PLANNING AND INFERENCE OF SEQUENTIAL ACCELERATED LIFE TESTS

LIU XIAO

(B. Eng, Harbin Institute of Technology, China)

A THESIS SUBMITTED

FOR THE DEGREE OF DOCTOR OF PHILOSOPHY

DEPARTMENT OF INDUSTRIAL AND SYSTEMS ENGINEERING

NATIONAL UNIVERSITY OF SINGAPORE

2009

Accelerated Life Test in Chinese Philosophy

When Heaven is about to place a great responsibility on a great man, it always first frustrates his spirit and will, exhausts his muscles and bones, exposes him to starvation and poverty, harasses him by troubles and setbacks so as to stimulate his spirit, toughen his nature and enhance his abilities.

--- Mencius, 372 – 289 BC

天将降大任于斯人也，必先苦其心志，劳其筋骨，饿其体肤，空乏其身，行拂乱其所为，所以动心忍性，增益其所不能。

---- 《孟子 告子下》

Acknowledgements

I am deeply indebted to my supervisor, Associate Professor TANG Loon Ching, the head of the Department of Industrial and Systems Engineering (ISE), National University of Singapore. He led me to and guided me in the world of reliability engineering. This dissertation would not have been possible without his patience, encouragement, expert advice, and strict requirement, which gave me the deepest impression during the past years.

Deepest gratitude is also due to the faculty members of the ISE department. I am grateful to Professor GOH Thong Ngee and Dr. NG Szu Hui for their valuable support and recommendation when I applied for my current research position in our department. I am also grateful to Professor XIE Min who provided me with valuable suggestions when I applied to the Ph. D program at NUS.

Sincere thanks also go to the ISE simulation laboratory technologist Ms. NEO Siew Hoon, Celine, and the ISE management assistant officer Ms. OW Lai Chun for their constant assistance.

To all my friends in Singapore, what else can I say? I do not list your names here as you are always on my mind. Thank you all. You are the sunshine of my life in the beautiful Singapore.

To my parents, grandparents, my wife REN Jia and my families, I started to live on campus when I was twelve, and left my hometown when I was eighteen. I wish I could spend more time with you. Your endless love and selfless support means everything in my life.

Table of Contents

Summary

This dissertation investigates several important problems in Accelerated Life Test (ALT). Both statistical inference (Chapter 3 and 4) and planning (Chapter 5, 6, 7 and 9) methods are proposed accompanied with numerical examples and simulation studies.

In the analysis of ALT data, some stress-life model is typically used to relate results obtained at stressed conditions to those at use condition. For example, the Arrhenius model has been widely used for accelerated testing involving high temperature. Motivated by the fact that some prior knowledge of the particular model parameters is usually available, a sequential constant-stress accelerated life testing (ALT) scheme is proposed in this dissertation (Chapter 3). Under this framework, test at the highest stress is firstly conducted to quickly yield preliminary information on key ALT model parameters. In reality, these parameters are usually difficult to be specified and have more bearing on the developed plans. Using both information obtained at the highest stress and that elicited from engineering experiences, prior distributions for model parameters at lower stress levels are deduced. Particularly, two basic Bayesian inference frameworks are presented, namely, the All-at-one Prior Distribution Construction (APC) and the Full Sequential Prior Distribution Construction (FSPC). Assuming Weibull failure times, this thesis 1) derives the closed-form expressions for estimating the smallest extreme value location parameter at each stress level; 2) compares the performance of the proposed Bayesian inference to that of Maximum Likelihood (ML) methods; and 3) assesses the risk of including

empirical engineering knowledge into ALT data analysis under the proposed framework. Step-by-step illustrations of both frameworks are presented using a published real-life ALT dataset.

This dissertation also addresses the applicability of the proposed inference method. In practice, the applications of Bayesian inference in ALT data analysis are typically limited by 1) the difficulty of quantifying prior knowledge into mathematical expressions, and 2) the potential risk of violating data objectivity when certain prior knowledge is incorporated. Hence, Chapter 4 proposes a Double-Stage Estimation procedure and establishes the closed-form relationships between the prior knowledge and the statistical precision/accuracy of certain estimates.

In the planning of ALT, preliminary estimates of unknown model parameters are often needed so as to assess the statistical efficiency of test plans. Very often, the margin of error is high and the requisite level of statistical precision cannot be achieved as planned. To enhance the robustness of ALT plan to misspecification of model parameters, approaches to planning sequential ALT are proposed. Under the proposed sequential scheme, test at the highest stress level is firstly planned and conducted. Then, both Bayesian (Chapter 5 and 6) and Maximum Likelihood (Chapter 7) based frameworks are proposed to incorporate the information obtained under the highest stress in the planning of subsequent tests under lower stresses. Under either framework, the large-sample approximation to posterior density is used, and both sample allocation and stress combinations at lower stress levels are optimized by minimizing the variance of certain reliability estimates at use condition. Sometimes,

since few or zero failures are obtained when the stress is low, an auxiliary acceleration factor, with its effect on product life distribution being well understood, is embedded into the Bayesian planning framework so as to amplify the failure probability under lower stresses (Chapter 6). Comprehensive simulation studies are conducted to compare the performance of the sequential testing scheme to that of the traditional non-sequential planning and testing. In Chapter 8, a case study that successfully employs the methods introduced in this dissertation is provided to reaffirm the strengths of the proposed planning and inference approaches for sequential accelerated life tests.

Chapter 9 proposes a Bayesian approach to planning an accelerated life test (ALT) for repairable systems with multiple *s*-independent failure modes. A power law process (PLP), that combines both proportional intensity (PL) and acceleration time (AT) approaches, is used for modeling the failure process of repairable systems under ALT. Based on the Bayesian *D*-optimality and *Ds*-optimality, this chapter develops optimal plans for ALT by invoking the general equivalence theorem. It also addresses the problem of prior elicitation, and derives the expression of the Fisher information matrix. Finally, a case study on testing diesel automotive engines is presented to illustrate how to use the proposed planning principle to obtain the 2-stress-level optimal plan and a compromise plan for 3-stress-level ALT.

List of Tables

List of Figures

List of Symbols

ALT	Accelerated Life Testing
AT	Accelerated Time
AVAR	Asymptotic Variance
BLUE	Best Linear Unbiased Estimator
Cdf	Cumulative Distribution Function
CSALT	Constant-Stress ALT
DSE	Double Stage Estimation
FMEA	Failure Modes and Effects Analysis
GET	General Equivalence Theorem
ILS	Iterative Least Squares
LS	Least Squares
MCMC	Markov Chain Monte-Carlo
ML	Maximum Likelihood
MLE	Maximum Likelihood Estimator/Estimation
MSE	Mean Squared Error
PI	Proportional Intensity
PLP	Power law Process
PSALT	Progressive Stress ALT
Pdf	Probability Density Function
QALT	Qualitative ALT

SALT	Sequential Accelerated Life Test
SEV	Smallest Extreme Value
SSALT	Step-Stress ALT
TTT	Total Time on Test
WR	Weighted Regression

ξ	An ALT plan
s	Stress level, possibly transformed
x	Standardized censoring time at stress level
u	Scaling factor
k	Number of stress levels*
$v(t)$	Failure intensity at time t
$\Lambda(t)$	Cumulative mean number of failures in the time interval $(0,t]$
$\Lambda_i(t)$	Cumulative mean number of failures in the time interval $(0,t]$ at stress i for $i = 1, 2, ..., m$
$\Lambda_0(t)$	Baseline cumulative mean number of failures in the time interval $(0,t]$ at base-line stress level
T	Failure time
α	Weibull scale parameter
μ	SEV location parameter

* In Chapter 9, k denotes the number of failure modes, whereas m denotes the number of stress levels

β	Weibull shape parameter
σ	SEV scale parameter
L	Likelihood function
l	Log-likelihood function
A_{ki}	Acceleration factor between level k and any lower stress level i
M_{ji}	Transformed A_{ki}
$T_i^{(T)}$	Transformed total time on test at stress level i
c_i	Censoring time at stress level i
ζ_i	Standardized c_i
N	Total number of testing units, i.e., the sample size
π_i	Proportion of systems allocated to stress i for $i = 1, 2, ..., m$, $\sum_{i=1}^{m} \pi_i = 1$
r_i	Number of failures at stress level i
ρ	Number of parameters of interest
t_{ij}	The jth failure at stress level i
y_{ij}	The jth failure at stress level i in log-scale
z_{ij}	The standardized jth failure at stress level i in log-scale
$\mathbf{I}(\cdot)$	Fisher information matrix
$U(\cdot)$	Utility function
$\phi(\cdot)$	Planning criterion
$d(\xi, x)$	Frechet derivative of criterion $\phi(\xi)$ at ξ in the direction of ξ_x
$\eta(\cdot)$	Relative D-efficiency of the plan
$\eta_a(\cdot)$	Adjusted relative D-efficiency of the plan

E_a	Activation energy, in electron-volts
k_B	Boltzmann Constant, 8.6171e-5 electron-volts per Celsius
Ψ_n	Polygamma Function
Γ	Gamma Function
ϕ_{SEV}	Pdf of Standard Smallest Extreme Value Distribution
ϕ_{NOR}	Pdf of Standard Normal Distribution
Φ_{SEV}	Cdf of Standard Smallest Extreme Value Distribution
Φ_{NOR}	Cdf of Standard Normal Distribution

Chapter 1. Introduction

1.1. Introduction to Accelerated Life Testing

Manufacturers today are facing strong pressure to develop newer products with more features and higher reliability. In line with the modern quality philosophy for producing high reliability products, this is achieved by improving the design and manufacturing processes, rather than relying on inspections. For example, Electronic Engine Controls (EEC) is one of the most complex and expensive components of the jet engine. Reliability must be designed into the EEC from the initial stage of design by considerations of hardware selection, manufacturing processes, software design, rigorous testing, fault detection and monitoring logic, and proper in-service trouble shooting procedures (Sikand et al 2005).

For this reason, various up-front reliability tests of materials, components and systems have been motivated in both product design and production phases. However, today's manufacturers usually do not have the luxury of collecting 100% of the information needed to make a bulletproof reliability analysis due to the strong pressure to shorten the time-to-market of their products. It is always a need to balance the gathering and analyzing of information against the timeliness of the decision being made. For some modern products which are designed to operate properly for tens of years, testing under normal operating conditions in a practical length usually causes zero or few failures. "No one wants to learn from mistakes, but we cannot learn

enough from successes to go beyond the state of the art". Without enough failures, engineers simply do not have enough information for estimating the time-to-failure distribution or the long-term performance of their products.

Hence, Accelerated Life Test (ALT), which precipitates timely information on product reliability, has been widely used. During an ALT, testing units (materials, components, systems, etc.) are subject to high level of stress (temperature, humidity, voltage, usage rate, and etc.) to yield short lives. The life data obtained at over-stressed conditions are then used to evaluate product reliability at normal operating conditions. Because of its irreplaceable role in estimating and improving product reliability, ALT has become one of the most important reliability programs in manufacturing industries facing the rapidly changing technologies and increasingly high customer expectations.

In the following sections, we shall see the basic functions as well as the classification of modern ALT.

1.1.1. Functions of Accelerated Life Testing

ALT carries multiple functions in product design and development. Usually, it is helpful to answer those important questions listed in Table 1.1 (Porter 2004).

From a product life cycle perspective, Yang (2007) classifies ALT into three categories: design ALT, qualification ALT, and production ALT. Within each category, the functions of test may not necessarily be the same. Design ALT carries functions involving 1) comparing and assessing material reliability; 2) determining optimum design alternatives; and 3) confirming the effectiveness of a design change. Once the

product design is done, qualification ALT is usually followed for design verification by testing product prototypes. Within this phase, ALT is primarily used to 1) demonstrate whether the design achieves the reliability target; and 2) estimate the reliability of the design. When the design verification is completed, ALT plays another important role in process validation, including 1) demonstration of the capability of the manufacturing process; and 2) estimation of the product reliability.

Table 1.1 Questions answered by ALT

Research	What are the boundaries of a new type of technology?
Development	What design features need correcting? What must be changed to make it work?
Validation	Does the product meet the life/performance requirements? How reliably?
Production	What production parameters affect the fabrication of the product? What are the optimal values and tolerances for the parameters?
Warranty	What causes the warranty failure? How can the warranty failure be reproduced? What corrects the warranty failure?
Life Extension	What residual life exists in a system at the end of its scheduled life? What performance envelope adjustments or maintenance schedule changes can be made to extend the useful life safely?

In summary, by analyzing failures obtained from ALT, reliability engineers are essentially aimed to find out ‘how’, ‘when’, and ‘why’ products fail at normal operation conditions. Answering the question ‘how’ requires the identification of potential design and manufacturing defects, namely, the identification of failure modes. Answering the question ‘when’ requires the quantification of product reliability for

critical failure modes (see Section 1.2). Finally, in order to remove or reduce products' deficiencies using better design, manufacturing, or component selection, the third question 'why' has to be answered.

In fact, failures obtained in product life test help to identify problems and thus provide opportunities to improve the design and manufacturing process. This reminds me of the ancient Chinese saying by *Mencius*, "When Heaven is about to place a great responsibility on a great man, it always first frustrates his spirit and will, exhausts his muscles and bones, exposes him to starvation and poverty, harasses him by troubles and setbacks so as to stimulate his spirit, toughen his nature and enhance his abilities".

1.1.2. Types of Accelerated Life Testing

In this dissertation, the focus is on quantitative ALTs that are used to obtain timely information on product *life distribution* at use conditions by testing products at higher-than-use conditions. Usually, this type of ALT can take form of 1) usage rate acceleration; 2) over stress acceleration; 3) changing level of control factor; and 4) tightening the failure threshold. Key reliability measures can be estimated by analyzing the failure data obtained from stressed conditions, and the highest stress level should be carefully chosen to accelerate the right failure mode without introducing irrelevant failure modes that are not of interest to reliability engineers.

When the life information at use conditions is not needed, however, there are other important types of accelerated tests, e.g. the Highly Accelerated Life Test (HALT), the Environmental Stress Testing (EST), the Environmental Stress Screening, and etc. In

general, these types of tests are used to expose design/manufacturing defects, and thus usually require smaller sample size.

In addition to different types of ALT, we will see different stress loading methods in Section 2.2. But it has to be always remembered that “it is not the test that is important, but the information (Porter 2004)”.

1.2. Statistics and Reliability Measures

As the only available powerful tool that effectively quantifies data/information uncertainty, statistics is used as the official mathematical language in reliability modeling and analysis which deal with the random nature of product failures. In the monograph “Statistical Methods in Reliability Engineering”, Meeker and Escobar (1998) provide detailed discussions on methods for data collection, analysis, and interpretation which are important for product reliability and design decisions.

In Figure 1.1a, the four basic statistical operations are presented (Efron 1982), namely, enumeration (data collection), summary, comparison, and inference. As a contrast, Figure 1.1b shows the four basic operations in ALT applications. It is very interesting to observe that every basic operation in ALT applications employs certain powerful tools from its counterpart in statistical operations. For example, an ALT project usually starts with test planning as it determines if failure data can be collected efficiently. Since products typically fail in a random manner, the knowledge of data collection (enumeration) in statistics plays an important role as it provides guidance of how an ALT should be planned given certain optimality criterion. After an ALT is

completed, testing results are briefly summarized using summary statistics such as the total number of failures at each testing condition, and simple comparison can thus be made based on these summary statistics. Finally, in order to quantify product reliability at use condition, or predict product reliability at a given time, or make decisions depending on product life distribution, engineers borrow the powerful tool of statistical inference that yields estimates with statistical significance by taking into account the random nature of product failure.

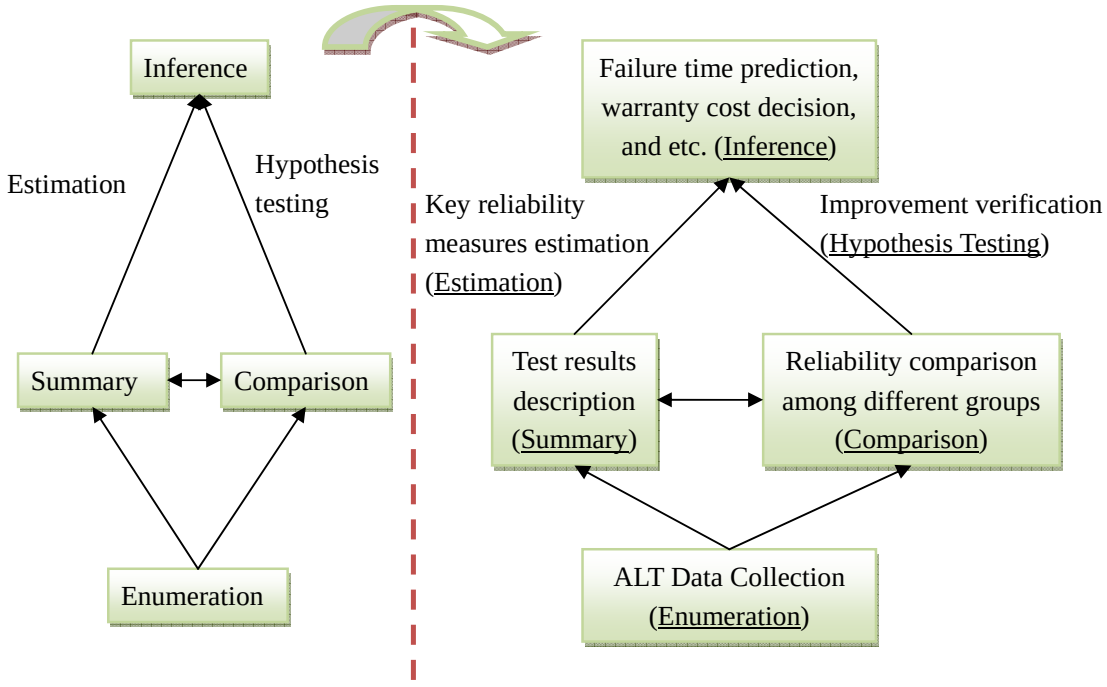

Figure 1.1 Mapping of basic operations from statistics to ALT

Several important reliability measures, which are defined using the language of statistics, are widely used in practice. Commonly used ones include the Reliability function--a probability that an item is functioning at any time, the mean time to failure

(MTTF), the life quantile, the failure/hazard rate, and etc.

1.3. Problems with Accelerated Life Testing

Current ALTs have problems that restrict their applications. Meeker and Escobar (1998) and Pascual et al. (2006) summarize the possible pitfalls of accelerated life testing. In this section, a discussion on those major problems is presented.

- For complex mechatronics systems/assemblies with multiple potential failure modes, it is difficult to lock on the target failure mode in an ALT. In other words, failure modes precipitated by ALTs might not be those occurring under normal operation conditions. Currently, most quantifiable ALTs are used to make an inference on certain key reliability measures for one particular failure mode. Hence, it is vitally important to make sure that failure produced by ALT is actually caused by one of the dominated failure modes in the field. However, this is not easy at all. On the one hand, severe testing environment might produce new/irrelevant failure modes, namely, these failure modes do not really exist under normal operation conditions. On the other hand, the sequence that different failure modes occur might also be shuffled under accelerated conditions. As shown in Figure 1.2, the target failure mode A is more likely to occur before the nuisance failure mode B under normal operation conditions, however, this order is switched under accelerated environment. Hence, the analysis of ALT data is sometimes beyond the

capability of reliability engineers or statisticians, it requires the participation of managers and senior design engineers, which challenges the teamwork of many companies. In practice, since the target failure mode is usually identified before a quantitative ALT by employing the methods such as Failure Modes and Effects Analysis (FMEA), engineers can use some special case-dependent techniques to keep those irrelevant failure modes from occurring. For instance, they can add some protections to those fragile components or links if their failure modes are not the primary concerns. Or, they can reduce the level of acceleration. Unfortunately, this results in the second problem as follows.

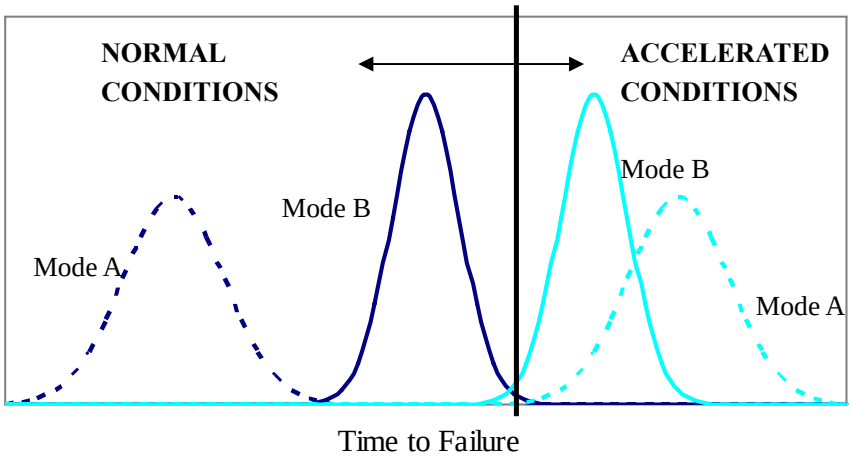

Figure 1.2 Illustration of the change in failure model occurrence order

- For complex mechatronics systems/assemblies, it is hard to achieve a high time compression. As discussed above, the level of acceleration may be reduced to lock on the target failure mode for an ALT. Sometimes, the highest level of acceleration is limited by the most fragile component of that system.

As shown in Figure 1.2, in order to produce failure mode A during an ALT, the actual acceleration level used should be much lower than that shown in the figure. Hence, it takes a long time, usually several months, to obtain enough failures that support an inference on product reliability with statistical significance.

- The current role of ALT prohibits the company from taking full advantage of the powerful technique of ALT. Although ALT now has been widely recognized as an indispensable part in product design/development, it is certainly not the most important part. Hence, the budget for reliability testing program must always be weighed against the expected benefits that can be obtained. The statistical sample size, for example, is frequently too large to be affordable as it largely affects the test cost, required capacity of test equipments, test time, and estimate accuracy (Yang 2007, pp. 240). Furthermore, as we have seen above, a successful ALT at the system-level not only requires efforts across different departments, but also sufficient time and financial supports. Unfortunately, these requirements can be very tedious for small companies which are not able to spend too much on reliability improvement. Hence, reliability programs will not be the top priority when decisions on resource distribution are made. The relationship between information, time, cost and engineering decisions in the development process should be explored to provide a common dialog for making sound decisions about what information to collect, what validation tools to use and what

resources to apply. Ultimately, if validation tools are selected and applied to provide the key information precisely when it is needed, the development process will not just be faster; it will be a truly efficient development process.

1.4. The Structure and Scope

This dissertation develops both data analysis and test planning methods for the proposed sequential constant-stress accelerated life testing. The structure of this dissertation is sketched in Figure 1.3.

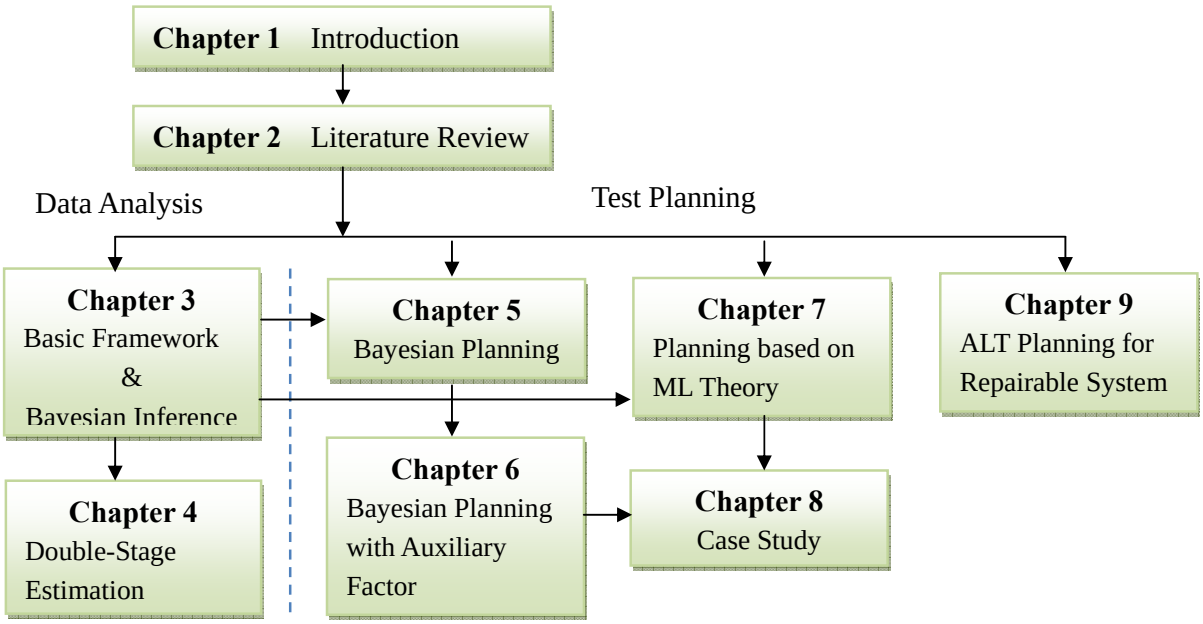

Figure 1.3 The structure of the thesis

In Chapter 2, a literature review, with discussions and illustrations, on statistical ALT modeling, inference and planning is firstly presented. The purpose of this literature review is not only to provide necessary background information of current

data analysis and test planning methods, but also to compare these methods in order to see both of their advantages and disadvantages.

Chapter 3 and 4 are focused on the analysis of ALT data.

Following the discussion, a sequential ALT (SALT) scheme, with its motivation clearly stated, is proposed in Chapter 3. Under this framework, test at the highest stress is firstly conducted to quickly yield preliminary information on key ALT model parameters. Then, using both the information obtained at the highest stress and that elicited from product engineers, prior distributions for model parameters at lower stress levels are constructed. Particularly, two basic Bayesian inference frameworks are developed, namely, the All-at-one Prior Distribution Construction (APC) and the Full Sequential Prior Distribution Construction (FSPC). Based on the assumption of Weibull failure times, this chapter is focused on the 1) derivation of closed-form expressions for estimating the smallest extreme value location parameter at each stress level; 2) performance comparison of the proposed Bayesian inference to that of Maximum Likelihood (ML) methods; and 3) assessment of the risk of including empirical engineering knowledge into ALT data analysis under the proposed framework.

Based on the results of Chapter 3, Chapter 4 goes one step further and proposes a double-stage estimation utilizing both initial estimates and prior knowledge. In particular, the relationship between prior knowledge and statistical precision/accuracy of certain estimates for reliability is investigated in detail.

Chapter 5 ~ 9 are focused on the planning of an ALT.

Based on the framework of sequential ALT proposed in Chapter 3, both Bayesian (Chapter 5 and 6) and Maximum Likelihood (Chapter 7) based planning methods are proposed to incorporate the information obtained under the highest stress in the planning of subsequent tests under lower stresses. Under either framework, the large-sample approximation to posterior density can be used, and both sample allocation and stress combinations at lower stress levels should be optimized by minimizing the variance of certain reliability estimates at use condition. Sometimes, since few or zero failures are obtained when the stress is low, an auxiliary acceleration factor, with its effect on product life distribution being well understood, can be embedded into the Bayesian planning framework so as to amplify the failure probability under lower stresses (Chapter 6). Comprehensive simulation studies are needed to compare the performance of the sequential testing scheme to that of the traditional non-sequential planning and testing. In Chapter 8, a real case study that successfully employs the methodologies introduced in this dissertation will be provided to reaffirm the strengths of the proposed planning and inference of sequential accelerated life tests.

Chapter 9 can be viewed as an independent chapter as the method proposed in this chapter does not apply to the framework of sequential ALT. In this chapter, we consider the situation when more than one failure modes are often of interest, and propose a Bayesian approach to planning an accelerated life test (ALT) for repairable systems with multiple *s*-independent failure modes. A power law process (PLP), that combines both proportional intensity (PL) and acceleration time (AT) approaches, is

used for modeling the failure process of repairable systems under ALT. Based on the Bayesian *D*-optimality and *Ds*-optimality, we develop optimal plans for ALT by invoking the general equivalence theorem. We also discuss the elicitation of prior distributions, and derive the expression of the Fisher information matrix. Finally, a case study on testing diesel automotive engines is presented to illustrate how to use the proposed planning principle to obtain the 2-stress-level optimal plan and a compromise plan for 3-stress-level ALT.

Chapter 2. Literature Review on Statistical ALT Modeling, Inference and Planning

2.1. Introduction

This chapter reviews the current development of Accelerated Life Testing (ALT) modeling, inference and planning. It involves 5 fundamental issues: Stress loadings, Data type, Statistical ALT model, ALT data analysis, and ALT planning. Figure 2.1 below sketches the organization structure of this chapter.

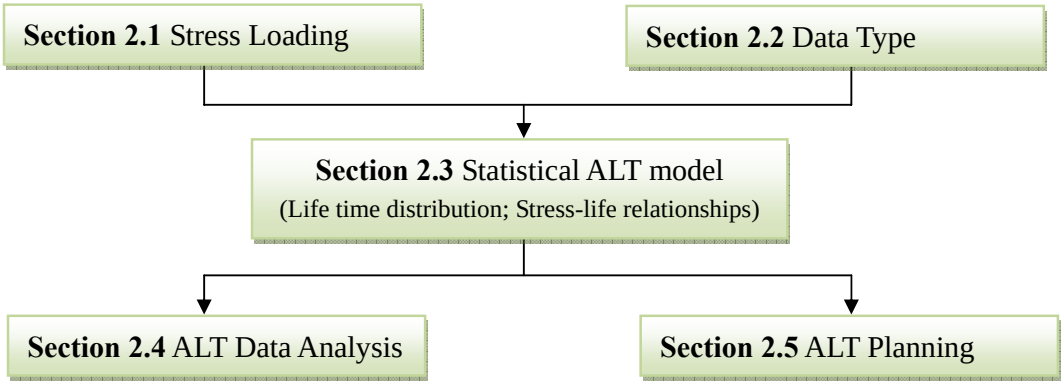

Figure 2.1 Organization of Chapter 2

2.2. Types of Stress Loadings

Stresses used in ALT typically include temperature, humidity, voltage, vibration, etc. and the most commonly adopted patterns of loading these stresses are constant-stress, step-stress, progressive stress loadings, cyclic stress loading, and etc. Accordingly, we have constant-stress ALT (CSALT), step-stress ALT (SSALT) and progressive-stress ALT (PSALT).

As shown in Figure 2.2a, stress applied to testing units does not vary with time in CSALT. In practice, test with this type of stress loading is most commonly conducted due to its simplicity. Methods for analyzing CSALT data are also relatively mature and empirically verified.

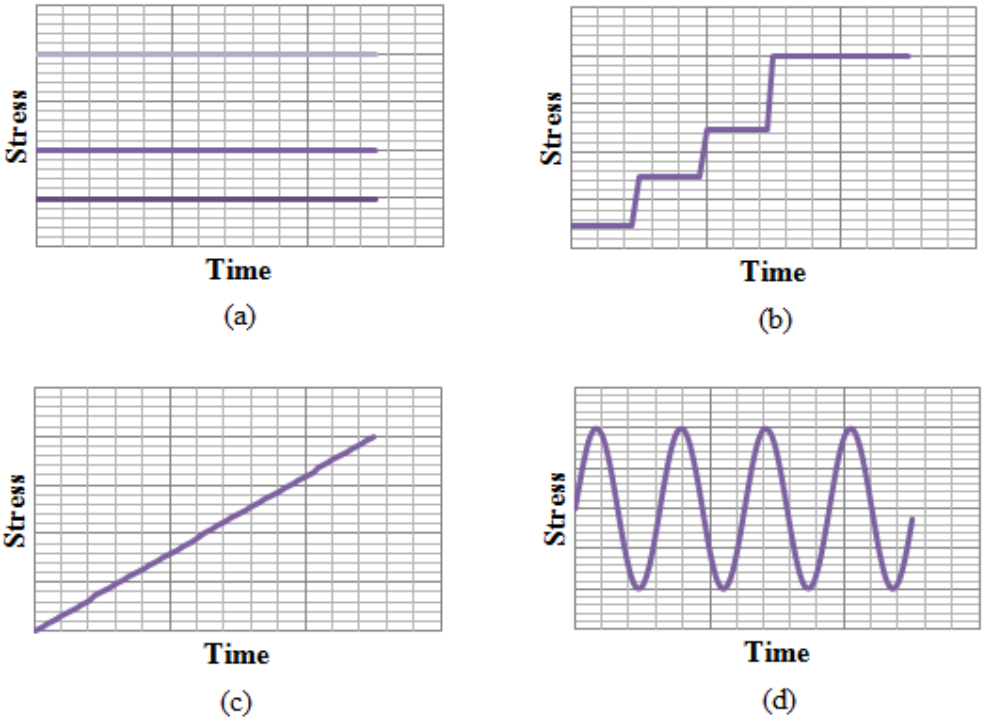

Figure 2.2 Stress loadings in ALT

For both SSALT and PSALT, stress applied to sample units is time-dependent. For SSALT, stress remains at a certain level for a period of time and jumps to a higher level at a pre-specified point as shown in Figure 2.2b. For PSALT, stress constantly increases with time as shown in Figure 2.2c. Both SSALT and PSALT have advantages in yielding failures quickly but impose challenges for modeling the data. In fact, the models are not well developed and might lead to less accurate conclusions. ALT with cyclic stresses shown in Figure 2.2d is also used in practice, e.g. Monroe and Pan

(2008). However, both the modeling and analysis for such an ALT become much more difficult, and necessary simplifications are usually needed.

More stress loading patterns can be found in Nelson (1990) and Yang (2007).

2.3. Data Type

"Reliability data are typically censored". This is the first distinguishing feature of reliability data summarized by Meeker and Escobar (1998).

For accelerated life tests, two stopping (censoring) rules are commonly adopted. One, test is stopped at a pre-specified time (known as time-censoring or type-I censoring). Two, test is stopped when a given number of failures has been observed (known as failure censoring or type-II censoring). Thus, what engineers usually have are some exact observations mixed with censored observations which provide a bound or bounds of actual failure times.

Typical data type in ALT includes: complete (exact) data, right censored data, and interval censored data.

- Complete (exact) data. As shown in Figure 2.3, unit A has failed before the test is done, hence, the exact failure time of unit A (C3) has been recorded and referred as a complete or exact observation.
- Right censored data. As shown in Figure 2.3, unit B has not failed before the test is done, hence, the actual failure time of unit B is unknown. In this case, what engineers observe is a lower bound (C) of the actual failure time, and this lower bound value is referred as a right censored observation. Right

censored data and complete data are the two most common and important data types appear in typical ALT datasets.

- Interval censored data. As shown in Figure 2.3, unit C has failed before the test is done, however, the failure time is roughly known as within an interval (C1~C2). This type of observation is referred as interval censored data which reflects uncertainty as to the exact time the units failed within an interval. Usually, it comes from tests or situations where the objects of interest are not constantly monitored (See Yang 2007, pp. 245 for detailed introduction to data collection methods).

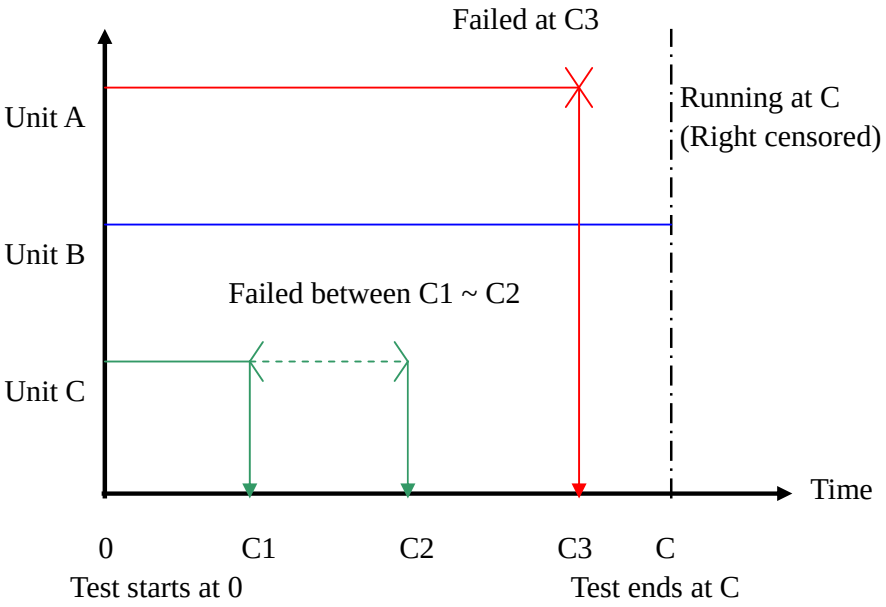

Figure 2.3 Illustration of exact data, right censored data, and interval censored data

2.4. Statistical Model of Constant-Stress ALT

A typical statistical model of constant-stress ALT consists of the following two

components as shown in Figure 2.4.

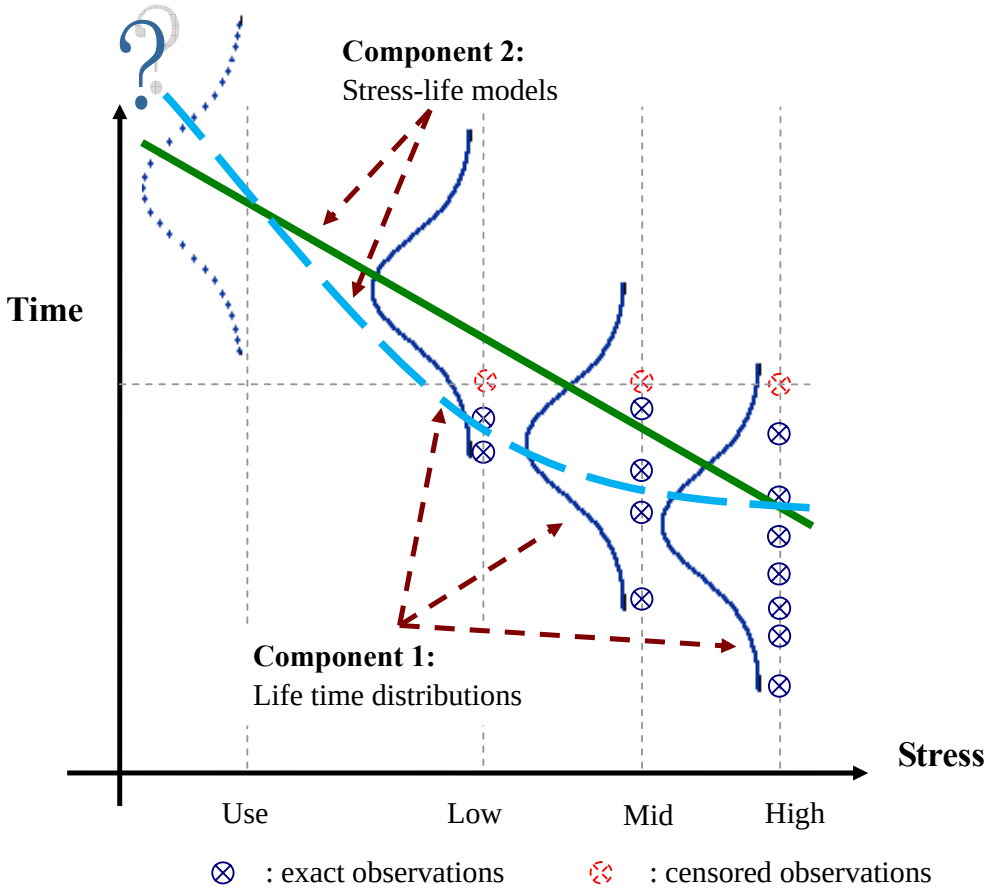

Figure 2.4 Statistical ALT model

Component 1: A life time distribution that models product's behavior at a particular stress level. This assumption might be avoided if non-parametric methods are used, but parametric models provide important practical advantages for most applications. This thesis therefore only focuses on parametric ALT models. Table 2.1 summarizes the characteristics of those life time distributions commonly used for reliability data modeling. More details can be found Leemis (1995), Meeker and Escobar (1998), Nelson (1990). Particularly, a relationships plot among continuous

univariate lifetime distributions is provided by Leemis (1995).

Component 2: A relationship (also called stress-life model) that quantifies the manner in which the life time distribution changes across different stress levels. Table 2.2 summarizes the characteristics of those commonly used stress-life models. In this table, the Acceleration Factor A_f is defined as the ratio of the life between the use level and a higher stress level. More details can be found in Nelson (1990), Meeker and Escobar (1998), and Livingston (2000).

Table 2.1 Characteristics of life-time distributions commonly used in ALT

Distribution	Key Characteristics	Remarks
Weibull	Probability density function: $f(t)=\frac{\beta}{\alpha}\left(\frac{t}{\alpha}\right)^{\beta-1}\exp\left[-\left(\frac{t}{\alpha}\right)^{\beta}\right],\quad t>0$ Cumulative density function: $F(t)=1-\exp\left[-\left(\frac{t}{\alpha}\right)^{\beta}\right],\quad t>0$ Reliability function: $R(t)=1-F(t)=\exp\left[-\left(\frac{t}{\alpha}\right)^{\beta}\right],\quad t>0$ MTTF: $MTTF=\alpha\cdot\Gamma\left(1+\frac{1}{\beta}\right)$	a) One of the most commonly used distributions in ALT and reliability data modeling; b) α is the scale parameter; β is the shape parameter; c) Appropriate for modeling life times having constant ($\beta=1$), strictly increasing ($\beta>1$), and strictly decreasing ($\beta<1$) failure rate; d) Log-location-scale parametric distribution; e) If T follows Weibull distribution with scale α and shape β, then, $Y=\log(T)$ follows smallest extreme value distribution with location $\mu=\log(\alpha)$ and scale $\sigma=1/\beta$;

	Failure rate: $h(t)=\frac{\beta}{\alpha}\left(\frac{t}{\alpha}\right)^{\beta-1}, \quad t>0$ TTFp: $t_p=\exp\left[\log(\alpha)+\Phi_{sev}^{-1}(p)\frac{1}{\beta}\right]$ $\Phi_{sev}^{-1}(z)=1-\exp\left[-\exp(z)\right]$	
Smallest Extreme Value	Probability density function: $f(y)=\frac{1}{\sigma}\phi_{sev}\left(\frac{y-\mu}{\sigma}\right), \quad -\infty<y<\infty$ $\phi_{sev}=\exp\left[z-\exp(z)\right]$ Cumulative density function: $F(y)=\Phi_{sev}\left(\frac{y-\mu}{\sigma}\right), \quad -\infty<y<\infty$ TTFp: $y_p=\mu+\Phi_{sev}^{-1}(p)\sigma$	a) If T follows Weibull distribution with scale α and shape β, then, $Y=\log(T)$ follows smallest extreme value distribution with location $\mu=\log(\alpha)$ and scale $\sigma=1/\beta$; b) Location-scale parametric distribution;

Exponential	Equivalent to Weibull distribution with $\beta = 1$	a) Model life data with constant failure data; b) Simple, even used in situations in which it does not apply;
Normal	Probability density function: $f(y) = \frac{1}{\sigma}\phi_{nor}\left(\frac{y-\mu}{\sigma}\right), \quad -\infty < y < \infty$ $\phi_{nor}(z) = \left(1/\sqrt{2\pi}\right)\exp\left(-z^2/2\right)$ Cumulative density function: $F(y) = \Phi_{nor}\left(\frac{y-\mu}{\sigma}\right), \quad -\infty < y < \infty$ $\Phi_{nor}(z) = \int_{-\infty}^{z}\phi_{nor}(w)dw$ TTFp: $y_p = \mu + \Phi_{nor}^{-1}(p)\sigma$	a) Useful to model life data when $\mu > 0$ and σ/μ is small; b) Not commonly used in reliability and ALT;
Lognormal	Probability density function: $f(t) = \frac{1}{\sigma t}\phi_{nor}\left[\left(\log(t) - \mu\right)/\sigma\right], \quad t > 0$	a) One of the most commonly used life time distribution in ALT and reliability modeling;

Cumulative density function:

$$F(t) = \Phi_{nor}\left[\left(\log(t) - \mu\right)/\sigma\right], \quad t > 0$$

Reliability function:

$$R(t) = 1 - \Phi_{nor}\left[\left(\log(t) - \mu\right)/\sigma\right], \quad t > 0$$

MTTF:

$$MTTF = \exp\left[\mu + 0.5\sigma^2\right]$$

Failure rate:

$$h(t) = f(t)/R(t), \quad t > 0$$

TTFp:

$$t_p = \exp\left[\mu + \Phi_{sev}^{-1}(p)\sigma\right]$$

b) Useful in degradation, fatigue data modeling;

c) $h(t)$ starts at zero, increases to a certain point, and decreases to zero.

Table 2.2 Characteristics of commonly used stress-life models

Model	Expression	Remarks
Arrhenius relationship	$A_f = \exp\left[\frac{E_a}{k}\cdot\left(\frac{1}{T_u}-\frac{1}{T_a}\right)\right]$ E_a : activation energy, ev k : Boltzmann's Constant $(8.6141\times10^{-5}$ ev/C) T_u : use temperature in Kelvin T_a : test temperature in Kelvin	a) Model product life as a function of temperature; b) Typical value of E_a is usually available from physical or chemical knowledge, empirical data, failure mechanisms, and etc.
Hallberg – Peck relationship	$A_f = \left(\frac{RH_a}{RH_u}\right)^3 \exp\left[\frac{E_a}{k}\cdot\left(\frac{1}{T_u}-\frac{1}{T_a}\right)\right]$ RH_a : use relative humidity RH_u : test relative humidity	a) Model product life as a function of temperature, humidity and bias. b) Usually used in highly accelerated stress test (HAST), temperature humidity bias (THB), and Autoclave (unbiased)

	E_a, k, T_u, T_a defined as above	
Eyring relationship	$A_f = \left(\frac{T_a}{T_u}\right)^m \exp\left[\frac{E_a}{k}\cdot\left(\frac{1}{T_u}-\frac{1}{T_a}\right)\right]$ E_a, k, T_u, T_a defined as above m: constant ranges from 0 to 1	a) Based on physical theory describing the effect that temperature has on a reaction rate
Inverse-Power relationship	$A_f = \left(\frac{V_a}{V_u}\right)^{-\beta_1}$ V_a: test voltage V_u: use voltage β_1: material-specific exponent	a) Useful for voltage acceleration;
Coffin – Mansion relationship	$A_f = \left(\frac{\Delta T_a}{\Delta T_u}\right)^m$ ΔT_a: thermal cycle temperature change in test environment	a) Thermo-Mechanical effects; b) Model effects of low-cycle fatigue induced by thermal stressing

	V_u : thermal cycle temperature change in use environment m : constant	c) m is derived from empirical data
NVM data retention T-Model	$A_f = \exp\left[\frac{T_a - T_u}{T_0}\right]$ T_a : test junction temperature in Kelvin T_u : use junction temperature in Kelvin T_0 : data-retention characteristic temperature	a) NVM is short for nonvolatile memory b) Model for data loss c) Dependent on the temperature, the dielectric properties, and the electric field strength

2.5. Inference Methods for Accelerated Life Testing Data

To quantify the reliability of product, some key reliability measures are to be estimated. Various methods have been proposed for ALT data analysis. Nelson (1990) classified these methods into the following 7 categories. In Table 2.3, a summary of these methods are presented.

- Graphical methods
- Least squares analysis (LS)
- Iterative least squares (ILS)
- Weighted regression (WR)
- Best linear unbiased estimator (BLUE)
- Maximum Likelihood (ML) methods
- Bayesian analysis

To review, illustrate, and compare these methods, consider a typical constant-stress ALT model as follows,

Suppose a number of specimens of sample size N are tested at k constant stress levels s_i for $i = 1,...,k$. Let s_k and s_0 respectively denotes the pre-specified highest stress and the design stress where certain product reliability is to be estimated, we parameterize s_i

$$x_i = (s_i - s_k)/(s_0 - s_k) \quad \text{or} \quad x_i = (s_i - s_0)/(s_k - s_0) \qquad \forall i = 0,1,...,k, \tag{2.1}$$

such that $x_0 = 1$ for $s = s_0$ and $x_k = 0$ for $s = s_k$ for the first type of parameterization;

whereas $x_0 = 0$ for $s = s_0$ and $x_k = 1$ at $s = s_k$ for the second type of parameterization. Regardless of the type of parameterization, the testing region is always $[0,1]$.

At any stress level s_i, $\forall i = 1,...,k$, n_i number of specimens is tested until a pre-specified censoring time c_i. The failure time T at any stress is assumed to follow a log-location-scale distribution

$$F(t) = \Phi\left(\left(\log(t) - \mu\right)/\sigma\right),$$

where μ and σ are respectively the location and scale parameter of failure time in log-scale. In particular, the location parameter μ depends on stress through a linear stress-life model

$$\mu_i = \beta_0 + \beta_1 x_i \tag{2.2}$$

and the shape parameter σ is a constant independent of stress.

It is noted that both Arrhenius and inverse power relationships can be linearized after proper parameterization. For example, the Arrhenius model can be linearized as

$$\begin{aligned} \mu &= \log A + \frac{\text{Activation energy}, E_a}{\text{Boltzmann constant}, k_B} \cdot \frac{1}{\text{Temp}} \\ &= \beta_0 + \beta_1 \cdot s \end{aligned} \tag{2.3}$$

where $\beta_0 = \log A$ $\beta_1 = E_a \cdot k_B^{-1}$ $s = 1/\text{Temp}$

The assumption of constant shape parameter σ is motivated by the fact that σ is usually associated with the underlying failure mechanism. Although controversial, this type of assumption is not uncommon in statistics. For example, in both linear regression analysis and ANOVA, statisticians often make similar assumptions that the dependent variables associated with different independent variables are normally distributed with the same variance. Certain techniques, as we shall see in Section 2.4.2,

have been developed to check the validity of this assumption. Meeter and Meeker (1994) discussed ALT plans with a non-constant scale parameter.

Parameters contained in this constant-stress ALT model are collected in the triplets $\boldsymbol{\varphi} = (\beta_0, \beta_1, \sigma)$.

In what follows, the first 5 methods are briefly reviewed. After that, detailed review of the ML methods and Bayesian analysis are respectively presented in Section 2.4.1 and Section 2.4.2.

Table 2.3 Summary of ALT data analysis methods

Method	Characteristics	Main limitations	Representative references
Graphical	Information visualization; Simple	Lack of rigorous analytic results	Klein and Moeschberger (2004), Nelson (1975a, 1982)
LS	Effective for complete data; Exact variance available	Difficult to handle censored data	Nelson (1975b), Kahn (1979), Teng and Yeo (2002)
Iterative LS	Updated version of LS to handle censored data	Lack of thorough studies on estimator bias	Schmee and Hahn (1979, 1981), Aitkin (1981)
WR	Weights on information obtained at each stress	Lack of thorough studies on estimator performance; No software available	Lawless (1982)
BLUE	Minimum variance unbiased linear estimator	Poor performance for heavy censoring	Nelson and Hahn (1972, 1973)
ML	Applicable for all stress loadings and data types; Automatically applied.	Asymptotic approximation inadequate for few failures	Nelson (1990), Meeker and Escobar (1998)
Bayesian	Prior knowledge included	Difficult to specify a priori; data objectivity is at risk	Barlow et al. (1988), Singpurwalla (2006) Zhang and Meeker (2006)

Graphical methods are extremely important in industrial applications to analyze ALT data based on the model above. They are simple and able to visualize critical information contained in dataset. Hence, they are ideal and powerful communication tools among engineers or between engineers and other people who are not familiar with statistical analysis. However, graphical methods have disadvantages due to the lack of analytic formulations. They usually do not reveal the underlying relationships among key statistical quantities, such as the relationship between sample size and statistical precision. Furthermore, different people might reach different conclusions based on the very same graph. In Nelson (1990), the author presented another disadvantage of graphical methods saying that such methods are difficult to quantify the statistical uncertainty by means of confidence intervals. Fortunately, commercial packages such Minitab and Reliasoft significantly mitigate this problem by automatically generating the confidence bounds for many important statistical plots. More details of the applications of graphical methods can be found in Nelson (1975a) and Klein and Moeschberger (2004).

The least squares method is a well known and simple analytic approach in regression analysis (Birkes and Dodge 1993, Chatterjee and Price 1991). In the literature, a least squares approach for the estimation of the inverse power law parameters assuming Weibull failure times can be found in Nelson (1975b). Only complete data were considered in this work, and the least squares estimates were assumed to be approximately normal. Kahn (1979) presented a least squares estimation for the inverse power law for ALT with type-II censoring. According to Kahn (1979),

the least squares estimator has many desirable properties: it is best linear unbiased and orthogonal for any sample size; the exact variance of the estimator is available; it is approximately normal for small number of stress levels provided a moderate number of failures is observed at each stress. However, the application of such method in ALT data analysis is limited as it is difficult to handle censored data. Much effort has been made to enhance the capability of the least squares method (Buckley and James 1979, Jin et al. 2006), but the modified versions of the method appear to be mathematically difficult thus less attractive to practitioners.

One of the modified versions of the least squares method was the iterative least squares found in Schmee and Hahn (1979, 1981) and Aitkin (1981). The salient feature of the iterative least squares is that the censored data are replaced by the value equal to its expected failure time conditioning on how long the specimen run without failure. Within each iteration, the value used to replace the censored data is updated based on the regression line fitted in previous iteration. Monte Carlo simulation shows that the iterative least squares method performs comparably to ML methods as discussed later. This is not surprising at all if we consider the fact that the iterative least squares procedure replaces the censored values with the expected values within each iteration.

The weighted regression method is somehow connected to the inference method introduced in Chapter 3. In this method, parameters at each stress level are separately estimated, and the stress-life relationship is then fitted using the weighted least square regression with weights being the inverse of the variance of estimators under each stress (Lawless 1982). Unfortunately, this method performs poorer than ML methods

in terms of the precision and accuracy of estimation.

The best linear unbiased estimators (BLUE) method was presented by Nelson and Hahn (1972, 1973). It performs comparable to ML estimators in terms of the mean squared error. However, for heavy censoring, ML methods are still better (Bugaighis 1988).

In the following two sections, a detailed review of ML methods and Bayesian analysis are provided. These two methods are most important in ALT data analysis and closely related to the study presented in Chapter 3 and Chapter 4.

2.5.1. Maximum Likelihood (ML) Methods for ALT Data Analysis

Maximum Likelihood (ML) methods the most widely used for analyzing ALT data. Such methods are straightforward (automatic) and applicable to almost all types of data and stress loadings. Hence, commercial packages, such as Reliasoft and Minitab, employ ML methods as the standard procedures in analyzing ALT data. In this section, I briefly review the ML methods in ALT data analysis. Important results can be found in Nelson (1982, 1990), Meeker and Escobar (1998), Pascual et al. (2006), Balakrishnan and Xie (2007a, 2007b).

The log-likelihood function corresponding the observed failure data Y is

$$l(\boldsymbol{\varphi};Y)=\sum_{i=1}^{k}\sum_{j=1}^{n_i}\left\{\kappa_{ij}\log\left(\frac{1}{\sigma}\phi\left(z_{ij}\right)\right)-\left(1-\kappa_{ij}\right)\exp\left(\zeta_i\right)\right\} \tag{2.4}$$

where the subscript "$_{ij}$" denote the *jth* failure at stress s_i; $\zeta_i=\left(\log\left(c_i\right)-\mu_i\right)\big/\sigma$ is the standardized censoring time; $z_{ij}=\left(\log\left(t_{ij}\right)-\mu_i\right)\big/\sigma=\left(y_{ij}-\mu_i\right)\big/\sigma$ is the standardized

failure time; and the index κ_{ij} =1when $z_{ij} < \zeta_i$ and κ_{ij} =0 otherwise;

The Maximum Likelihood Estimate (MLE) $\hat{\boldsymbol{\varphi}}$ is the value that maximizes the equation (2.4), that is, the efficient score equals zero at $\hat{\boldsymbol{\varphi}}$

$$U_{\cdot}(\boldsymbol{\varphi})\Big|_{\boldsymbol{\varphi}=\hat{\boldsymbol{\varphi}}} = \frac{\partial l(\boldsymbol{\varphi};Y)}{\partial \boldsymbol{\varphi}}\Bigg|_{\boldsymbol{\varphi}=\hat{\boldsymbol{\varphi}}} = 0 \tag{2.5}$$

Particularly, $\hat{\boldsymbol{\varphi}}$ is asymptotically normally distributed with its variance-covariance matrix given by

$$\hat{\boldsymbol{\Sigma}}_{\boldsymbol{\varphi}} = \left[-\hat{\mathbf{I}}_{\boldsymbol{\varphi}}\right]\Big|_{\boldsymbol{\varphi}=\hat{\boldsymbol{\varphi}}} = \begin{bmatrix} \widehat{\mathrm{var}}(\hat{\beta}_0) & \widehat{\mathrm{cov}}(\hat{\beta}_0,\hat{\beta}_1) & \widehat{\mathrm{cov}}(\hat{\beta}_0,\hat{\sigma}) \\ & \widehat{\mathrm{var}}(\hat{\beta}_0) & \widehat{\mathrm{cov}}(\hat{\beta}_1,\hat{\sigma}) \\ & & \widehat{\mathrm{var}}(\hat{\sigma}) \end{bmatrix}, \tag{2.6}$$

where $\hat{\mathbf{I}}_{\boldsymbol{\varphi}} = \dfrac{\partial^2 l(\boldsymbol{\varphi};Y)}{\partial \boldsymbol{\varphi}^2}\Bigg|_{\boldsymbol{\varphi}=\hat{\boldsymbol{\varphi}}}$ is the information observed at $\boldsymbol{\varphi} = \hat{\boldsymbol{\varphi}}$.

2.4.1.1 Illustration of MLE: Temperature-ALT on Device-A

An illustration of the application of MLE is given below using the dataset presented in Appendix. In this test, engineers analyzed the temperature-accelerated life test data on a particular device. Three temperature levels are involved in the test. At each level, the failure data are modeled by Weibull distribution $F(t) = \Phi\left(\left(\log(t) - \mu\right)/\sigma\right)$. A linear stress-life relationship $\mu_i = \beta_0 + \beta_1 s_i$ is assumed with s_i equals the inverse of the temperature (in Kelvin). The scale parameter σ is a constant, independent of temperature.

Applying the ML methods to the device-A data, we have the maximum likelihood estimate $\hat{\boldsymbol{\varphi}}$ of $\boldsymbol{\varphi} = (\beta_0, \beta_1, \sigma)$ by maximizing the equation (2.7). Numerical methods are often needed at this step.

$$l(\boldsymbol{\varphi};Y)=\sum_{i=1}^{3}\sum_{j=1}^{n_i}\left\{\kappa_{ij}\log\left(\frac{1}{\sigma}\phi_{SEV}\left(z_{ij}\right)\right)-\left(1-\kappa_{ij}\right)\exp\left(\zeta_i\right)\right\} \tag{2.7}$$

Based on the large-sample theory, the variance-covariance matrix of $\hat{\boldsymbol{\varphi}}$ is computed using the following equation (2.8), see Nelson and Meeker (1978)

$$\hat{\boldsymbol{\Sigma}}_{\boldsymbol{\varphi}}=\left[-\hat{\mathbf{I}}_{\boldsymbol{\varphi}}\right]^{-1}\Big|_{\boldsymbol{\varphi}=\hat{\boldsymbol{\varphi}}}=\left[-\sum_{i}^{k}\sum_{j}^{n_i}\hat{\mathbf{i}}_{\boldsymbol{\varphi}}^{ij}\right]^{-1}\Bigg|_{\boldsymbol{\varphi}=\hat{\boldsymbol{\varphi}}} \tag{2.8}$$

In equation (2.8), $\hat{\mathbf{i}}_{\boldsymbol{\varphi}}^{ij}$ is the observed Fisher information contributed by the *jth* failure at stress level i

$$\hat{\mathbf{i}}_{\boldsymbol{\varphi}}^{ij}=\begin{bmatrix}A_{00}\left(z_{ij},\zeta_i\right) & A_{01}\left(z_{ij},\zeta_i\right) & B_0\left(z_{ij},\zeta_i\right)\\ A_{01}\left(z_{ij},\zeta_i\right) & A_{11}\left(z_{ij},\zeta_i\right) & B_1\left(z_{ij},\zeta_i\right)\\ B_0\left(z_{ij},\zeta_i\right) & B_1\left(z_{ij},\zeta_i\right) & C\left(z_{ij},\zeta_i\right)\end{bmatrix}\Bigg|_{\boldsymbol{\varphi}=\hat{\boldsymbol{\varphi}}}$$

where

$$A_{ab}=\frac{\partial^2 l}{\partial\beta_a\partial\beta_b}=\left(\frac{-g_a g_b}{\sigma^2}\right)\left[\kappa_{ij}e^{z_{ij}}+\left(1-\kappa_{ij}\right)e^{\zeta_i}\right],\quad g_0=x_0, g_1=x_k,\quad a,b=0,1$$

$$B_a=\frac{\partial^2 l}{\partial\beta_a\partial\sigma}=\left(\frac{-g_a}{\sigma^2}\right)\left\{-x_a\left[\kappa_{ij}\left(e^{z_{ij}}-1\right)+\left(1-\kappa_{ij}\right)e^{\zeta_i}\right]+\kappa_{ij}z_{ij}e^{z_{ij}}+\left(1-\kappa_{ij}\right)\zeta_i e^{\zeta_i}\right\},\quad a=0,1$$

$$C=\frac{\partial^2 l}{\partial\sigma^2}=\left(\frac{-1}{\sigma^2}\right)\left\{-2\left[\kappa_{ij}\left(z_{ij}e^{z_{ij}}-z_{ij}-1\right)+\left(1-\kappa_{ij}\right)\zeta_i e^{\zeta_i}\right]+\kappa_{ij}\left(1+z_{ij}^{\,2}e^{z_{ij}}\right)+\left(1-\kappa_{ij}\right)\zeta_i^{\,2}e^{\zeta_i}\right\} \tag{2.9}$$

Table 2.4 and 2.5 below present the analysis outputs generated by MINITAB. In Table 2.4, both the MLE $\hat{\boldsymbol{\varphi}}$ and its 95% confidence interval are presented. Very often, these results are visualized by Figure 2.5, which is known as the relation plot in MINITAB. On this plot, both failure times at each stress level and the estimated stress-life model (for 10% percentile, $y_{.1}$) are plotted.

Table 2.4 Regression table

Predictor	Standard		Z	P	95.0% Normal CI	
	Coef.	Error			Lower	Upper
β_0	7.5155	0.1853	40.57	0.000	7.1524	7.8786
β_1	5.1218	0.7889	6.49	0.000	3.5755	6.6680
σ	0.7085	0.1033			0.5323	0.9429

Log-Likelihood -77.279

Table 2.5 Table of percentile

Percent	Stress		Percentile	Standard Error	95.0% Normal CI	
	Temp.	Standard			Lower	Upper
10	283K	1	11.0429	0.5323	9.9994	12.0863

The result in Table 2.5 can be visualized using another plot. Figure 2.6 presents the smallest extreme value multiple probability plot for each stress level (including the design level) based on the fitted model. The estimated percentile $\hat{y}_{.1}(1)$ at the use level as well as its confidence interval can now be immediately read from this plot.

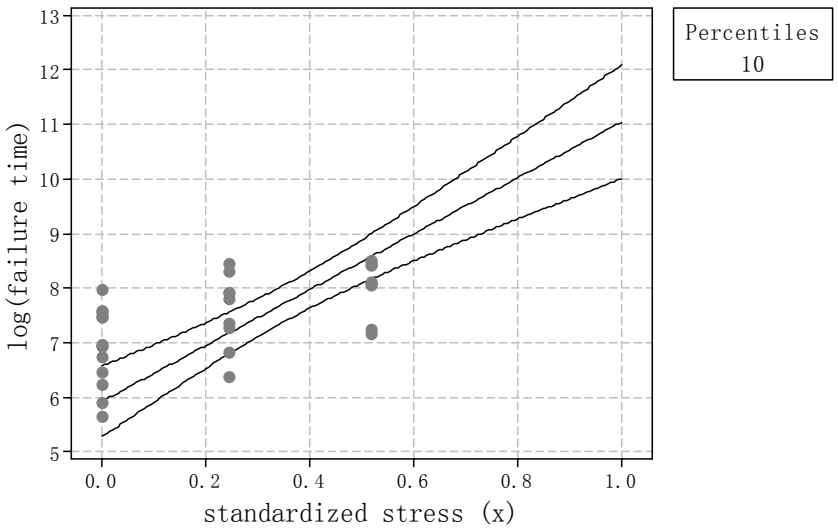

Figure 2.5 Relation plot for log (failure time), Y

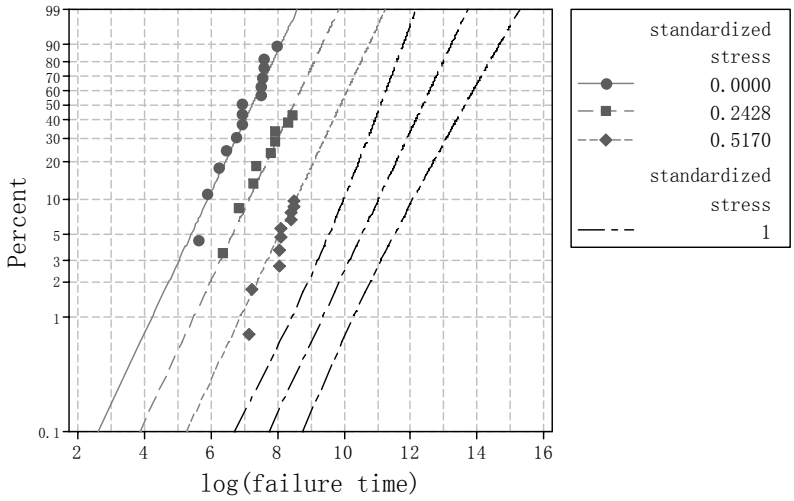

Figure 2.6 Smallest extreme value multiple probability plot for log (failure time), *Y*

2.4.1.2 Checking Model Assumptions

An important part of ALT analysis is checking for departures from model assumptions. In fact, this is a critical step for any parametric method before drawing conclusions from the data. Meeker and Escobar (1998) suggested 4 commonly used regression model diagnostics, including 1) plot of standardized residuals versus fitted values; 2) probability plot of standardized residuals; 3) other residual plots; and 4) Sensitivity analysis. Chatterjee and Price (1991) and Birkes and Dodge (1993) also provided elegant discussions on the detection/correction of regression model violations.

However, all the diagnostics above suffer from one common difficulty in checking the validity of ALT model assumptions. In a typical ALT dataset, failure data at each stress level are usually censored to the right. Heavily censoring is also not uncommon at lower stress levels. This feature makes the above methods 1) ~ 3) very difficult to interpret, particularly the plot of standardized residuals versus fitted values. Hence, this

dissertation only highlights 2 most effective techniques: the multiple-probability plot of ML estimates with a fitted acceleration relationship, and the sensitivity analysis.

Figure 2.6 is the multiple smallest extreme value probability plot of ML estimates with a fitted acceleration relationship. In this figure, the *cdf* estimated from the fitted model are plotted on a smallest extreme value probability plot. Since the deviation of each data point from linearity at each stress level is not strong, thus the assumed Weibull-Arrhenius ALT model with constant σ is adequate to model the Device-A data.

Instead of answering the question whether the model assumptions are valid, which can be very difficult for heavily censored data, sensitivity analysis examines the consequence of potential assumption violations by assessing the degree to which estimates depend on model assumptions. In practice, ALT data analysis is not just a pure statistical problem. It involves multiple decisions considering multiple (conflicting) objectives. Hence, knowing the consequence of possible assumption violations is essential for decision makings when those residual/probability plots fail to effectively validate the model. In Chapter 3 and 4, sensitivity analysis is widely used to detect the effect of uncertain inputs on both statistical precision and accuracy.

2.4.1.3 Drawback of ML Methods

A drawback of ML theory is that the approximate variances and confidence limits for estimators are accurate only for tests with enough failures. Recall equation (2.6), the ML estimate $\hat{\boldsymbol{\varphi}}$ is asymptotically normally distributed with variance $\hat{\boldsymbol{\Sigma}}_{\varphi}$. Hence, when the number of failures is small, the normal approximation becomes inadequate. This is

one of the reasons that strongly motivates various Bayesian inference methods described below.

2.5.2. Preliminaries on Bayesian Analysis in Reliability

When the number of failures is small, which is typically the case in practice, asymptotic approximations could be grossly inaccurate. When this happens, it is better to consider Bayesian approach particularly when prior empirical information is available. However, before reviewing the Bayesian methods for ALT data analysis, we shall first introduce some preliminaries of Bayesian analysis in reliability engineering.

2.5.2.1 Bayes' Law

The Bayes' Law, a straightforward mathematical result, is one of the fundamental rules of mathematical probability theory. It is concerned with reversing the order of the statements in a conditional probability.

Let A and B denote two events, $\mathcal{H}$ denote the background information, then, the Bayes' Law has the following three equivalent forms

$$P(B|A;\mathcal{H}) = \frac{P(A|B;\mathcal{H})P(B;\mathcal{H})}{P(A;\mathcal{H})} \quad ; \tag{2.10a}$$

or

$$P(B|A;\mathcal{H}) = \frac{P(A|B;\mathcal{H})P(B;\mathcal{H})}{\sum P(A|B;\mathcal{H})P(B;\mathcal{H})} \quad ; \tag{2.10b}$$

or

$$P(B|A;\mathcal{H}) \propto P(A|B;\mathcal{H})P(B;\mathcal{H}) \quad ; \tag{2.10c}$$

It is interesting to note that Thomas Bayes (1702-1761) might not be the person who derived this law that bears his name; it could be a Cambridge mathematician Saunderson (Singpurwalla 2006). In addition, the great French mathematician Laplace (1749-1827) also set out a mathematical system of inductive reasoning based on probability, which we would today recognize as a huge contribution to Bayes' Law.

2.5.2.2 The Bayes Paradigm in Reliability Engineering

The Bayesian paradigm for statistical inference is a probabilistic view of the world that all uncertainty should only be described by probability and its calculus, and that probability is personal or subjective (Singpurwalla 2006).

To understand the Bayesian paradigm from a reliability engineering point of view, let A in equation (2.10) represent the data, and B represent explanations about the probability mechanism generating the data, we then have

$$\begin{aligned} f(\theta|X;\mathcal{H}) &= \frac{f(X|\theta;\mathcal{H})\cdot f(\theta;\mathcal{H})}{f(X;\mathcal{H})} \\ &= \frac{f(X|\theta;\mathcal{H})\cdot f(\theta;\mathcal{H})}{\sum f(X|\theta;\mathcal{H})\cdot f(\theta;\mathcal{H})} \\ &\propto f(X|\theta;\mathcal{H})\cdot f(\theta;\mathcal{H}) \end{aligned} \tag{2.11}$$

Here, the term $f(X|\theta;\mathcal{H})$ is known as the probability model for data X with parameter θ. For example, let X be the failure data of a product obtained from a life test, then, $f(X|\theta;\mathcal{H})$ can be a probability distribution, say, the Weibull distribution, that quantifies the uncertainty of X. In addition, we also note that in this example, $f(X|\theta;\mathcal{H})$ is exactly the likelihood function corresponding to the observed data X of the density $f(X|\theta;\mathcal{H})$.

The term $f(\theta;\mathcal{H})$ is the prior distribution for parameter θ that quantifies the uncertainty of the unknown parameter θ. Usually, the prior distribution is specified subjectively (see Berger (1985)), and this subjectivity has been the center of debate. It is certainly true that the use of Bayesian methods in reliability engineering might sometimes risk the objectivity of the analysis, but as we shall see in this thesis, subjective judgment or empirical knowledge can also be valuable for reliability analysis and experiment planning, provided that we have a proper way to utilize them. For ALT problems that will be discusses in this thesis, the Bayesian methods are particularly important when sample sizes or the number of failures insufficient. Section 2.5.4 provides a more detailed discussion on the debate of using Bayesian methods in reliability engineering.

2.5.2.4 Illustrative Example: Bayesian Analysis for Repairable Systems

A simple numerical example is presented in this section to illustrate the use of Bayesian approaches in analyzing real-life reliability data. Consider a scenario in facilities management industry in which the total number of failures is large due to a large pool of similar repairable systems but the number of failures for a single system is very small due to relative short observation intervals (compare to lifetime of the system). This situation arises when systematic recording failure data is newly instituted, and its initial results and benefits need to be presented. Table 2.6 presents a set of heavily interval-censored data from a fleet of repairable systems obtained in an observation period T. It can be seen that only about 10% of the 1616 systems

experienced one or more failures (repairs) during the observation period.

In what follows, we shall employ and compare three Bayesian approaches in analyzing the data presented in Table 2.6, namely, the naïve Bayesian approach, the Bayesian estimation based on single system, and the Bayesian analysis based on the Dirichlet-Multinomial model.

Table 2.6 Summary of failure data from a large fleet of repairable systems

Age Group (year)	Total No. of systems	No. of systems with 0 failure	No. of systems with 1 failure	No. of systems with 2 failures	No. of systems with 3 failures	No. of systems with more than 3 failures
9 ~ 12	232	215	15	1	1	0
12 ~ 15	206	179	18	3	2	4
15 ~ 17	240	209	28	2	0	1
17 ~ 18	175	154	17	4	0	0
18 ~ 19	202	184	17	1	0	0
19 ~ 20	390	360	17	5	4	4
20 ~ 21	171	159	8	1	3	0
Total	1616	1460	120	17	10	9

- Naïve Bayesian Approach.

We firstly assume that the failure process of a single system i follow a homogeneous Poisson process (HPP) with intensity λ_i, i.e.

$$f(n_i|\lambda_i) = \frac{(\lambda_i T)^{n_i}}{n_i!} \cdot \exp(-\lambda_i T)$$

where n_i is the number of failures of system i during the observation period T.

Conventionally, if all N systems are similar, not necessarily to be identical, it is possible to further assume that these λ_i are drawn from a certain prior distribution, say,

a Gamma distribution $p(\lambda_i)$

$$p(\lambda_i) = \frac{\beta^{\alpha}}{\Gamma(\alpha)} \cdot \lambda_i^{\alpha-1} \cdot \exp(-\lambda_i \beta)$$

Then, the posterior distribution of λ_i is easily found using the Bayes' Rule

$$p(\lambda_i | n_i, T) = \frac{(\beta+T)^{\alpha+n_i}}{\Gamma(\alpha+n_i)} \cdot \lambda_i^{\alpha+n_i-1} \cdot \exp(-\lambda_i(\beta+T))$$

Here, since Gamma distribution is the conjugate distribution of Poisson distribution, the posterior $p(\lambda_i | n_i, T)$ is still a Gamma distribution with parameters $(\alpha+n_i, \beta+T)$. Next, as suggested by Frohner (1985a, 1985b), a simple mixture of $p(\lambda_i | n_i, T)$ is used to obtain the posterior distribution of λ

$$p(\lambda) = \frac{1}{N}\sum_{i=1}^{N} p(\lambda_i | n_i, T)$$

Figure 2.7 shows the obtained distribution $p(\lambda)$ and the prior distribution $p(\lambda_i)$. Particularly, the hyper-parameters α and β are chosen as

$$\alpha = \frac{\hat{\mu}^2}{\hat{\sigma}^2} \quad \beta = \frac{\hat{\mu}}{\hat{\sigma}^2}$$

where $\hat{\mu} = \frac{1}{N \cdot T}\sum_i^N n_i, \hat{\sigma}^2 = \frac{1}{N-1}\sum_i^N (n_i - \hat{\mu})^2$.

One of the advantages of this naïve Bayesian approach is that it allows a certain level of heterogeneity among systems. However, such a method is termed as the naïve approach since the mixed distribution $p(\lambda)$ neither converges to the true distribution nor to any particular distribution (Fisher 1990). Moreover, as can be seen in Figure 2.7, the probability density approaches infinite as the failure intensity approaches zero. Apparently, this is logically incorrect.

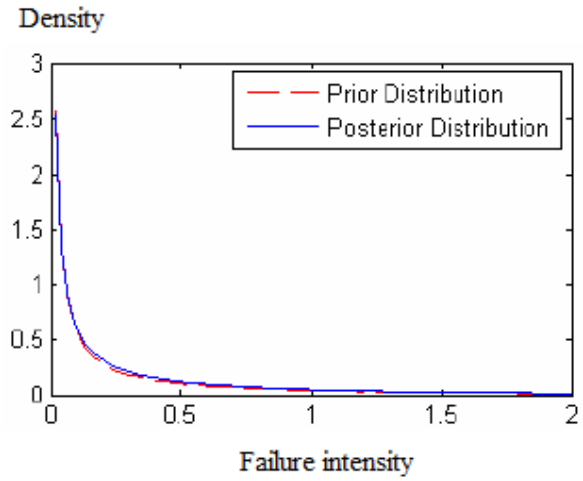

Figure 2.7 Posterior density $p(\lambda)$ and the prior distribution $p(\lambda_i)$

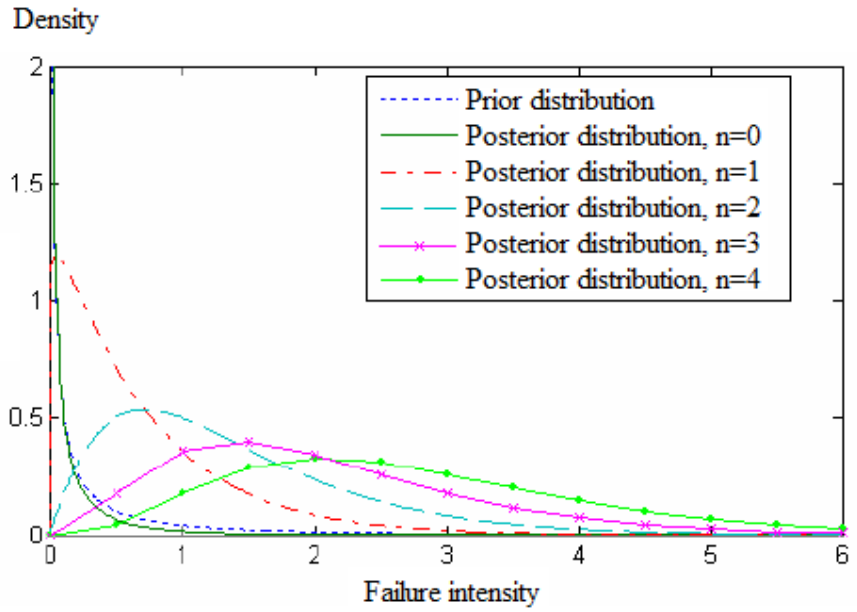

Figure 2.8 Plot of posterior distributions for different n_i

- Bayesian Estimation Based on Single System

Instead of mixing the posterior distribution of λ_i, one may simply focuses on individual system and uses the prior information elicited from the entire system population. Again, we assume HPP failure process, and employ the conjugate Gamma

prior distribution. Figure 2.8 plots the posterior distributions of λ_i for different number of failures n_i observed in T.

Then, the Bayesian prediction distribution of the number of failures $\tilde{n}_i$ for system i within a given future time interval T' is (Rigdon and Basu, 2000)

$$p(\tilde{n}_i) \propto \frac{\beta^{\alpha} \cdot T'^{n_i} \cdot \Gamma(\alpha + n_i + \tilde{n}_i)}{\tilde{n}_i ! \cdot \Gamma(\alpha) \cdot (\beta + T + T')^{\alpha + n_i + \tilde{n}}}$$

The plot of $p(\tilde{n}_i)$ given different n_i is shown in Figure 2.9.

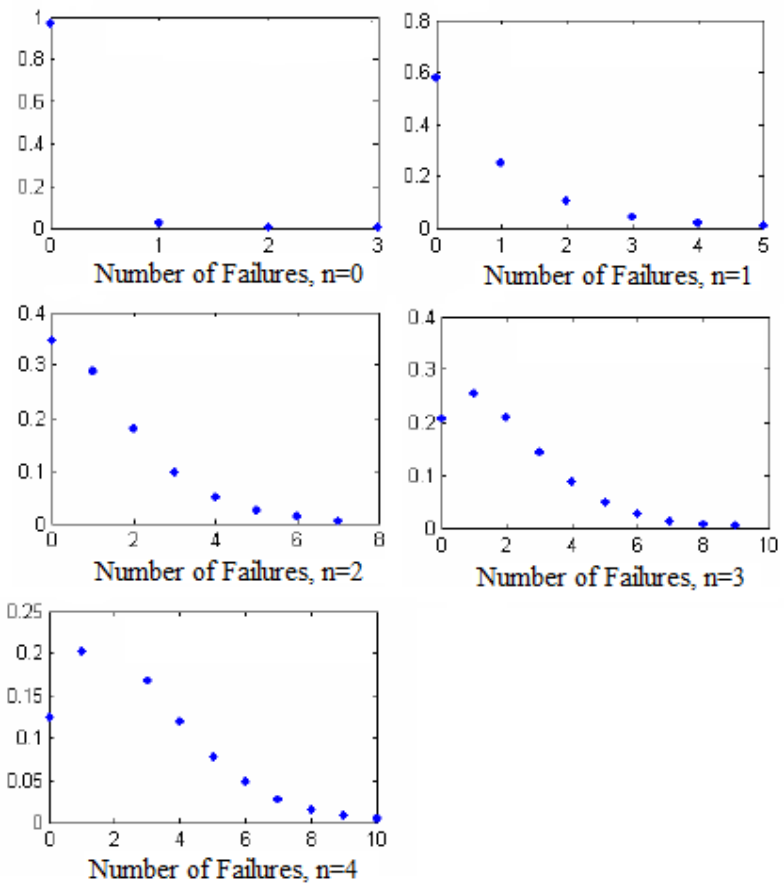

Figure 2.9 Plot of $p(\tilde{n}_i)$ for different n_i

In predicting the number of failures of a repairable system, the uncertainty in the estimation for λ_i should be combined with the variability in the distribution $p(\tilde{n}_i)$. In

the classical paradigm, it is difficult to combine these two sources of uncertainty. In the Bayesian paradigm, however, such an analysis is straightforward.

- Bayesian Estimation Based on Dirichlet-Multinomial Model

Methods presented above all focus on the estimation of intensity and adopts the assumption of HPP. In practice, however, the intensity is neither known nor observable, and the assumption of HPP is might be a controversial one as the intensity of a system usually changes as time.

Instead of focusing on the intensity, one might employ a Dirichlet-Multinomial model and directly focus on the number of failures of a single system in the short time interval T. Given a fleet of systems N, define a vector $K = (k_0, k_1, k_2, k_3, k_{3+})$ with its element k_j denoting the number of systems that experienced *j* failures during the time T. Clearly, k_j follows a Multinomial distribution with parameter $Q = (q_0, q_1, q_2, q_3, q_{3+})$

$$P(K) = \frac{\sum_{i=1}^{5} k_i!}{\prod_{i=1}^{5} k_i!} \prod_{i=1}^{5} q_i^{k_i} \quad 0 \le q_i \le 1, \sum_{i}^{5} q_{i=1} = 1$$

Then, as a conjugate distribution of Multinomial distribution, Dirichlet distribution is naturally chosen as the prior distribution for parameter Q. Then, we have

$$P(Q) = \frac{\Gamma(\sum_{i=1}^{5} u_i)}{\prod_{i=1}^{5} u_i} \prod_{i=1}^{5} q_i^{u_i - 1}$$

where $u_i > 0$ are constants specifying the Dirichlet distribution. Here, since we do not have any information on the failure history, a non-informative prior distribution is used by letting $u_j \to 0$. Given the observation $K = (k_0, k_1, k_2, k_3, k_{3+})$, the posterior distribution of $Q = (q_0, q_1, q_2, q_3, q_{3+})$ is still a Dirichlet distribution with parameter $(u_0 + k_0, u_1 + k_1, u_2 + k_2, u_3 + k_3, u_{3+} + k_{3+})$. Then, we have

$$\hat{q}_i = E(q_i) = \frac{u_i + k_i}{\sum_i^5 (u_i + k_i)}$$

with its variance given by,

$$\text{var}(\hat{q}_i) = \frac{(u_i + k_i)((\sum_i^5 (u_i + k_i)) - (u_i + k_i))}{(\sum_i^5 (u_i + k_i))^2 (1 + \sum_i^5 (u_i + k_i))}$$

Figure 2.10 shows the interval estimation with 95% confidence of the number of systems that experience i failures in the future time interval $T' = T$ for $i = 0,1,2,3,3+$. It is seen that, the length of the estimated interval becomes wider as the number of failures becomes bigger. This is because fewer data are collected for systems experiencing more failures.

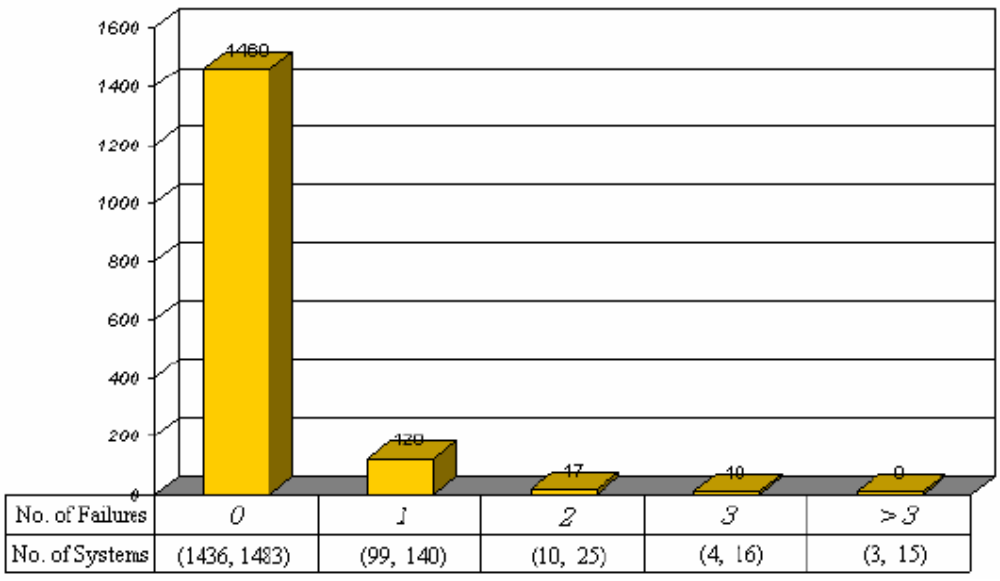

Figure 2.10 Estimated numbers of systems experiencing i failures for $i = 0,1,2,3,3+$

As seen above, the Bayesian approach based on the Dirichlet-Multinomial model directly focuses on the number of failures, thus circumvent the difficulty of handing the failure intensity. However, one apparent drawback of such an approach is that the

prediction interval must have the same length as that of the observation interval.

2.5.3. Bayesian Methods for ALT Data Analysis

As we have seen above, unlike ML methods, which can be viewed as an automatic procedure, Bayesian methods do not have a uniform or consistent form. Each method has its unique features. This difference usually arises in how the model is constructed or how the prior information is introduced into the analysis.

Some early studies of Bayesian methods for ALT data analysis were presented by De Groot and Goel (1988), Barlow et al. (1988), Mazzuchi and Singpurwalla (1988), etc. A survey of these early studies can be found in Viertl (1988). Meinhold and Singpurwalla (1983, 1987) and Singpurwalla (2006) presented a very interesting exploration of the application of the Kalman filter in ALT data analysis. In their work, the Kalman filter, which is popularly used by control engineers, is interpreted using a Bayesian formulation. Some new results (after 1990) of Bayesian methods for ALT data analysis were presented in Achcar and Louzada-Neto (1992), Van Dorp et al. (1996), Van Dorp and Mazzuchi (2004, 2005), Tojeiro et al. (2004). In what follows, I briefly discuss several typical Bayesian methods for analyzing ALT data. Some ideas will be borrowed and re-visited in Chapter 3, 4 and 5.

Barlow et al. (1988) presented an elegant Bayesian analysis of the stress-rupture life of Kevlar/epoxy spherical pressure vessels. This is one of the pioneering studies of Bayesian methods in ALT data analysis, and provides several wonderful ideas for the inference and planning methods presented in Chapter 3, 4 and 5. In their work, failure

time T at each stress level i is assumed to follow Weibull distribution with scale parameter α_i and shape parameter β_i . Therefore, given a constant prior distribution $\vartheta(\alpha_i, \beta_i)$, the posterior distribution $\pi(\alpha_i, \beta_i)$ at that stress level is given by

$$\pi(\alpha_i, \beta_i) \propto L(\alpha_i, \beta_i; T) \cdot \vartheta(\alpha_i, \beta_i) \tag{2.10}$$

where $L(\alpha_i, \beta_i; T)$ is the likelihood function of (α_i, β_i) given data T . Then, the prior density on (α, β) at use condition can be extrapolated from the derived posterior distributions $\pi(\alpha_i, \beta_i)$ at each accelerated stress level.

This work is without any doubt a successful exploration of Bayesian methods in ALT data analysis, however, for heavily censored data, the flat or diffuse prior density is an especially poor choice. From this perspective of view, the practical impact of this type of Bayesian analysis is very much limited despite of its theoretical achievements. In fact, it does not significantly over-perform ML method when a well constructed parametric ALT model is available. Of course, the use of non-informative prior distributions to a great extent avoids the potential risk of violating data objective by incorporating some subjective or empirical engineering knowledge.

In fact, based on the ALT model given in Section 2.3, the posterior distribution $\pi(\boldsymbol{\varphi})$ can be directly derived from the prior distribution $\vartheta(\boldsymbol{\varphi})$ as shown in equation (2.11). Zhang and Meeker (2006) actually employed this idea and proposed a Bayesian method for ALT planning

$$\pi(\boldsymbol{\varphi}) \propto L_Y(\boldsymbol{\varphi}; Y) \cdot \vartheta(\boldsymbol{\varphi}) \tag{2.11}$$

Instead of maximizing $L_Y(\boldsymbol{\varphi}; Y)$ as ML method does, the posterior distribution is maximized to yield the Bayesian estimate $\hat{\boldsymbol{\varphi}}$. Based on the large sample theory, $\hat{\boldsymbol{\varphi}}$ is

normally distributed with mean $\hat{\boldsymbol{\varphi}}$ and variance matrix $\hat{\boldsymbol{\Sigma}}_{\boldsymbol{\varphi}}$ (Berger 1985)

$$\hat{\boldsymbol{\Sigma}}_{\boldsymbol{\varphi}} = \left[-\left(\hat{\mathbf{I}}_{\boldsymbol{\varphi}} + \mathbf{I}^{\vartheta} \right) \right]^{-1} \Big|_{\boldsymbol{\varphi}=\hat{\boldsymbol{\varphi}}} \tag{2.12}$$

where $\hat{\mathbf{I}}_{\boldsymbol{\varphi}}$ is still the Fisher information observed at $\hat{\boldsymbol{\varphi}}$, whereas $\mathbf{I}^{\vartheta}$ is the information contained in the prior distribution $\vartheta(\boldsymbol{\varphi})$.

From equation (2.12), the advantage as well as the essence of Bayesian method is immediately seen. By combining the information obtained from the data and certain empirical knowledge, a more precise estimate $\hat{\boldsymbol{\varphi}}$ can be obtained. When the number of failure is large, the information $\mathbf{I}^{\vartheta}$ contained in the prior distribution is overshadowed by the information $\hat{\mathbf{I}}_{\boldsymbol{\varphi}}$ obtained from the data (i.e. $\det(\mathbf{I}^{\vartheta}) < \det(\hat{\mathbf{I}}_{\boldsymbol{\varphi}})$), hence, the result obtained from equation (2.12) depends more on objective data. On the other hand, when the information $\hat{\mathbf{I}}_{\boldsymbol{\varphi}}$ obtained from data is vague, the prior knowledge then plays a dominant role in data analysis. Hence, when the prior knowledge is not reliable, the Bayesian method might violate the objectivity of the analysis. This is the most controversial part of Bayesian theory and greatly limits the application of this method.

2.5.4. Comments on Fisherian and Bayesian Inference for ALT Data

There has been a long-running debate between Fisherian (Frequentist) and Bayesian inference. Anyone who have read Efron (1986) and those discussions attached to that paper must be able to feel the heat of such debate. Luckily, this debate should not exist in ALT data analysis. Careful engineers will not apply his/her procedures mechanically, be them Fisherian or Bayesian. All they need are cautions when they quantify their

valuable empirical knowledge. When the prior information is vague, they may immediately drop it when presented with sharper information from tests. On the other hand, if certain reliable information, say, the range of the activation energy, on products reliability is available, Bayesian approach is the only best available way so far to employ this valuable information that is accumulated from years practice.

Sir Ronald Aylmer Fisher
1890 ~ 1962

Thomas Bayes
1702 ~ 1761

As discussed in the first section of this dissertation, the key question in ALT is how to balance the gathering and analyzing of information against the timeliness of the decision being made. Engineers usually have multiple conflicting objectives in conducting an experiment. Both cost and time-to-market considerations prohibit long test duration and large sample size. Hence, the ultimate purpose of an ALT is sometimes not to “seize the high ground of scientific objectivity (Efron, 1986)”. This further encourages the use of Bayesian methods in ALT analysis. Just like the great Euclid set 5 Axiom in “The thirteen books of the Elements” as the basic rules 2000 years ago, why don’t we also set some ground rules for ALT data analysis in order to make the results logically sound? Say, the reliability

of the upgraded version is not worse than the original product; or, the MTTF of such product is between some interval; or, the activation energy of consumer electronics is typically within the interval [0.5, 1.5], and etc.

Lindley (1975) has foreseen a Bayesian 21st century. Using engineering knowledge in ALT data analysis may yield inaccurate results from time to time, but in recent decades, advancement in information technology has greatly facilitated the documentation and sharing of past engineering knowledge. It is thus timely for us to explore enabling statistical techniques that conveniently incorporate empirical engineering knowledge while keeping the risk of violating the data objectivity in check. But two issues are of paramount importance for Bayesian methods, 1) the way to quantify prior information; and 2) the robustness of the method to prior information. We therefore address these two problems in this study.

2.6. Planning Methods for Accelerated Life Testing

The first ALT plan was derived by Chernoff (1962) based on Exponential failure times. This section reviews important ALT planning approaches in the literature.

2.6.1. Planning Based on Maximum Likelihood (ML) Theory

To plan a constant-stress ALT, one needs to choose 1) the stress level combinations while fixing the highest stress level, and 2) the number of test units allocated to each stress level. The pioneering ideas of modern ALT plans based on ML theory were conceived by Nelson and Kielpinski (1976), Nelson and Meeker (1978), Meeker

(1984), and Nelson (1990). Nelson and Kielpinski (1976) and Nelson and Meeker (1978) presented the ML theory for large sample statistically optimum constant-stress ALT plans with two stress levels. Meeker (1984) and Meeker and Hahn (1985) extended the above results and presented good compromise plans with more than two stress levels. They proposed a 4:2:1 allocation ratio for low, middle and high stress levels for constant-stress ALT plans and gave the optimum low stress level by assuming that the middle stress is the average of the high and low stress levels. The 4:2:1 plan was then extended under other test constraints by Yang (1994) and Yang and Jin (1994). Tang et al. (2002) proposed two approaches that optimize both low and middle stress and their respective allocations for three-stress compromise constant-stress ALT plans. Meeter and Meeker (1994) presented the plan that considered non-constant log time-to-failure scale parameter. Compared to the statistically optimum constant-stress ALT plan with two stress levels, compromise plans improve the robustness to misspecification of unknown inputs by sacrificing some statistical efficiency. In practice, the obtained optimum plan is usually evaluated by simulation techniques (Meeker et al. 2005).

Given the prior information or pre-specified values of ALT model parameters, an optimum plan is typically the one that minimizes the asymptotic variance of the MLE of certain reliability measure at use condition (known as *c*-optimal). Other planning criteria have also been used. Meeker and Escobar (1995) minimized the determinant of the covariance matrix for the model parameters. Tang and Xu (2005) proposed a framework which considers multiple (conflicting) objectives in ALT planning.

Step-stress ALT plans can be found in Alhadeed and Yang (2002), Tang (2003, 2005), etc. For ALT plans with other type of stress loadings, one may refer to the comprehensive review given by Nelson (2005).

2.6.2. Robustness of ALT Plans and Bayesian Planning Methods

Bayesian planning enhances the robustness of ALT plans to mis-specification of ALT model as well as model parameters.

When the most commonly used *c*-optimal criterion is adopted, the asymptotic variance of the MLE is the key quantity used in determining the optimum plan. This quantity depends on the "planning information" which consists of empirical knowledge or guessed values of the unknown life time distribution and the stress-life model. Since these models as well as their parameters are never known exactly, assuming they are known at the planning stage might lead to a false sense of statistical precision. In fact, one pitfall of ALT is to fail to recognize that although statistical confidence limits account for estimator variability, they do not account for model uncertainty. Hence, much effort has been made to enhance the robustness of an ALT plan using Bayesian planning methods.

Early results in this area were given by De Groot and Goel (1979, 1988). Zhang and Meeker (2006) recently presented a general Bayesian planning framework where the optimum plan $\boldsymbol{\xi}$ minimizes the pre-posterior expectation of the posterior variance over the marginal distribution of all possible unobserved failure data $\mathbf{t}$

$$C(\boldsymbol{\xi}) = E_{\mathbf{t}|\boldsymbol{\xi}}\left[\text{var}_{\boldsymbol{\varphi}|\mathbf{t},\boldsymbol{\xi}}\left(\text{reliability measure of interest}\right)\right] \tag{2.13}$$

This work closely follows the classical framework of the constant-stress ALT planning (see Nelson and Kielpinski 1976, Nelson and Meeker 1978). However, instead of specifying exact values for those unknown model parameters, prior distributions are assigned to each parameter $\boldsymbol{\varphi} = [\beta_0, \beta_1, \sigma]$ to increase the robustness of the plan.

Chaloner and Larntz (1992) not only used prior distribution for unknown model parameters, but also assigned weights to different failure-time distribution and the optimum plan can therefore be viewed as a result of model-averaging. The optimum plan $\boldsymbol{\xi}$ is found by minimizing

$$C(\boldsymbol{\xi}) = \sum_{i=1}^{2} \lambda_i E\left(\pi_1 E_l + \pi_1 E_q\right)$$

where

λ : weight given to Weibull and Lognormal distributions (2.14)

π : weight given to linear or quadratic stress-life models

E_l: expection over the unknown parameters assuming linear model

E_l: expection over the unknown parameters assuming quadratic model

Verdinelli at el. (1993) and Singpurwalla (2006) proposed an interesting Bayesian planning method by maximizing the (Shannon) mutual information. The optimum plan $\boldsymbol{\xi}$ is found by maximizing

$$C(\boldsymbol{\xi}) = E_{\mathbf{t}|\boldsymbol{\xi}} E_{t_u|\mathbf{t},\boldsymbol{\xi}} \left[\log \frac{p(t_u|\mathbf{t},\boldsymbol{\xi})}{p(t_u)} \right]$$

where (2.15)

$\mathbf{t}$: the observed value

t_u: the predicted value for time u

Compare equation (2.13) and (2.15), the similarity is immediately seen. In equation (2.13), the optimum plan D maximizes the expected Fisher information

on $\boldsymbol{\varphi}$ given the unobserved data $\mathbf{t}$, while in equation (2.15), the optimum plan D maximizes the mutual information between the predicted value t_u and $\mathbf{t}$. In fact, predicting t_u is equivalent to estimating the model parameter $\boldsymbol{\varphi}$. Hence, the Zhang and Meeker's Bayesian criterion is very much closely or similar to that of Verdinelli and Singpurwalla's. An elementary but elegant introduction to information-theoretic theory can be found in Haykin (1999, Chapter 10). Pascual and Montepiedra (2003a, 2003b) and Pascual (2006) thoroughly discussed the robustness of an ALT plan and proposed planning approach robust to misspecification of ALT models. In Table 2.7, studies on the robustness in ALT plans are summarized.

Table 2.7 Summary of studies focusing on the robustness of ALT plans

Category	Selected References	Descriptions
Robustness w.r.t. specified model parameters	Nelson and Hahn (1972, 1973)	Monte-Carlo simulation
	Ginebra and Sen (1998)	Minimax approach
	De Groot and Goel (1979, 1988), Verdinelli at el. (1993), Singpurwalla (2006), Zhang and Meeker (2006)	Bayesian planning; Quantify the uncertainty using prior distributions
Robustness w.r.t. assumed life time distribution	Chaloner and Larntz (1992)	Bayesian model-averaging
	Pascual and Montepiedra (2003a)	Weighted sum of asymptotic sample ratios (ASRs)
	Pascual and Montepiedra (2003b)	Minimax plan minimize ASRs
Robustness w.r.t. assumed stress-life model	Pascual (2006)	Bias-robust estimator

2.6.3. The Equivalence Theorem

Very often, numerical methods are needed to obtain optimum ALT plans by maximizing certain criteria $\phi(\xi)$. Hence, in order to verify the global optimality of the developed ALT plans, the general equivalence theorem (GET) introduced by Whittle (1973) has been used (e.g. Chaloner and Larntz (1992), Zhang and Meeker (2006), Pascual (2007), etc).

Let ξ_x be a one-point plan that allocates all units to stress x. Then, the Frechet derivative of criterion $\phi(\xi)$ at ξ in the direction of ξ_x is defined as,

$$d(\xi, x) = \lim_{\varepsilon \downarrow 0} \left(\varepsilon^{-1} \left[\phi\{(1-\varepsilon)\xi + \varepsilon\xi_x\} - \phi(\xi) \right] \right)$$

The GET says that, if $\phi(\xi)$ is concave, $\phi(\xi^*)$ is the global maximum iff $\sup d(\xi^*, x) = 0$. The concavity of the planning criteria $\phi_i(\xi)$ for $i = 1, 2, ..., 5$ is guaranteed here as discussed in Chaloner and Verdinelli (1995).

2.7. Asymptotic Theory

In subsequent chapters, asymptotic results are repeatedly used. The importance of the use of the asymptotic theory is to obtain good approximate solutions when exact solutions are computationally difficult to find (which is often the case in practice). Mathematically, the following regularity conditions are required (Cox and Hinkley 2000):

- The parameter space of the ALT model parameter, $\boldsymbol{\varphi}$, has finite dimension, is closed and compact, and the true parameter value is interior to the parameter

space;

- The probability distributions defined by any two different values of $\boldsymbol{\varphi}$ are distinct;
- The first three derivatives of the log-likelihood, $l(\boldsymbol{\varphi};Y)$, with respect to $\boldsymbol{\varphi}$ exist in the neighborhood of the true parameter value almost surely. Further, in such a neighborhood, N^{-1} times the absolute value of the third derivative is bounded above by a function of Y, whose expectation exists;
- The identity, $E\{U_{\cdot}(\boldsymbol{\varphi})U_{\cdot}^{T}(\boldsymbol{\varphi});\boldsymbol{\varphi}\} = \mathbf{I}_{\boldsymbol{\varphi}}$, holds and the information $\mathbf{I}_{\boldsymbol{\varphi}}$ is finite and positive definite in the neighborhood of the true parameter value.

It is not difficult to see that, these conditions are satisfied in all problems to be discussed below.

Chapter 3. A Sequential ALT Framework and Its Bayesian Inference

3.1. Introduction

This chapter presents the basic framework of sequential accelerated life testing (SALT) and a Bayesian approach for analyzing SALT data.

In analyzing ALT data, the accuracy of the extrapolation is determined by the statistical method used to fit the stress-life model. As we have discussed in Chapter 2, various fitting methods based on Maximum Likelihood (ML) methods have been proposed. ML methods are straightforward and applicable to almost all types of data and stress loadings. Since the ML estimator is asymptotically normal, confidence limits for such an estimator can be easily approximated. However, when the number of failures is small, which is typically the case in practice, asymptotic approximations could be grossly inaccurate. When this happens, it is better to consider Bayesian approach particularly when prior empirical information is available. Under a general Bayesian framework, unknown parameters are replaced with prior distributions. In Table 3.1, we summarize some typical Bayesian approaches for ALT applications, classified by the type of failure time distributions, unknown parameters and their prior distributions. These methods are able to incorporate prior knowledge into data analysis in the face of small sample size and short test duration, but the difficulty in specifying a reasonable priori distribution sometimes significantly limits their applications (Nelson, 1990).

Here, it is necessary to point out that engineering applications and scientific research are serving different purposes. In addition to seizing the high ground of scientific objectivity, reliability engineers always pursue multiple (conflicting) objectives, typically including cost and time-to-market considerations, in product testing projects. This strongly motivates the use of previous knowledge/data as long as the risk is acceptable. In recent decades, advancement in information technology has greatly facilitated the documentation and sharing of past engineering knowledge. It is thus timely for us to explore enabling statistical techniques that conveniently incorporate empirical engineering knowledge while keeping the risk of violating the data objectivity in check.

In this chapter, we shall see a sequential constant-stress ALT scheme and its Bayesian inference approach. Conducting an accelerated life test (ALT) sequentially is an important strategy that allows for the step-by-step (sequential) exploration on products' reliability. This is particularly desirable for newly developed materials or devices for which the uncertainty associated to ALT model and model parameters are still high. In practice, performing an ALT sequentially also helps to save the sample size and requires fewer testing equipments, even though a longer testing duration is sometimes needed as in all sequential experiments. Assuming Exponential failure times, an important work on the optimal sequential ALT design was presented by Bessler et al (1962). Given the observations at different testing stress levels, the authors extended the key result of Chernoff (1959) and presented an approach that selects the optimal testing stress combination for the remaining units, if more tests are

needed, by maximizing the Kullback-Leibler information number for the statistical hypothesis of interest. This framework has the major advantage in saving sample size, but it is usually time consuming and requires more testing equipments, say, temperature chambers, as tests at different stresses need to be conducted at each stage of the sequential testing. Other results on sequential ALT are also found in the literature. Morris (1987) proposed the adaptive design for ALT under destructive inspection, and Edgeman and Lin (1997) considered the analysis of sequential ALT data based on the inverse-Gaussian failure distribution.

Under the scheme to be proposed in this chapter, test at the highest stress level is firstly conducted to quickly generate failures. This is the case when preliminary information of the product reliability is needed. Traditionally, this information plays an important role in test planning; however, as we shall soon see, it is also very useful for statistical inference. In some practical situations, test at the highest stress level has to be firstly conducted simply due to the lack of testing equipments. There might be no way to simultaneously carry out all test runs under different temperatures with only one temperature chamber. Using the information obtained at the highest stress, a Bayesian inference framework is employed to analyze the data coming from lower stress testing levels. Particularly, the following three issues are addressed: 1). the performance of the Bayesian inference in terms of both statistical accuracy and precision; 2). the applicability of the inference method, i.e. whether the prior distribution can be easily specified; 3). the effects of prior knowledge, namely, the robustness of the proposed method.

Figure 3.1 below shows the organization of this chapter. Section 3.2 and 3.3 respectively describes the sequential ALT scheme and the Bayesian inference frameworks. In Section 3.4, a step-by-step illustration of the proposed method can be found. In Section 3.5, the robustness of the proposed method is investigated by simulation. Further discussions are provided in Chapter 4 which contains a theoretical study of the effect of the specified model parameter values.

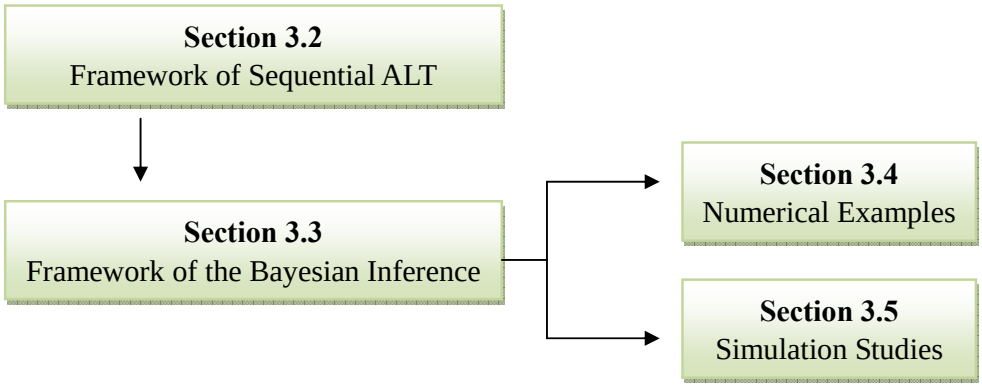

Figure 3.1 Organization of Chapter 3 and Chapter 4

Table 3.1 Typical Bayesian applications in ALT

Reference	Assumed Distribution of Failure Times	Unknown Parameter	Prior Distribution
Van Dorp et al. (1996, 2004, 2005)	Exponential and Weibull	Failure rate (transformed)	Dirichlet distribution
Pathak et al. (1991)	Exponential	Failure rate λ; Time transformation parameter θ	Gamma distribution for λ; Truncated Pareto, or Uniform, or Uniform-Truncated Pareto composite for θ
Chaloner and Larntz (1992)	Lognormal or Weibull	Probability that the lifetime is less than the censoring time at use stress and the highest stress, $P_{D,}P_H$	Beta distribution for $\log(P_D/(1-P_D))$ and $\log(P_H/(1-P_H))$
Achar and Louzada-Neto (1992)	Weibull	Accelerated model parameters and the shape parameter of the lifetime distribution (Weibull)	Non-informative distribution
De Groot and Goel (1988)	Exponential	Tampering coefficient and failure rate	Gamma distribution
Barlow et al. (1988)	Weibull	Scale and shape parameters of the lifetime distribution (Weibull)	Constant
Zhang and Meeker (2006)	Weibull	Accelerated model parameters and the scale parameter of the log-lifetime distribution (SEV)	Lognormal

3.2. The Framework of Sequential Accelerated Life Testing

A sequential constant-stress ALT scheme can be modeled as follows,

1). the Sequential Test Procedure:

- The test involves $k\,(k \geq 2)$ constant stress levels s_i organized in a strictly increasing order

  $$s_0 \leq s_1 < s_2 < \ldots < s_k ,$$

  where s_0 is the design stress where the given reliability measures are to be estimated, and s_k is the highest stress which is pre-specified.

- Test at the highest stress level s_k is firstly conducted until a pre-specified censoring time c_k if the type-I censoring is adopted, or a pre-specified number of items has failed if the type-II censoring is adopted (Nelson 1990).

- After the test at s_k is completed, tests at lower stresses s_i, $\forall i = 1,\ldots,k-1$ are conducted until a pre-specified censoring time c_i $(\forall i = 1,\ldots,k-1)$ if the type-I censoring is adopted, or a pre-specified number of items has failed if the type-II censoring is adopted.

2). *Assumptions:*

- At each stress level, the failure time T follows the Weibull distribution with scale α and shape β. Hence, the logarithm failure time Y follows smallest extreme value (SEV) distribution with location μ and scale σ

  $$F\left(y;\mu,\sigma\right) = 1 - \exp\left(-\exp\left(\left(y-\mu\right)/\sigma\right)\right) \quad \text{where} \quad \mu = \log\left(\alpha\right) \quad \sigma = 1/\beta$$

- The scale parameter σ does not depend on the stress level.

- The location parameter μ depends on the stress, or a function of it, through a linear stress-life function $\varphi: \mu_i = \log(\alpha_i) = \beta_0 + \beta_1 \cdot f(s_i)$.

3.3. The Framework of Bayesian Inference

Categorized by how prior distributions at lower stress level are constructed, the proposed Bayesian inference method has two frameworks, namely, the All-at-one Prior Distribution Construction (APC) and the Full Sequential Prior Distribution Construction (FSPC).

As illustrated in Figure 3.2a, the framework of APC includes 4 steps.

- Step 1. Derive the posterior distribution $\pi(\mu_k)$. APC starts at the highest stress level by deriving the posterior distribution $\pi(\mu_k)$ for the location parameter μ_k. Since the number of failures at the highest stress level is expected to be large, a non-informative prior distribution is chosen here as it does not raise any risk of violating the data objectivity.
- Step 2. Construct prior distributions for lower stress levels ($i = 1, 2, ..., k-1$). When the posterior distribution $\pi(\mu_k)$ is derived, prior distributions $\vartheta(\mu_i)$ for all lower stress levels are simultaneously constructed given a pre-specified prior distribution $\vartheta(\beta_1)$. For the Arrhenius model, specifying the prior distribution $\vartheta(\beta_1)$ is equivalent to specifying the prior distribution $\vartheta(E_a)$ of the activation energy E_a. In practice, E_a has been well defined particularly for consumer electronics. Its value or range is generally available from past experience, physical/chemical knowledge, or engineering handbooks.

- Step 3. Derive posterior distributions for lower stress levels ($i = 1, 2, ..., k-1$). When $\vartheta(\mu_i)$ at lower stress levels have been constructed, posterior distributions $\pi(\mu_i)$ can be derived using the Bayesian rule.
- Step 4. Fit an appropriate stress-life model to the estimates $\hat{\mu}_i$ found in above steps ($i = 1, 2, ..., k$).

FSPC differs from APC in how prior distributions $\vartheta(\mu_i)$ at lower stress levels ($i = 1, 2, ..., k-1$) are constructed. Given the prior distribution $\vartheta(\beta_1)$, the analysis based on FSPC moves downwards from the highest stress level to the lowest. The prior distribution $\vartheta(\mu_i)$ at any lower stress i ($i = 1, 2, ..., k-1$) is constructed from those posterior distributions $\pi(\mu_j)$ that have already been derived ($j = i+1, ..., k$). For example when $k = 3$, the prior distribution $\vartheta(\mu_2)$ is derived from $\pi(\mu_3)$ and $\vartheta(\beta_1)$; whereas $\vartheta(\mu_1)$ is derived from $\pi(\mu_2)$ and $\pi(\mu_3)$. The framework of FSPC with $k = 3$ is illustrated in Figure 3.2b.

Compared to APC, FSPC is more robust to the prior information on β_1. However, it becomes less preferred when this prior information is accurate. Detailed discussions on this trade-off are presented in simulation studies.

In both APC and FSPC, we fit a stress-life model to $\hat{\mu}_i$ in the last step. This is similar to the weighted regression approach used by Lawless (1982). In that approach, the unknown parameter μ_i at each stress level is separately estimated, and the stress-life relationship is found using least-square method with weights being the amount of information obtained at each level.

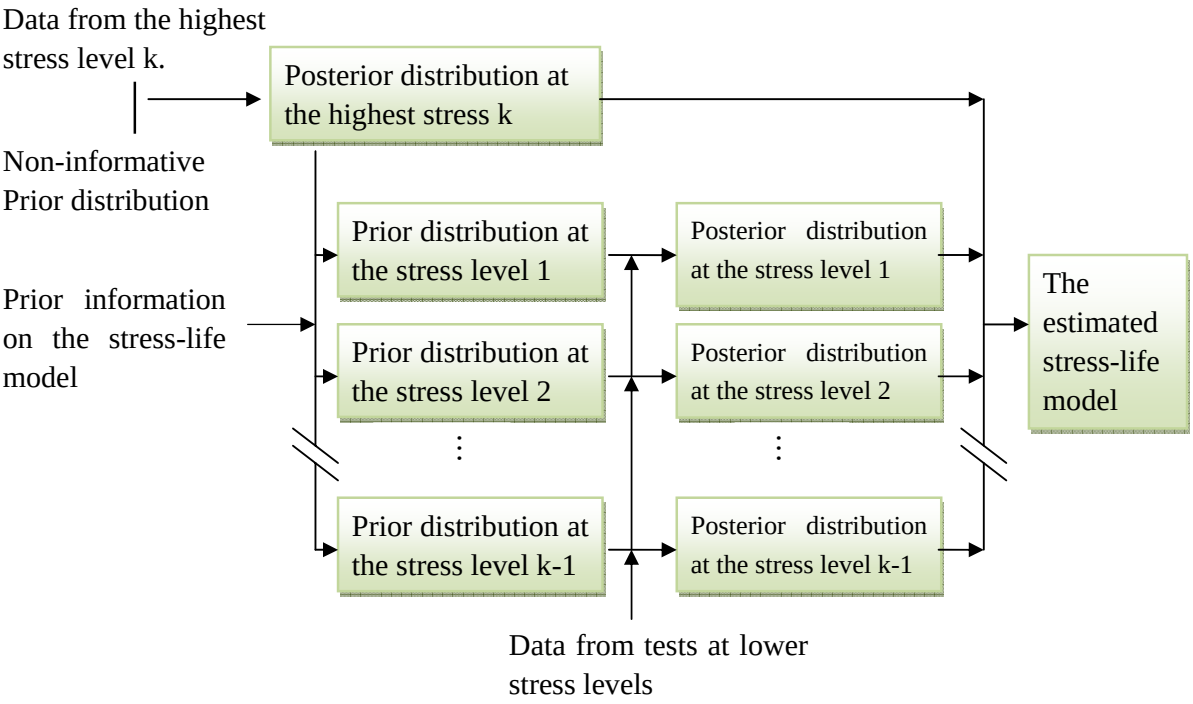

(a)

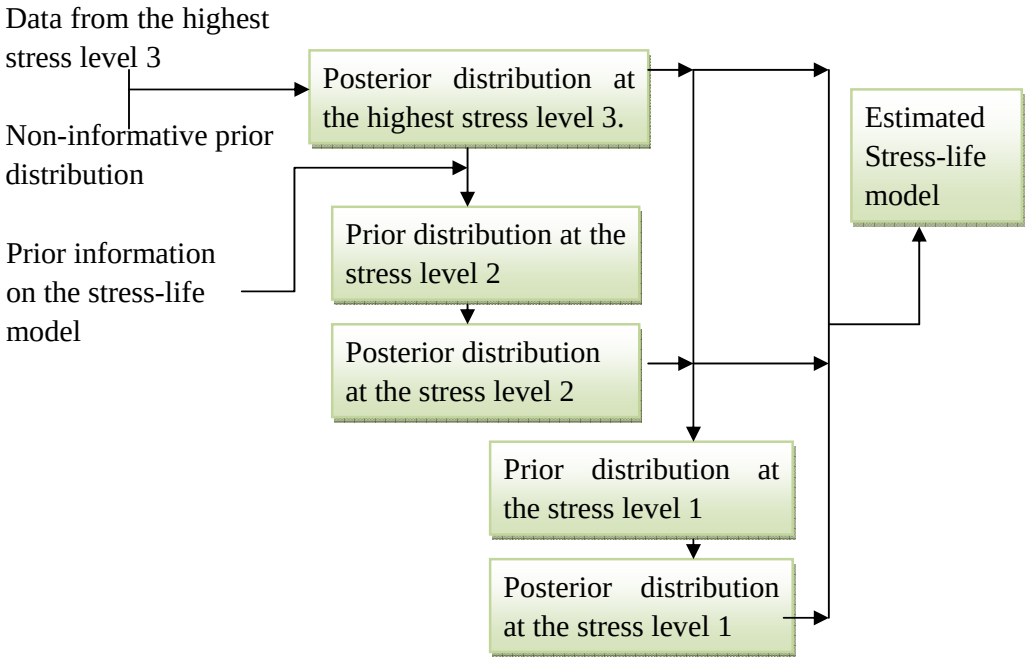

(b)

Figure 3.2 Framework of the Bayesian inference (a) APC (b) FSPC

3.4. Numerical Examples

In this section, step-by-step illustrations of the proposed inference method are presented using a real-life dataset.

3.4.1. A temperature-accelerated life test

Hooper and Amster (1990) present a temperature-accelerated life test for a certain device-A. The data are available in the Appendix as well as Meeker and Escobar (1998). In this constant-stress ALT,

1). Testing units, which have the normal operation temperature T_0 equals $283K$, are tested at 3 temperature levels $T_1 = 313K, T_2 = 333K, T_3 = 353K$. To facilitate the analysis, let $s_i = 1/T_i$, and standardize s_i as $x_i = (s_i - s_0)/(s_k - s_0)$;

2). At any stress level x_i ($i = 1, 2, 3$), n_i units are tested, and r_i number of failures are observed at a censoring time c;

Here, $n_1 = 100, n_2 = 20, n_3 = 15, r_1 = 10, r_2 = 9, r_3 = 14$, and $c = 5000hrs$;

3). Failure times at each stress level x_i ($i = 1, 2, 3$) follow Weibull distribution with scale parameter α_i and shape parameter β. Let t_{ij} be the *jth* failure obtained from stress level s_i, the logarithm of failure time $y_{ij} = \log\left(t_{ij}\right)$ therefore follows the smallest extreme value distribution

$$F(y) = 1 - \exp\left[-\exp\left[\left(y - \mu\right)/\sigma\right]\right];$$

4). The Arrhenius model is chosen to describe the dependency of μ_i on temperature, i.e. $\mu_i = \log A + \dfrac{\text{Activation energy}, E_a}{\text{Boltzmann constant}, k_B} \cdot \dfrac{1}{T_i}$. Then, we have the linear stress-life

model $\varphi(x_i;\Phi)$ as

$$\mu_i = \varphi(x_i;\Phi) = \beta_0 + \beta_1 \cdot x_i$$
$$\text{where } \beta_0 = \log A + E_a \cdot k_B^{-1} \cdot s_0 \quad \beta_1 = E_a \cdot k_B^{-1} \cdot (s_k - s_0) \tag{3.1}$$

5). σ is a constant independent of temperature.

3.4.2. Analyze Device-A data using APC framework

A step-by-step illustration of APC is presented in this section. To make the illustration clearer, we only focus on the estimation of (β_0, β_1) and assume σ equals to its maximum likelihood estimate 0.7 (Nelson & Meeker 1978). Although the application of the Bayesian inference framework is not restricted to situations in which σ is known (see Chapter 4), two reasons motivate this simplification: 1) the closed-form solution of $\hat{\sigma}$ is not available; 2) the estimates $(\hat{\beta}_0, \hat{\beta}_1)$ are not sensitive to $\hat{\sigma}$. At the end of this section, we provide a sensitivity analysis to justify this point.

APC involves the following 4 steps to analyze the Device-A data.

- STEP 1: Derive the Posterior Distribution $\pi(\mu_3)$ of μ_3

Suppose the test at the highest temperature level $T_3 = 353K$ has been firstly conducted, the first step of APC is to derive the posterior distribution $\pi(\mu_3)$ of μ_3. Since the number of failures (14 failures out of 15 items) is large enough, $\pi(\mu_3)$ is derived from a non-informative prior distribution $\vartheta(\mu_3)$ using the Bayesian rule. Figure 3.3a shows the posterior distribution $\pi(\mu_3)$.

If the mode of $\pi(\mu_3)$, i.e., the generalized MLE (Berger 1985), is chosen to be the estimate of μ_3, we then have

$$\left.\frac{\partial In\left[\prod_{j=1}^{r_k}\frac{1}{\sigma}\cdot\exp\left(\frac{y_{kj}-\mu_k}{\sigma}-\exp\left(\frac{y_{kj}-\mu_k}{\sigma}\right)\right)\cdot\prod_{j=1}^{n_k-r_k}\exp\left(-\exp\left(\frac{c_k-\mu_k}{\sigma}\right)\right)\right]}{\partial\mu_k}\right|_{\mu_k=\hat{\mu}_k} = 0$$

$$\Rightarrow \hat{\mu}_k = \sigma\cdot\left[\log\left(\sum_{j=1}^{r_k} t_{kj}^{1/\sigma}+\left(n_k-r_k\right)\cdot c_k^{1/\sigma}\right)-\log\left(r_k\right)\right]$$

$$\Rightarrow$$

$$\hat{\mu}_3 = \sigma\cdot\left[\log\left(\sum_{j=1}^{r_3} t_{3j}^{1/\sigma}+\left(n_3-r_3\right)\cdot c_3^{1/\sigma}\right)-\log\left(r_3\right)\right] = 7.48$$

(3.2)

In fact, $\pi(\mu_3)$ is asymptotically normal with mean $\hat{\mu}_3$ and variance: (Cox and Hinkley 2000)

$$\text{var}\left(\hat{\mu}_3\right) = \left[-\frac{\partial^2 l(\mu_3)}{\partial {\mu_3}^2}\right]^{-1}_{\mu_3=\hat{\mu}_3} = 0.036$$

$$\text{where}\quad l(\mu_3) = \sum_{i=1}^{r_3}\left(\log\frac{1}{\sigma}+\frac{y_i-\mu_3}{\sigma}-\exp\left\{\frac{y_i-\mu_3}{\sigma}\right\}\right)+\sum_{i=1}^{n_3-r_3}\left(-\exp\left\{\frac{\log c_3-\mu_3}{\sigma}\right\}\right)$$

(3.3)

Hence, we approximate $\pi(\mu_3)$ using the normal curve as shown in Figure 3.3b. As can be seen later, this approximation plays an important role in constructing the prior distributions $\vartheta(\mu_2)$ and $\vartheta(\mu_1)$.

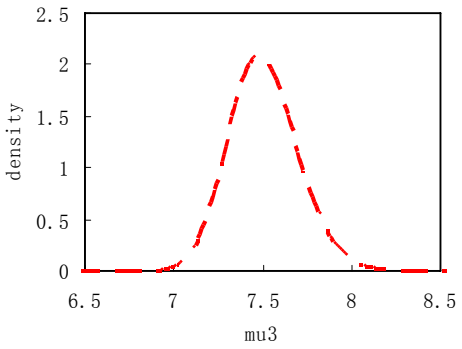

(a)

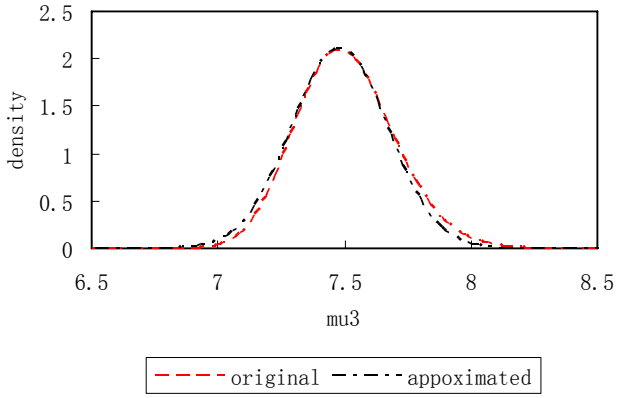

(b)

Figure 3.3 Posterior distribution $\pi(\mu_3)$ (a) original (b) approximated

- STEP 2: Construct the Prior Distributions of μ_2 and μ_1

Step 2 involves constructing the prior distributions $\vartheta(\mu_2)$ and $\vartheta(\mu_1)$ based on $\pi(\mu_3)$ and particular engineering knowledge on the slope β_1 (or E_a equivalently),

$$\mu_i = \mu_3 + \beta_1 \cdot (x_i - 1) \quad \forall i = 1,2$$
$$\text{where } \beta_1 = E_a \cdot k_B^{-1} \cdot (s_k - s_0) \tag{3.4}$$

As seen in equation (3.4), $\vartheta(\mu_i)$ can be constructed from $\pi(\mu_3)$ if the information on E_a is available. In practice, information on E_a is generally available from previous experience, physical/chemical knowledge, or MIL-STD and handbooks. For many

consumer electronics products, E_a for various failure mechanisms are roughly within some typical ranges. In this example, our engineering knowledge suggests a uniform distribution $\vartheta(E_a)$ defined on the interval $[E_a^- = 0.5, E_a^+ = 0.8]$. Although arbitrary form of $\vartheta(E_a)$ is allowed, the uniform distribution is clearly an easy choice considering the applicability of the proposed method in practice.

Recall that $\pi(\mu_3)$ is asymptotically normal, the *pdf* of $\vartheta(\mu_2)$ and $\vartheta(\mu_1)$ can be written as follows,

$$\vartheta(\mu_i) \propto \frac{1}{(2\pi \cdot \mathrm{var}(\hat{\mu}_3))^{1/2}} \cdot \int_{a_i^-}^{a_i^+} \exp\left\{-\frac{(\mu_i - a)^2}{2\,\mathrm{var}(\hat{\mu}_3)}\right\} \cdot \frac{1}{a_i^+ - a_i^-} da$$

$$= \frac{2}{a_i^+ - a_i^-} \cdot \left(\mathrm{erf}\left\{\frac{\mu_i - a_i^-}{(2\,\mathrm{var}(\hat{\mu}_3))^{1/2}}\right\} - \mathrm{erf}\left\{\frac{\mu_i - a_i^+}{(2\,\mathrm{var}(\hat{\mu}_3))^{1/2}}\right\} \right)$$

where (3.5)

$$a_i^- = \hat{\mu}_3 + E_a^- \cdot k_B^{-1} \cdot (s_k - s_0) \cdot (x_i - 1)$$

$$a_i^+ = \hat{\mu}_3 + E_a^+ \cdot k_B^{-1} \cdot (s_k - s_0) \cdot (x_i - 1)$$

Figure 3.4a and 3.4b respectively shows the prior distribution $\vartheta(\mu_2)$ and $\vartheta(\mu_1)$.

Apparently, the spread of $\vartheta(\mu_1)$ is wider than that of $\vartheta(\mu_2)$. This is because the distance between stress level 1 and 3 is farther than that between stress level 2 and 3, as a result, the uncertainty on μ_i becomes larger as the distance from stress level i to 3 increases. That is, uncertainty over the value of E_a leads to an information loss. In the extreme case when E_a is specified to an exact value, i.e. $E_a^- = E_a^+$, the information loss is zero in constructing $\vartheta(\mu_1)$ and $\vartheta(\mu_2)$.

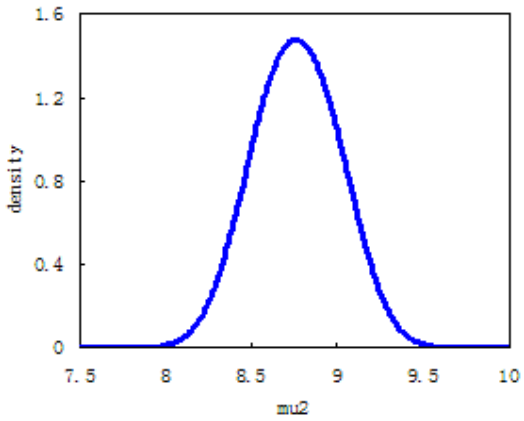

(a)

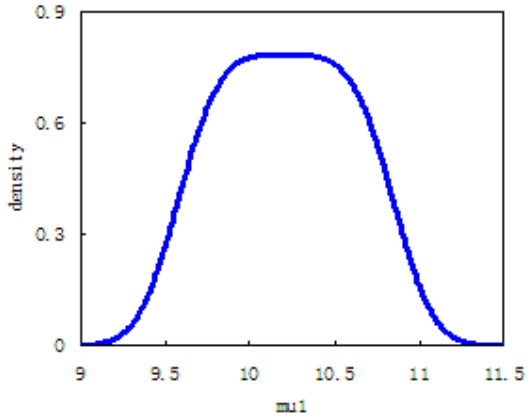

(b)

Figure 3.4 Constructed prior distribution (a) $\vartheta(\mu_2)$ (b) $\vartheta(\mu_1)$

- STEP 3: Derive the Posterior Distributions of μ_2 and μ_1

Apply the Bayes rule, the posterior distributions $\pi(\mu_2)$ and $\pi(\mu_1)$ are shown in Figure 3.5a and 3.5b.

Again, $\pi(\mu_2)$ and $\pi(\mu_1)$ can be approximated by (Berger1985)

$$N\left(\hat{\mu}_i, \left[I^{\vartheta(\mu_i)}(\mathbf{Y}_i)\right]^{-1}\right) \qquad \forall i = 1,2$$

$$\text{where} \quad I^{\vartheta(\mu_i)}(\mathbf{Y}_i) = -\left[\frac{\partial^2}{\partial \mu^2}\log\left(f(\mathbf{Y}_i|\mu_i)\cdot\vartheta(\mu_i)\right)\right]_{\mu_i=\hat{\mu}_i} \tag{3.6}$$

Hence, the posterior distribution $\pi(\mu_2)$ is approximately $N(8.81, 0.033)$ and the

posterior distribution $\pi(\mu_1)$ is approximately $N(10.13, 0.05)$. In Figure 3.5a and 3.5b, the approximated curves are also plotted. As clearly seen, these curves well approximate $\pi(\mu_2)$ and $\pi(\mu_1)$. As the number of failures at the lowest stress level 1 is relatively small, the large sample approximation of $\pi(\mu_1)$ appears to be slightly worse than that of $\pi(\mu_2)$.

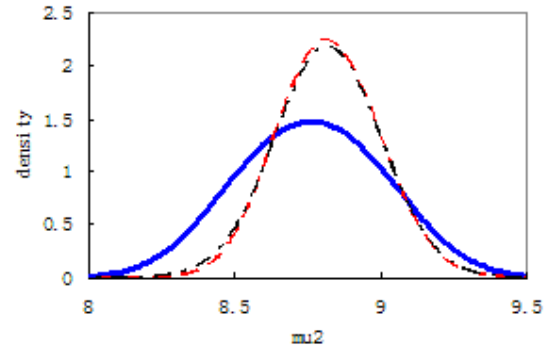

(a)

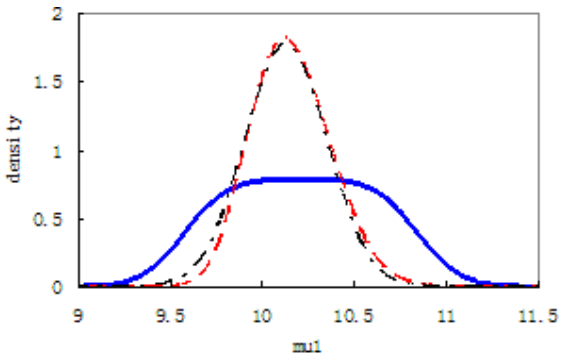

(b)

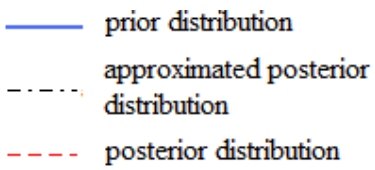

Figure 3.5 Posterior distribution (a) original and approximated posterior distribution $\pi(\mu_2)$ (b) original and approximated posterior distribution $\pi(\mu_1)$

Then, the estimate $\hat{\mu}_i$ is the root of the following equation,

$$\left.\frac{\partial \pi(\mu_i)}{\partial \mu_i}\right|_{\mu_i=\hat{\mu}_i} = 0 \quad \Rightarrow$$

$$-\frac{r_i}{\sigma} + \left(\frac{1}{\exp(\mu_i)}\right)^{1/\sigma} \cdot \frac{1}{\sigma} \cdot \left(\sum_{j=1}^{r_i} t_{ij}^{1/\sigma} + (n_i - r_i) \cdot c_i^{1/\sigma}\right) + \kappa(\mu_i) = 0 \qquad \forall i = 1,2 \tag{3.7}$$

$$\text{where} \quad \kappa(\mu_i) = \sqrt{\frac{2}{\pi \cdot \text{var}(\hat{\mu}_3)}} \cdot \frac{\exp\left(-\frac{(\mu_i - a_i^-)^2}{2\,\text{var}(\hat{\mu}_3)}\right) - \exp\left(-\frac{(\mu_i - a_i^+)^2}{2\,\text{var}(\hat{\mu}_3)}\right)}{\text{erf}\left(\frac{\mu_i - a_i^-}{\sqrt{2\,\text{var}(\hat{\mu}_3)}}\right) - \text{erf}\left(\frac{\mu_i - a_i^+}{\sqrt{2\,\text{var}(\hat{\mu}_3)}}\right)}$$

- STEP 4: Estimate the Stress-Life Model

Substitute $\hat{\mu}_3 = 7.48$, $\hat{\mu}_2 = 8.81$ and $\hat{\mu}_1 = 10.13$ into the model $\mu_i = \beta_0 + \beta_1 x_i$, we have

$$\mathbf{X}\boldsymbol{\Phi}^T = \mathbf{M}^T$$

$$\text{where} \quad \boldsymbol{\Phi} = [\beta_0, \beta_1]$$

$$\mathbf{X} = \begin{bmatrix} 1, x_1 \\ 1, x_2 \\ 1, x_3 \end{bmatrix} \tag{3.8}$$

$$\mathbf{M} = [\mu_1, \mu_2, \mu_3]$$

It follows that

$$\hat{\beta}_0 = \hat{\mu}_0 = \sum_{i=1}^{k} u_i \cdot \hat{\mu}_i = 12.64 \quad , \quad \text{var}(\hat{\beta}_0) = \sum_{i=1}^{k} u_i^2 \cdot \text{var}(\hat{\mu}_i) = 0.21$$

$$\hat{\beta}_1 = \sum_{i=1}^{k} v_i \cdot \hat{\mu}_i = -5.21 \quad , \quad \text{var}(\hat{\beta}_1) = \sum_{i=1}^{k} v_i^2 \cdot \text{var}(\hat{\mu}_i) = 0.32$$

$$\hat{E}_a = \hat{\beta}_1 \cdot k_B / (s_k - s_0) = 0.65$$

where (3.9)

$$k = 3$$

$$u_i = \frac{\sum_{j=1}^{k} x_j^2 - x_j \cdot \sum_{j=1}^{k} x_j}{k \cdot \sum_{j=1}^{k} x_j^2 - \sum_{j=1}^{k} x_j \cdot \sum_{j=1}^{k} x_j}$$

$$v_i = \frac{k \cdot x_j - \sum_{j=1}^{k} x_j}{k \cdot \sum_{j=1}^{k} x_j^2 - \sum_{j=1}^{k} x_j \cdot \sum_{j=1}^{k} x_j}$$

Figure 3.6 illustrates how APC works in analyzing Device-A data.

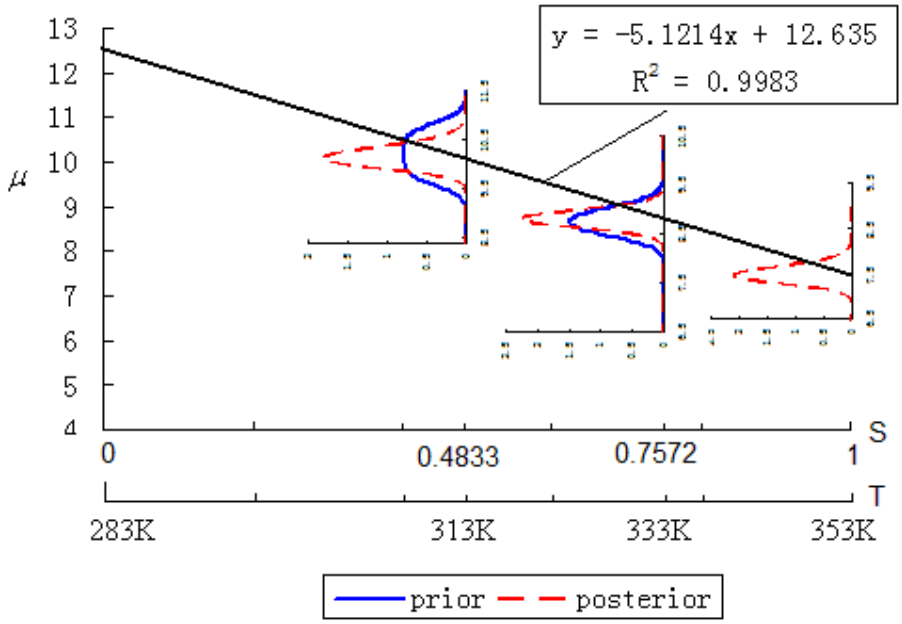

Figure 3.6 Analyze the device-A data using APC

As mentioned at the beginning, the analysis above is based on a particular value of σ. Figure 3.7 below gives the sensitivity analysis of $\hat{\mu}_0$ for different σ. The values 0.514 and 0.906 are respectively the lower and upper confidence bound of the MLE of σ at 95% confidence level. It is seen from the Figure 3.7, the relative variation of $\hat{\mu}_0$ is less than 6% when σ ranges between 0.514 and 0.906.

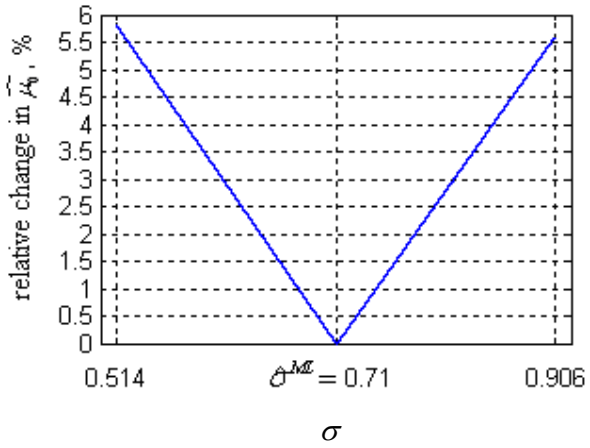

Figure 3.7 Sensitivity analysis of $\hat{\mu}_0$

3.4.3. Analyze Device-A data using FSPC framework

In APC, the prior information on E_a is directly used to construct both $\vartheta(\mu_2)$ and $\vartheta(\mu_1)$. Hence, inaccurate information might lead to poor estimates $\hat{\mu}_2$ and $\hat{\mu}_1$. To enhance the robustness of the Bayesian inference, we present below the full sequential prior distribution construction (FSPC) framework for analyzing Device-A data. Compared to APC, FSPC only uses the prior information on E_a to construct $\vartheta(\mu_2)$; while $\vartheta(\mu_1)$ is constructed from $\pi(\mu_2)$ and $\pi(\mu_3)$.

Similar to APC, the sequential analysis of FSPC also includes 4 steps.

- STEP 1: Derive the Posterior Distribution of μ_3

From the result of section 3.4.2, we have $\pi(\mu_3) \sim N\left(\hat{\mu}_3 = 10.13, \text{var}(\hat{\mu}_3) = 0.036\right)$.

- STEP 2: Construct the Prior Distribution of μ_2 and Derive the Posterior Distribution of μ_2

From the result of section 3.4.2, $\pi(\mu_2)$ asymptotically follows normal distribution $N\left(\hat{\mu}_2 = 8.82, \text{var}(\hat{\mu}_2) = 0.033\right)$.

- STEP 3: Construct the Prior Distribution of μ_1 and Derive the Posterior Distribution of μ_1

Unlike the framework of APC where the prior distribution $\vartheta(\mu_1)$ is constructed from $\vartheta(E_a)$ and $\pi(\mu_3)$, FSPC allows $\vartheta(\mu_1)$ to be constructed based on the derived posterior distributions $\pi(\mu_2)$ and $\pi(\mu_3)$. Given $\pi(\mu_2)$ and $\pi(\mu_3)$, the preliminary estimated value $\tilde{\mu}_1$ of μ_1 can be easily obtained in (3.10). It is normally distribution with mean $\tilde{\mu}_1$ and variance $\text{var}(\tilde{\mu}_1)$

$$\tilde{\mu}_i = \frac{\hat{\mu}_2(x_3 - x_1) - \hat{\mu}_3(x_2 - x_1)}{x_3 - x_2} = 10.33$$
$$\text{var}(\tilde{\mu}_i) = \left(\frac{x_3 - x_1}{x_3 - x_2}\right)^2 \text{var}(\hat{\mu}_2) + \left(\frac{x_2 - x_1}{x_3 - x_2}\right)^2 \text{var}(\hat{\mu}_3) = 0.19 \quad (3.10)$$

Hence, we naturally choose $N\left(\tilde{\mu}_1 = 10.33, \text{var}\left(\tilde{\mu}_1\right) = 0.19\right)$ shown in Figure 3.8a as the prior distribution $\vartheta\left(\mu_1\right)$.

Then, the posterior distribution $\pi\left(\mu_1\right)$ is derived using the Bayesian rule,

$$\pi(\mu_1 \mid \text{data from stress level 1}) \propto \vartheta(\mu_1) \cdot L(\text{data from stress level 1})$$

Figure 3.8b shows the posterior distribution $\pi\left(\mu_1\right)$. Again, if the mode of $\pi\left(\mu_1\right)$ is chosen as the Bayesian estimate, we have $\hat{\mu}_1 = 10.17$. In addition, based on equation (3.6), $\pi\left(\mu_1\right)$ is approximated by $N\left(\hat{\mu}_1 = 10.17, \left[I^{\vartheta(\mu_1)}\left(\mathbf{Y}_1\right)\right]^{-1} = 0.042\right)$. The approximated curve is also given in Figure 3.8b.

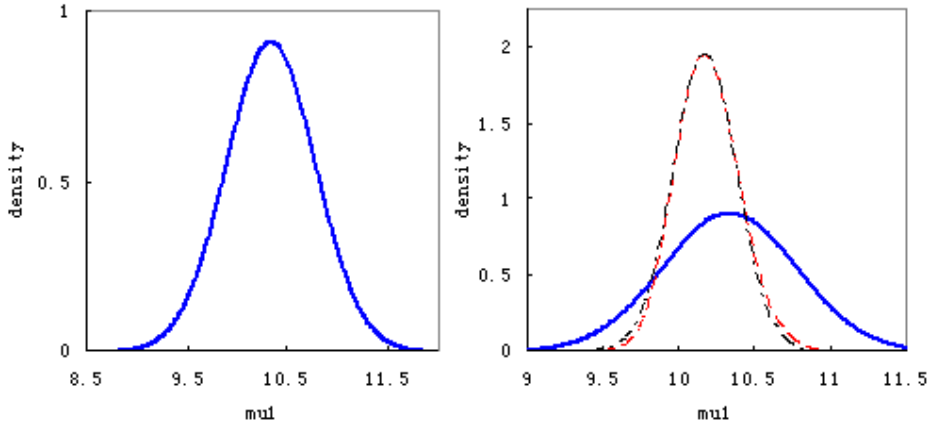

(a) (b)

Figure 3.8 Prior and posterior distribution

(a) prior distribution $\vartheta\left(\mu_1\right)$ (b) posterior distribution $\pi\left(\mu_1\right)$ with approximated curve

- STEP 4: Estimate the Stress-Life Model

Substitute $\hat{\mu}_3 = 7.48$, $\hat{\mu}_2 = 8.82$ and $\hat{\mu}_1 = 10.17$ into the model $\mu_i = \beta_0 + \beta_1 x_i$, we have

$$\mathbf{X}\boldsymbol{\Phi}^T = \mathbf{M}^T$$
$$\text{where} \quad \boldsymbol{\Phi} = [\beta_0, \beta_1]$$
$$\mathbf{X} = \begin{bmatrix} 1, x_1 \\ 1, x_2 \\ 1, x_3 \end{bmatrix} \tag{3.11}$$
$$\mathbf{M} = [\mu_1, \mu_2, \mu_3]$$

It follows that

$$\hat{\beta}_0 = \hat{\mu}_0 = \sum_{i=1}^{k} u_i \cdot \hat{\mu}_i = 12.71 \quad , \quad \text{var}(\hat{\beta}_0) = \sum_{i=1}^{k} u_i^2 \cdot \text{var}(\hat{\mu}_i) = 0.18$$
$$\hat{\beta}_1 = \sum_{i=1}^{k} v_i \cdot \hat{\mu}_i = -5.20 \quad , \quad \text{var}(\hat{\beta}_1) = \sum_{i=1}^{k} v_i^2 \cdot \text{var}(\hat{\mu}_i) = 0.29 \tag{3.12}$$
$$\hat{E}_a = \hat{\beta}_1 \cdot k_B / (s_k - s_0) = 0.64$$

Figure 3.9 illustrates how FSPC works in analyzing Device-A data.

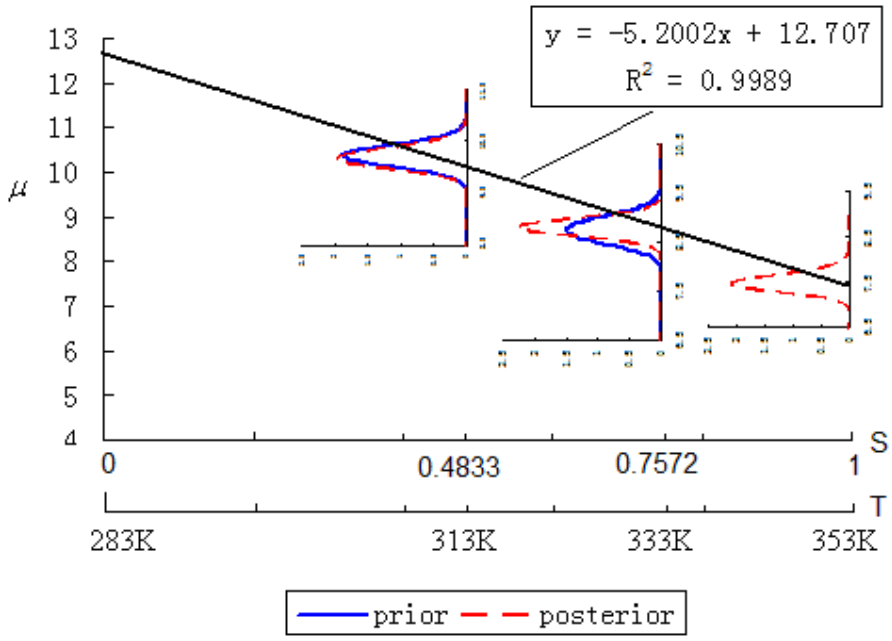

Figure 3.9 Analyze the device-A data using FSPC

3.5. Simulation Studies

Simulation studies are conducted to examine the performance of the proposed Bayesian inference method. In particular, we address the following three questions,

Q1: What are the effects of the prior knowledge?

Q2: Given different prior knowledge about the activation energy, how does the proposed Bayesian inference method compare to MLE in terms of estimation accuracy and precision?

Q3: How does the robustness of FSPC compared to that of APC?

3.5.1. Failure Data Generation

The Device-A ALT plan is again used in the simulation study. In each simulation run, failure data are generated based on the values given in (3.13)

$$\begin{aligned} &\sigma = 0.71 \quad , \quad E_a = 0.61 \quad , \quad \log A = -12.65 \\ &\mu_i = \beta_0 + \beta_1 x_i = \log A + E_a \cdot k_B{}^{-1} \cdot s_0 + E_a \cdot k_B{}^{-1} \cdot (s_k - s_0) \cdot x_i \end{aligned} \tag{3.13}$$

3.5.2. Quantify the Prior Knowledge

Let the prior knowledge about E_a has the form given by equation (3.14). That is, the pre-specified E_a is uniformly distributed on an interval with its length controlled by τ. These intervals might either *tightly* cover the true value of E_a, or *loosely* cover the true value of E_a, or even *miss* the true value of E_a. These are the scenarios that engineers might encounter in practice, and their effects are of our interest

$$E_a \sim uniform\left(\tilde{E}_a - \tau, \tilde{E}_a + \tau\right) \tag{3.14}$$

3.5.3. Simulation Design

We propose 20 combinations of $\left(\tilde{E}_a, \tau\right)$ for a particular censoring time. As seen in Table 3.2, the censoring time has three levels: 2500hrs, 5000hrs, and 10000hrs; for each censoring time, $\tilde{E}_a$ has five levels:0.5, 0.55, 0.61(the true value), 0.65, and 0.7; for each $\tilde{E}_a$, the precision control factor τ has four levels: 0, 0.1, 0.2, and 0.3. Hence, there are total 60 "censoring time-$\tilde{E}_a$-τ" combinations in the simulation study. For each combination, 10e6 simulation runs are repeated. In each run, the failure times are generated, and the estimate $\hat{\mu}_0$ is derived using APC, FSPC and MLE.

Table 3.2 Simulation design table

2500hrs		5000hrs		10000hrs	
$\tilde{E}_a = 0.5$	$\tau = 0$ $\tau = 0.1$ $\tau = 0.2$ $\tau = 0.3$	$\tilde{E}_a = 0.5$	$\tau = 0$ $\tau = 0.1$ $\tau = 0.2$ $\tau = 0.3$	$\tilde{E}_a = 0.5$	$\tau = 0$ $\tau = 0.1$ $\tau = 0.2$ $\tau = 0.3$
$\tilde{E}_a = 0.55$	$\tau = 0$ $\tau = 0.1$ $\tau = 0.2$ $\tau = 0.3$	$\tilde{E}_a = 0.55$	$\tau = 0$ $\tau = 0.1$ $\tau = 0.2$ $\tau = 0.3$	$\tilde{E}_a = 0.55$	$\tau = 0$ $\tau = 0.1$ $\tau = 0.2$ $\tau = 0.3$
$\tilde{E}_a = 0.61$	$\tau = 0$ $\tau = 0.1$ $\tau = 0.2$ $\tau = 0.3$	$\tilde{E}_a = 0.61$	$\tau = 0$ $\tau = 0.1$ $\tau = 0.2$ $\tau = 0.3$	$\tilde{E}_a = 0.61$	$\tau = 0$ $\tau = 0.1$ $\tau = 0.2$ $\tau = 0.3$
$\tilde{E}_a = 0.65$	$\tau = 0$ $\tau = 0.1$ $\tau = 0.2$ $\tau = 0.3$	$\tilde{E}_a = 0.65$	$\tau = 0$ $\tau = 0.1$ $\tau = 0.2$ $\tau = 0.3$	$\tilde{E}_a = 0.65$	$\tau = 0$ $\tau = 0.1$ $\tau = 0.2$ $\tau = 0.3$
$\tilde{E}_a = 0.7$	$\tau = 0$ $\tau = 0.1$ $\tau = 0.2$ $\tau = 0.3$	$\tilde{E}_a = 0.7$	$\tau = 0$ $\tau = 0.1$ $\tau = 0.2$ $\tau = 0.3$	$\tilde{E}_a = 0.7$	$\tau = 0$ $\tau = 0.1$ $\tau = 0.2$ $\tau = 0.3$

3.5.4. Analysis of Simulation Outputs

Simulation results are contained in Table 3.3 ~ 3.5.

Table 3.3 Simulation results (censoring time = 2500hrs)

$\tilde{E}_a$	τ	APC			FSPC			MLE		
		Bias	Var.	MSE	Bias	Var.	MSE	Bias	Var.	MSE
$\tilde{E}_a = 0.5$	$\tau = 0$	-0.5992	0.0255	0.3846	-0.2132	0.1481	0.1936	0.1061	0.4228	0.4341
	$\tau = 0.1$	-0.0134	0.1980	0.1981	0.0063	0.2456	0.2456	0.1061	0.4228	0.4341
	$\tau = 0.2$	0.0933	0.2920	0.3006	0.0486	0.2778	0.2802	0.1061	0.4228	0.4341
	$\tau = 0.3$	0.1533	0.3515	0.3750	0.0904	0.3000	0.3082	0.1061	0.4228	0.4341
$\tilde{E}_a = 0.55$	$\tau = 0$	-0.3372	0.0296	0.1433	-0.1046	0.1629	0.1739	0.1061	0.4228	0.4341
	$\tau = 0.1$	0.0709	0.2647	0.2697	0.0444	0.2669	0.2688	0.1061	0.4228	0.4341
	$\tau = 0.2$	0.1398	0.3415	0.3610	0.0752	0.2905	0.2961	0.1061	0.4228	0.4341
	$\tau = 0.3$	0.1829	0.3838	0.4172	0.1024	0.3037	0.3141	0.1061	0.4228	0.4341
$\tilde{E}_a = 0.61$	$\tau = 0$	0.0020	0.0343	0.0343	0.0438	0.1766	0.1782	0.1061	0.4228	0.4341
	$\tau = 0.1$	0.1498	0.3271	0.3496	0.0998	0.2918	0.3018	0.1061	0.4228	0.4341
	$\tau = 0.2$	0.1870	0.3827	0.4176	0.1069	0.3017	0.3131	0.1061	0.4228	0.4341
	$\tau = 0.3$	0.2176	0.4106	0.4579	0.1207	0.3088	0.3233	0.1061	0.4228	0.4341
$\tilde{E}_a = 0.65$	$\tau = 0$	0.2330	0.0376	0.0919	0.1393	0.1935	0.2129	0.1061	0.4228	0.4341
	$\tau = 0.1$	0.1965	0.3521	0.3907	0.1385	0.3003	0.3195	0.1061	0.4228	0.4341
	$\tau = 0.2$	0.2173	0.3999	0.4471	0.1298	0.3102	0.3271	0.1061	0.4228	0.4341
	$\tau = 0.3$	0.2406	0.4283	0.4862	0.1339	0.3137	0.3316	0.1061	0.4228	0.4341
$\tilde{E}_a = 0.7$	$\tau = 0$	0.5483	0.0426	0.3432	0.2681	0.2147	0.2806	0.1061	0.4228	0.4341
	$\tau = 0.1$	0.2568	0.3629	0.4289	0.1869	0.3109	0.3458	0.1061	0.4228	0.4341
	$\tau = 0.2$	0.2530	0.4148	0.4788	0.1630	0.3093	0.3358	0.1061	0.4228	0.4341
	$\tau = 0.3$	0.2666	0.4469	0.5180	0.1470	0.3200	0.3416	0.1061	0.4228	0.4341

Table 3.4 Simulation results (censoring time = 5000hrs)

$\tilde{E}_a$	τ	APC			FSPC			MLE		
		Bias	Var.	MSE	Bias	Var.	MSE	Bias	Var.	MSE
$\tilde{E}_a = 0.5$	$\tau = 0$	-0.4491	0.0222	0.2239	-0.1013	0.1117	0.1220	0.0616	0.2127	0.2165
	$\tau = 0.1$	-0.0016	0.1176	0.1176	0.0144	0.1469	0.1471	0.0616	0.2127	0.2165
	$\tau = 0.2$	0.0547	0.1577	0.1607	0.0339	0.1555	0.1566	0.0616	0.2127	0.2165
	$\tau = 0.3$	0.0753	0.1679	0.1736	0.0478	0.1580	0.1603	0.0616	0.2127	0.2165
$\tilde{E}_a = 0.55$	$\tau = 0$	-0.2475	0.0224	0.0847	-0.0333	0.1128	0.1139	0.0616	0.2127	0.2165
	$\tau = 0.1$	0.0430	0.1471	0.1490	0.0329	0.1519	0.1529	0.0616	0.2127	0.2165
	$\tau = 0.2$	0.0729	0.1680	0.1733	0.0451	0.1568	0.1588	0.0616	0.2127	0.2165
	$\tau = 0.3$	0.0849	0.1715	0.1787	0.0539	0.1572	0.1601	0.0616	0.2127	0.2165
$\tilde{E}_a = 0.61$	$\tau = 0$	0.0063	0.0281	0.0281	0.0456	0.1211	0.1227	0.0616	0.2127	0.2165
	$\tau = 0.1$	0.0772	0.1641	0.1701	0.0545	0.1568	0.1597	0.0616	0.2127	0.2165
	$\tau = 0.2$	0.0865	0.1719	0.1794	0.0584	0.1587	0.1622	0.0616	0.2127	0.2165
	$\tau = 0.3$	0.0960	0.1737	0.1829	0.0593	0.1563	0.1598	0.0616	0.2127	0.2165
$\tilde{E}_a = 0.65$	$\tau = 0$	0.1873	0.0324	0.0675	0.1005	0.1260	0.1361	0.0616	0.2127	0.2165
	$\tau = 0.1$	0.0945	0.1653	0.1743	0.0693	0.1555	0.1603	0.0616	0.2127	0.2165
	$\tau = 0.2$	0.0959	0.1727	0.1819	0.0642	0.1561	0.1602	0.0616	0.2127	0.2165
	$\tau = 0.3$	0.1051	0.1754	0.1864	0.0628	0.1550	0.1590	0.0616	0.2127	0.2165
$\tilde{E}_a = 0.7$	$\tau = 0$	0.4361	0.0346	0.2248	0.1569	0.1321	0.1567	0.0616	0.2127	0.2165
	$\tau = 0.1$	0.1013	0.1683	0.1786	0.0910	0.1532	0.1615	0.0616	0.2127	0.2165
	$\tau = 0.2$	0.1119	0.1712	0.1837	0.0794	0.1556	0.1619	0.0616	0.2127	0.2165
	$\tau = 0.3$	0.1133	0.1768	0.1896	0.0707	0.1570	0.1620	0.0616	0.2127	0.2165

Table 3.5 Simulation results (censoring time = 10000hrs)

$\tilde{E}_a$	τ	APC			FSPC			MLE		
		Bias	Var.	MSE	Bias	Var.	MSE	Bias	Var.	MSE
$\tilde{E}_a = 0.5$	$\tau = 0$	-0.2721	0.0278	0.1018	-0.0483	0.0830	0.0857	0.0557	0.1163	0.1194
	$\tau = 0.1$	0.0003	0.0723	0.0723	0.0105	0.0865	0.0864	0.0557	0.1163	0.1194
	$\tau = 0.2$	0.0293	0.0885	0.0893	0.0209	0.0900	0.0894	0.0557	0.1163	0.1194
	$\tau = 0.3$	0.0384	0.0920	0.0935	0.0291	0.0900	0.0908	0.0557	0.1163	0.1194
$\tilde{E}_a = 0.55$	$\tau = 0$	-0.1462	0.0281	0.0495	-0.0030	0.0870	0.0867	0.0557	0.1163	0.1194
	$\tau = 0.1$	0.0251	0.0858	0.0864	0.0211	0.0880	0.0875	0.0557	0.1163	0.1194
	$\tau = 0.2$	0.0370	0.0912	0.0926	0.0269	0.0900	0.0897	0.0557	0.1163	0.1194
	$\tau = 0.3$	0.0436	0.0929	0.0948	0.0306	0.0900	0.0906	0.0557	0.1163	0.1194
$\tilde{E}_a = 0.61$	$\tau = 0$	0.0095	0.0306	0.0306	0.0354	0.0879	0.0892	0.0557	0.1163	0.1194
	$\tau = 0.1$	0.0386	0.0891	0.0906	0.0315	0.0890	0.0886	0.0557	0.1163	0.1194
	$\tau = 0.2$	0.0424	0.0921	0.0939	0.0332	0.0898	0.0909	0.0557	0.1163	0.1194
	$\tau = 0.3$	0.0490	0.0930	0.0969	0.0340	0.0898	0.0909	0.0557	0.1163	0.1194
$\tilde{E}_a = 0.65$	$\tau = 0$	0.1275	0.0313	0.0476	0.0564	0.0840	0.0867	0.0557	0.1163	0.1194
	$\tau = 0.1$	0.0510	0.0894	0.0920	0.0396	0.0870	0.0882	0.0557	0.1163	0.1194
	$\tau = 0.2$	0.0492	0.0921	0.0946	0.0378	0.0900	0.0908	0.0557	0.1163	0.1194
	$\tau = 0.3$	0.0511	0.0932	0.0958	0.0338	0.0900	0.0903	0.0557	0.1163	0.1194
$\tilde{E}_a = 0.7$	$\tau = 0$	0.2830	0.0344	0.1135	0.0938	0.0820	0.0908	0.0557	0.1163	0.1194
	$\tau = 0.1$	0.0670	0.0899	0.0944	0.0518	0.0860	0.0889	0.0557	0.1163	0.1194
	$\tau = 0.2$	0.0558	0.0923	0.0954	0.0434	0.0900	0.0903	0.0557	0.1163	0.1194
	$\tau = 0.3$	0.0545	0.0936	0.0966	0.0383	0.0900	0.0911	0.0557	0.1163	0.1194

Based on the results, we first plot the bias of $\hat{\mu}_0$ against $\left(\tilde{E}_a, \tau\right)$ for different censoring time in Figure 3.10.

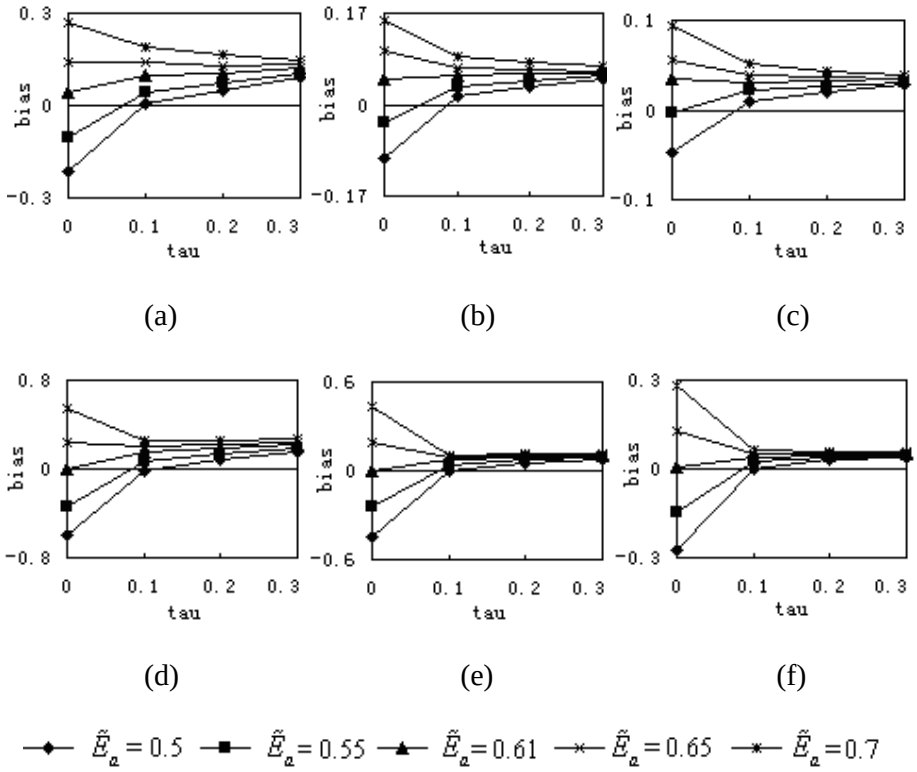

Figure 3.10 Effects of $(\tilde{E}_a, \tau)$ on the bias of $\hat{\mu}_0$

(a) APC is used, and the censoring time is 2500 hrs. (b) APC is used, and the censoring time is 5000 hrs. (c) APC is used, and the censoring time is 10000 hrs. (d) FSPC is used, and the censoring time is 2500 hrs. (e) FSPC is used, and the censoring time is 5000 hrs. (f) FSPC is used, and the censoring time is 10000 hrs.

The plot suggests the following observations.

O1: The longer the test duration, the smaller the bias of $\hat{\mu}_0$. Given a certain level of τ, the more accurate the specified $\tilde{E}_a$, the smaller the bias of $\hat{\mu}_0$. When $\tilde{E}_a$ is over-specified (under-specified), the estimate $\hat{\mu}_0$ has a positive (negative) bias.

O2: Regardless of the $\tilde{E}_a$ value, the bias of $\hat{\mu}_0$ converges to a positive value as the

tolerance τ grows. This is because when τ becomes larger, the estimate $\hat{\mu}_0$ depends more on the failure data and less on our prior knowledge. Since the data are time censored to the right, it is therefore not surprising to see a positively biased $\hat{\mu}_0$. This also explains why the bias is actually small when $\tilde{E}_a$ is under-specified and τ is moderate. For example, when $\tilde{E}_a$ =0.5 and τ =0.1, the bias of $\hat{\mu}_0$ is the smallest for both APC and FSPC. That is, the effect of under-specifying $\tilde{E}_a$ cancels that of time censoring.

O3: FSPC depends less on the expert knowledge compared to APC, hence, FSPC yields smaller bias than APC when $\tilde{E}_a$ deviates from 0.61. However, when the specified $\tilde{E}_a$ is close to the true value, APC yields a smaller bias than FSPC. This is a trade-off.

The pre-specified $\left(\tilde{E}_a, \tau\right)$ not only affects the bias but also the variance of $\hat{\mu}_0$. The variance of $\hat{\mu}_0$ against $\left(\tilde{E}_a, \tau\right)$ for different censoring time is plotted in Figure 3.11. For both APC and FSPC, the bigger the tolerance τ, the higher the uncertainty of the prior knowledge, and the bigger the variance of $\hat{\mu}_0$. If we compare both bias and variance of the estimates given by all these 3 methods, another two important observations are found in Figure 3.12.

O4: FSPC is more robust than APC to the variation of $\left(\tilde{E}_a, \tau\right)$. Although both the absolute bias and variance of $\hat{\mu}_0$ yielded by FSPC vary with $\left(\tilde{E}_a, \tau\right)$, the variation is much smaller compared to the results given by APC. Of course, APC has certain advantages in two situations. 1) When the activation energy E_a is accurately pre-specified (i.e. $\tilde{E}_a$ is near 0.61 and τ is small), APC gives the estimate with smaller bias and variance; 2) When $\tilde{E}_a$ is under-specified, say 0.5, and τ is moderate, say 0.1,

APC also gives the estimate with small bias and moderate variance. As we have explained above, this is due to the cancellation of effects between under-specifying $\tilde{E}_a$ and time censoring.

O5: Either APC or FSPC gives smaller variance of $\hat{\mu}_0$ than MLE particularly when the test duration is long. This is indeed the advantage of the proposed Bayesian inference over MLE, although the estimate obtained from the former method could be more biased for some $(\tilde{E}_a, \tau)$ combinations. Fortunately, when the test duration is long FSPC is robust enough in the sense that the surface of the absolute bias given by FSPC is flat and close to the surface given by MLE.

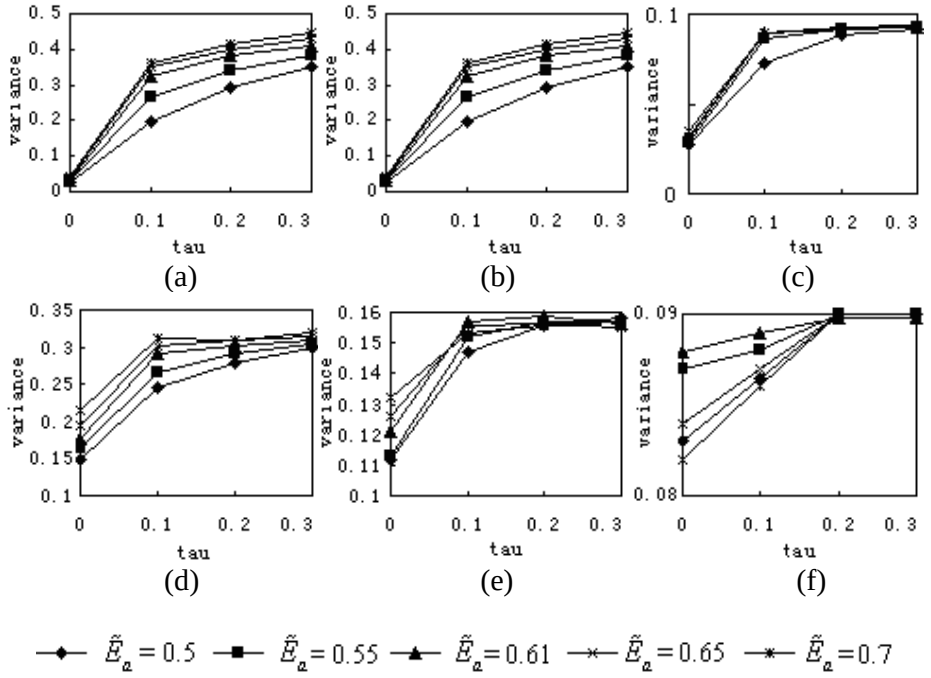

Figure 3.11 Effects of $(\tilde{E}_a, \tau)$ on the variance of $\hat{\mu}_0$

(a) APC is used, and the censoring time is 2500 hrs. (b) APC is used, and the censoring time is 5000 hrs. (c) APC is used, and the censoring time is 10000 hrs. (d) FSPC is used, and the censoring time is 2500 hrs. (e) FSPC is used, and the censoring time is 5000 hrs. (f) FSPC is used, and the censoring time is 10000 hrs.

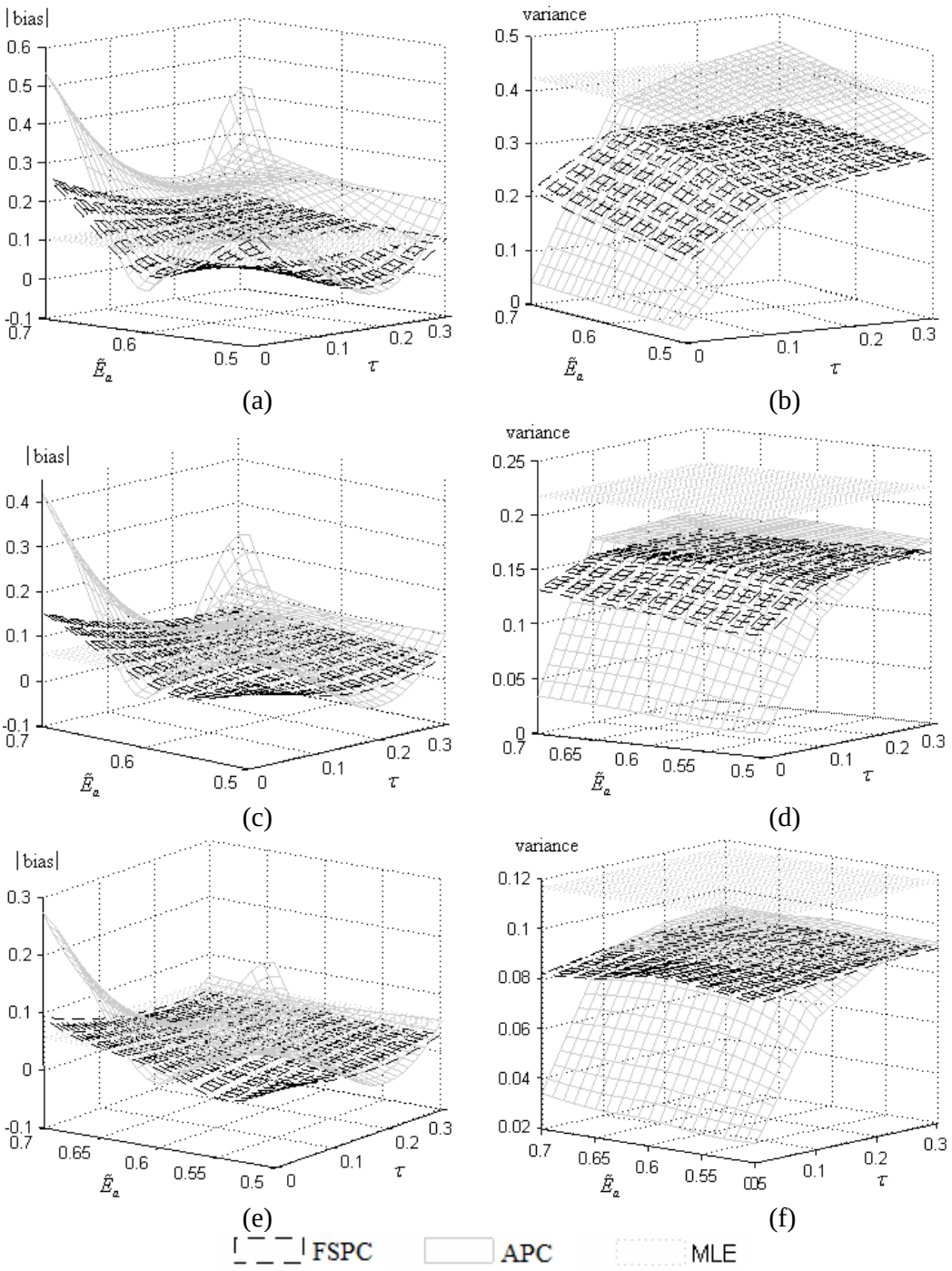

Figure 3.12 Comparison of both bias and variance among APC, FSPC and MLE (a) bias of $\hat{\mu}_0$, censoring time: 2500hrs (b) variance of $\hat{\mu}_0$, censoring time: 2500hrs (c) bias of $\hat{\mu}_0$, censoring time: 5000hrs (d) variance of $\hat{\mu}_0$, censoring time: 5000hrs (e) bias of $\hat{\mu}_0$, censoring time: 10000hrs (f) variance of $\hat{\mu}_0$, censoring time: 10000hrs.

Chapter 4. Double-Stage Estimation Utilizing Initial Estimates and Prior Knowledge

In Chapter 3, we have seen how some prior knowledge of key ALT model parameters can be used in analyzing sequential ALT data. This chapter considers the inference problem for an important type of sequential accelerated life tests (ALT), and proposes an easy-to-apply double-stage estimation (DSE) procedure which utilizes both preliminary testing results and empirical engineering knowledge. A step-by-step description of the procedure is provided. The bias, (asymptotic) variance and mean-squared-error of the estimator are also derived so as to measure the risk of incorporating prior engineering knowledge into the data analysis. Finally, a simulation study is presented to compare the performance of DSE to that of MLE, and visualize the risk associated to the DSE procedure. To facilitate the use of the proposed procedure, a computer program coded under the MATLAB® Graphical User Interface Design Environment (GUIDE) is provided and available from the author.

4.1. Introduction

Recall a typical parametric model of constant-stress ALT that consists of two components:

Components 1: A log-location-scale distribution that models failure time T at any testing stress

$$F(t) = \Phi[(\log t - \mu)/\sigma] \quad ,$$

where μ and σ is respectively the location and scale parameters, and Φ is the standardized location-scale Cdf.

Components 2: A linear stress-life relationship that describe the manner in which the life time distribution changes across different stress levels

$$\mu_i = \beta_0 + \beta_1 \cdot s_i \quad , \quad \sigma = \text{unknown constant} \qquad \forall i = 0,1,...,k \tag{4.1}$$

where s_i denotes the possibly transformed testing stress. Clearly, this model involves 3 model parameters $\boldsymbol{\varphi} = (\beta_0, \beta_1, \sigma)$.

Based on the framework of sequential ALT presented in Chapter 3, the test at the highest testing stress level s_k yields the initial estimate $\hat{\boldsymbol{\theta}}_k = (\hat{\mu}_k, \hat{\sigma})$. Then, from the prior knowledge on β_1, we also obtain the initial estimate $\tilde{\boldsymbol{\theta}}_i$ of $\boldsymbol{\theta}_i$ at any lower stress level for $i = 1, 2, ..., k-1$

$$\tilde{\boldsymbol{\theta}}_i = (\hat{\mu}_k + \beta_1(s_i - s_k), \hat{\sigma}) \qquad \forall i = 1, 2, ..., k-1 \tag{4.2}$$

On the other hand, test at stress s_i also yields a *local* estimate $\hat{\boldsymbol{\theta}}_i$ of $\boldsymbol{\theta}_i$. If $\hat{\boldsymbol{\theta}}_i$ implies that the initial estimate $\tilde{\boldsymbol{\theta}}_i$ is reasonable, we "shrink" $\hat{\boldsymbol{\theta}}_i$ towards $\tilde{\boldsymbol{\theta}}_i$ to yield the final estimate of $\hat{\boldsymbol{\theta}}_i$

$$\hat{\boldsymbol{\theta}}_i = \Gamma(\hat{\boldsymbol{\theta}}_i, \tilde{\boldsymbol{\theta}}_i) \tag{4.3}$$

where Γ is the shrinkage rule to be determined in this chapter.

The main object of the double-stage estimation above is to save sample size or test duration by utilizing initial estimates and prior information and yet to retain high efficiency. Readers might recognize that this is exactly the fundamental idea of double-stage shrinkage estimator (DSSE) discussed in Al-Bayyati and Arnold (1972).

In what follows, we formally propose a double-stage estimator, and quantify the bias, asymptotic variance of such an estimator given initial estimates and prior knowledge.

4.1.1. The Model

The SALT model presented in Section 3.2 is used throughout this chapter.

4.2. The Double-Stage Estimation

As discussed above, initial estimates obtained at the highest stress s_k and the prior knowledge on β_1 could be used together for data analysis at lower stress levels s_i for $i = 1, 2, ..., k-1$. As shown in Figure 4.1, the double-stage estimation of ALT data involves the following steps,

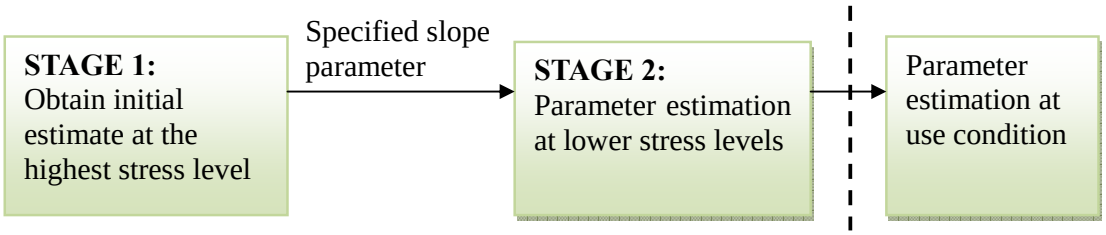

Figure 4.1 A flow chart of ALT data analysis using the double-stage estimation

4.2.1. STAGE 1: Obtain the Initial Estimate

At the highest stress s_k, the log-likelihood function corresponding to the observed (log) failure data $\mathbf{y}_k = (y_{k,1}, y_{k,2}, \cdots, y_{k,n_k})$ is given by

$$l(\boldsymbol{\theta}_k; \mathbf{y}_k) = \sum_{j=1}^{n_k} \left\{ \kappa_{k,j} \left(\log \frac{1}{\sigma} + \frac{y_{k,j} - \mu_k}{\sigma} - \exp\left(\frac{y_{k,j} - \mu_k}{\sigma} \right) \right) - (1 - \kappa_{k,j}) \exp\left(\frac{y_{k,j} - \mu_k}{\sigma} \right) \right\} \quad (4.4)$$

where the subscript "$(\cdot)_{i,j}$" corresponds to the *jth* observation at stress s_i, and κ is defined as

$$\kappa = \begin{cases} 0 & \text{for right-censored observation} \\ 1 & \text{for exact observation} \end{cases}$$

Numerically maximizing (4.4) yields the MLE

$$\hat{\boldsymbol{\theta}}_k = \arg\max l(\boldsymbol{\theta}_k ; \mathbf{y}_k), \tag{4.5}$$

with asymptotic covariance matrix

$$\hat{\Sigma}_{\hat{\boldsymbol{\theta}}_k} = \begin{pmatrix} \mathrm{var}(\hat{\mu}_k) & \mathrm{cov}(\hat{\mu}_k, \hat{\sigma}_k) \\ \mathrm{cov}(\hat{\mu}_k, \hat{\sigma}_k) & \mathrm{var}(\hat{\sigma}_k) \end{pmatrix} = \left(-\frac{\partial^2 l(\boldsymbol{\theta}_k ; \mathbf{y}_k)}{\partial \boldsymbol{\theta}_k^{\,2}} \right)^{-1}_{\boldsymbol{\theta}_k = \hat{\boldsymbol{\theta}}_k}$$

Hence, given an empirically specified β_1, the initial estimate, $\tilde{\boldsymbol{\theta}}_i$, of $\boldsymbol{\theta}_i$ at low stresses, $\{s_i\}_{i=1}^{k-1}$, are obtained through the stress-life relationship

$$\tilde{\boldsymbol{\theta}}_i = (\hat{\mu}_k + \beta_1 (s_i - s_k), \hat{\sigma}_k) \qquad \forall i = 1, ..., k-1 \quad , \tag{4.6}$$

with asymptotic covariance matrix $\hat{\Sigma}_{\tilde{\boldsymbol{\theta}}_i} = \hat{\Sigma}_{\hat{\boldsymbol{\theta}}_k}$.

4.2.2. STAGE 2: Obtain the Shrinkage Estimates

As the sequential test proceeds to the 2nd stage, n_i observations, $\mathbf{y}_i = (y_{i,1}, \cdots, y_{i,n_i})$, at each low stress s_i are obtained. Using these observations, we obtain the MLE of $\boldsymbol{\theta}_i$

$$\widehat{\boldsymbol{\theta}}_i = \arg\max l(\boldsymbol{\theta}_i ; y_i) \qquad \forall i = 1, ..., k-1 \quad , \tag{4.7}$$

where $\widehat{\boldsymbol{\theta}}_i$ is referred as the local estimate of $\boldsymbol{\theta}_i$.

To obtain the shrinkage estimate of $\boldsymbol{\theta}_i$, it is proposed to maximize the log-likelihood function

$$\begin{aligned} & l(\boldsymbol{\theta}_i ; \mathbf{y}_k, \mathbf{y}_i) \\ & = \sum_{j=1}^{n_k} \left\{ \kappa_{k,j} \left(-\log\sigma + \frac{\log A_i + y_{k,j} - \mu_i}{\sigma} - \exp\left(\frac{\log A_i + y_{k,j} - \mu_i}{\sigma} \right) \right) \right\} \\ & \qquad \left\{ -(1 - \kappa_{k,j}) \exp\left(\frac{\log A_i + y_{k,j} - \mu_i}{\sigma} \right) \right\} \\ & + \sum_{j=1}^{n_i} \left\{ \kappa_{i,j} \left(-\log\sigma + \frac{y_{i,j} - \mu_i}{\sigma} - \exp\left(\frac{y_{i,j} - \mu_i}{\sigma} \right) \right) - (1 - \kappa_{i,j}) \exp\left(\frac{y_{i,j} - \mu_i}{\sigma} \right) \right\} \end{aligned} \tag{4.8}$$

where $A_i = \exp(\beta_1(s_i - s_k))$ is known as the time-scale factor (Meeker and Escobar 1998).

That is, given the specified β_1, we map the data, $\mathbf{y}_k$, observed at s_k to s_i according to

$$\begin{aligned}\mathbf{y}_i' &= f(\mathbf{y}_k;\beta_1) \\ &= \beta_1(s_i - s_k) + \mathbf{y}_k = \log A_i + \mathbf{y}_k \quad \forall i = 1,2,\cdots,k-1\end{aligned}, \tag{4.9}$$

as if $\mathbf{y}_i'$ was collected from s_i.

Then, the shrinkage estimates $\hat{\boldsymbol{\theta}}_i$ are obtained as

$$\hat{\boldsymbol{\theta}}_i = \arg\max l(\boldsymbol{\theta}_i;\mathbf{y}_k,\mathbf{y}_i) \qquad \forall i = 1,...,k-1 \quad , \tag{4.10}$$

with asymptotic covariance matrix

$$\hat{\Sigma}_{\hat{\boldsymbol{\theta}}_i} = \begin{pmatrix} \mathrm{var}(\hat{\mu}_i) & \mathrm{cov}(\hat{\mu}_i,\hat{\sigma}_i) \\ \mathrm{cov}(\hat{\mu}_i,\hat{\sigma}_i) & \mathrm{var}(\hat{\sigma}_i) \end{pmatrix} = \left(-\frac{\partial^2 l(\boldsymbol{\theta}_i;\mathbf{y}_k,\mathbf{y}_i)}{\partial \boldsymbol{\theta}_i^{\,2}} \right)^{-1}_{\boldsymbol{\theta}_i = \hat{\boldsymbol{\theta}}_i} \qquad \forall i = 1,...,k-1$$

In order to see the shrinkage structure clearly, we assume σ to be known. It follows from (4.10) that

$$\exp\left(\frac{\hat{\mu}_i}{\sigma}\right) = \frac{r_k}{r_k + r_i}\exp\left(\frac{\tilde{\mu}_i}{\sigma}\right) + \frac{r_i}{r_k + r_i}\exp\left(\frac{\widehat{\mu}_i}{\sigma}\right) \quad \forall i = 1,2,\cdots,k-1, \tag{4.11}$$

or equivalently

$$\hat{\alpha}_i^{\,\beta} = \frac{r_k}{r_k + r_i}\tilde{\alpha}_i^{\,\beta} + \frac{r_i}{r_k + r_i}\widehat{\alpha}_i^{\,\beta} \qquad \forall i = 1,2,\cdots,k-1. \tag{4.12}$$

We see that from (4.11), $\hat{\mu}_i$ is always between $\tilde{\mu}_i$ and $\widehat{\mu}_i$, i.e. $(\hat{\mu}_i - \tilde{\mu}_i)/(\hat{\mu}_i - \widehat{\mu}_i) < 0$, and the ratio $|\hat{\mu}_i - \tilde{\mu}_i| / |\hat{\mu}_i - \widehat{\mu}_i|$ is monotone increasing as r_i / r_k. The interpretation of this observation is clear: as more failures are obtained at low stresses, the shrinkage estimate moves towards the local estimate. Similar observation also holds for (4.12). Also note that, equation (4.12) is exactly of the form of the equation (1) in Al-Bayyati and Arnold (1972), where the shrinkage estimator is a

linear combination of initial and local estimators.

Remark 4.1. Instead of using MLE, the best linear unbiased estimates (BLUE), $\hat{\boldsymbol{\theta}}_i$, based on order statistics can also be obtained given an empirically specified value of β_1. Interested readers might consult the method described in Nelson and Hahn (1972, 1973).

4.2.3. Obtain the Least-Squares Estimates

The generalized least squares can now be used to find the estimate, $\hat{\boldsymbol{\varphi}}$. Let

$$\hat{\mu} = (\hat{\mu}_1, \hat{\mu}_2, \cdots, \hat{\mu}_k)^T \quad , \quad V = \begin{pmatrix} \mathrm{var}(\hat{\mu}_1) & & \\ & \mathrm{var}(\hat{\mu}_2) & \\ & & \ddots \\ & & & \mathrm{var}(\hat{\mu}_k) \end{pmatrix} \quad ,$$

and define the design matrix

$$S = \begin{pmatrix} 1, & 1, & \cdots, 1 \\ s_1, & s_2, & \cdots, s_k \end{pmatrix}^T ,$$

the estimate $\hat{\boldsymbol{\varphi}}$ is then given by

$$\begin{pmatrix} \hat{\beta}_0 \\ \hat{\beta}_1 \end{pmatrix} = \left(S^T V^{-1} S\right)^{-1} \left(S^T V^{-1} \hat{\mu}\right) \quad , \qquad (4.13)$$
$$\hat{\sigma} = \left(\sum_{i=1}^{k} \mathrm{var}^{-1}(\hat{\sigma}_i)\right)^{-1} \sum_{i=1}^{k} \hat{\sigma}_i \, \mathrm{var}^{-1}(\hat{\sigma}_i)$$

with covariance matrix

$$\hat{\Sigma}_{\hat{\boldsymbol{\varphi}}} = \hat{\sigma}^2 \cdot \left(\begin{array}{c|c} \left(S^T V^{-1} S\right)^{-1} & \\ \hline & \left(\sum_{i=1}^{k} \mathrm{var}^{-1}(\hat{\sigma}_i)\right)^{-1} \end{array}\right) \quad . \qquad (4.14)$$

If the 100p-th life quantile, $y_p(s_0)$, at use stress is of interest, we have

$$\hat{y}_p(s_0) = \hat{\beta}_0 + \hat{\beta}_1 s_0 + z_p \hat{\sigma} \qquad z_p = \log(-\log(1-p)), \tag{4.15}$$

with variance

$$\text{var}(\hat{y}_p(s_0)) = (1, s_0, z_p)\hat{\Sigma}_{\hat{\beta}_1}(1, s_0, z_p)^T \tag{4.16}$$

Remark 4.2. In section 4.2.3, a linear stress-life relationship is fitted to the estimate, $\hat{\boldsymbol{\theta}}_i$, at each testing stress, $\{s_i\}_{i=1}^k$, weighted by the *amount of information* obtained at that level. This important idea in ALT data analysis can also be found in Nelson and Hahn (1972, 1973), as well as in the weighted regression approach presented by Lawless (1982).

4.3. Quantifying the Effects of Prior Knowledge

As discussed, it is of paramount importance to measure the risk of using the empirically specified β_1. Hence, this section derives the bias, (asymptotic) variance, and MSE of the estimator, $\hat{y}_p(s_0)$, for any given value of β_1.

In order to obtain the following analytic results, we are forced to assume σ to be a known constant since the closed-form solution of σ does not exist for (4.5), (4.7) and (4.10). In practice, the preliminary estimate of σ can be obtained numerically from the test at the highest stress, i.e. from (4.5).

4.3.1. The Bias

4.3.1.1. When the Slope Parameter is Correctly Specified

Let β_1^* denotes the (unknown) true value of β_1, we have

Lemma 4.1. For a known σ and $\beta_1 = \beta_1^*$, $\hat{y}_p(s_0)$ obtained in (4.15) is biased and has the bias

$$\begin{aligned}\text{bias}\left\{\hat{y}_p(s_0)\right\} &= E\left\{\hat{y}_p(s_0)\right\} - y_p(s_0) \\ &= (1, s_0)(S^T V^{-1} S)^{-1}(S^T V^{-1} b)\end{aligned} \quad , \tag{4.17}$$

where

$$b = \sigma \cdot \begin{pmatrix} \psi(0, r_k + r_1) - \log(r_k + r_1) \\ \vdots \\ \psi(0, r_k + r_{k-1}) - \log(r_k + r_{k-1}) \\ \psi(0, r_k) - \log(r_k) \end{pmatrix} \quad ,$$

for type-II censoring, and

$$b \approx \sigma \cdot \begin{pmatrix} \psi(0, r_k + r_1 + 2) - \log(r_k + r_1 + 2) \\ \vdots \\ \psi(0, r_k + r_{k-1} + 2) - \log(r_k + r_{k-1} + 2) \\ \psi(0, r_k + 1) - \log(r_k + 1) \end{pmatrix} \quad ,$$

for type-I censoring, and ψ is a Polygamma function.

Proof. Let

$$\lambda_i = \begin{cases} 0 & i = k \\ 1 & i = 1, 2, ..., k-1 \end{cases} \quad ,$$

we obtain the MLE, $\hat{\mu}_i$, from (4.5) and (4.10)

$$\hat{\mu}_i = \sigma \cdot (\log(Z_i^{(T)} + \lambda_i \cdot A_i^{1/\sigma} \cdot Z_k^{(T)}) - \log(r_i + \lambda_i \cdot r_k)) \qquad \forall\ i = 1, 2, ..., k\,, \tag{4.18}$$

where $Z_i^{(T)} = \sum_{j=1}^{n_i} \left(\kappa_{i,j} t_{i,j}^{1/\sigma} + \left(1 - \kappa_{i,j}\right) c_i^{1/\sigma} \right)$.

Here, $\hat{\mu}_i$ are biased with its bias given by

$$\begin{aligned}\text{bias}\left\{\hat{\mu}_i\right\} &= E\left\{\hat{\mu}_i\right\} - \mu_i \\ &= \sigma \cdot E\left\{ \log\left(\frac{Z_i^{(T)} + \lambda_i \cdot A_i^{1/\sigma} \cdot Z_k^{(T)}}{\alpha_i^{1/\sigma}} \right) - \log\left(r_i + \lambda_i \cdot r_k\right) \right\} \qquad \forall\ i = 1, 2, ..., k\end{aligned} \tag{4.19}$$

When $\beta_1 = \beta_1^*$, it is easy to see that the statistic

$$X_i = 2\alpha_i^{-1/\sigma} \cdot (Z_i^{(T)} + \lambda_i \cdot A_i^{1/\sigma} \cdot Z_k^{(T)}) \quad ,$$

follows the chi-square distribution with degree of freedom, $2(r_i + \lambda_i \cdot r_k)$, under type-II censoring (Meeker and Escobar 1998). For type-I censoring, we can approximate X_i by the chi-square distribution with degree of freedom, $2(r_i + 1 + \lambda_i(r_k + 1))$. This follows that

$$\sigma^{-1} \cdot \text{bias}\{\hat{\mu}_i\} = \begin{cases} \psi(0,(r_i + 1 + \lambda_i(r_k + 1))) - \log(r_i + \lambda_i \cdot r_k) & \text{for type-I censoring} \\ \psi(0,(r_i + \lambda_i r_k)) - \log(r_i + \lambda_i \cdot r_k) & \text{for type-II censoring} \end{cases} \tag{4.20}$$

and from equations (4.13) and (4.15), we obtain

$$\text{bias}\left\{\hat{y}_p(s_0)\right\} = (1, s_0)\left(S^T V^{-1} S\right)^{-1}\left(S^T V^{-1} b\right) \quad ,$$

as was to be proved.

4.3.1.2. When the Slope Parameter is Incorrectly Specified

In practice, however, the specified value of β_1 never equals β_1^*. Define

$$\begin{aligned} &\beta_1 = \beta_1^* + e \\ &A_i^{1/\sigma} = (A_i^*)^{1/\sigma} \cdot \delta_i \\ &A_i^* = \exp(\beta_1^*(s_i - s_k)) \\ &\delta_i = \exp(\sigma^{-1} e(s_i - s_k)) \end{aligned}$$

we have

Lemma 4.2. For a known σ and $\beta_1 = \beta_1^* + e$, $\hat{y}_p(s_0)$ obtained in (4.15) is biased and has the bias

$$\begin{aligned} \text{bias}\left\{\hat{y}_p(s_0)\right\} &= E\left\{\hat{y}_p(s_0)\right\} - y_p(s_0) \\ &= (1, s_0)(S^T V^{-1} S)^{-1}(S^T V^{-1}(\text{bias}\{\hat{\mu}_1\}, \text{bias}\{\hat{\mu}_2\}, ..., \text{bias}\{\hat{\mu}_k\})^T) \end{aligned} \tag{4.21}$$

where $\text{bias}\{\hat{\mu}_i\} = \sigma \cdot E\{\log(X_i / 2 + (\delta_i - 1) \cdot \lambda_i \cdot X_k / 2) - \log(r_i + \lambda_i \cdot r_k)\}$.

Proof. It follows from equation (4.19) that

$$\text{bias}\{\hat{\mu}_i\} = \sigma \cdot E\left\{\log\left(X_i/2 + (\delta_i - 1)\cdot\lambda_i \cdot X_k/2\right) - \log\left(r_i + \lambda_i \cdot r_k\right)\right\} \quad \forall i = 1,...,k\,. \tag{4.22}$$

Numerical methods, such as the Monte-Carlo method, are needed to evaluate this equation. When $e = 0$, equation (4.22) and (4.19) are exactly the same.

Finally, from equations (4.13) and (4.15), it is immediately that

$$\text{bias}\{\hat{y}_p(s_0)\} = (1, s_0)(S^T V^{-1} S)^{-1}(S^T V^{-1}(\text{bias}\{\hat{\mu}_1\}, \text{bias}\{\hat{\mu}_2\}, ..., \text{bias}\{\hat{\mu}_k\})^T) \quad ,$$

as was to be proved.

4.3.1.3. Bias of the Estimator on Lower Stress Levels

For estimates at each lower stress levels, we have another two interesting results summarized by Lemma 4.3 and Lemma 4.4.

Lemma 4.3: If the shape parameter β is known and the acceleration factor A_{ki} is correctly specified, for any positive constant κ we have,

$$\lim_{c_i, c_k \to \infty} E(\hat{\alpha}_i^{\beta}) = \alpha_i^{\beta} \qquad \forall i = 1, 2, ..., k-1$$

Proof: Given the observations (r_i , r_k , $\mathbf{t}_k$), $E(\hat{\alpha}_i^{\beta})$ at any lower stress test level s_i for $i = 1, 2, ..., k-1$ is given by

$$E(\hat{\alpha}_i^{\beta} \,|\, r_i, r_k, \mathbf{t}_k) = E\left(\left(\sum_{j=1}^{r_i} t_{ij}^{\beta} + \sum^{n_i - r_i} c_i^{\beta} + A_{ki}^{\beta} \cdot \left(\sum_{j=1}^{r_k} t_{kj}^{\beta} + \sum^{n_k - r_k} c_k^{\beta}\right)\right) / (r_i + r_k) \right) \tag{4.23}$$

Define the failure probability $P_i = 1 - \exp(-(c_i/\alpha_i)^{\beta})$ of an item at stress level s_i, we then have,

$$\begin{aligned} E\left(\hat{\alpha}_i^{\beta} \,|\, r_k, \mathbf{t}_k\right) &= \sum_{m=0}^{n_i} \Pr(r_i = m) E\left(\hat{\alpha}_i^{\beta} \,|\, r_i, r_k, t_{kj}\right) \\ &= \sum_{m=0}^{n_i} \binom{n_i}{m} P_i^m \left(1 - P_i\right)^{n_i - r_i} \frac{1}{r_k + m} \left(\sum_{j=1}^{m} E\left(t_{ij}^{\beta}\right) + \sum^{n_i - m} c_i^{\beta} + A_{ki}^{\beta} \left(\sum_{j=1}^{r_k} t_{kj}^{\beta} + \sum^{n_k - r_k} c_k^{\beta} \right) \right) \end{aligned}$$

(4.24)

It follows that,

$$E\left(\hat{\alpha}_i^{\beta}\middle|r_k\right)=\int_0^{c_k}E\left(\hat{\alpha}_i^{\beta}\middle|r_k,t_{kj}\right)\cdot f_k\left(t\right)dt$$
$$=\sum_{m=0}^{n_i}\binom{n_i}{m}P_i^k\left(1-P_i\right)^{n_i-F_i}\frac{1}{r_k+m}\left(\sum_{j=1}^{m}E\left(t_{ij}^{\beta}\right)+\sum^{n_i-m}c_i^{\beta}+A_{ki}^{\beta}\left(\sum_{j=1}^{r_k}E\left(t_{kj}^{\beta}\right)+\sum^{n_k-r_k}c_k^{\beta}\right)\right)$$

(4.25)

Finally,

$$E\left(\hat{\alpha}_i^{\beta}\right)=\sum_{m=1}^{n_k}P\left(r_k=m\right)E\left(\hat{\alpha}_i^{\beta}\middle|r_k\right)=\sum_{m=1}^{n_k}\frac{\binom{n_k}{m}P_k^m\left(1-P_k\right)^{n_k-m}}{1-\left(1-P_n\right)^{n_k}}E\left(\hat{\alpha}_i^{\beta}\middle|r_k=m\right)\qquad(4.26)$$

Equation (4.26) implies that, when the acceleration factor A_{ki} is correctly specified to its true value A_{ki}^{*}, for any positive constant κ we have,

$$\lim_{c_i,c_k\to\infty}E(\hat{\alpha}_i^{\beta})=\alpha_i^{\beta}\qquad\forall i=1,2,...,k-1\qquad(4.27)$$

Lemma 4.4: Let $A_{ki}^{*}=\sqrt[1/\beta]{M_{ki}^{*}}$, $A_{ki}^{(+)}=A_{ki}^{*}+\gamma_{ki}$, and $A_{ki}^{(-)}=A_{ki}^{*}-\gamma_{ki}$, then, the following result hold iff $\beta=1$

$$\lim_{c_i,c_k\to\infty}(E(\hat{\alpha}_i;A_{ki}^{(+)})+E(\hat{\alpha}_i;A_{ki}^{(-)}))=0\qquad\forall i=1,2,...,k-1$$

Proof: When A_{ki} is falsely specified as $A_{ki}=A_{ki}^{*}+e_{ki}$, for any lower stress level s_i we have

$$\lim_{c_i,c_k\to\infty}E(\hat{\alpha}_i^{\beta})=(n_i\alpha_i^{\beta}+(A_{ki}^{*}+e_{ki})^{\beta}n_k\alpha_k^{\beta})/(n_i+n_k)\qquad(4.28)$$

If failure times follow Exponential distribution, i.e. $\beta=1$, equation (4.28) yields,

$$\lim_{c_i,c_k\to\infty}E(\hat{\alpha}_i)=\alpha_i+\frac{n_k\alpha_k}{n_i+n_k}\cdot e_{ki}\qquad(4.29)$$

Hence, when $\beta=1$, we have

$$\lim_{c_i, c_k \to \infty} (E(\hat{\alpha}_i \mid A_{ki}^{(+)}) + E(\hat{\alpha}_i \mid A_{ki}^{(-)})) = 0 \qquad \forall i = 1, 2, ..., k-1 \tag{4.30}$$

It equation (4.29), $\lim_{c_i, c_k \to \infty} E\left(\hat{\alpha}_i^{\beta}\right)$ is a linear function of the error e. When the ratio between n_i and n_k increases, the term $n_k \alpha_k e/(n_i + n_k)$ becomes smaller which implies that the effect of the specified slope parameter vanishes as n_i/n_k approaches infinity. On the other hand, when n_i is small compared to n_k, the estimation results heavily depend on the specified slope parameter.

As a simple illustration, Figure 4.2 illustrates how the expectation $E(\hat{\alpha}_i^{\beta})$ varies with the test duration given that A_{ki} is correctly specified. When test duration is zero, $\hat{\alpha}_i^{\beta}$ is unbiased since $A_{ki} = A_{ki}^*$. As test proceeds, the bias grows towards the positive side since most data are censored during this phase. After a certain point, the bias decreases and eventually goes to zero.

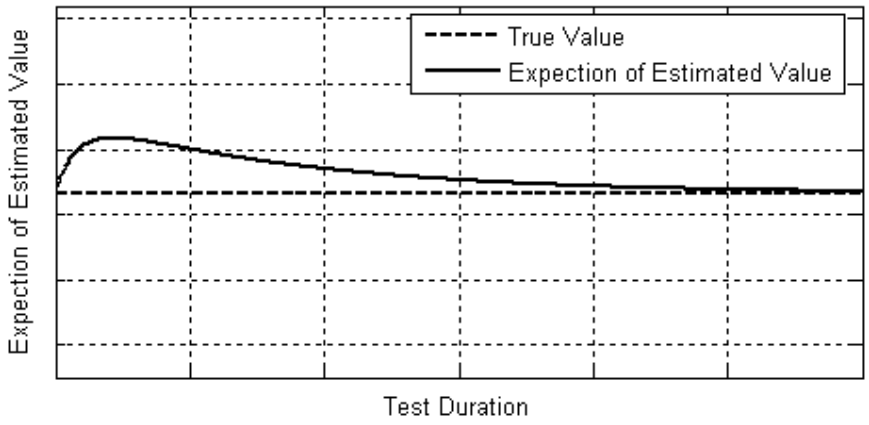

Figure 4.2 The bias of $\hat{\alpha}_i^{\beta}$ against test duration for any lower stress level i

When $A_{ki} \neq A_{ki}^*$, Figure 4.3 shows the effect of test duration on $E(\hat{\alpha}_i^{\beta})$ with $\beta = 1$. As seen in this figure, over-specifying and under-specifying A_{ki} have a symmetric effect on $\lim_{c_i, c_k \to \infty} E(\hat{\alpha}_i^{\beta})$ as implied by equation (4.29). As test duration becomes larger, the

distances between two neighboring curves converges to a constant which can be evaluated by equation (4.29).

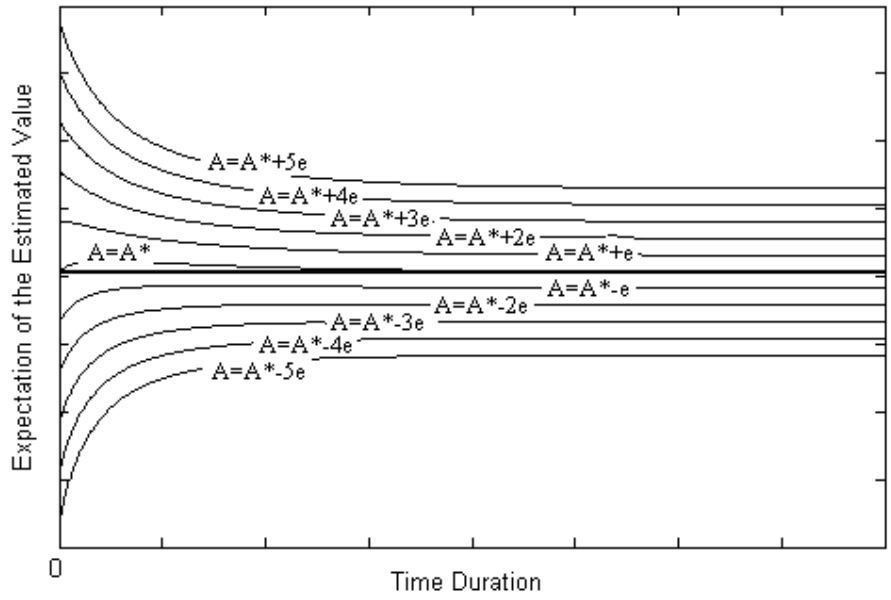

Figure 4.3 $E(\hat{\alpha}_i^{\beta})$ against test duration for any lower stress level i ($\beta = 1$)

Particularly when $\beta \neq 1$, over-specifying and under-specifying A_{ki} have an asymmetric effect on the value of $\lim_{c_i, c_k \to \infty} E(\hat{\alpha}_i^{\beta})$. This is shown in Figure 4.4.

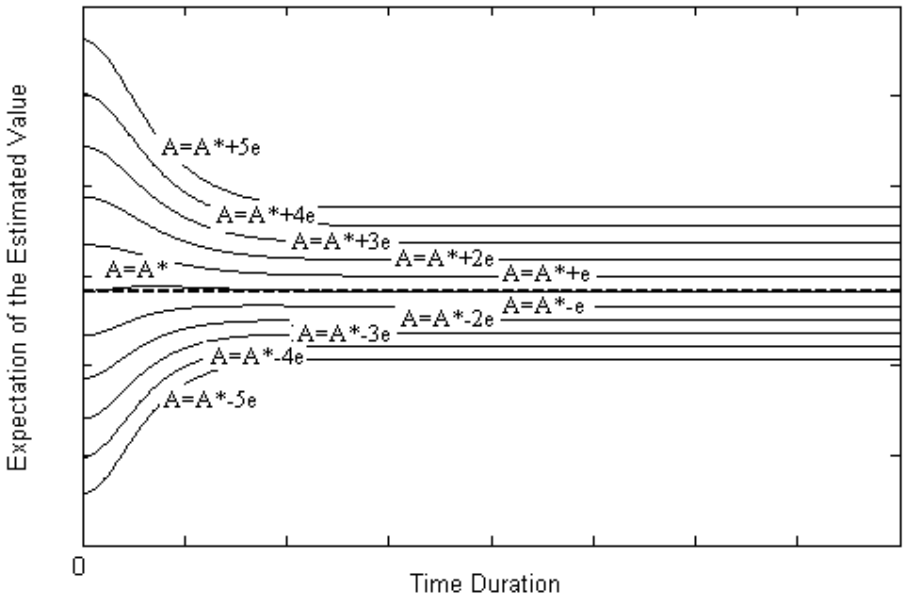

Figure 4.4 $E(\hat{\alpha}_i^{\beta})$ against test duration for any lower stress level i ($\beta = 2$)

4.3.2. The Mean-Squared-Error

Generally speaking, the main object of the double-stage estimation above is to save sample size or test duration by utilizing initial estimates and prior information and yet to retain high efficiency. However, as we have seen, the estimator is biased by incorporating the prior information. Therefore, the mean-squared-error of the estimator could be used to decide if the double-stage estimation should be used (see e.g. Al-Bayyati and Arnold 1972). Assuming the shape parameter β is known, the mean-squared-error (MSE) of $\hat{y}_p(s_0)$ is directly computed by,

$$\mathrm{MSE}\left\{\hat{y}_p(s_0)\right\} = \mathrm{bias}^2\left\{\hat{y}_p(s_0)\right\} + (1, s_0, z_p)\hat{\Sigma}_{\hat{\Phi}}(1, s_0, z_p)^T \tag{4.31}$$

4.4. Numerical Study

A simulation study is presented in this section to 1) compare the performance of DSE to that of MLE, and 2) visualize the risk associated to DSE.

A temperature-accelerated life test is used in this section. This real-life ALT was firstly reported by Hooper and Amster (1990). Table 4.1 summarizes the testing plan.

Table 4.1 A three-stress-level temperature-accelerated life test

Sequential testing stage	Condition	Temp	Stress level (11605 / Temp)	Censoring time (hrs)	Sample size
	Use	293K	39.6075		
Stage 1	High	353K	32.8754	5000	15
Stage 2	Low	313K	37.0767	5000	100
	Mid	333K	34.8498	5000	20

For this ALT, the log-lifetime under any temperature is assumed to follow the SEV distribution. The scale parameter σ is assumed to be constant independent of temperature, and the location parameter μ depends on temperature through the

Arrhenius life-stress relationship

$$\mu = \beta_0 + E_a \cdot 11605 / \text{Temp},$$

where E_a is the activation energy.

The objective of this ALT is to estimate the 0.1 life quantile $y_{.1}$ at the use temperature.

The simulation study is designed as follows.

1). *Generation of Failure Times*

To generate SEV failure times at each testing stress, the following values are used

$$\boldsymbol{\varphi}^* = (\phi_0^*, E_a^*, \sigma^*) = (-13.2043, 0.6302, 0.7084)$$

These values are the MLE of $\boldsymbol{\varphi}$ obtained using the original dataset published in Hooper and Amster (1990), and reprinted in Meeker and Escobar (1998).

2). *Simulation Procedure:*

Step-1: Simulate the testing data using $\boldsymbol{\varphi}^*$ and the plan given in Table 4.1.

Step-2a: Obtain the estimate, $\hat{y}_{.1}^{MLE}$, of $y_{.1}$ using MLE.

Step-2b: Set $E_a = 0.2\text{eV}$ (which is 31% of the true value, $E_a^* = 0.63\text{eV}$).

Step-3b: Obtain the estimate, $\hat{y}_{.1}^{DSE}$, of $y_{.1}$ using DSE.

Step-4b: If $E_a < 1\text{eV}$ (which is 160% of the true value, E_a^*), then, $E_a = E_a + 0.05$ and

go to *Step-3b*.

Otherwise, go to *Step-5*.

Step-5: Start the next iteration from *Step-1*

In this simulation study, 500 iterations are completed.

4.4.1. Simulation Results

Simulation results, i.e. the estimates, $\hat{y}_{.1}^{MLE}$ and $\hat{y}_{.1}^{DSE}$, obtained within each iteration are plotted in Figure 4.5. In this figure, $\hat{y}_{.1}^{*}$ is the (unknown) true value of $\hat{y}_{.1}$ calculated from $\boldsymbol{\varphi}^{*}$.

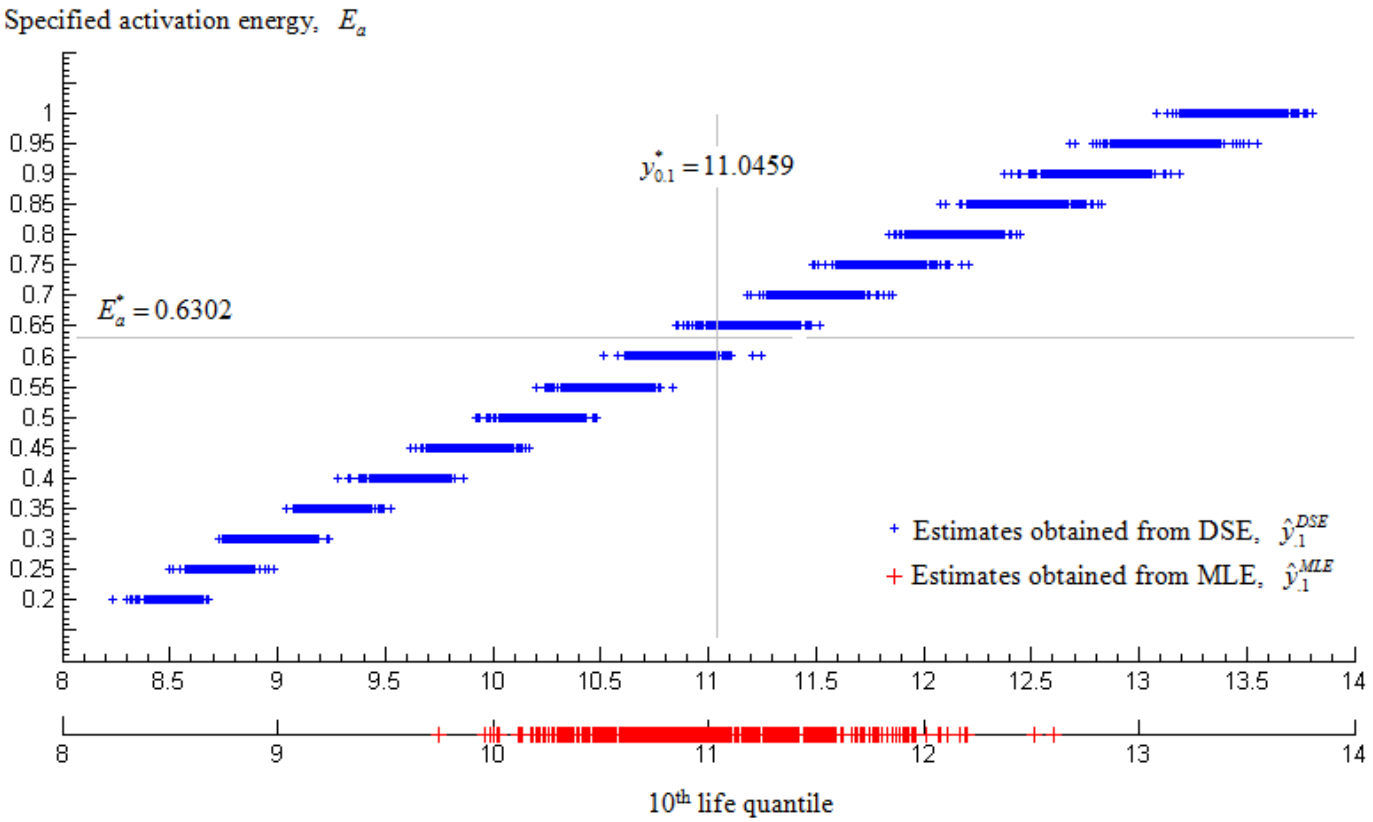

Figure 4.5 $b[\hat{y}_{.5}{}^{(MLE)}]$ and $b[\hat{y}_{.5}{}^{(DSE)}]$ against the specified activation energy E_a

The trade-off of using DSE is immediately seen from Figure 4.5. We define the relative risk

$$\eta = \mathrm{MSE}(\hat{y}_{.1}^{DSE}) / \mathrm{MSE}(\hat{y}_{.1}^{MLE}) \quad , \tag{4.32}$$

and plots η against the specified E_a in Figure 4.6. As seen in this figure, $\eta \le 1$ when E_a ranges from 0.47 to 0.78 , which are respectively 75% and 124% of the true value E_a^*.

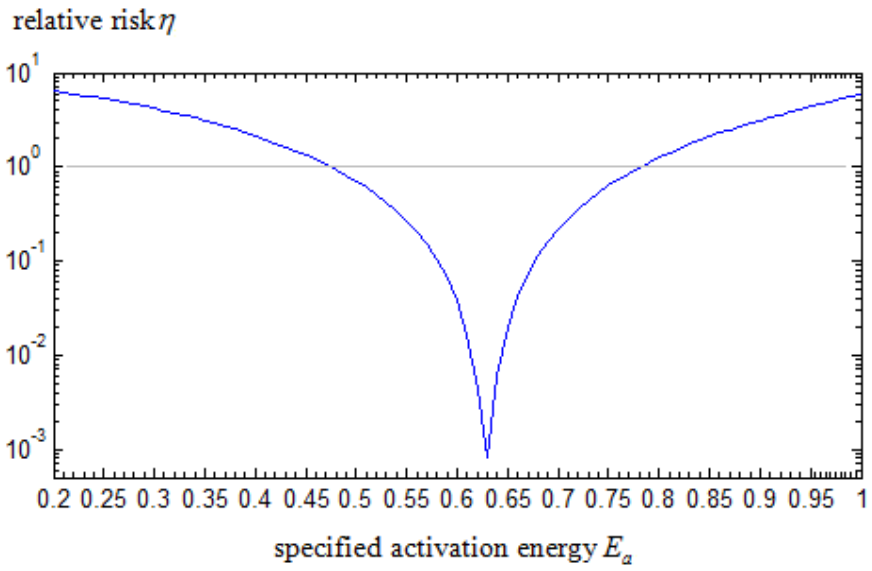

Figure 4.6 Plot of relative risk against the specified activation energy

Let E_a^+ and E_a^- respectively denote the upper and lower bound of E_a within which $\eta \le 1$, we extend the test duration from 5000 to 8000 to see how E_a^+ and E_a^- are changed correspondingly. Figure 4.7 plots both E_a^+ and E_a^- for different censoring times. It is seen that, the interval between E_a^+ and E_a^- becomes slightly wider as the test duration increases. This observation can be briefly explained by: since more failures are observed at low stresses for longer test duration, the shrinkage estimate at each stress is getting closer to the local estimate, and $\hat{y}_{.1}^{DSE}$ become less dependent on the

specified value of E_a.

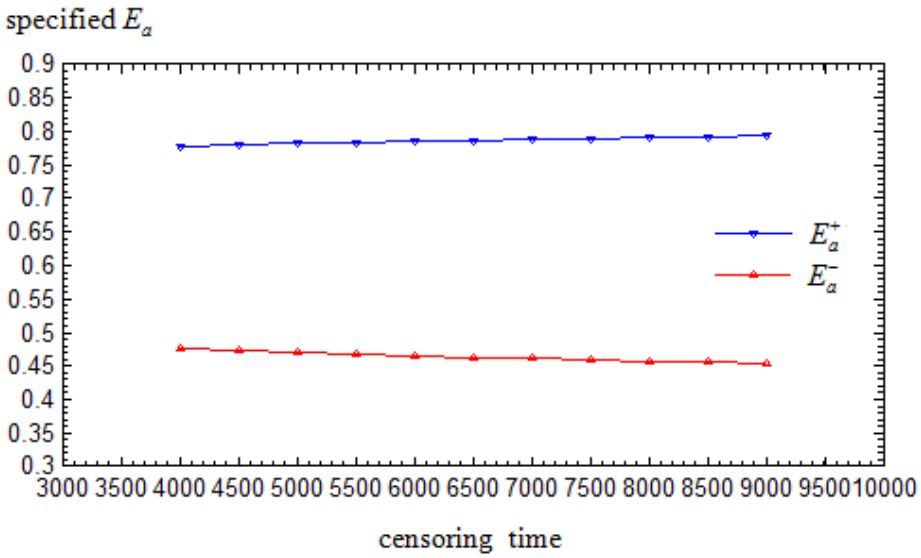

Figure 4.7 Plot of E_a^- and E_a^+ against censoring time

Remark 4.3. A natural extension of the DSE procedure can be immediately seen, namely, instead of specifying an exact value of β_1, a prior distribution $\vartheta(\beta_1)$ that quantifies the uncertainty over β_1 can be used. The resulting sequential Bayesian analysis is described in Liu and Tang (2009).

4.4.2. The Computerized Implementation

GUIDE, the MATLAB® graphical user interface development environment, provides a set of tools for creating graphical user interface (GUI). Hence, in order to facilitate the use of the proposed DSE method, the procedure is coded using the MATLAB® GUIDE.

Figure 4.8 shows the GUI of the DSE procedure for analyzing sequential ALT data. The 4 modules are briefly described as follows:

Module 1: Data import/input from workspace. Basic information, including testing

stress levels, use stress, censoring time, and the empirically specified slope parameter are the required inputs of this module. In addition, users are also required either input or import testing data. It is noted that in the censoring column, the text “0” and “1” respectively denotes the exact and right-censored observation.

Module 2: DSE procedure. Given the input of module 1, this module performs the DSE procedure and estimates key reliability measures, such as the stress-life model, covariance matrix of the estimate for model parameters, and important life-quantiles often used in practice.

Module 3: Weibull probability plot for the fitted model. Following the analysis in module 2, this module automatically generates the Weibull probability plot for the fitted model.

Module 4: Risk assessment. Given a possible deviation of the pre-specified slope parameter as well as the life-quantile of interest, this module estimates the bias, and MSE of the quantile estimator.

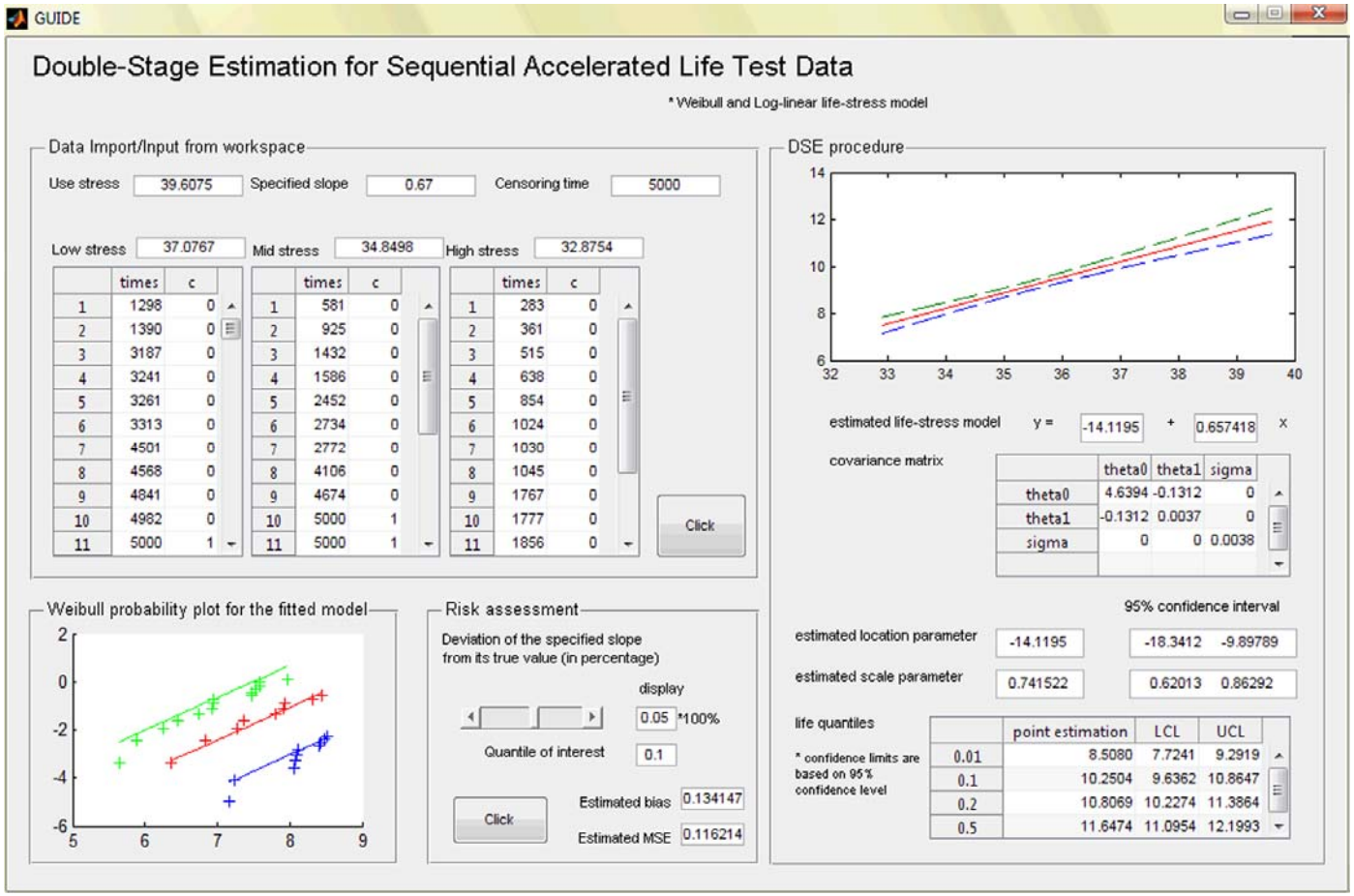

Figure 4.8 Graphical user interface (GUI) of MAT-DSE

Chapter 5. Bayesian Planning of Sequential ALT

5.1. Introduction

From this chapter onwards, our focus is turned to ALT planning problems.

Based on the sequential test scheme, this chapter describes a Bayesian planning method for sequential constant-stress ALT (A planning method for sequential ALT that is based on the likelihood theory is presented in Chapter 7). As discussed in Chapter 2, in planning of Accelerated Life Tests, preliminary estimates of unknown model parameters are often needed so as to assess the statistical efficiency of a test plan. Very often, the margin of error is high and the requisite level of statistical precision cannot be achieved as planned. Hence, test at the highest stress level is firstly planned and conducted under the sequential scheme. As we shall see in this chapter, a Bayesian framework is then deployed to incorporate the information obtained at the highest stress level in the planning of subsequent accelerated tests at lower stress levels. Under this framework, the normal approximation to posterior density is used, and both the optimum sample allocation and stress combinations at lower stress levels are chosen to minimize the pre-posterior variance of the estimate of the percentile of the time to failure at use condition. We shall see in this chapter how the proposed test scheme can be applied to design ALTs with 2 and 3 constant stress levels. A comprehensive simulation study can also be found that compares the performance of the sequential testing scheme to that of the traditional non-sequential testing. It can be seen that the robustness of an ALT plan can be greatly enhanced using the proposed approach without affecting the total test duration.

To plan a constant-stress ALT, one needs to decide 1) the stress level combinations and 2) the sample allocation to each stress level. Meeker and Escobar (1993) summarized the characterization of one- and two-factor constant-stress ALT test plans.

Most ALT plans involve constant stress loading. Very often, the lifetime at each stress is assumed to follow a log-location-scale life time distribution such as Weibull or Lognormal. A simple linear stress-life relationship between the location parameter and some function of stress are employed, and the scale parameter is assumed to be a constant independent of stress. Hence, three parameters are of interest in such a constant-stress ALT model, i.e., the scale parameter of the life time distribution, the intercept parameter of the linear stress-life relationship, and the slope parameters of the linear stress-life relationship. Each of these parameters has its own physical interpretation. The scale parameter is closely related to the failure mechanism; the intercept parameter is usually the median life (or a function of it) under a particular stress; and the slope parameter is the reflection of both product properties and acceleration mechanism. For example, under a temperature acceleration scheme in which the Arrhenius model is usually appropriate, there exists a one-to-one correspondence between the value of the slope parameter and the Arrhenius activation energy -- a property of the product in response to operation temperature.

The pioneering ideas of modern ALT planning techniques were conceived by Nelson and Kielpinski (1976), Nelson and Meeker (1978), Meeker (1984), and Nelson (1990). Given the prior information or pre-specified values of all three ALT model parameters, an optimum plan is typically the one that minimizes the asymptotic variance of the Maximum Likelihood Estimate (MLE) of certain reliability measure at use condition (*c*-optimality). Other planning criteria, such as the maximization of determinant of the Fisher information matrix for model parameters (*D*-optimality),

have also been used (e.g. Meeker and Escobar (1993)). Tang and Xu (2005) proposed a framework which considers multiple (conflicting) objectives in ALT planning. For a comprehensive review of different planning criteria, one may refer to Chaloner and Verdinelli (1995), and Pilz (1991). Recently, Pascual (2007) presented an ALT planning approach considering competing risks, and Meeker et al. (2005) discussed how to evaluate the developed optimum plans via simulation.

For many applications, the product life percentile at use condition is of interest. Then, the *c*-optimality criterion becomes appropriate. When the *c*-optimality is adopted as in most ALT plans, the asymptotic variance of the MLE is used as a yardstick in determining the optimum plan. As discussed in Chernoff (1972), the asymptotic variance depends on the "best guess" of the unknown model parameter values, and the developed plan is also known as the local optimal plan. Hence, assuming the model parameters are known at the planning stage might lead to a false sense of statistical precision. This is one of the key motivations of using Bayesian design methods. Although there has been a long-run debate on the theoretical framework of Bayesian approach, the primary consideration in practice is whether the method yields good result after balancing all potential risks and conflicting objectives. For example, Zhang and Meeker (2006) recently presented a general Bayesian method for planning ALTs. Instead of specifying exact values for those unknown model parameters, prior distributions are assigned to each parameter to enhance the robustness of the plan. Chaloner and Larntz (1992) not only used priors, but also assigned weights to different lifetime distributions and life-stress models. Pascual (2006) addressed the possibility of bias arising from mis-specifying the ALT model and developed a robust planning method. Comprehensive reviews of ALT planning can be found in the excellent books authored by Nelson (1990) and Meeker and Escobar (1998).

The sequential testing scheme presented in this chapter is motivated by the following observations from practice. First, it is difficult to specify the unknown model parameters at the planning stage. As we have discussed above, misspecification of model parameters leads to a false sense of statistical precision. When tests at all stress levels are simultaneously done, there are a few adjustments engineers can do when they finally realize that some model parameters are mis-specified.

Second, the degree of difficulty in specifying the unknown model parameters is different, i.e. the amount of prior information we have on each unknown parameter is usually not the same. Zhang and Meeker (2006) have already provided a discussion on this issue. If we assume a log-location-scale failure-time distribution as well as a log-linear stress-life model, it might be relatively easier for us to specify the value of the slope parameter. In the case of the Arrhenius model, specifying the slope parameter is equivalent to specifying the Arrhenius activation energy. For many applications, the ranges of the activation energy for typical failure mechanisms have already been well defined particularly for consumer electronics. This even allows some ALT to be conducted at only one extreme stress level (e.g. MIL-STD-883). On the other hand, the specification of the intercept parameter and the scale parameter appears to be much more difficult. The value of the intercept parameter might be specified from product/design specifications, or prior knowledge from similar products, but the margin of the specification error is usually so high that easily lead to a poor plan which provides a false sense of statistical precision. For the scale parameter, what engineers usually know is whether it is larger or smaller than a certain value, say 1.

Third, the values of the intercept and the slope parameters are directly related to the logarithm life at various stress levels. Conducting the ALT in a sequential manner will help in specifying the intercept parameter. Moreover, in situations where ALT with

more than one stress level cannot be simultaneously run, sequential testing is commonly adopted. Hence, when the test results of the first batch of units become available, engineers should be able to use this fresh information to plan or adjust the subsequent tests. For more discussions on sequential testing and design of experiment, one may refer to Chernoff (1972), Pilz (1991), Wetherill and Glazebrook (1986), and Michlin et al. (2008).

In the rest of the chapter, we first present 1) the statistical model of a constant-stress ALT in Section 5.1.2; 2) the framework of the sequential ALT planning and inference in Section 5.2; 3) numerical examples that illustrates the application of the proposed method in Section 5.3; and 4) simulation studies that compare the performance of the sequential planning to that of the traditional non-sequential planning in Section 5.4.

5.1.1. The Model

The model presented in Section 3.2 is still in use. However, in order to facilitate the discussion of this chapter, new notations and different parameterization are introduced. Hence, the full model is given as follows,

- k stress levels are involved in the test. Very often, the stress s_i (possibly transformed) is parameterized as (Nelson (1990), pp. 320)

  $$x_i = (s_i - s_k)/(s_0 - s_k) \quad \text{for } i = 0,1,...,k\,. \tag{5.1}$$

  In (5.1), s_k is the highest stress and is specified; s_0 is the design stress where a given percentile is to be estimated. Clearly, $x_0 = 1$ at s_0; and $x_k = 0$ at s_k.

- N specimens are available for the test. At each stress level x_i, n_i number of specimens are tested untill a pre-specified time c_i (type-I censored). Let r_i be the

number of failures at stress x_i and the failure time T follows Weibull distribution. Hence, the logarithm failure time Y follows the Smallest Extreme Value (SEV) distribution with location μ_i and scale σ_i, i.e.,

$$F(y;\boldsymbol{\theta}) = 1 - \exp(-\exp((y-\mu_i)/\sigma_i)) \quad \text{where } \boldsymbol{\theta} = (\mu, \sigma).$$

In this chapter, y_{ij} denotes the logarithm failure time of the jth unit at stress i, and is standardized as $z_{ij} = (y_{ij} - \mu_i)/\sigma_i$. Similarly, we also standardize the censoring time as $\zeta_i = (\log(c_i) - \mu_i)/\sigma_i$, and define an index κ_{ij} such that κ_{ij} =1 if $z_{ij} < \zeta_i$; otherwise κ_{ij} =0;

- The location parameter μ depends on stress through a linear stress-life model

$$\mu_i = \beta_0 + \beta_1 x_i \tag{5.2}$$

From equation (5.1), we have $\beta_0 = \mu_k$ and $\beta_1 = \mu_0 - \mu_k$. It is also noted that many important stress-life models, including the Arrhenius model and Inverse Power relationship can both be expressed by (5.2) after certain parameterizations (Nelson (1990)).

- The scale parameter σ is a constant independent of stress, i.e. $\sigma = \sigma_0 = \sigma_1 = ... = \sigma_k$

The 100p-th percentile of the SEV distribution $y_p(x_0) = \beta_0 + \beta_1 x_0 + u_p \cdot \sigma_0$ at the design stress x_0 is to be estimated, where $u_p = \ln[-\ln(1-p)]$.

5.2. The Framework of the Sequential ALT Planning

The framework of the sequential ALT planning is sketched in Figure 5.1. As seen in Figure 5.1, the sequential planning involves 2 stages. At stage 1, the test at the highest

stress level x_H is firstly planned and conducted in order to yield preliminary information on (β_0, σ). This information is then used in stage 2 as one of the planning inputs.

To plan the test at the highest stress x_H, one needs to specify the values of (β_0, σ). Although the margin of specification error is high as discussed above, useful information on (β_0, σ) are still obtainable after the test since enough failures are expected under the highest stress in most applications. At stage 2, both the optimum sample allocation and stress combinations for tests at lower stress levels are generated using the information obtained under the highest stress as well as the prior information on β_1. Details are presented below.

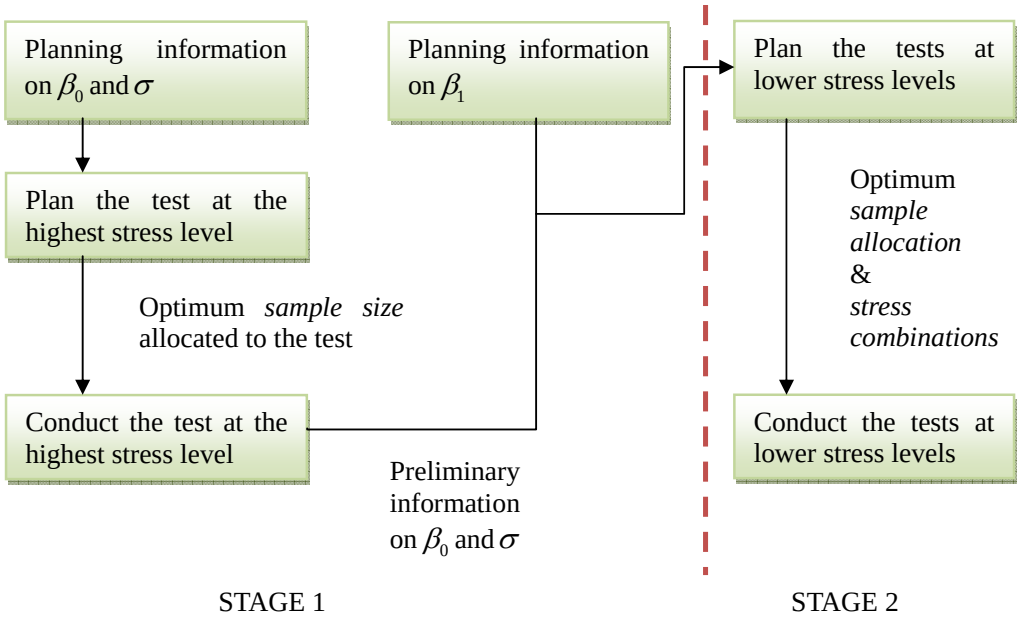

Figure 5.1 Framework of the sequential ALT planning based on Bayesian method

5.2.1. STAGE 1: Planning for Test at the Highest Stress Level

To plan the test at the highest stress level x_H, one needs to:

- Specify the values of μ_H and σ_H. Note that, μ_H equals the intercept parameter β_0 of the stress-life model and σ is a constant independent of stress.
- Specify the test duration c_H and a reasonable number of failures R_H to be expected for the test at the highest stress. Here, it is essential to see enough failures under the highest stress since results obtained at this stage is used as planning information for stage 2. Hence, given the test duration, an expected number of failures must be specified. In practice, the upper bound of R_H is usually limited by cost considerations.

Given the specified values of μ_H, σ_H, c_H and R_H, the number of units needed for the test at x_H can be calculated as

$$n_H = R_H \cdot (1 - \exp(-(c_H / \exp(\mu_H))^{1/\sigma_H}))^{-1} \tag{5.3}$$

Preliminary information on (μ_H, σ_H) is obtained by analyzing the failure data obtained at the highest stress. Using the Bayes rule (Carlin and Louis (2000)), the posterior distribution $\pi(\mu_H, \sigma_H)$ can be found in (5.4). Here, since the number of failures is expected to be large at the highest stress, a constant prior distribution of (μ_H, σ_H) is used as it does not risk the objectivity of our analysis

$$\pi(\mu_H, \sigma_H) \propto \exp\left\{\sum_{j=1}^{n_H}\left(\kappa_{Hj}\left(\log(1/\sigma_H) + z_{Hj} - \exp(z_{Hj})\right) - (1-\kappa_{Hj})\exp\zeta_H\right)\right\} \tag{5.4}$$

If the mode of the posterior distribution is taken as the Bayesian estimate, $\hat{\boldsymbol{\theta}}_H = [\hat{\mu}_H, \hat{\sigma}_H]$ is the value that maximizes $\pi(\mu_H, \sigma_H)$ and is sometimes called

the generalized maximum likelihood estimate (Berger (1985), pp. 133). Based on the large sample theory (Berger (1985), pp. 244), the posterior density $\pi(\mu_H, \sigma_H)$ asymptotically follows bivariate normal distribution as shown in (5.5), where $l(\boldsymbol{\theta}_H)$ is the likelihood function of $\boldsymbol{\theta}_H$; $\hat{\boldsymbol{\Sigma}}_H$ is the covariance matrix; and $\hat{\mathbf{I}}_H$ is the Fisher information observed at $\hat{\boldsymbol{\theta}}_H$

$$\hat{\boldsymbol{\theta}}_H \sim N\left(\hat{\boldsymbol{\theta}}_H, \hat{\boldsymbol{\Sigma}}_H\right)$$
$$\text{where} \quad \hat{\mathbf{I}}_H = \left.\frac{\partial^2 \log l(\boldsymbol{\theta}_H)}{\partial \boldsymbol{\theta}_H{}^2}\right|_{\boldsymbol{\theta}=\hat{\boldsymbol{\theta}}} \quad , \quad \hat{\boldsymbol{\Sigma}}_H = \left[-\hat{\mathbf{I}}_H\right]^{-1} \tag{5.5}$$

Based on the results above, the estimate $\hat{y}_p(0)$ of the 100p-th life percentile at the highest stress x_H equals $\hat{\mu}_H + u_p \cdot \hat{\sigma}_H$, and its posterior variance $\text{var}(\hat{y}_p(0))$ is calculated by $[1, u_p]\hat{\boldsymbol{\Sigma}}_H[1, u_p]'$.

5.2.2. STAGE 2: Planning for Tests at Lower Stress Levels

To plan the tests at lower stress levels, one needs to:

- Specify the sample size and the test duration available for tests at lower stress levels.
- Specify the total number of stress levels for tests under lower stresses.
- Obtain the information on (μ_H, σ_H) yielded at the highest stress.
- Specify a possible range $[\beta_1^-, \beta_1^+]$ for the value of β_1. In practice, usually only the prior bounds of β_1 is known (see e.g. Pilz (1991), pp. 16), we therefore assume that any value within the range $[\beta_1^-, \beta_1^+]$ is equally likely to be true.

5.2.2.1 Deduction of the Prior Distribution

Given the range of β_1 and the approximated posterior distribution $\pi(\mu_H, \sigma_H)$, the prior distribution $\vartheta(\mu_i, \sigma_i)$ of (μ_i, σ_i) at any stress x_i can be constructed using the relationships $\mu_i = \mu_H + \beta_1 x_i$ and $\sigma_0 = \sigma_1 = ... = \sigma_k$. Equation (5.6) gives the *pdf* of the deduced prior distribution $\vartheta(\mu_i, \sigma_i)$. Similar ideas of prior distribution construction but for different problems can be found in Barlow et al. (1988), and Meinhold and Singpurwalla (1987)

$$\begin{aligned}\vartheta(\mu_i, \sigma_i) &= (2\pi \operatorname{var}(\hat{\mu}_k) \operatorname{var}(\hat{\sigma}))^{-1} \cdot (1-\rho^2)^{-1/2} \\ &\int_{\omega_i^-}^{\omega_i^+} \exp\left(-\left(\frac{(\mu_i - \omega_i)^2}{\operatorname{var}(\hat{\mu}_k)} - \frac{2\rho(\mu_i - \omega_i)(\sigma - \hat{\sigma})}{\operatorname{var}(\hat{\mu}_k)\operatorname{var}(\hat{\sigma})} + \frac{(\sigma - \hat{\sigma})^2}{\operatorname{var}(\hat{\sigma})} \right) \Big/ 2(1-\rho^2) \right) \cdot \frac{1}{\omega_i^+ - \omega_i^-} d\omega_i \\ &= \frac{1}{2^{3/2}(\pi \operatorname{var}(\hat{\sigma}))^{1/2}(\omega_i^- - \omega_i^+)} \cdot \exp\left[-\frac{(\sigma - \hat{\sigma})^2}{2\operatorname{var}(\hat{\sigma})} \right] \cdot \left[\operatorname{erf}(\psi_i^-) - \operatorname{erf}(\psi_i^+) \right] \\ &\qquad \forall i = 1, 2, ..., k-1 \end{aligned} \tag{5.6}$$

where

$$\omega_i = \hat{\mu}_H + \beta_1 x_i, \quad \omega_i^- = \hat{\mu}_H + \beta_1^- x_i, \quad \omega_i^+ = \hat{\mu}_H + \beta_1^+ x_i, \quad \rho = \operatorname{cov}(\hat{\mu}_H, \hat{\sigma}_H) / \operatorname{var}(\hat{\mu}_H) \operatorname{var}(\hat{\sigma}_H)$$

$$\psi_i^- = -\frac{\mu_i \cdot \operatorname{var}^{1/2}(\hat{\sigma}_H) - \omega_i^- \cdot \operatorname{var}^{1/2}(\hat{\sigma}_H) - \rho(\sigma_i - \hat{\sigma}_H) \cdot \operatorname{var}^{1/2}(\hat{\mu}_H)}{(2\operatorname{var}(\hat{\mu}_H)\operatorname{var}(\hat{\sigma}_H)(1-\rho^2))^{1/2}}$$

$$\psi_i^+ = -\frac{\mu_i \cdot \operatorname{var}^{1/2}(\hat{\sigma}_H) - \omega_i^+ \cdot \operatorname{var}^{1/2}(\hat{\sigma}_H) - \rho(\sigma_i - \hat{\sigma}_H) \cdot \operatorname{var}^{1/2}(\hat{\mu}_H)}{(2\operatorname{var}(\hat{\mu}_H)\operatorname{var}(\hat{\sigma}_H)(1-\rho^2))^{1/2}}$$

erf is the error function given by the definite integral $\operatorname{erf}(z) = 2\pi^{1/2} \int_0^z e^{-t^2} dt$

5.2.2.2 Approximation of the Posterior Distribution

A critical step is to evaluate the large-sample approximate covariance matrix $\boldsymbol{\Sigma}_i$ of the preposterior distribution, $\pi(\boldsymbol{\theta}_i)$, by conditioning on $\beta_1 = \tilde{\beta}_1$, a value sampled from the prior distribution $\vartheta(\beta_1)$. Note that, given $\beta_1 = \tilde{\beta}_1$, the preposterior distribution, $\pi(\boldsymbol{\theta}_i)$, at

lower testing stress x_i (for $i = 1, ..., H-1$) can be approximated by a bivariate normal distribution with covariance matrix

$$\boldsymbol{\Sigma}_i = (\mathbf{I}_{\boldsymbol{\theta}_i} + \mathbf{I}^{\vartheta_i})^{-1} \qquad \mathbf{I}^{\vartheta_i} = -\partial^2 \log \vartheta(\boldsymbol{\theta}_i) / \partial \boldsymbol{\theta}_i^{\,2} \text{ and } \mathbf{I}_{\boldsymbol{\theta}_i} = E[-\partial^2 l(\boldsymbol{\theta}_i) / \partial \boldsymbol{\theta}_i^{\,2}] \qquad (5.7)$$

where $\mathbf{I}^{\vartheta_i}$ and $\mathbf{I}_{\boldsymbol{\theta}_i}$ are evaluated at $\boldsymbol{\theta}_i = (\hat{\mu}_H + \tilde{\beta}_1 x_i, \hat{\sigma}_H)$.

In equation (5.7), $\mathbf{I}^{\vartheta_i} = \partial^2 \log \vartheta(\boldsymbol{\theta}_i) / \partial \boldsymbol{\theta}_i^{\,2}$ is the information on $\boldsymbol{\theta}_i$ contained in the prior distribution $\vartheta(\mu_i, \sigma_i)$. Since the closed-from of $\vartheta(\mu_i, \sigma_i)$ has been derived in equation (5.6), conventional numerical differentiation method can be used to evaluate $\mathbf{I}^{\vartheta_i}$ (see Friedman and Kandel (1994)). $\mathbf{I}_{\boldsymbol{\theta}_i}$ is the information expected to obtain from the test at stress x_i conditioning on $\beta_1 = \tilde{\beta}_1$. The closed-form expression of $\mathbf{I}_{\boldsymbol{\theta}_i}$ can be easily derived as follows

$$\mathbf{I}_{\boldsymbol{\theta}_i} = E[-\partial^2 l(\boldsymbol{\theta}_i) / \partial \boldsymbol{\theta}_i^{\,2}] = n_i \cdot \begin{pmatrix} I_{11} & I_{12} \\ I_{12} & I_{22} \end{pmatrix},$$

where

$$\sigma^2 \cdot I_{11} = B - (1 - \Phi(\zeta)) \exp(\zeta)$$
$$\sigma^2 \cdot I_{12} = \sigma^2 \cdot I_{21} = A + B + C + (1 - \Phi(\zeta))G,$$
$$\sigma^2 \cdot I_{22} = A + D + E + F + (1 - \Phi(\zeta))H$$

and

$$A = 1 - \exp(-\exp(\zeta)) \quad B = \exp(-\exp(\zeta)) + \exp(\zeta - \exp(\zeta)) - 1$$
$$C = -1 + \exp(-\exp(\zeta))(1 + \zeta(1 + \exp(\zeta))) + E_1(\exp(\zeta)) + \gamma$$
$$D = -2\zeta \exp(-\exp(\zeta)) - 2E_1(\exp(\zeta)) - 2\gamma$$
$$E = -2 + 2\exp(-\exp(\zeta))(1 + \zeta(1 + \exp(\zeta))) + 2E_1(\exp(\zeta)) + 2\gamma$$
$$G = -\zeta \exp(\zeta) - \exp(\zeta) \quad H = -2\zeta \exp(\zeta) - \zeta^2 \exp(\zeta)$$
$$F = \int_{-\infty}^{\zeta} x^2 \exp(2x - \exp(x)) dx$$

$E_1(x)$ is the exponential integral defined as $\int_x^{\infty} t^{-1} \exp(-t) dt$

γ is the Euler's constant, which is approximately 0.577216

$\Phi(z) = 1 - \exp(-\exp(z))$ is the standard SEV Cdf

After $\boldsymbol{\Sigma}_i$ has been found, the preposterior expectation $E_{\beta_1}(\text{var}(y_p(x_i)))$ of the posterior variance $\text{var}(y_p(x_i))$ at the stress x_i is computed by averaging $\text{var}(y_p(x_i))$ over the specified range of β_1 as shown in equation (5.8)

$$E_{\beta_1}(\text{var}(y_p(x_i))) = \int_{\beta_1^-}^{\beta_1^+} (1, u_p)\boldsymbol{\Sigma}_i(1, u_p)^T \vartheta(\beta_1) d\beta_1 \qquad \forall i = 1, ..., H-1 \qquad (5.8)$$

The Monte-Carlo integration method can be used here to evaluate (5.8) (see Robert and Casella (1999)).

5.2.2.3 The Bayesian Planning Problem

To derive an appropriate plan for tests at lower stress levels for $i = 1, 2, ..., k-1$, both sample allocation n_i and stress level combinations x_i must be chosen according to a certain planning criterion. In this chapter, the optimal plan for tests at lower stresses minimizes the preposterior expectation $E_{\beta_1}(\text{var}(y_p(1)))$ of the posterior variance $y_p(1)$ at use stress. This is done by optimizing the stresses $(x_1, x_2, ..., x_{k-1})$ on which the tests are to be conducted, and the number of samples $(n_1, n_2, ..., n_{k-1})$ allocated to each chosen stress.

Let

$$\mathbf{X} = \begin{pmatrix} 1 & \cdots & 1 & 1 \\ x_1 & \cdots & x_{H-1} & x_H \end{pmatrix}^T$$

be the design matrix; $\boldsymbol{\Lambda}$ be the diagonal matrix given by

$$\boldsymbol{\Lambda} = \begin{pmatrix} E_{\beta_1}(\text{var}(y_p(x_1))) & & & \\ & \ddots & & \\ & & E_{\beta_1}(\text{var}(y_p(x_{H-1}))) & \\ & & & \text{var}(y_p(0)) \end{pmatrix}$$

and $\mathbf{1} = (1,1)$. The sequential optimum ALT plan can be obtained by solving the

following

$$\begin{aligned} &\text{Min} \quad E_{\beta_1}(\text{var}(y_p(1))) = \mathbf{1}(\mathbf{X}^T\boldsymbol{\Lambda}^{-1}\mathbf{X})^{-1}\mathbf{1}^T \\ &\text{s.t.} \quad \sum_{i=1}^{H} n_i = N \quad n_i \geq 0 \quad \text{and} \quad 0 < x_{H-1} < \cdots < x_1 \leq 1 \end{aligned} \quad . \tag{5.9}$$

Note that while $\text{var}(y_p(0)) = (1, u_p)\hat{\boldsymbol{\Sigma}}_H(1, u_p)^T$, $E_{\beta_1}(\text{var}(y_p(x)))$ for all low stresses need to be evaluated numerically. Fortunately, in practice, the number of lower stress levels is typically no more than three and additional constraints are imposed to reduce the dimensionality of the solution space. An example will be given later.

It is noted that the Bayesian planning approach presented above is based on the approximate normality. Hence, Clyde (1993) suggested several approaches that can be used to ensure the normality of the posterior distribution. One may also refer to Kass and Slate (1994) for useful diagnostics for posterior normality.

In the next section, numerical examples are presented to illustrate the application of the proposed sequential ALT planning. Simulation studies are conducted after that.

5.3. Numerical Examples

The numerical example presented below is taken from examples 20.1 ~ 20.4 of Meeker and Escobar (1998). In this example, engineers responsible for the adhesive bond reliability need to estimate the 0.1 percentile of failure-time distribution at the use operating temperature of 50ºC. 300 units and 183 days are available for the test. Existing engineering knowledge suggests that Weibull distribution is a reasonable model for the bond failure times and the Arrhenius relationship is an appropriate underlying stress-life model when the operating temperature ranges from 50ºC to 120ºC.

Both ALT plans with 2 and 3 stress levels are developed in this section using the

proposed method. To make the presentation clear, a simple summary of planning steps are presented as below,

Stage 1: Planning the test at the highest stress Level x_H. This step determines the number of units to be tested at the highest stress level. By analyzing the data collected at the highest stress, preliminary information on (β_0, σ) is obtained.

Stage 2: Planning the tests at lower stress levels. Based on the information obtained at the highest stress, and the prior knowledge about the slope parameter β_1, prior distributions for parameters μ and σ at lower stresses are derived. Both sample allocation and stress level combination at lower stresses are then optimized.

5.3.1. Planning an ALT with 2 Stress Levels

5.3.1.1 STAGE 1: Planning the test at the Highest Stress Level x_H

The test at the highest stress level x_H is firstly planned and conducted. Given the planning values $\beta_0 = 4.72$ and $\sigma = 0.6$, we generate (using equation (5.3)) the contour plot of the sample size n_H versus the expected number of failures R_H and the censoring time c_H.

As seen in Figure 5.2, more units are needed for a larger value of R_H given the test duration. Let $R_H = 15$ and $c_H = 60$ days, n_H is approximately 50 from Figure 5.2.

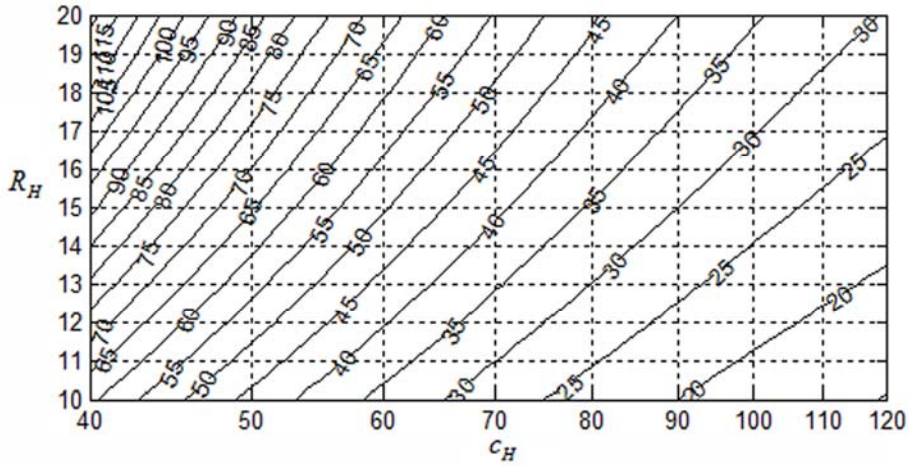

Figure 5.2 Contour plot of n_H against R_H and c_H

Suppose the test at the highest stress x_H has been conducted and 50 failure times are obtained as shown in Table 5.1. These data are simulated assuming the model parameters $\overline{\beta}_0 = 4$ and $\overline{\sigma} = 0.8$; and "_" denotes the censored data.

Table 5.1 Failure times at the highest stress level x_H

Failure Times at x_H (day)
33.3, 48.4, 39.3, 58.8, 47.4, 60.0, 33.6, 19.4, 38.0, 28.6, 60.0, 53.2, 17.7, 25.4, 44.5, 34.6, 16.9, 60.0, 31.7, 60.0 ,49.2, 60.0, 10.953, 60.0, 18.8, 3.3, 1.4, 17.3, 46.8, 40.9, 60.0, 28.4, 60.0, 4.2, 21.9, 49.6, 20.6, 60.0, 46.6, 6.4, 25.2, 60.0, 13.6, 29.5, 60.0, 60.0, 31.3, 29.4, 54.3, 34.0

Based on the data in Table 5.1, the posterior distribution $\pi(\mu_H, \sigma_H)$ shown in Figure 5.3 is derived from a constant prior distribution of (μ_H, σ_H). Here, $\hat{\mu}_H = 3.87$, $\hat{\sigma}_H = 0.65$, and $\hat{\boldsymbol{\Sigma}}_H = [-\hat{\mathbf{I}}_H]^{-1} = \begin{bmatrix} 0.0112, 0.0003; \\ 0.0003, 0.0086 \end{bmatrix}$.

As discussed, the posterior distribution $\pi(\mu_H, \sigma_H)$ can be approximated by a bivariate normal distribution $N([\hat{\mu}_H, \hat{\sigma}_H], [-\hat{\mathbf{I}}_H]^{-1})$ using equation (5.5). Figure 5.4 shows the approximated distribution. In practice, the quality of this type of approximation, which is substantially determined by the sample size, can be simply quantified by special hypothesis tests, say, the Kolmogorov-Smirnov (KS) tests as

shown in the example given by Martz et al (1988). In addition, one may also refer to Kass and Slate (1994) for diagnostics of posterior normality.

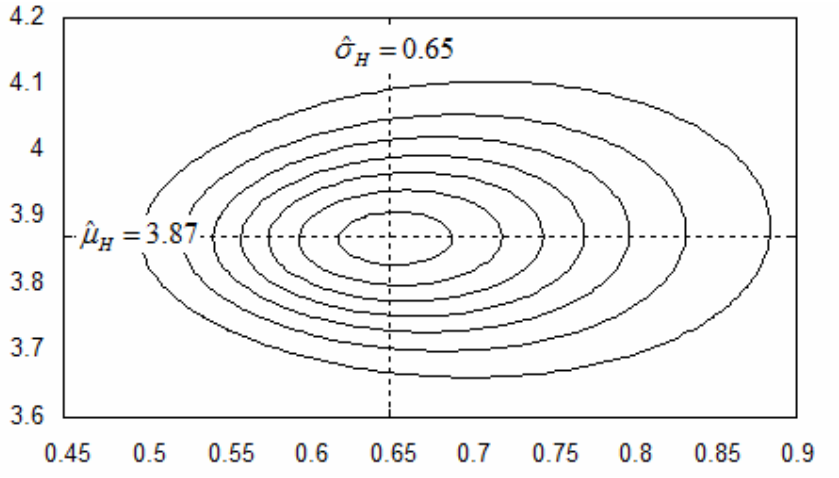

Figure 5.3 Posterior distribution $\pi(\mu_H, \sigma_H)$

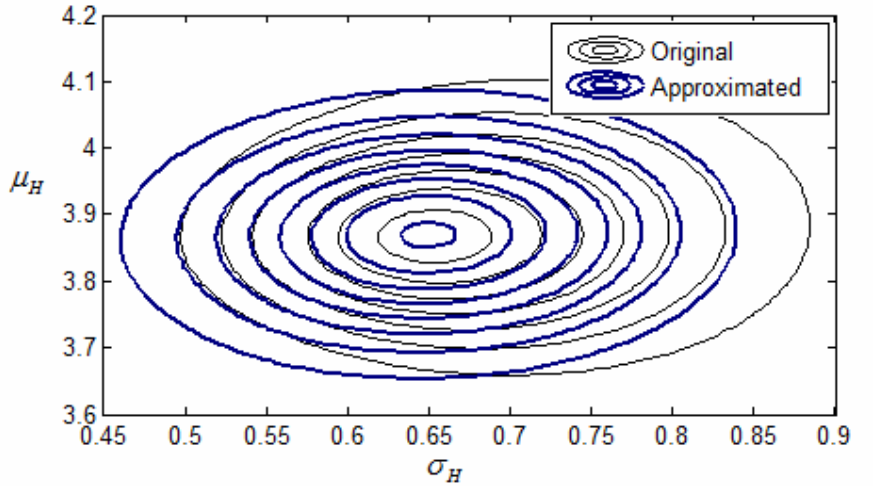

Figure 5.4 Approximation of the posterior distribution $\pi(\mu_H, \sigma_H)$

5.3.1.2 STAGE 2: Planning the Test at the Low Stress Level x_L

- Quantify the Value of the Slope Parameter

In this example, the Arrhenius model is employed for modeling the dependency of μ on temperature T, i.e.

$$\mu = \log A + \frac{\text{Activation energy, } E_a}{\text{Boltzmann constant, } k_B = 8.6171 \times 10^{-5}} \cdot \frac{1}{T}$$

Let $s = 1/T$ and $x = (s - s_k)/(s_0 - s_k)$, the re-parameterization of the Arrhenius model yields the linear stress-life model as

$$\mu = \beta_0 + \beta_1 x$$

where $\beta_0 = \log A + \frac{E_a}{k_B} \cdot s_k \quad \beta_1 = \frac{E_a}{k_B} \cdot (s_0 - s_k)$

Hence, specifying the value of β_1 here is equivalent to specifying the Arrhenius activation energy E_a. In this project, the activation energy of the adhesive bond is thought to be within the range of (0.6, 0.8), then, the slope parameter β_1 is roughly within the interval (3.84, 5.12) as $\beta_1 = E_a \cdot k_B^{-1} \cdot (s_k - s_0)$.

- Deduction of the Prior Distribution for (μ_i, σ_i)

At any lower stress level $x_i \in (0,1]$, the prior distribution $\vartheta(\mu_i, \sigma_i)$ of (μ_i, σ_i) is obtained from equation (5.6). In Figure 5.5, we present two examples of the constructed prior distributions respectively at the stress $x_i = 0.5$ and $x_i = 1$.

As discussed, the prior distribution is deduced based on the approximated posterior distribution $\pi(\mu_H, \sigma_H)$ and the interval of β_1. Hence, we are seeing the sports field shaped contour of the constructed prior distribution, especially when $x_i = 1$. This observation suggests that the uncertainty over μ_i grows as the distance between x_i and x_H becomes larger; or equivalently, the prior information on μ_i becomes vague when the distance between x_i and x_H increases.

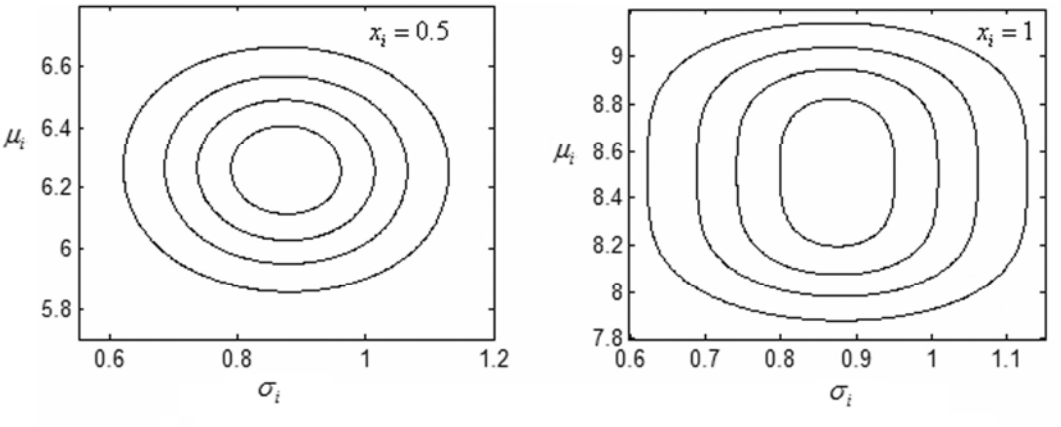

Figure 5.5 Examples of the constructed prior distribution $\vartheta(\mu_i, \sigma_i)$

- Optimize the Location of x_L

250 units and 123 days are left to conduct the test at the low stress level x_L. Using equation (5.7), the approximate posterior distribution $\pi(\mu_i, \sigma_i)$ of (μ_i, σ_i) at stress x_i can be derived. For this adhesive bond reliability test, engineers are interested in the 0.1 percentile of the failure time distribution at use condition. Hence, given the information yielded by the test at the highest stress level x_H, the optimum x_L^* minimizes $E_{\beta_1}(\text{var}(y_{0.1}(1)))$ at use condition. This is done by solving equations (5.9). Figure 5.6 plots $E_{\beta_1}(\text{var}(y_{0.1}(1)))$ against stress x_L. The optimum $x_L^* = 0.8\,(62^{\circ}\text{C})$ can be directly read from the figure.

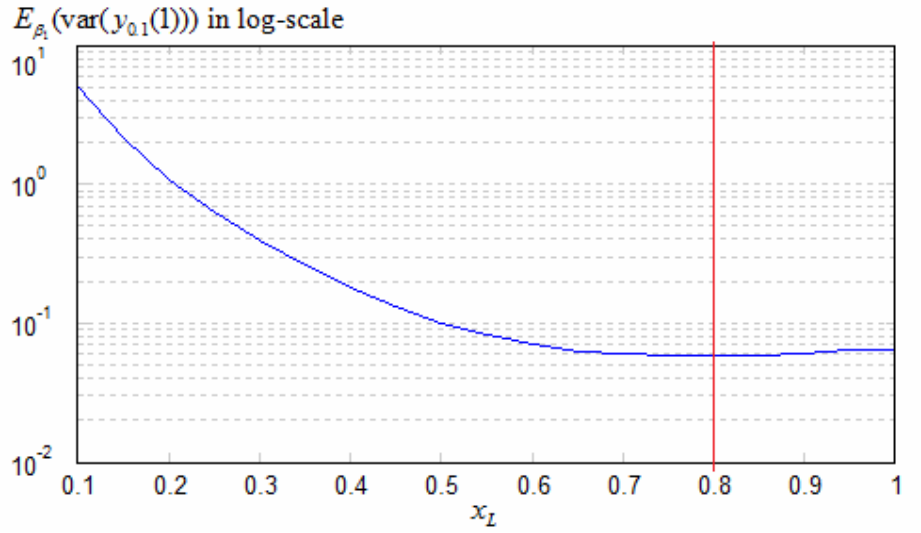

Figure 5.6 Plot of $E_{\theta|D}[\text{var}(y_p(1))]$ against stress x_L

Compared to the conventional non-sequential (static) planning (Meeker and Escobar, 1998, Chapter 20), the sequential ALT planning reduces the range of extrapolation in estimating the 0.1 percentile at use condition. This is because an informative prior distribution has been constructed for (μ_L, σ_L). Hence, we can further push the optimum x_L^* towards the design level. More details are presented in simulation studies.

- Effect of the Specified Range of β_1

In the planning above, the activation energy of the adhesive bond is thought to be within the range (0.6, 0.8), that is, the slope parameter β_1 is roughly within (3.84, 5.12). Suppose now we extend the upper bound of the activation energy to 0.9, i.e. the range of the slope parameter β_1 becomes (3.84, 5.76). This modification indicates a higher perceived bond reliability, i.e. fewer failures are expected at a particular lower stress level. Intuitively, the optimum x_L^* should be increased from the current level 0.8 so as to produce more failures. This is confirmed by the new optimal x_L^* =0.7 (68ºC).

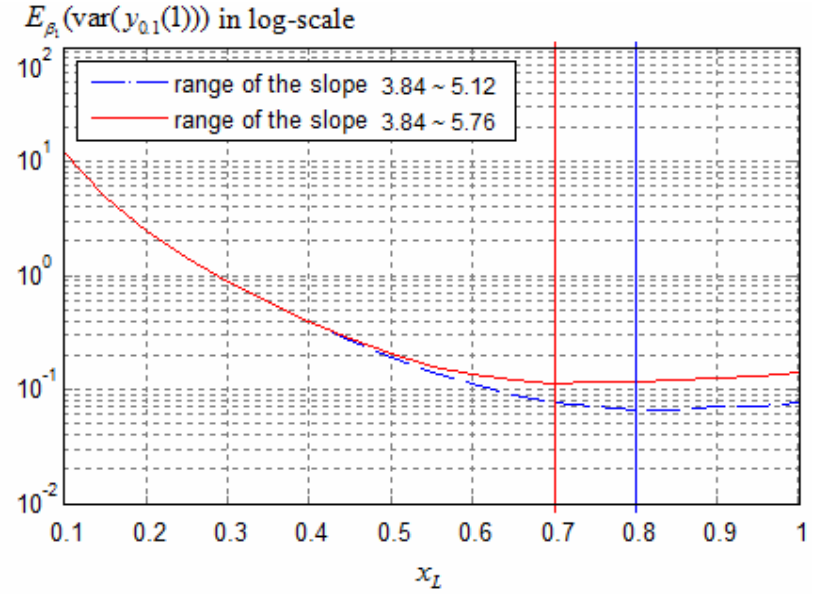

Figure 5.7 Effect of the pre-specified interval of β_1

5.3.2. Planning of a Compromise ALT with 3 stress Levels

ALT plans with two stress levels are known to be less robust against modeling error as discussed in both Nelson (1990) and Meeker and Escobar (1998). In fact, they are usually used as benchmarks for more practical compromise plans which consist of more than two stress levels. In this section, we shall illustrate the approach to planning tests at both middle and low stresses, given the testing results obtained from the highest stress.

For meaningful inference, the minimum expected number of failures R_L and R_M at both x_L and x_M need to be specified. Typically, at least 4 or 5 failures should be obtained as suggested in Meeker and Escobar (1998). As the key role of having the middle stress level is to check for curvature in the stress-life relationship, we set the middle stress x_M at the mid-point of x_L and x_H, i.e. $x_M = (x_L + x_H)/2 = x_L/2$.

Suppose $n_M = \pi \cdot n_{L+M}$ units are allocated to the middle stress level,

where $n_{L+M} = N - n_H$ is the remaining testing units and $0 \le \pi \le 1$. In our formulation, both π and the low stress level x_L are the decision variables in the following optimization problem which involves non-linear constraints

$$\begin{aligned} &Min: E_{\beta_1}(\text{var}(y_{0.1}(1)); x_L, \pi) \\ &s.t. \\ &n_{L+M} \cdot (1-\pi) \cdot p(x_L) \ge R_L \quad , \quad n_{L+M} \cdot \pi \cdot p(x_M) \ge R_M \\ &0 = x_H < x_L = 2x_M \le 1 \quad , \quad 0 \le \pi \le 1 \end{aligned} \tag{5.10}$$

where $p(x_L)$ and $p(x_M)$ respectively denotes the failure probability at the low and middle stress level. From the prior distribution $\vartheta(\mu_L, \sigma_L)$ and $\vartheta(\mu_M, \sigma_M)$ obtained using equation (5.6), we have

$$p(x_L) = \int_{-\infty}^{\infty}\int_{0}^{\infty} (1-\exp(-\exp(\zeta_L)))\vartheta(\mu_L, \sigma_L) d\sigma_L d\mu_L$$
$$p(x_M) = \int_{-\infty}^{\infty}\int_{0}^{\infty} (1-\exp(-\exp(\zeta_M)))\vartheta(\mu_M, \sigma_M) d\sigma_M d\mu_M$$

For the optimization problem (5.10), Figure 5.8 depicts the feasible region S when $R_L = R_M = 5$ (see the later numerical example). It is noted that, the feasible region S will be empty if the sample size n_{L+M} is too small to achieve the minimum number of failures R_L and R_M required. In addition, the feasible region is not convex as the curve $n_{L+M} \cdot \pi \cdot p(x_M) = R_M$ is not convex w.r.t. x_L, and the curve $n_{L+M} \cdot (1-\pi) \cdot p(x_L) = R_L$ is not concave w.r.t. x_L.

To solve the optimization problem (5.10) with nonlinear constraints, the interior penalty function method (Fiacco and McCormick (1968)) can be used. By adding some multiple of the negative of the inverse of the constraint equations, this method modifies the function $E_{\beta_1}(\text{var}(y_{0.1}(1)))$ to form a new unconstrained objective function

$$F(x_L,\pi,k)=E_{\beta_1}(\mathrm{var}(y_{0.1}(1));x_L,\pi)-k\sum_{i=1}^{6}g_i^{-1},\quad k>0$$

$$\text{where}\quad g_1=R_L-n_{L+M}\cdot(1-\pi)\cdot p(x_L),\ g_2=R_M-n_{L+M}\cdot\pi\cdot p(x_M) \tag{5.11}$$

$$g_3=x_L-1,\ g_4=-x_L,\ g_5=\pi-1,\ g_6=-\pi$$

If a monotonically decreasing sequence $\{k^{(i)}\}, k^{(i)}\downarrow 0$, is chosen in (5.11), we can easily find the optimum point $(x_L^{(i)},\pi^{(i)})$ that minimizes the unconstrained object function $F(x_L,\pi,k^{(i)})$. Fiacco and McCormick (1968) have shown that

$$\lim_{i\to\infty}(x_L^{(i)},\pi^{(i)})=(x_L^*,\pi^*)$$

where (x_L^*,π^*) is the optimum point for problem (5.10).

Figure 5.8 depicts the trajectory of $(x_L^{(i)},\pi^{(i)})$ as $k^{(i)}$ decreases. Within each iteration, $(x_L^{(i)},\pi^{(i)})$ is found by the well known Newton-Raphson method.

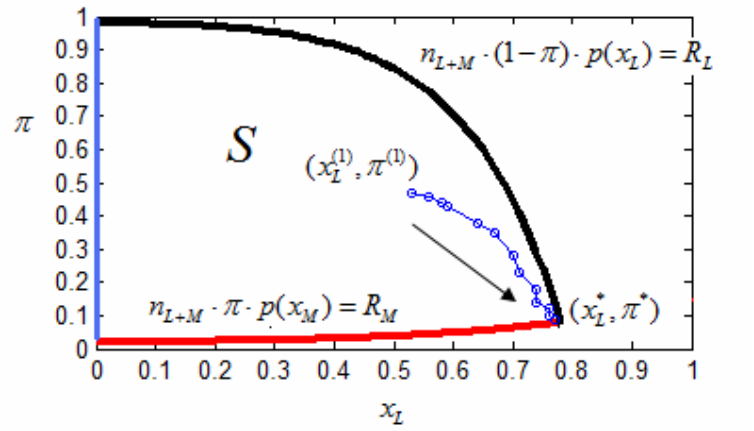

Figure 5.8 Results of applying the penalty function method

It is seen that the optimum point $(x_L^*,\pi^*)=\lim_{i\to\infty}(x_L^{(i)},\pi^{(i)})$ is found at the extreme corner of the feasible region S which is approximately $(0.78,0.08)$. Similar result is plotted in Figure 5.9, where the response value represents the $E_{\beta_1}(\mathrm{var}(y_{0.1}(1));x_L,\pi)$ in log-scale.

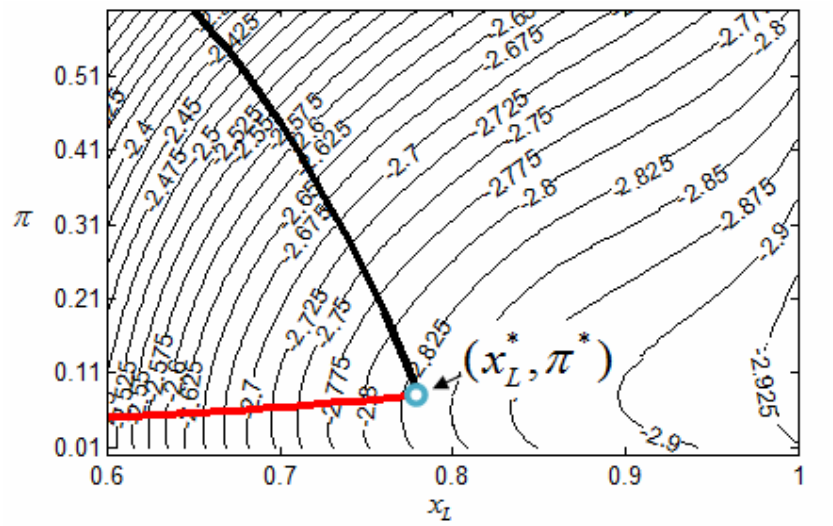

Figure 5.9 The optimum point lies on the extreme corner of the feasible region

Substitute $x_L^* = 0.78$ and $\pi^* = 0.08$ into the equation (5.10), we obtain $E_{\beta_1}(\text{var}(y_{0.1}(1)); x_L^*, \pi^*) = 0.0588$. Table 5.2 summarizes the compromise plan for the adhesive bond test.

Table 5.2 Compromise sequential ALT plan

Condition	Temp. T_i	Stress x_i	Test Duration c_i	Sample Allocation, n_i	Expected Failures, R_i
Use	50ºC	1			
Low	63ºC	0.78	123days	230	5
Mid	89ºC	0.39	123days	20	5
High	120ºC	0	60days	50	15

(The pre-posterior expectation $E_{\beta_1}(\text{var}(y_{0.1}(1)))$ of $\text{var}(y_{0.1}(1)$ is approximately 0.0588)

The above plan can be validated by simulation as follows. Suppose now the tests are conducted at $x_L^* = 0.78$ and $x_M^* = 0.39$ based on the plan given in Table 5.2. Table 5.3 presents the simulated failure data using the assumed model parameters $\bar{\beta}_0 = 4$, $\bar{\beta}_1 = 4.5$, and $\bar{\sigma} = 0.8$. As we can see, 5 failures are obtained from

the test at x_L ; 4 failures are obtained from the test at x_M .

Table 5.3 Simulated failure times at $x_L^* = 0.78$ and $x_M^* = 0.39$

Failure times at $x_L = 0.78$	Failure times at $x_M = 0.39$
22.8	46.1
44.8	62.5
59.1	86.2
84.4	98.9
87.7	101.7
105.2	123 (×15)
123 (×224)	

("_" denotes the censored data)

Using equation (5.6), the prior distribution $\vartheta(\mu_i, \sigma_i)$ of (μ_i, σ_i) at both stress levels x_L^* and x_M^* can be constructed. Then, the estimates $(\hat{\mu}_i, \hat{\sigma}_i)$ at these 2 stress levels are those values that maximize the posterior distribution $\pi(\mu_i, \sigma_i)$. This is equivalent to maximizing equation (5.12)

$$\log \pi(\mu_i, \sigma_i) = \log(\vartheta(\mu_i, \sigma_i)) + \sum_{j=1}^{n_i} (\kappa_{ij}(-\log \sigma_i + z_{ij} - \exp(z_{ij})) - (1-\kappa_{ij})\exp(\zeta_{ij})) + \text{Constant} \tag{5.12}$$

Then, we obtain $\hat{\mu}_L = 7.24$, $\hat{\sigma}_L = 0.664$ and $\hat{\mu}_M = 5.28$, $\hat{\sigma}_M = 0.594$. Similar to equation (5.7), the posterior distribution $\pi(\mu_i, \sigma_i)$ is asymptotically normally distributed with mean $\hat{\boldsymbol{\theta}}_i$ and variance matrix $\hat{\boldsymbol{\Sigma}}_i$ as given by equation (5.13), where $\hat{\mathbf{I}}_{\boldsymbol{\theta}_i}$ is the Fisher information observed at $\hat{\boldsymbol{\theta}}_i = (\hat{\mu}_i, \hat{\sigma}_i)$

$$\begin{aligned} &\hat{\boldsymbol{\theta}}_i = [\hat{\mu}_i, \hat{\sigma}_i] \quad , \quad \hat{\boldsymbol{\Sigma}}_i = [-(\hat{\mathbf{I}}_{\boldsymbol{\theta}_i} + \mathbf{I}^{\vartheta_i})]^{-1} \\ &\text{where} \quad \hat{\mathbf{I}}_{\boldsymbol{\theta}_i} = \partial^2 \log l(\boldsymbol{\theta}_i) / \partial \boldsymbol{\theta}_i^{\,2} \big|_{\boldsymbol{\theta}_i = \hat{\boldsymbol{\theta}}_i} , \quad \mathbf{I}^{\vartheta_i} = \partial^2 \log \vartheta(\boldsymbol{\theta}_i) / \partial \boldsymbol{\theta}_i^{\,2} \end{aligned} \tag{5.13}$$

Then, we have

$$\hat{\boldsymbol{\Sigma}}_L = \begin{bmatrix} 0.0381, 0.0061; \\ 0.0061, 0.0042 \end{bmatrix}, \quad \hat{\boldsymbol{\Sigma}}_M = \begin{bmatrix} 0.0162, 0.0020; \\ 0.0020, 0.0068 \end{bmatrix}$$

Figure 5.10 shows the approximated posterior distributions of (μ_i, σ_i) as well as the prior distributions for both stress levels $x_L^* = 0.78$ and $x_M^* = 0.39$.

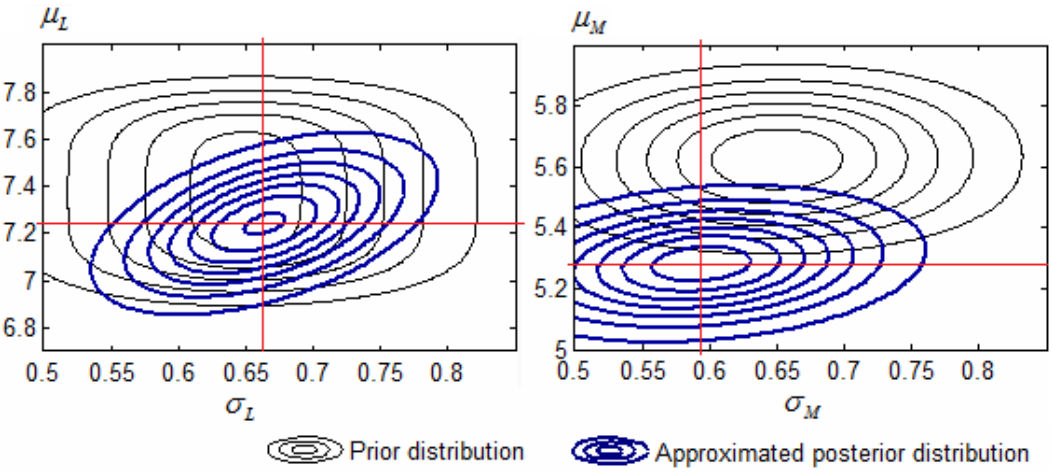

Figure 5.10 Approximated posterior distributions $\pi(\mu_M, \sigma_M)$ and $\pi(\mu_L, \sigma_L)$

Finally, the 10th life percentile at use condition is given by

$$\hat{y}_{.1}(1) = \mathbf{1}(\mathbf{X}^T \mathbf{\Lambda}^{-1} \mathbf{X})^{-1} (\mathbf{X}^T \mathbf{\Lambda}^{-1} \mathbf{Y}) = 6.728 \quad , \tag{5.14}$$

with variance

$$\text{var}(\hat{y}_{.1}(1)) = \mathbf{1}(\mathbf{X}^T \mathbf{\Lambda}^{-1} \mathbf{X})^{-1} \mathbf{1}^T = 0.0541 \quad , \tag{5.15}$$

where

$$\mathbf{X} = \begin{pmatrix} 1 & 0.78 \\ 1 & 0.39 \\ 1 & 0 \end{pmatrix} \qquad \mathbf{Y} = \begin{pmatrix} \hat{y}_{.1}(0.78) \\ \hat{y}_{.1}(0.39) \\ \hat{y}_{.1}(0) \end{pmatrix} \qquad \mathbf{\Lambda} = \begin{pmatrix} \text{var}(\hat{y}_{.1}(0.78)) & & \\ & \text{var}(\hat{y}_{.1}(0.39)) & \\ & & \text{var}(\hat{y}_{.1}(0)) \end{pmatrix}$$

and

$$\hat{y}_{.1}(0.78) = \hat{\mu}_L + u_{.1}\hat{\sigma}_L = 5.746, \quad \text{var}(\hat{y}_{.1}(0.78)) = (1, u_{.1})\hat{\mathbf{\Sigma}}_L (1, u_{.1})^T = 0.0318$$
$$\hat{y}_{.1}(0.39) = \hat{\mu}_M + u_{.1}\hat{\sigma}_M = 3.943, \quad \text{var}(\hat{y}_{.1}(0.39)) = (1, u_{.1})\hat{\mathbf{\Sigma}}_M (1, u_{.1})^T = 0.0492$$
$$\hat{y}_{.1}(0) = \hat{\mu}_H + u_{.1}\hat{\sigma}_H = 2.407, \quad \text{var}(\hat{y}_{.1}(0)) = (1, u_{.1})\hat{\mathbf{\Sigma}}_H (1, u_{.1})^T = 0.053$$

We see that $\text{var}(\hat{y}_{.1}(1)) = 0.0541$ is close to the preposterior expectation of the

large-sample approximate posterior variance $E_{\beta_1}(\text{var}(y_{0.1}(1))) = 0.0544$.

5.4. Comparison of the Sequential Plan with Static Plan

Simulation studies are conducted in this section to compare the performance of the sequential ALT planning to that of the traditional static (non-sequential) ALT planning. The comparison is based on both the statistically optimum test plan with 2 stress levels and compromise plan with 3 stress levels. For the static planning, plans are generated by the commonly used Maximum Likelihood (ML) method described by Meeker & Escobar (1998), and the simulated failure data is then analyzed using the Maximum Likelihood Estimation (MLE). For the sequential planning, plans are generated sequentially using the method proposed in this chapter, and the simulated failure data are analyzed by the proposed method as shown in the numerical example above.

5.4.1. Generation of Failure Data

We assume that the logarithm failure times at each stress level follow the SEV distribution with a constant scale parameter σ. The location parameter μ is a linear function of the standardized stress, i.e. $\mu = \beta_0 + \beta_1 x, x \in [0,1]$. Failure times are simulated using the assumed values $\overline{\beta}_0 = 4$, $\overline{\beta}_1 = 4.5$, and $\overline{\sigma} = 0.8$.

Particularly, when the sequential planning is used, the test at the high stress level x_H is conducted first. Again, 15 failures are expected within 60 days for this test run.

5.4.2. Simulation Design

To examine the effects of misspecification of model parameters, we consider 9 scenarios of how these parameters are (mis)specified as given in Table 5.4.

Table 5.4 Simulation design

Simulation Scenarios	Pre-specified β_0	Pre-specified β_1		Pre-specified σ
		Non-sequential Planning	Sequential Planning	
1	(0)	(0)	$(-)\sim(+)$	(0)
2	$(-)$	$(-)$	$(-)\sim(+)$	$(-)$
3	$(-)$	$(-)$	$(-)\sim(+)$	$(+)$
4	$(-)$	$(+)$	$(-)\sim(+)$	$(-)$
5	$(-)$	$(+)$	$(-)\sim(+)$	$(+)$
6	$(+)$	$(-)$	$(-)\sim(+)$	$(-)$
7	$(+)$	$(-)$	$(-)\sim(+)$	$(+)$
8	$(+)$	$(+)$	$(-)\sim(+)$	$(-)$
9	$(+)$	$(+)$	$(-)\sim(+)$	$(+)$

Similar to DOE, "$(+)$" implies that the model parameter is over-specified to its upper bound "$\cdot^{+}$"; "$(-)$" implies that the model parameter is specified to its lower bound "$\cdot^{-}$"; and "(0)" implies that the model parameter is correctly specified.

In our design, we set the upper bound $\beta_0^{+}=5$, which is 25% higher than its true value; the lower bound $\beta_0^{-}=3$, which is 25% lower than its true value. Since the slope parameter is usually easier to be specified in practice, we let the upper bound $\beta_1^{+}=5$,

which is 12.55% higher than its true value; the lower bound $\beta_1^- = 4$, which is 12.55% lower than its true value. Further, we let $\sigma^+ = 1$, which is 25% higher than its true value; $\sigma^- = 0.6$, which is 25% lower than its true value. When the sequential planning method is used, the pre-specified range of β_1 is always $[\beta_1^-, \beta_1^+]$.

For each scenario, 100 simulation runs are conducted. Within each simulation run, optimum ALT plans are generated using both sequential and static planning methods. Under each generated plan, failure times are simulated, and the 0.1 percentile $y_{0.1}(1)$ is estimated.

5.4.3. Simulation Results

Simulation results are presented in Table 5.5. For each simulation scenario, planning outputs using both methods are given in columns "Outputs". There are two sub-columns under "Std. Dev": sub-column "A" is the asymptotic standard error (for static planning) or the pre-posterior expectation of the posterior standard error (for sequential planning) of the estimate $\hat{y}_{0.1}(1)$ given by the developed plans, denoted as $\text{Ase}(\hat{y}_{0.1}(1))$; sub-column "B" is the sample standard deviation of the estimate $\hat{y}_{0.1}(1)$ calculated from 100 repeated simulation runs, denoted as $\text{SD}(\hat{y}_{0.1}(1))$. For each simulation run, the estimate $\hat{y}_{0.1}(1)$ is plotted as shown in Figure 5.11.

Table 5.5 Comparison between the sequential and static ALT plan with 2 stress levels

	Static Planning				Sequential Planning			
	Inputs	Outputs	Std. Dev.		Inputs	Outputs	Std. Dev.	
			A	B			A	B
1	$\beta_0 = 4$ $\beta_1 = 4.5$ $\sigma = 0.8$ $c = 183$ $n = 300$	$n_H = 61$ $n_L = 239$ $x_L = 0.51$ $(T_L = 81^0\text{C})$	0.242	0.384	$\beta_0 = 4,\ \sigma = 0.8$ $\beta_1 \sim uniform(4,5)$ $c = 183\quad n = 300$ $R_H = 15$	$c_H = 60, c_L = 123$ $n_H = 22,\ n_L = 278$ $x_L = 0.85\ (T_L = 59^0\text{C})$	0.269	0.207
2	$\beta_0 = 3$ $\beta_1 = 4$ $\sigma = 0.6$ $c = 183$ $n = 300$	$n_H = 50$ $n_L = 250$ $x_L = 0.7$ $(T_L = 68^0\text{C})$	0.107	0.319	$\beta_0 = 3,\ \sigma = 0.6$ $\beta_1 \sim uniform(4,5)$ $c = 183\quad n = 300$ $R_H = 15$	$c_H = 60, c_L = 123$ $n_H = 15,\ n_L = 285$ $x_L = 0.8\ (T_L = 62^0\text{C})$	0.310	0.227
3	$\beta_0 = 3$ $\beta_1 = 4$ $\sigma = 1$ $c = 183$ $n = 300$	$n_H = 58$ $n_L = 242$ $x_L = 0.7$ $(T_L = 68^0\text{C})$	0.167	0.267	$\beta_0 = 3,\ \sigma = 1$ $\beta_1 \sim uniform(4,5)$ $c = 183\quad n = 300$ $R_H = 15$	$c_H = 60, c_L = 123$ $n_H = 16,\ n_L = 284$ $x_L = 0.9\ (T_L = 56^0\text{C})$	0.320	0.229
4	$\beta_0 = 3$ $\beta_1 = 5$ $\sigma = 0.6$ $c = 183$ $n = 300$	$n_H = 68$ $n_L = 232$ $x_L = 0.53$ $(T_L = 80^0\text{C})$	0.137	0.334	$\beta_0 = 3,\ \sigma = 0.6$ $\beta_1 \sim uniform(4,5)$ $c = 183\quad n = 300$ $R_H = 15$	$c_H = 60, c_L = 123$ $n_H = 15,\ n_L = 285$ $x_L = 0.8\ (T_L = 62^0\text{C})$	0.310	0.227
5	$\beta_0 = 3$ $\beta_1 = 5$ $\sigma = 1$ $c = 183$ $n = 300$	$n_H = 50$ $n_L = 250$ $x_L = 0.69$ $(T_L = 69^0\text{C})$	0.194	0.272	$\beta_0 = 3,\ \sigma = 1$ $\beta_1 \sim uniform(4,5)$ $c = 183\quad n = 300$ $R_H = 15$	$c_H = 60, c_L = 123$ $n_H = 16,\ n_L = 284$ $x_L = 0.9\ (T_L = 56^0\text{C})$	0.320	0.229

6	$\beta_0 = 5$	$n_H = 87$	0.405	0.622	$\beta_0 = 5$, $\sigma = 0.6$	$c_H = 60, c_L = 123$	0.250	0.168
	$\beta_1 = 4$	$n_L = 213$			$\beta_1 \sim uniform(4,5)$	$n_H = 16$, $n_L = 224$		
	$\sigma = 0.6$	$x_L = 0.35$			$c = 183$ $n = 300$	$x_L = 0.95$ $(T_L = 53^0\text{C})$		
	$c = 183$	$(T_L = 92^0\text{C})$			$R_H = 15$			
	$n = 300$							
7	$\beta_0 = 5$	$n_H = 57$	0.378	0.287	$\beta_0 = 5$, $\sigma = 1$	$c_H = 60, c_L = 123$	0.274	0.212
	$\beta_1 = 4$	$n_L = 243$			$\beta_1 \sim uniform(4,5)$	$n_H = 16$, $n_L = 224$		
	$\sigma = 1$	$x_L = 0.59$			$c = 183$ $n = 300$	$x_L = 0.95$ $(T_L = 53^0\text{C})$		
	$c = 183$	$(T_L = 75^0\text{C})$			$R_H = 15$			
	$n = 300$							
8	$\beta_0 = 5$	$n_H = 95$	0.528	0.721	$\beta_0 = 5$, $\sigma = 0.6$	$c_H = 60, c_L = 123$	0.250	0.168
	$\beta_1 = 5$	$n_L = 205$			$\beta_1 \sim uniform(4,5)$	$n_H = 16$, $n_L = 224$		
	$\sigma = 0.6$	$x_L = 0.28$			$c = 183$ $n = 300$	$x_L = 0.95$ $(T_L = 53^0\text{C})$		
	$c = 183$	$(T_L = 96^0\text{C})$			$R_H = 15$			
	$n = 300$							
9	$\beta_0 = 5$	$n_H = 74$	0.509	0.405	$\beta_0 = 5$, $\sigma = 1$	$c_H = 60, c_L = 123$	0.274	0.212
	$\beta_1 = 5$	$n_L = 226$			$\beta_1 \sim uniform(4,5)$	$n_H = 16$, $n_L = 224$		
	$\sigma = 1$	$x_L = 0.47$			$c = 183$ $n = 300$	$x_L = 0.95$ $(T_L = 53^0\text{C})$		
	$c = 183$	$(T_L = 84^0\text{C})$			$R_H = 15$			
	$n = 300$							

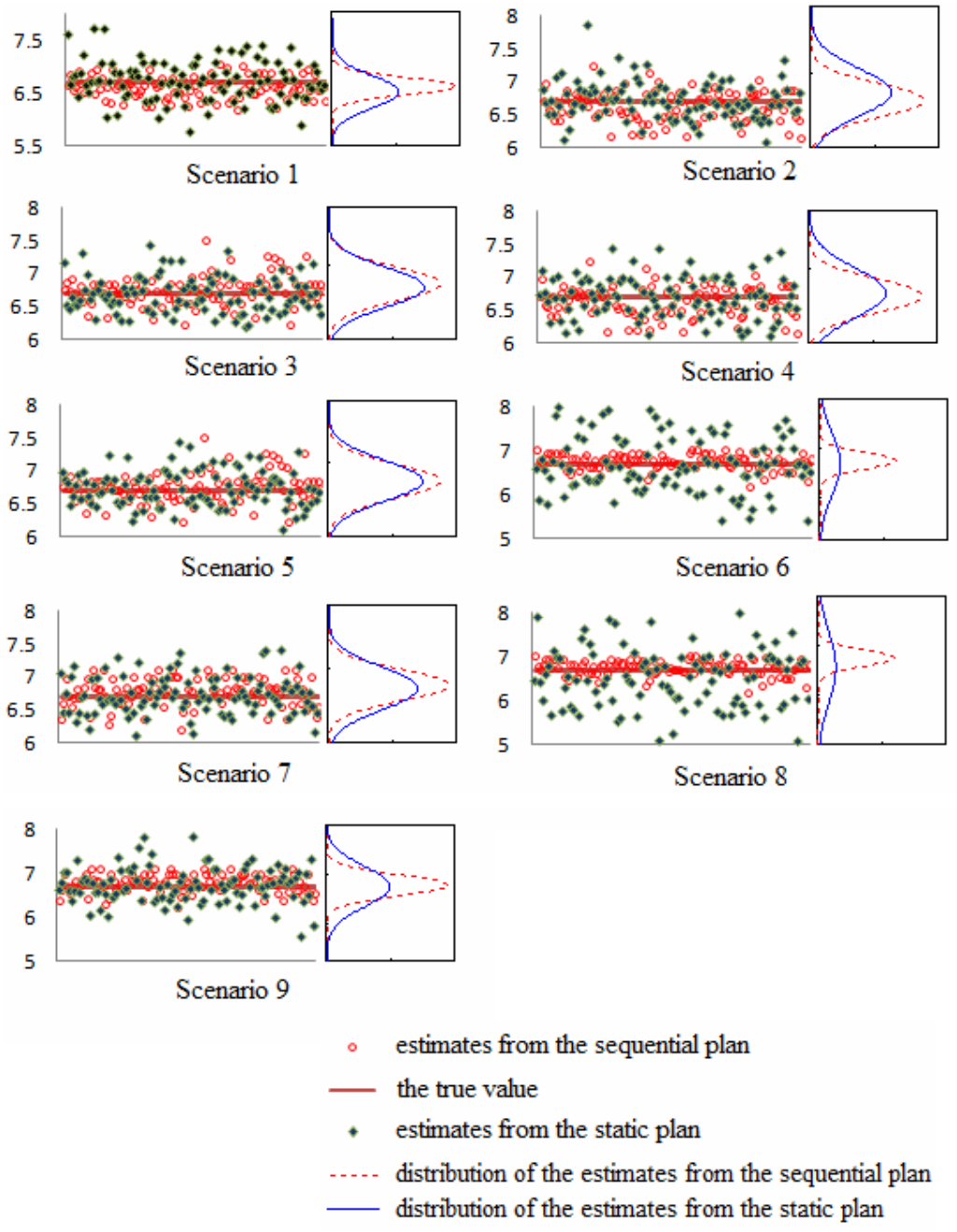

Figure 5.11 Plot of estimated $\hat{y}_{0.1}(1)$ of each simulation run for all scenarios

Three key observations from the simulation results presented in Table 5 and Figure 11 are:

- The sequential ALT plan yields an estimate $\hat{y}_{0.1}(1)$ with higher precision

For both planning methods, Figure 5.12 depicts the standard deviation of $\hat{y}_{0.1}(1)$ (both the $\text{Ase}(\hat{y}_{0.1}(1))$ given in the sub-column "A" and the sample standard deviation $\text{SD}(\hat{y}_{0.1}(1))$ given in the sub-column "B") for each simulation scenario. It is clear that the sequential plan consistently yields smaller $\text{SD}(\hat{y}_{0.1}(1))$ than the non-sequential static plan for all scenarios.

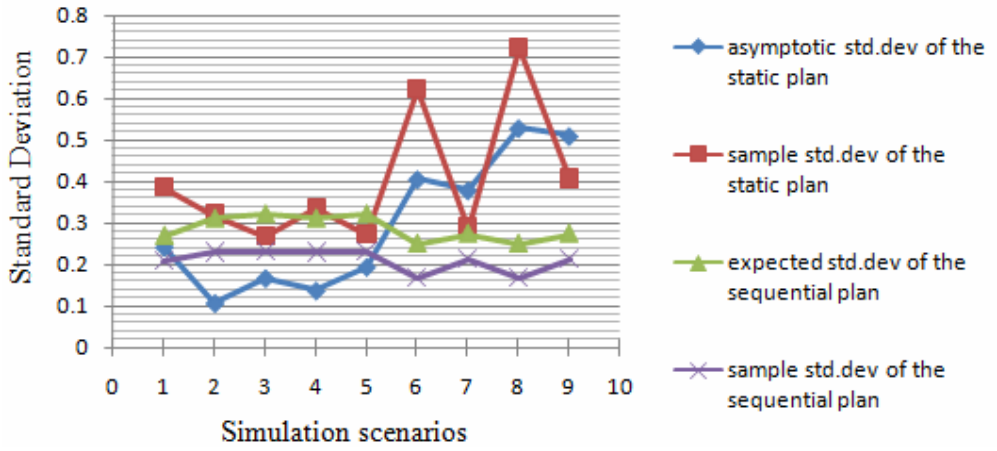

Figure 5.12 Plot of standard deviation of $\hat{y}_{0.1}(1)$ for all simulation scenarios

In addition, based on the plot in Figure 5.12, the sequential plan appears to provide a conservative planning result since the $\text{Ase}(\hat{y}_{0.1}(1))$ given by the sequential plan is larger than the sample standard deviation $\text{SD}(\hat{y}_{0.1}(1))$ for all scenarios. However, this conclusion does not always hold. Recall that the sequential plan is developed (averaged) over a specified range $[\beta_1^-, \beta_1^+]$ of β_1. Conceivably, when the true value of β_1 is small, say, somewhere near β_1^-, more failures might be obtained at lower stress levels than it is expected, thus the sample standard deviation $\text{SD}(\hat{y}_{0.1}(1))$ tends to be

smaller than the pre-posterior expectation $\text{Ase}(\hat{y}_{0.1}(1))$. On the other hand, $\text{SD}(\hat{y}_{0.1}(1))$ can be larger than $\text{Ase}(\hat{y}_{0.1}(1))$ if the true value of β_1 is larger than it is expected.

In fact, it is not easy to conclude that which (pre-specified) parameter(s) causes the dramatic change of $\text{SD}(\hat{y}_{0.1}(1))$ for the static plan. What might be helpful here is to compute the "effect" of each (pre-specified) parameter using the method that has been widely applied to analyze the results of a 2^3 factorial experiment, namely, we estimate the "effect" of each parameter and their interactions by (Montgomery and Runger, (2003))

$$\text{Effect} = \frac{\text{Contrast}}{2^{3-1}} \tag{5.16}$$

The results are presented in Table 5.6. It can be seen that the intercept parameter β_0 , the slope parameter β_1, and their interaction have relatively larger effect on $\text{SD}(\hat{y}_{0.1}(1))$ for the static plan. This observation supports the third motivation of the proposed sequential planning discussed in the introduction. By conducting the ALT in a sequential manner helps in specifying the intercept parameter β_0 . By using a prior distribution of β_1 addresses the uncertainty associated to the slope parameter. Therefore, it is possible to enhance the robustness of the plan against mis-specification of model parameters.

Table 5.6 Effect of pre-specified model parameters and their interactions

	β_0	β_1	σ	$\beta_0\ \beta_1$	$\beta_0\ \sigma$	$\beta_1\ \sigma$	$\beta_0\ \beta_1\ \sigma$
Effect	0.1945	-0.2075	0.043	-0.1180	0.0655	0.0185	-0.009

- Sequential ALT plan is more robust to the misspecification of model parameters.

As clearly seen in Figure 5.12, both $\text{Ase}\left(\hat{y}_{0.1}(1)\right)$ and $\text{SD}\left(\hat{y}_{0.1}(1)\right)$ yielded by the sequential plan remain stable across different scenarios, that is, the sequential plan is robust to the pre-specified model parameters. We compute the relative error (*RE*) between $\text{Ase}\left(\hat{y}_{0.1}(1)\right)$ and $\text{SD}\left(\hat{y}_{0.1}(1)\right)$ for both plans. Figure 5.13 plots the computed *RE* (in its absolute value) for each scenario. It is seen that, the *RE* curve of the sequential plan is considerably stable and always under the *RE* curve of the static plan. This observation supports the conclusion that the robustness of an ALT plan can be greatly improved using the sequential testing scheme even without affecting the total test duration at times.

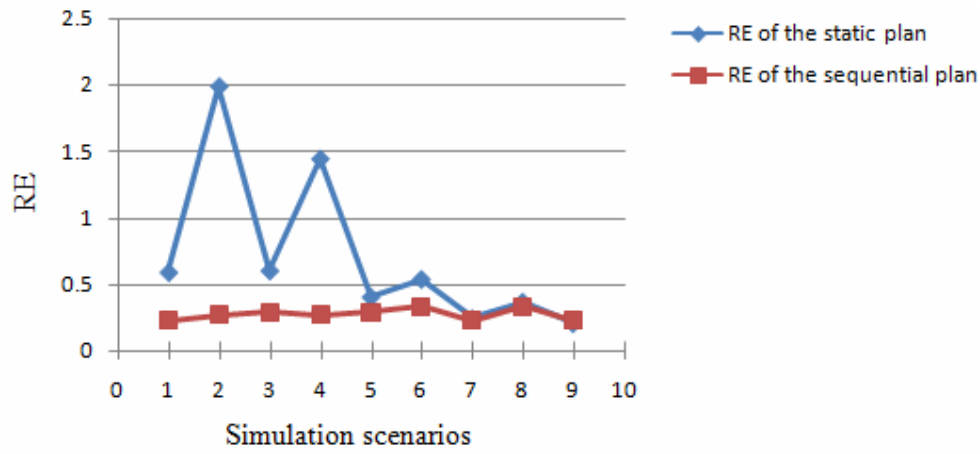

Figure 5.13 Plot of RE for all simulation scenarios

- The sequential ALT plan decreases the degree of extrapolation.

In choosing levels of the accelerating variable, it is necessary to balance extrapolation in the accelerating variable with extrapolation in time (Meeker and Escobar (1998), Chapter 20). Hence, we compare the optimum low stress level for both sequential and static plan under each simulation scenario. The results are shown in Figure 5.14.

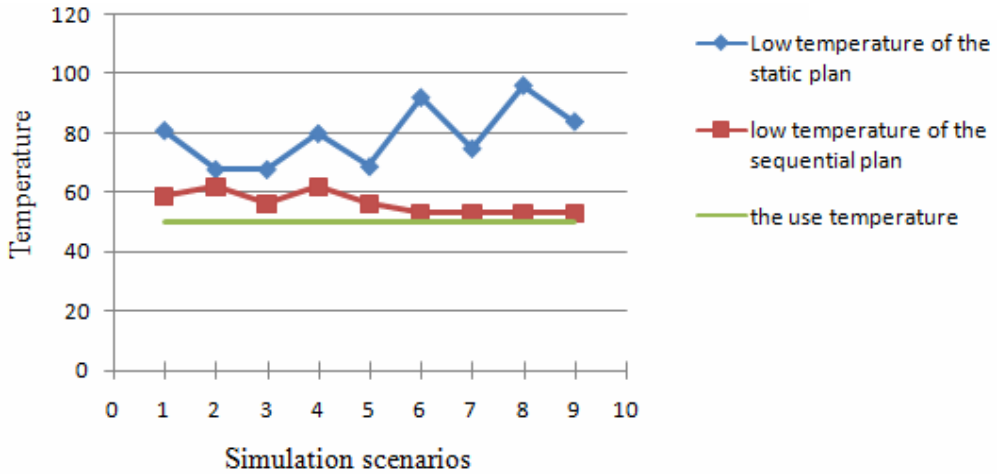

Figure 5.14 The optimum low temperature level for all simulation scenarios

As seen from the figure, the optimum low stress level can be further push towards the use condition if the sequential test plan is adopted. As discussed above, this is because an informative prior distribution of (μ_i, σ_i) is constructed for test planning at the low stress. In addition, it is also observed that the optimum low temperature yielded by the sequential plan does not vary dramatically across different simulation scenarios, namely, the sequential ALT plan is less sensitive to the pre-specified planning values.

5.4.4. Comparison of the Sequential Plan with Compromise Plan

The comparison above is based on two-level optimal plans. Such plans are known not to be robust to mis-specification of planning values, but usually used as benchmarks for more practical compromise plans which consist of more than two stress levels (Meeker and Escobar, (1998)). For example, the 4:2:1 test plan proposed in Meeker and Hahn (1985) is a special type of compromise plan which allocates 4/7, 2/7, and 1/7 of all units to three equally-spaced stress levels x_L, $x_M = (x_L + x_H)/2$, and $x_H = 0$. In this section, we present a comparison study between the proposed

sequential plan and the 4:2:1 static compromise plan based on the adhesive bond example presented above. All numerical settings remain unchanged.

In order to design a meaningful and fair comparison study, two issues must be addressed,

♦ For the static compromise planning, both sample size allocation and stress level combination for all stress levels are simultaneously optimized. For the proposed sequential planning, however, the sample allocation at the highest stress is firstly determined using a different approach. Hence, it is appropriate to compare the proposed sequential plan to the 4:2:1 plan as the sample allocation to each stress level can be fixed for both sequential and static plans.

♦ The testing duration c_H at the highest stress for the sequential plan must be pre-determined. In this comparison study, we consider three testing durations as $c_H = 30$, $c_H = 60$ and $c_H = 90$. For each c_H, all the 9 scenarios listed in Table 4 are studied.

The comparison results are presented in Table 5.7. In this table, p_U and p_H are respectively the failure probability at use condition and the highest stress level; "Ase" is the asymptotic standard error (for static plan) or the pre-posterior expectation of the posterior standard error (for sequential plan) of the estimate $\hat{y}_{0.1}(1)$ given by the testing plans; "ASR" is known as the asymptotic sample ratio which is defined as

$$\text{ASR} = \left| \frac{\text{Ase}(\hat{y}_{0.1}(1)) - \text{Ase}^*(\hat{y}_{0.1}(1))}{\text{Ase}^*(\hat{y}_{0.1}(1))} \right| \times 100\% \qquad (5.17)$$

where $\text{Ase}^*(\hat{y}_{0.1}(1))$ is the "Ase" when all model parameters are correctly specified, i.e. the $\text{Ase}(\hat{y}_{0.1}(1))$ for the simulation scenario 1.

Clearly, ASR measures the robustness of the developed plans to the mis-specification of model parameters. This idea is partially borrowed from Pascual

and Montepiedra (2003). In their work, the authors used the ASR, defined in a different way, to measure the planning robustness against mis-specification of failure time model.

Figure 5.15 plots the ASR for both the static 4:2:1 plan and sequential plan under all simulation scenarios. It is immediately seen that the ASR of the sequential plan is smaller than that of the 4:2:1 plan. Particularly, when the test duration at the highest stress is short, say $c_H = 30$, the sequential plan appears to be more sensitive to the pre-specified model parameters. This is because the preliminary information on β_0 and σ is vague when not enough failures are obtained at the highest stress, and the developed plan dependents more on the specified model parameters which can be mis-specified.

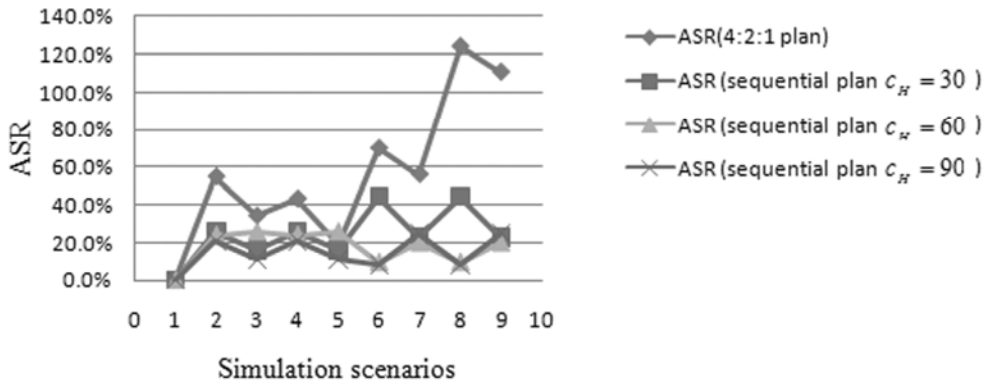

Figure 5.15. Plot of ASR for all simulation scenarios

In addition, it is interesting to observe that the lowest stress level x_L yielded by the sequential plan is 1 or very much close to 1. As we have discussed above, this is due to an informative prior distribution on (μ_L, σ) has been used. Hence, to ensure enough failures, it is highly recommended to specify a minimum number of failures R_L at stress x_L as we did in the numerical example. On the other hand, if little information on β_0 and σ is obtained from the test at the highest stress, or the prior knowledge on β_1 is

vague, the lower stress level x_L will become higher so as to generate more failures.

Table 5.7 Comparison between the sequential plan and the static 4:2:1 ALT plan

Scenario	4:2:1 Plan						Sequential Plan, $c_H = 30$				Sequential Plan, $c_H = 60$				Sequential Plan, $c_H = 90$			
	p_U	p_H	x_L	p_L	Ase	ASR	x_L	p_L	Ase	ASR	x_L	p_L	Ase	ASR	x_L	p_L	Ase	ASR
1	.0162	.9893	.51	.2270	.2868	1	1	.0134	.2478	1	.98	.0090	.2528	1	.98	.0081	.2629	1
2	.0493	.9999	.70	.3188	.1288	55.0%	.96	.0236	.1828	26.2%	.98	.0107	.1915	24.3%	1	.006	.2008	20.6%
3	.1537	.9999	.84	.2759	.1884	34.3%	1	.0786	.2081	16.0%	1	.0563	.2129	25.8%	1	.0429	.2251	11.0%
4	.0095	.9999	.54	.3569	.1625	43.3%	.96	.0236	.1828	26.2%	.98	.0107	.1915	24.3%	1	.006	.2008	20.6%
5	.0595	.9999	.67	.2736	.2316	19.2%	1	.0786	.2081	16.0%	1	.0563	.2129	25.8%	1	.0429	.2251	11.0%
6	.0018	.7578	.36	.1245	.4880	70.2%	1	.0003	.3578	44.4%	1	.0002	.2771	9.6%	1	.0002	.2735	8.2%
7	.0223	.7086	.59	.1099	.4480	56.2%	1	.0074	.3042	22.8%	1	.0065	.3030	19.9%	1	.0058	.3156	24.8%
8	.0003	.7578	.29	.1236	.6435	124.3%	1	.0003	.3578	44.4%	1	.0002	.2771	9.6%	1	.0002	.2735	8.2%
9	.0083	.7086	.47	.1109	.6051	111.0%	1	.0074	.3042	22.8%	1	.0065	.3030	19.9%	1	.0058	.3156	24.8%

Chapter 6. Bayesian Planning of Sequential ALT with Stepwise Loaded Auxiliary Acceleration Factor

6.1. Introduction

It is extremely important to obtain enough number of failures from an ALT. However, one challenge today in both ALT planning and inference is that failures can still be elusive at lower stress levels when product reliability is high, see e.g. the case study presented in Section 6.4. To mitigate this problem, the common remedy is to specify a minimum number of failures at low stress levels. But this inevitably leads to a longer test duration which may not always be feasible. As a result, the low stress level is typically elevated to meet the time constraint. This results in high, sometimes intolerable, degree of extrapolation in estimating product reliability at use stress. Motivated by a real-case application shown in Section 6.4, an auxiliary acceleration factor (AAF) is introduced in this chapter to further amplify the failure probability at low stress levels. Particularly, as illustrated by Figure 6.1, we shall embed the AAF into the framework of sequential Bayesian ALT planning, and obtain optimal sequential ALT plans with a selected AAF. Several important problems with practical significance shall be addressed in this article, including the modeling of a sequential ALT with an AAF, the choice of an AAF as well as its loading profile, the Bayesian optimal planning problem of a sequential ALT with AAF, and the robustness of the sequential testing plan against mis-specification of model parameters.

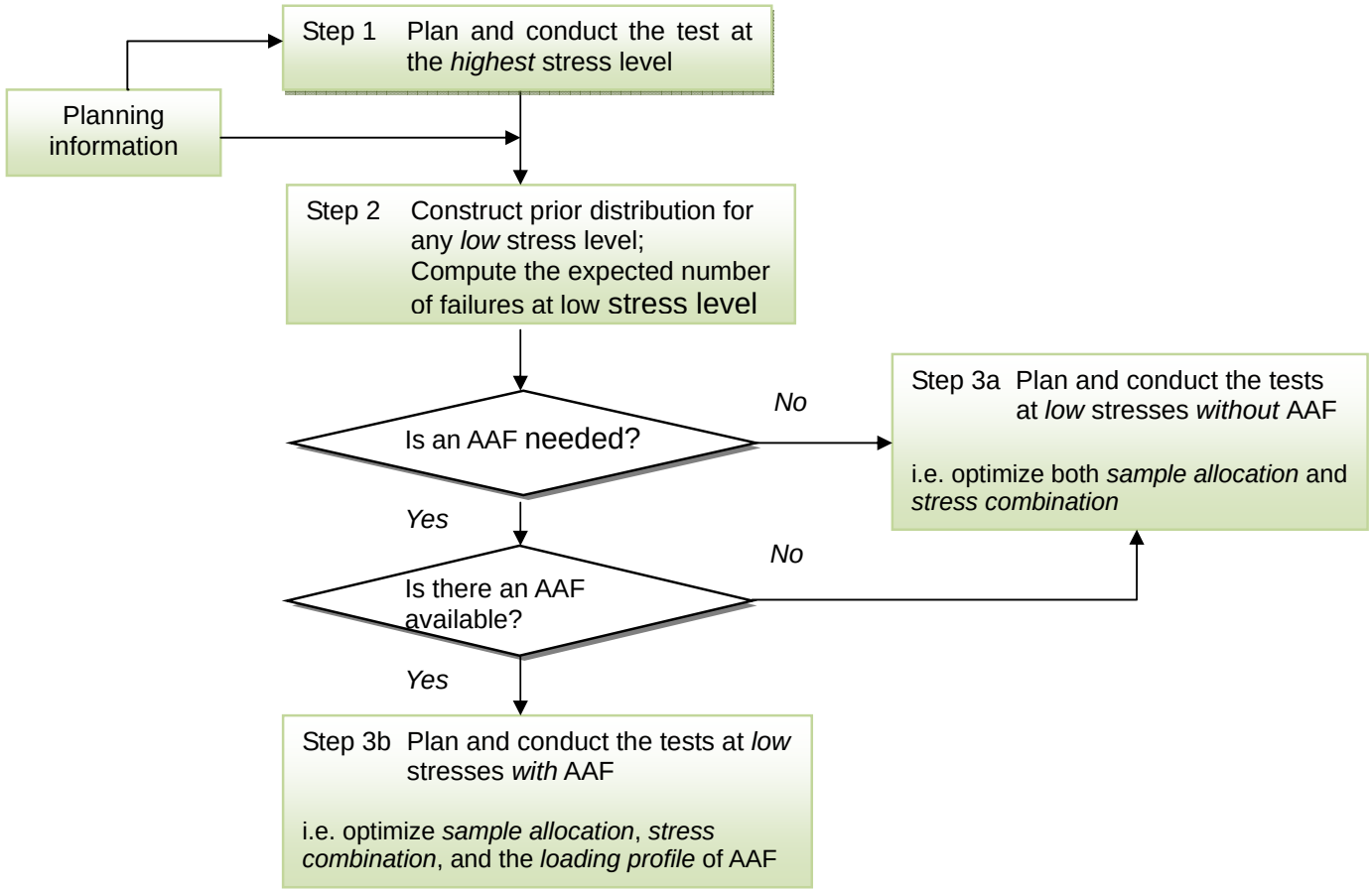

Figure 6.1 Framework of planning a sequential ALT with auxiliary acceleration factor (AAF)

In what follows, we provide comprehensive discussions on both the background and motivation of the problem addressed in this chapter, and explain in detail the framework of sequential ALT planning with AAF as sketched by Figure 6.1.

6.1.1. Motivations of Using an Auxiliary Acceleration Factor

Although an ALT can be sequentially conducted, the number of failures might be elusive at low stresses as seen in the case study presented in Section 6.4. In fact, this is not a trivial situation nowadays when product reliability is getting higher. Not seeing enough failures usually makes it extremely difficult to estimate product reliability, or to discover product deficiencies. To mitigate this problem, one common practice is to add an additional constraint that specifies the minimum number of failures expected to obtain, see Meeker and Escobar (1998). However, as shown in the case study provided in Section 6.4, this constraint leads to a longer test duration which may not always be feasible. As a result, the low stress level is forced to be elevated to meet the time constraint. This results in high, sometimes intolerable, degree of extrapolation in estimating product reliability at use stress.

Hence, an auxiliary acceleration factor (AAF), with its effect on product life well defined, is introduced in this chapter to further amplify the failure probability of testing units at low stress levels (step 3b in Figure 6.1). For one example, one can intentionally change the level of one or more controllable factors, say, the size of the prototype, so as to amplify the failure probability of testing units, see e.g. Bai and Yun (1996). For another example, in a reliability test of certain micro relays operating at difference levels of silicone vapor (ppm), the usage rate (Hz) might be used as an auxiliary factor if the effect of usage rate on product reliability is well defined, see e.g. Yang (2005). In the temperature-accelerated life test presented in Section 6.4, the

humidity level controlled in the chamber will be used as an auxiliary acceleration factor as its effect on our product life is well understood; also see Livingston (2000).

In fact, we have seen similar ideas in the literature as the one to use an auxiliary acceleration factor. In the study of design of experiment (DOE), Joseph and Wu (2004) and Jeng et al. (2008) proposed a method known as FAMe--the failure amplification method. For such a method, an amplification factor with known effect is proposed to ensure an adequate number of failures during an experiment. However, the distinction here is that, FAMe is developed for system optimization while ALT is used for reliability estimation at user condition through extrapolation.

No matter what factor is chosen as the AAF, it is extremely important to make sure that it accelerates the right failure mode which is of our interest. Therefore, a careful modeling of AAF is a must as discussed in detail in Section 6.2.

6.1.2. Organization

The remainder of this chapter is organized as follows. Section 6.2 presents the ALT model and a Bayesian planning criterion based on which our analysis will be carried on. Section 6.3 describes the approach for planning a sequential ALT with auxiliary acceleration factor at low stress levels. The developed plan simultaneously optimizes the sample allocation, stress level combination, and loading pattern of the auxiliary acceleration factor. In Section 6.4, we present the motivating case study of this study to demonstrate the application of proposed planning method.

6.2. The ALT Model and a Bayesian Planning Criterion

6.2.1. The ALT Model with Auxiliary Acceleration Factor

Consider a constant-stress ALT that involves $k(\geq 2)$ stress levels. At each stress level, n_i number of specimen is tested until a pre-specified time c_i. Let s_k denote the highest stress which is pre-fixed, and s_0 denote the design stress where a given reliability measure is to be estimated, we standardize stress s

$$x = (s - s_k) / (s_0 - s_k) \tag{6.1}$$

, such that $x_0 = 1$ for the design stress s_0; $x_k = 0$ for the highest stress s_k. Hence, the testing region is defined on $X = [0,1]$ where the highest testing stress is pre-fixed.

At any stress, we assume that product life follows Weibull distribution. That is, the logarithm of product life follows Smallest Extreme Value (SEV) distribution with its cumulative distribution function (Cdf) given by

$$F(y) = \Phi_{SEV}[(y - \mu) / \sigma] \tag{6.2}$$

Here, μ and σ are respectively the location and scale parameters of product life y in log-scale; $\Phi_{SEV} = 1 - \exp(-\exp(z))$ is the standardized SEV Cdf.

As discussed in the introduction, an auxiliary acceleration factor (AAF) will be chosen to amplify the failure probability of testing units at low stress levels. Let v denote the level of AAF; $v_{\max}$ denotes the maximum allowable level of AAF; and v_{use} denotes the nominal level of AAF when no auxiliary acceleration is applied, we then standardize v

$$h = (v - v_{use}) / (v_{\max} - v_{use}) \tag{6.3}$$

such that $h = 0$ for $v = v_{use}$ and $h = 1$ for $v = v_{max}$. Note that, the standardization of v is different with that of s in (1) for the convenience of presentation in the following sections. After an AAF has been incorporated, the testing region is expanded to a unit square.

Furthermore, the stress-life relationship is assumed to be

$$\mu = \beta_0 + \beta_1 x + \beta_2 h \quad , \quad \sigma \text{ is a unknown constant} \tag{6.4}$$

where β_0 and β_1 are unknown parameters to be estimated, whereas β_2 is the known effect (possibly needs to be verified) of the chosen AAF. In practice, many commonly used stress-life models, such as the higher usage model proposed in Yang (2005), the Arrhenius and Hallberg-Peck relationships considered in Section 6.4, can all be easily linearized into the form of (6.4). In addition, as σ is closely related to the failure mechanism, it is reasonable to assume σ to be a constant as long as the failure mechanism of interest does not change. Apparently, if no auxiliary acceleration factor is used, i.e. $h = 0$, the stress-life model in (6.4) is simplified to $\mu = \beta_0 + \beta_1 x$ with $\mu_k = \beta_0$ as $x_k = 0$; and $\mu_0 = \beta_0 + \beta_1$ as $x_0 = 1$.

6.2.2. A Bayesian Planning Criterion

A Bayesian planning approach is used in this chapter, and the goal of the test is to estimate the 100p-th percentile $y_p(x)$ of the SEV distribution at use stress where $x = 1$ and $h = 0$. Collect the parameter (μ_i, σ) in a vector $\boldsymbol{\theta}_i = (\mu_i, \sigma)$ for $i = 0, 1, ..., k$, $y_p(1)$ is given as

$$y_p(1) = \mu_0 + u_p \cdot \sigma = \mathbf{c}\boldsymbol{\theta}_0^T \tag{6.5}$$

where $u_p = \Phi_{SEV}^{-1}(p) = \log(-\log(1-p))$ and $\mathbf{c} = [1, u_p]$.

Clearly, given a testing plan $\boldsymbol{\xi}$, the posterior variance $\text{var}(y_p(1))$ depends on the (unobserved) failure data $\mathbf{t}$. Hence, a pre-posterior expectation of the posterior variance over the marginal distribution of $\mathbf{t}$ is naturally chosen to obtain a Bayesian test planning criterion as follows

$$\begin{aligned} C(\boldsymbol{\xi}) &= -E_{\mathbf{t}|\boldsymbol{\xi}}[\text{var}(y_p(1))] \\ &= -E_{\mathbf{t}|\boldsymbol{\xi}}[\mathbf{c}\,\text{var}(\boldsymbol{\theta}_0)\mathbf{c}^T] \end{aligned} \tag{6.6}$$

That is, the optimal plan maximizes $C(\boldsymbol{\xi})$ in (6.6), or equivalently, minimizes the pre-posterior expectation of the posterior variance $\text{var}(y_p(1))$.

6.3. Planning of a Sequential ALT with Auxiliary Acceleration Factor

We formally present in this section the sequential planning approach for constant-stress ALT with a stepwise loaded auxiliary acceleration factor at lower stress levels.

6.3.1. Planning and Inference for Test at the Highest Stress Level

The planning of test at the highest stress level can be done using the method described in Section 5.2.1. In what follows, however, we introduce a different planning approach which takes into account the uncertainty in collecting failure data.

Under the sequential ALT planning scheme depicted by Figure 6.1, test at the highest stress level is firstly planned and conducted. As failures are usually relatively easier to obtain at the highest stress, there is no strong motivation to use any auxiliary acceleration stress. In practice as seen in Section 6.4, engineers may not even know at this moment an auxiliary acceleration factor will be needed for subsequent tests.

To plan the test at the highest stress x_k, one needs to,

- Specify the test duration c_k, and the number of failures r_k expected to obtain.
- Specify the values for parameters μ_k and σ, based on which the reliability of testing units at stress x_k is calculated by $R_k = \exp[-(c_k / \exp(\mu_k))^{1/\sigma}]$.
- Specify a confidence level α.

Given the planning information above, the number of units to be tested at the highest stress x_k can be easily found by solving the following equation

$$\sum_{i=0}^{r_k-1} C_{n_k}^{i} (1-R_k)^i R_k^{n_k-i} = 1-\alpha \tag{6.7}$$

That is, the probability of seeing less-than-r_k failures is $1-\alpha$. Equation (6.7) is also known as the Bogey testing which are commonly used for product reliability demonstration, and the value $1-\alpha$ is sometimes referred as the consumer's risk, see Yang (2007, pp.384). Here, the specified value of r_k should at least be 4 or 5 so as to yield enough information for both reliability assessment and subsequent tests planning.

Suppose that the test at x_k has been conducted and we have observed failure data $\mathbf{y}_k$. The posterior distribution $\pi(\boldsymbol{\theta}_k | \mathbf{y}_k)$ is directly derived applying the Bayes' rule

$$\pi(\boldsymbol{\theta}_k | \mathbf{y}_k) \propto \vartheta(\boldsymbol{\theta}_k) \cdot L(\boldsymbol{\theta}_k; \mathbf{y}_k)$$

where $\boldsymbol{\theta}_k = (\mu_k, \sigma)$; $\vartheta(\boldsymbol{\theta}_k)$ is prior distribution of $\boldsymbol{\theta}_k$; and $L(\boldsymbol{\theta}_k; \mathbf{y}_k)$ is the likelihood function of $\boldsymbol{\theta}_k$. In the context of ALT, since the number of failures is expected to be large enough at the highest stress, we let $\vartheta(\boldsymbol{\theta}_k)$ be a constant so as to protect the data objectivity and obtain the posterior distribution as follows

$$\pi(\boldsymbol{\theta}_k | \mathbf{y}_k) \propto \prod_{j=1}^{n_k} \exp\{\kappa_{kj} \cdot (-\log\sigma + z_{kj} - \exp(z_{kj})) - (1-\kappa_{kj}) \cdot \exp(\zeta_k)\} \tag{6.8}$$

where the subscript "- $_{kj}$ " is associated to the *jth* observation at the stress x_k ; $z=(y-\mu)/\sigma$ is the standardized failure time; $\zeta_i=(\log c_i-\mu_i)/\sigma$ is the standardized censoring time; and κ =1for exact failure data while κ =0 for censored data.

Throughout this chapter, the mode of the posterior distribution is used as the Bayesian estimate, i.e. $\hat{\boldsymbol{\theta}}_k=[\hat{\mu}_k,\hat{\sigma}]=\arg\max_{\boldsymbol{\theta}_k}\pi(\boldsymbol{\theta}_k|\mathbf{y}_k)$. In Berger (1985), this type of estimate is known as the Generalized Maximum Likelihood Estimate (GMLE).

Under the framework of sequential ALT plan, the derived $\pi(\boldsymbol{\theta}_k|\mathbf{y}_k)$ will then be used in Section 6.3.2.1 to construct the prior distributions $\vartheta(\boldsymbol{\theta}_i)$ for $\boldsymbol{\theta}_i$ at lower stress levels ($i=1,...,k-1$). For simplicity, we approximate the $\pi(\boldsymbol{\theta}_k|\mathbf{y}_k)$ by a bivariate normal distribution with mean $\hat{\boldsymbol{\theta}}_k$ and variance $\hat{\boldsymbol{\Sigma}}_k$

$$\boldsymbol{\theta}_k|\mathbf{y}_k\sim N(\hat{\boldsymbol{\theta}}_k,\hat{\boldsymbol{\Sigma}}_k)\qquad \hat{\boldsymbol{\Sigma}}_k=[-\hat{\mathbf{I}}_{\boldsymbol{\theta}_k}]^{-1},\quad \hat{\mathbf{I}}_k=[\partial^2 l(\boldsymbol{\theta}_k;\mathbf{y}_k)/\partial\boldsymbol{\theta}_k^2]_{\boldsymbol{\theta}_k=\hat{\boldsymbol{\theta}}_k} \tag{6.9}$$

where $l(\boldsymbol{\theta}_k;\mathbf{y}_k)$ is the log-likelihood function of $\boldsymbol{\theta}_k$, and $\hat{\mathbf{I}}_{\boldsymbol{\theta}_k}$ is the Fisher information observed at $\hat{\boldsymbol{\theta}}_k$. Based on the results derived above, the estimated 100p-th percentile $\hat{y}_p(0)$ at the highest stress level $x_k=0$ is estimated by $\hat{\mu}_k+u_p\cdot\hat{\sigma}$ with asymptotic variance $\mathbf{c}\hat{\boldsymbol{\Sigma}}_k\mathbf{c}^T$.

It is noted that, the normal approximation in (6.9) might not be a necessary step, but it certainly facilitates the construction of prior distribution as we shall soon see below, and greatly simplifies the proposed method for industrial application. Hence, what is truly necessary is to check the quality of the approximation, as well as the posterior normality of $\pi(\boldsymbol{\theta}_k|\mathbf{y}_k)$, see Martz et.al (1988) and Kass and Slate (1994). Generally speaking, as a reasonable large number of failures can usually be obtained at the highest stress level, the normal approximation here is expected to be appropriate in

many applications.

6.3.2. Planning Tests at Lower Stress Levels

6.3.2.1 Construction of Prior Distribution

Results obtained from the test at the highest stress level are then used to construct the prior distribution $\vartheta(\boldsymbol{\theta}_i)$ of $\boldsymbol{\theta}_i$ at any given lower stress x_i for $i = 1, 2, ..., k-1$, using the approach described in Section 5.2.2.1. That is, given a specified range $[\beta_1^-, \beta_1^+]$ of the slope parameter β_1, and the normally approximated $\pi(\boldsymbol{\theta}_k | \mathbf{y}_k)$

$$\pi(\boldsymbol{\theta}_k | \mathbf{y}_k) = (2\pi \operatorname{var}(\hat{\mu}_k) \operatorname{var}(\hat{\sigma}))^{-1} \cdot (1-\rho^2)^{-1/2} \cdot \exp\left(-\left(\frac{(\mu_k - \hat{\mu}_k)^2}{\operatorname{var}(\hat{\mu}_k)} - \frac{2\rho(\mu_k - \hat{\mu}_k)(\sigma - \hat{\sigma})}{\operatorname{var}(\hat{\mu}_k)\operatorname{var}(\hat{\sigma})} + \frac{(\sigma - \hat{\sigma})^2}{\operatorname{var}(\hat{\sigma})} \right) \Big/ 2(1-\rho^2) \right)$$

we obtain the prior distribution $\vartheta(\boldsymbol{\theta}_i)$ by changing the variable as $\mu_k = \mu_i - \beta_1 x_i$

$$\vartheta(\boldsymbol{\theta}_i) = (2\pi \operatorname{var}(\hat{\mu}_k) \operatorname{var}(\hat{\sigma}))^{-1} \cdot (1-\rho^2)^{-1/2} \int_{\omega_i^-}^{\omega_i^+} \exp\left(-\left(\frac{(\mu_i - \omega_i)^2}{\operatorname{var}(\hat{\mu}_k)} - \frac{2\rho(\mu_i - \omega_i)(\sigma - \hat{\sigma})}{\operatorname{var}(\hat{\mu}_k)\operatorname{var}(\hat{\sigma})} + \frac{(\sigma - \hat{\sigma})^2}{\operatorname{var}(\hat{\sigma})} \right) \Big/ 2(1-\rho^2) \right) \cdot \frac{1}{\omega_i^+ - \omega_i^-} d\omega_i$$

$$= \frac{1}{2^{3/2}(\pi \operatorname{var}(\hat{\sigma}))^{1/2}(\omega_i^- - \omega_i^+)} \cdot \exp\left[-\frac{(\sigma - \hat{\sigma})^2}{2\operatorname{var}(\hat{\sigma})} \right] \cdot \left[\operatorname{erf}(\psi_i^-) - \operatorname{erf}(\psi_i^+) \right] \quad \forall i = 1, 2, ..., k-1$$

where erf is the error function given by the definite integral $\operatorname{erf}(z) = 2\pi^{-1/2} \int_0^z e^{-t^2} dt$

$$\omega_i = \hat{\mu}_k + \beta_1 x_i$$

$$\omega_i^- = \hat{\mu}_k + \beta_1^- x_i, \quad \omega_i^+ = \hat{\mu}_k + \beta_1^+ x_i, \quad \rho = \operatorname{cov}(\hat{\mu}_k, \hat{\sigma}) / \operatorname{var}(\hat{\mu}_k) \operatorname{var}(\hat{\sigma})$$

$$\psi_i^- = \frac{-\mu_i \operatorname{var}^{1/2}(\hat{\sigma}) + \omega_i^- \operatorname{var}^{1/2}(\hat{\sigma}) + \rho(\sigma - \hat{\sigma}) \operatorname{var}^{1/2}(\hat{\mu}_k)}{(2\operatorname{var}(\hat{\mu}_k)\operatorname{var}(\hat{\sigma})(1-\rho^2))^{1/2}}$$

$$\psi_i^+ = \frac{-\mu_i \operatorname{var}^{1/2}(\hat{\sigma}) + \omega_i^+ \operatorname{var}^{1/2}(\hat{\sigma}) + \rho(\sigma - \hat{\sigma}) \operatorname{var}^{1/2}(\hat{\mu}_k)}{(2\operatorname{var}(\hat{\mu}_k)\operatorname{var}(\hat{\sigma})(1-\rho^2))^{1/2}}$$

(6.10)

It is noted that, since the prior knowledge about β_1 always involves a certain

amount of uncertainty, the information on μ_i and σ contained in $\vartheta(\boldsymbol{\theta}_i)$ decays as the low stress x_i moving away from the highest stress x_k where $\pi(\boldsymbol{\theta}_k \mid \mathbf{y}_k)$ is derived. In other words, the prior distribution $\vartheta(\boldsymbol{\theta}_i)$ must become diffuse as x_i approaches 1. In the case study provided in Section 6.4, we shall revisit this issue and provide more detailed illustrations.

6.3.2.2 The Choice of an Auxiliary Acceleration Factor

As we have discussed in Section 6.1.3, failures can be extremely difficult to obtain if the stress level is low. Hence, a possible auxiliary acceleration factor, with its effects well understood, can be used to amplify the failure probability so as to maximize the information obtained at lower stress levels.

In practice, it turns out to be important to carefully select an AAF, if it exists, as well as its maximum level so that the failure mode of interest does not change. In addition, it is also desirable to verify the pre-specified effect of the AAF after an ALT has been done. As we have seen in Section 6.2.1, the modeling of an ALT with AAF certainly requires stronger assumptions than that of a normal constant-stress ALT, hence, as long as the "amplification" target can be achieved, it is not always necessary to set the AAF to a high level throughout the test. In other words, we need to load the AAF with a target that specifies how much we are going to amply the failure probability.

Based on the considerations above, the step-stress stress loading scheme is naturally chosen for AAF, and the LCEM cumulative exposure model proposed in Tang (2003) is correspondingly adopted. It has been shown by Tang (2003) that, the LCEM model includes the well-known Nelson's cumulative exposure model as its special case under Weibull lifetime assumption. More importantly, it enables us to

derive the optimal loading pattern with a given time compression target which is defined as the ratio between the "equivalent time-to-failure at use condition" and "the actual time-to-failure at testing condition". In what follows, we consider a simple two-step step-stress loading pattern for AAF, although the approach can be quite easily generalized to accommodate multiple-step step-stress loading patterns.

A simple two-step step-stress loading pattern for AAF at a low stress level x_i can be illustrated by Figure 6.2. As seen from the figure, the level of AAF is initially set to $h_{i,1}$ where $h_{\text{use}} \le h_{i,1} \le h_{\max}$. At time τ_i, the level of AAF is elevated to $h_{i,2} = h_{\max} = 1$ and the test is continued until the censoring time c_i. Of course, the original acceleration factor is held on a level of x_i during the entire testing process, i.e.

$$h = \begin{cases} h_{i,1} & 0 \le t < \tau_i \\ h_{i,2} = h_{\max} & \tau_i \le t < c_i \end{cases} \quad \text{and} \quad x = x_i \quad 0 \le t < c_i$$

Here, the holding time τ_i, low level $h_{i,1}$ of AAF, and x_i need to be optimized in the test planning to be discussed in Section 6.3.2.5.

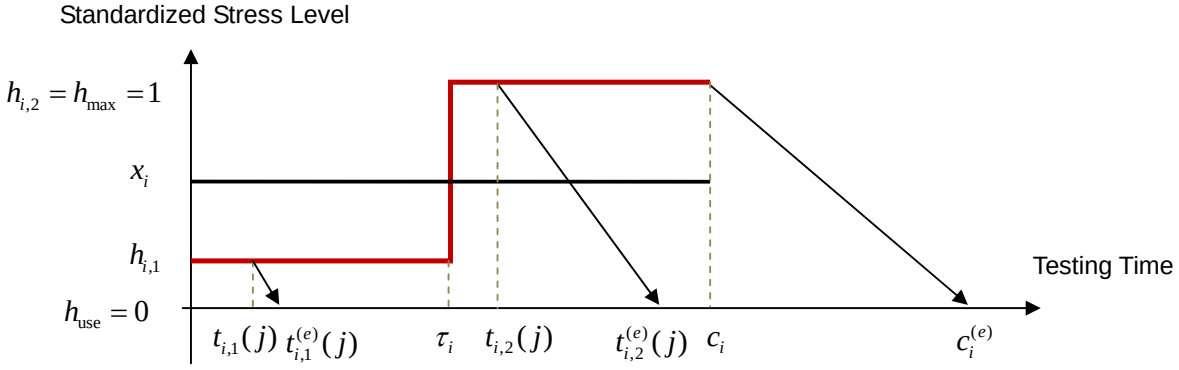

Figure 6.2 Illustration of a two-step step-stress loading of an auxiliary acceleration factor at stress x_i based on the LCEM exposure cumulative model

6.3.2.3 The Likelihood Function and Time Compression Target

To obtain the likelihood function, we need to translate the test times over different

AAF levels to a common reference stress. Let $t_{i,1}(j)$ be the *jth* failure at the testing condition $(x_i, h_{i,1})$, then, based on the LCEM model, its equivalent failure time of at condition $(x_i, h_{\text{use}} = 0)$ is

$$t_{i,1}^{(e)}(j) = \frac{\exp(\mu_{i,0})}{\exp(\mu_{i,1})} \cdot t_{i,1}(j) \tag{6.11}$$

where $\mu_{i,0} = \beta_0 + \beta_1 x_i + \beta_2 h_{\text{use}} = \beta_0 + \beta_1 x_i$ and $\mu_{i,1} = \beta_0 + \beta_1 x_i + \beta_2 h_{i,1}$

Let $t_{i,2}(j)$ be the *jth* failure at the testing condition $(x_i, h_{i,2})$, then, based on the LCEM model, its equivalent failure time of at condition $(x_i, h_{\text{use}} = 0)$ is

$$t_{i,2}^{(e)}(j) = \frac{\exp(\mu_{i,0})}{\exp(\mu_{i,1})} \cdot \tau_i + \frac{\exp(\mu_{i,0})}{\exp(\mu_{i,2})} \cdot (t_{i,2}(j) - \tau_i) \tag{6.12}$$

where $\mu_{i,2} = \beta_0 + \beta_1 x_i + \beta_2 h_2 = \beta_0 + \beta_1 x_i + \beta_2$

For each censored observation, the equivalent censoring time is

$$c_i^{(e)} = \frac{\exp(\mu_{i,0})}{\exp(\mu_{i,1})} \cdot \tau_i + \frac{\exp(\mu_{i,0})}{\exp(\mu_{i,2})} \cdot (c_i - \tau_i) \tag{6.13}$$

Hence, let $r_{i,1}$ and $r_{i,2}$ respectively denote the number of failures obtained within $[0, \tau_i)$ and $[\tau_i, c_i)$, the log-likelihood function of $\boldsymbol{\theta}_i = (\mu_i, \sigma)$ at testing condition $(x_i, h_{\text{use}} = 0)$ is given by

$$\begin{aligned} l(\boldsymbol{\theta}_i) = & \sum_{j=1}^{r_{i,1}} \{-\log(\sigma) + z_{i,1}^{(e)} - \exp(z_{i,1}^{(e)})\} + \sum_{j=1}^{r_{i,2}} \{-\log(\sigma) + z_{i,2}^{(e)}(j) - \exp(z_{i,2}^{(e)}(j))\} \\ & + (n_i - r_{i,1} - r_{i,2}) \exp(\zeta_i^{(e)}) \end{aligned} \tag{6.14}$$

where

$$z_{i,1}^{(e)}(j) = (\log(t_{i,1}^{(e)}(j)) - \mu_{i,0}) / \sigma$$
$$z_{i,2}^{(e)}(j) = (\log(t_{i,2}^{(e)}(j)) - \mu_{i,0}) / \sigma$$
$$\zeta_i^{(e)} = (\log(c_i^{(e)}) - \mu_{i,0}) / \sigma$$

Furthermore, from equation (6.13), we define a time compression target ψ_i at stress x_i based on the LCEM cumulative exposure model

$$\psi_i = \frac{\text{equivalent test duration, } c_i^{(e)}}{\text{actual test duration, } c_i} = \frac{\frac{\exp(\mu_{i,0})}{\exp(\mu_{i,1})} \cdot \tau_i + \frac{\exp(\mu_{i,0})}{\exp(\mu_{i,2})} \cdot (c_i - \tau_i)}{c_i} = \frac{\exp(-h_{i,1}\beta_2) \cdot \tau_i + \exp(-\beta_2) \cdot (c_i - \tau_i)}{c_i} \tag{6.15}$$

It is not difficult to see that $1 \le \psi_i \le e^{\beta_2}$. Particularly, $\psi_i = 1$ corresponds to the situation when no AAF is used (i.e. $\tau_i = c_i$), whereas $\psi_i = e^{\beta_2}$ corresponds to the situation when AAF is set to its maximum value $h_{\max}$ throughout the test (i.e. $\tau_i = 0$).

6.3.2.4 The Information Matrix at Low Stresses

Conditioning on a particular $\tilde{\beta}_1 \in [\beta_1^-, \beta_1^+]$, the pre-posterior distribution of $\boldsymbol{\theta}_i$ at any lower stress level x_i can be approximated by a bivariate normal distribution with covariance matrix $\boldsymbol{\Sigma}_i$ given by Berger (1985, p. 224)

$$\boldsymbol{\Sigma}_i = [-(\mathbf{I}_{\boldsymbol{\theta}_i} + \mathbf{I}^{\vartheta_i})]^{-1} \qquad \forall i = 1, \ldots, k-1 \tag{6.16}$$

where $\mathbf{I}_{\boldsymbol{\theta}_i}$ given in (6.17) is the information expected to be obtained from the test at x_i conditioning on $\beta_1 = \tilde{\beta}_1$

$$\mathbf{I}_{\boldsymbol{\theta}_i} = E(\partial^2 l(\boldsymbol{\theta}_i) / \partial \boldsymbol{\theta}_i^2) \tag{6.17}$$

and $\mathbf{I}^{\vartheta_i}$ is obtained from the constructed prior distribution $\vartheta(\boldsymbol{\theta}_i)$

$$\mathbf{I}^{\vartheta_i} = \partial^2 \log(\vartheta(\boldsymbol{\theta}_i)) / \partial \boldsymbol{\theta}_i^2 \tag{6.18}$$

Common numerical differentiation method is needed in order to evaluate $\mathbf{I}^{\vartheta_i}$, see e.g. Friedman and Kandel (1994)). In practice, this can be easily done as the closed-from of $\vartheta(\boldsymbol{\theta}_i)$ has already been derived in equation (6.10).

The closed-form expression of $\mathbf{I}_{\boldsymbol{\theta}_i}$ can be derived as follows,

At any low stress level x_i, n_i testing units are tested for c_i units of time. Suppose an AAF is loaded following the m-step step-stress loading profile as follows

$$h_i = \begin{cases} h_{i,1} & 0 = \tau_{i,0} \le t < \tau_{i,1} \\ h_{i,2} & \tau_{i,1} \le t < \tau_{i,2} \\ \vdots & \\ h_{i,m} & \tau_{i,m-1} \le t < \tau_{i,m} = c_i \end{cases}$$

, where $\tau_{i,q}$ is the stress changing time of AAF for $q = 0,1,...,m$.

Then, the information expected to be obtained from the test at low stress level x_i consists of $(m+1)$ components as follows

$$\mathbf{I}_{\boldsymbol{\theta}_i} = \mathbf{I}_{\boldsymbol{\theta}_i,[\tau_{i,0},\tau_{i,1})} + \mathbf{I}_{\boldsymbol{\theta}_i,[\tau_{i,1},\tau_{i,2})} + \quad \cdots \quad + \mathbf{I}_{\boldsymbol{\theta}_i,[\tau_{m-1},\tau_m)} + \mathbf{I}_{\boldsymbol{\theta}_i,[\tau_m,\infty)}$$

where

$\mathbf{I}_{\boldsymbol{\theta}_i,[\tau_{i,q},\tau_{i,q+1})}$ is the expected Fisher information obtained from failure data in the interval $[\tau_{i,q},\tau_{i,q+1})$ for $q = 0,1,...,m-1$

$\mathbf{I}_{\boldsymbol{\theta}_i,[\tau_m,\infty)}$ is the expected Fisher information obtained from censored data

Under any testing condition $(x_i, h_{i,q})$ for $q = 0,1,...,m$, we have assumed that the failure times follow Weibull distribution. Hence, the logarithm failure times follows smallest extreme value (SEV) distribution with location $\mu_{i,q}$ and scale σ. Furthermore, let $t^{(e)}$ denote the equivalent test time at reference condition $(x_i, h_{\text{use}} = 0)$ based on the LCEM model, we define the standardized equivalent failure time in log-scale as

$$z^{(e)} = (\log(t^{(e)}) - \mu_{i,0}) / \sigma$$

and correspondingly the standardized stress changing time of AAF

$$\zeta_q^{(e)} = (\log(\tau_{i,q}^{(e)}) - \mu_{i,0}) / \sigma \qquad \forall q = 0,1,...,m$$

Using the above parameterization, the information expected to be obtained from

one observation within the interval $[\tau_0, \tau_1)$ is

$$
\begin{aligned}
i_{\boldsymbol{\theta}_i,[\tau_0,\tau_1)} &= -E\{\partial^2[-\log\sigma + z^{(e)} - e^{z^{(e)}}] / \partial \boldsymbol{\theta}_i^{\,2}; z^{(e)}\} \\
&= (\Phi_{SEV}(\zeta_1^{(e)}))^{-1} \cdot \int_{-\infty}^{\zeta_1^{(e)}} \partial^2[-\log\sigma + z^{(e)} - e^{z^{(e)}}] / \partial \boldsymbol{\theta}_i^{\,2} \cdot e^{(z^{(e)} - e^{z^{(e)}})} dz^{(e)} \\
&= -\frac{1}{\sigma^2} \cdot \begin{bmatrix} E(-e^{z^{(e)}}) & E(1 - e^{z^{(e)}} - z^{(e)} e^{z^{(e)}}) \\ E(1 - e^{z^{(e)}} - z^{(e)} e^{z^{(e)}}) & E(1 + 2z^{(e)} - 2z^{(e)} e^{z^{(e)}} - (z^{(e)})^2 e^{z^{(e)}}) \end{bmatrix} \\
&= -\frac{1}{\sigma^2} \cdot (\Phi_{SEV}(\zeta_1^{(e)}))^{-1} \cdot \begin{bmatrix} -A & 1 - A - C \\ 1 - A - C & 1 + 2B - 2C - D \end{bmatrix}
\end{aligned}
$$

where

$A = E(e^{z^{(e)}}) = \exp(-\exp(\zeta_1^{(e)})) \cdot (\exp(\exp(\zeta_1^{(e)})) - \exp(\zeta_1^{(e)}) - 1)$

$B = E(z^{(e)}) = -\zeta_1^{(e)} \exp(-\exp(\zeta_1^{(e)})) - \gamma + Ei(-\exp(\zeta_1^{(e)}))$

$C = E(z^{(e)} e^{z^{(e)}}) = 1 - \exp(-\exp(\zeta_1^{(e)})) \cdot (1 + \zeta_1^{(e)}(1 + \exp(\zeta_1^{(e)}))) - \gamma + Ei(-\exp(\zeta_1^{(e)}))$

$D = E((z^{(e)})^2 e^{z^{(e)}}) = \int_{-\infty}^{\zeta_1^{(e)}} \exp(2z^{(e)} - \exp(z^{(e)})) \cdot (z^{(e)})^2 dz^{(e)}$

γ : Euler-Mascheroni Constant

$Ei(x)$: Exponential Integral, $-\int_{-x}^{\infty} t^{-1} e^{-t} dt$ for $x \le 0$

The information expected to be obtained from one observation within the interval $[\tau_{i,q}, \tau_{i,q+1})$ for $q = 1, 2, ..., m-1$ is

$$
\begin{aligned}
i_{\boldsymbol{\theta}_i,[\tau_{i,q},\tau_{i,q+1})} &= -E\{\partial^2[-\log\sigma + z^{(e)} - e^{z^{(e)}}] / \partial \boldsymbol{\theta}_i^{\,2}; z^{(e)}\} \\
&= -(\Phi_{SEV}(\zeta_{q+1}^{(e)}) - \Phi_{SEV}(\zeta_q^{(e)}))^{-1} \cdot \int_{\zeta_q^{(e)}}^{\zeta_{q+1}^{(e)}} \partial^2[-\log\sigma + z^{(e)} - e^{z^{(e)}}] / \partial \boldsymbol{\theta}_i^{\,2} \cdot e^{(z^{(e)} - e^{z^{(e)}})} dz^{(e)} \\
&= -\frac{1}{\sigma^2} \cdot \begin{bmatrix} E(-e^{z^{(e)}}) & E(1 - e^{z^{(e)}} - z^{(e)} e^{z^{(e)}}) \\ E(1 - e^{z^{(e)}} - z^{(e)} e^{z^{(e)}}) & E(1 + 2z^{(e)} - 2z^{(e)} e^{z^{(e)}} - (z^{(e)})^2 e^{z^{(e)}}) \end{bmatrix} \\
&= -\frac{1}{\sigma^2} \cdot (\Phi_{SEV}(\zeta_{q+1}^{(e)}) - \Phi_{SEV}(\zeta_q^{(e)}))^{-1} \cdot \begin{bmatrix} -A' & 1 - A' - C' \\ 1 - A' - C' & 1 + 2B' - 2C' - D' \end{bmatrix}
\end{aligned}
$$

where

$$A' = E(e^{z^{(e)}}) = (e^{-e^{\zeta_{q+1}^{(e)}}}(-1-e^{\zeta_{q+1}^{(e)}})) - (e^{-e^{\zeta_q^{(e)}}}(-1-e^{\zeta_q^{(e)}}))$$

$$B' = E(z^{(e)}) = (-\zeta_{q+1}^{(e)}e^{-e^{\zeta_{q+1}^{(e)}}} + Ei(-e^{\zeta_{q+1}^{(e)}})) - (-\zeta_q^{(e)}e^{-e^{\zeta_q^{(e)}}} + Ei(-e^{\zeta_q^{(e)}}))$$

$$C' = E(z^{(e)}e^{z^{(e)}}) = (e^{-e^{\zeta_{q+1}^{(e)}}}(-1-\zeta_{q+1}^{(e)} - \zeta_{q+1}^{(e)}e^{\zeta_{q+1}^{(e)}}) + Ei(-e^{\zeta_{q+1}^{(e)}}))$$
$$-(e^{-e^{\zeta_q^{(e)}}}(-1-\zeta_q^{(e)} - \zeta_q^{(e)}e^{\zeta_q^{(e)}}) + Ei(-e^{\zeta_q^{(e)}}))$$

$$D' = E((z^{(e)})^2 e^{z^{(e)}}) = \int_{\zeta_q^{(e)}}^{\zeta_{q+1}^{(e)}} \exp(2z^{(e)} - \exp(z^{(e)})) \cdot (z^{(e)})^2 dz^{(e)}$$

and the information expected to be obtained from one censored observation is

$$i_{\boldsymbol{\theta}_i,[\tau_m,\infty]} = -\partial^2 \exp(z^{(e)}) / \partial \boldsymbol{\theta}_i^{\,2}\Big|_{z^{(e)}=\zeta_m^{(e)}}$$
$$= \frac{1}{\sigma^2} \cdot \begin{bmatrix} -e^{\zeta_m^{(e)}} & -e^{\zeta_m^{(e)}} - \zeta_m^{(e)}e^{\zeta_m^{(e)}} \\ -e^{\zeta_m^{(e)}} - \zeta_m^{(e)}e^{\zeta_m^{(e)}} & -2\zeta_m^{(e)}e^{\zeta_m^{(e)}} - (\zeta_m^{(e)})^2 e^{\zeta_m^{(e)}} \end{bmatrix}$$

Hence, $\mathbf{I}_{\boldsymbol{\theta}_i}$ is given by

$$\mathbf{I}_{\boldsymbol{\theta}_i} = \mathbf{I}_{\boldsymbol{\theta}_i,[\tau_{i,0},\tau_{i,1})} + \mathbf{I}_{\boldsymbol{\theta}_i,[\tau_{i,1},\tau_{i,2})} + \quad \cdots \quad + \mathbf{I}_{\boldsymbol{\theta}_i,[\tau_{m-1},\tau_m)} + \mathbf{I}_{\boldsymbol{\theta}_i,[\tau_m,\infty)}$$
$$= [n_i \cdot P_{i,1}] \cdot i_{\boldsymbol{\theta}_i,[\tau_{i,0},\tau_{i,1})} + \sum_{q=1}^{m-1} [n_i \cdot P_{i,q}] \cdot i_{\boldsymbol{\theta}_i,[\tau_{i,1},\tau_{i,2})} + [n_i \cdot P_{i,m}] \cdot i_{\boldsymbol{\theta}_i,[\tau_m,\infty)}$$

where

$[\cdot]$: round to the nearest integer

$P_{i,1} = \Phi_{SEV}(\zeta_1^{(e)}), \quad P_{i,q} = \Phi_{SEV}(\zeta_{q+1}^{(e)}) - \Phi_{SEV}(\zeta_q^{(e)}), \quad P_{i,m} = 1 - \Phi_{SEV}(\zeta_m^{(e)})$

In the equation above, $[n_i \cdot P_{i,q}]$ for $q = 1, 2, ..., m-1$ is the expected number of failures within the interval $[\tau_{i,q}, \tau_{i,q+1})$, and $[n_i \cdot P_{i,m}]$ is the expected number of censored data. It is easily seen that $\mathbf{I}_{\boldsymbol{\theta}_i}$ depends on the specified β_2 only through $[n_i \cdot P_{i,q}]$ for $q = 1, 2, ..., m$.

Finally, based on the $\boldsymbol{\Sigma}_i$ at stress x_i conditioning on $\beta_1 = \tilde{\beta}_1$, the preposterior expectation $E_{\beta_1}(\text{var}(y_p(x_i)))$ of the posterior variance $\text{var}(y_p(x_i))$ at stress x_i is computed by averaging $\text{var}(y_p(x_i))$ over the specified range of β_1, i.e.

$$E_{\beta_1}(\text{var}(y_p(x_i))) = \frac{1}{\beta_1^+ - \beta_1^-}\int_{\beta_1^-}^{\beta_1^+} \text{var}(y_p(x_i))d\beta_1 = \frac{1}{\beta_1^+ - \beta_1^-}\int_{\beta_1^-}^{\beta_1^+} [1, u_p]\boldsymbol{\Sigma}_i[1, u_p]'d\beta_1$$

(6.19)

6.3.2.5 The Planning of Tests at Low Stresses

We are now ready to formulate the planning problem of tests at low stress levels with AAF. To summarize, given (i) the data $\mathbf{y}_k$ obtained at the highest stress $x_k = 0$, (ii) the specified range of the slope parameter β_1, and (iii) the time compression target, the developed ALT plan optimizes the (i) sample allocations, (ii) stress combinations, and (iii) the loading profiles of the AAF at lower stresses, so that the preposterior expectation $E_{\beta_1}(\text{var}(y_p(1)))$ of the posterior variance $y_p(1)$ at use stress $x_0 = 1$ is minimized. This optimization problem is formulated as follows

Let

$$\mathbf{X} = \begin{pmatrix} 1 & 1 & \cdots & 1 \\ x_1 & x_2 & \cdots & x_k \end{pmatrix}'$$

be the design matrix; $\boldsymbol{\Lambda}$ be the diagonal matrix given by

$$\boldsymbol{\Lambda} = \begin{pmatrix} E_{\beta_1}(\text{var}(y_p(x_1))) & 0 & 0 & 0 \\ 0 & E_{\beta_1}(\text{var}(y_p(x_2))) & 0 & 0 \\ \vdots & \vdots & \ddots & \vdots \\ 0 & 0 & 0 & \text{var}(y_p(x_k)) \end{pmatrix}$$

and $\mathbf{1} = (1,1)$. The optimum ALT plan can be obtained by solving

$$\begin{aligned} &\text{Min} \quad E_{\beta_1}(\text{var}(y_p(1))) = \mathbf{1}(\mathbf{X}^T\boldsymbol{\Lambda}^{-1}\mathbf{X})^{-1}\mathbf{1}^T \\ &\text{s.t.} \quad \text{target time compression } \psi_i, \forall i = 1,...,k-1 \\ &\qquad (x_1, x_2, ..., x_{k-1}) \in \mathbb{R}^{k-1} : 0 \le x_i \le 1 \\ &\qquad (n_1, n_2, ..., n_{k-1}) \in \mathbb{R}^{k-1} : \sum_{i=1}^{k-1} n_i = N - n_k \quad , \quad n_k > 0 \end{aligned} \tag{6.20}$$

6.4. Case Study: Temperature-ALT of an Electronic Controller

A case study, which is indeed the motivation of our study, is presented in this section to illustrate the sequential Bayesian ALT planning approach with an AAF. It deals with an ALT project in which engineers assessed the reliability of a newly developed cost reduction electronic controller.

Facing the escalating pressure from competitors, the company lately developed a new electronic controller with lower cost. Although a slight decline in reliability is expected, the 10% life quantile of the controller under normal operation conditions must still be larger than two years. To quickly assess if the new design meets this reliability target, product engineers launched this two-stress constant-stress ALT on 120 controller prototypes within one and a half month, i.e. 75days. More than one failure modes were carefully monitored in the actual testing, however, only one dominate failure mode, namely, the soft starter (SS) failure, is considered in this section for a clear illustration of the proposed planning approach.

Temperature was initially chosen as the acceleration factor. The use temperature of the controller is defined as 45^0C, while the highest temperature allowed in the test is 85^0C. Other environment factors, involving the relatively humidity (RH), on/off cycle frequency, voltage level was respectively set to the use level, i.e. 60%, 10sec on/60sec off, 220V50Hz.

Weibull distribution was used to model the SS lifetime as strongly indicated by historical data. Hence, the logarithm failure time follows the Smallest Extreme Value (SEV) distribution with location parameter μ and scale parameter σ. Furthermore, the

way that μ changes with temperature is assumed to follow the Arrhenius model as in (6.21), and the scale parameter σ is a constant independent of stress

$$\mu(T) = \beta_0 + \frac{Ea}{k} \times \frac{1}{T} \tag{6.21}$$

where T is the Kelvin temperature used in test; Ea is the activation energy in electron-volts; and $k = 8.6171 \times 10^{-5}$ is the Boltzmann's constant.

6.4.1. Test Design and Data Analysis at the High Stress Level

Based on the framework of sequential ALT plan presented in Figure 6.1, the ALT started from testing the units from the high temperature level 85^0C. It is noted that engineers did not realize at this moment that an auxiliary acceleration factor would be used in the subsequent testing.

Using equation (6.7), Figure 6.3 below plots the calculated minimum sample size given different expected number of failures r_k and consumer' risk $1-\alpha$.

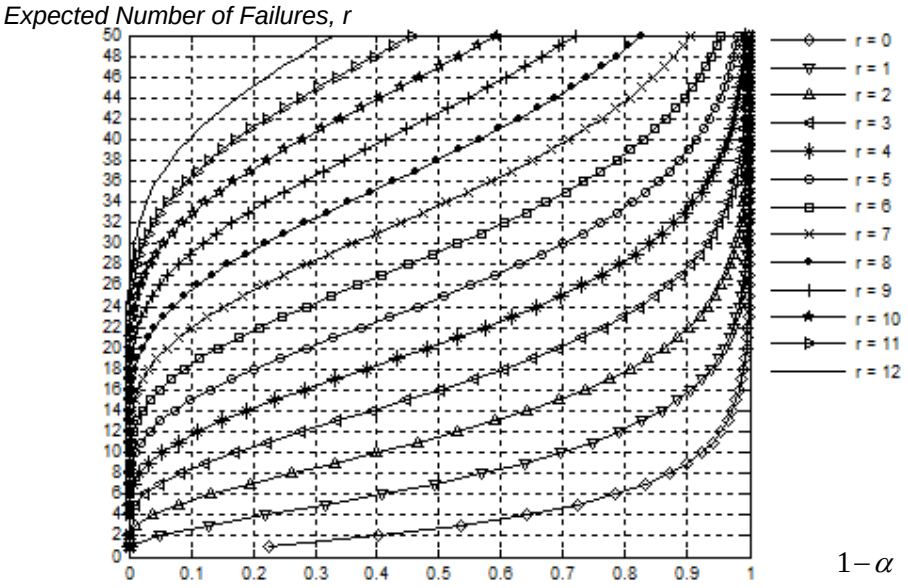

Figure 6.3 Sample sizes for different values of r and $(1-\alpha)$

In this project, 6 failures were expected and the confidence level α was chosen as 0.9, hence, 44 controller prototypes were tested at 85^0C as indicated by Figure 6.3. The recorded SS failure times are presented in Table 6.1. To protect proprietary information, data here are simulated and re-scaled from the fitted model of the original application.

Table 6.1 Failure times at the highest temperature

Failure Times (hrs)									
79.559	210.47	590.03	400.56	491.41	138.94	673.98	109.4	149.95	204.7
425.32	643.31	117.15	328.99	351.87	720×29				

Using equations (6.8) and (6.9), the posterior distribution $\pi(\boldsymbol{\theta}_2)$ was derived and approximated by a bivariate normal distribution $N(\hat{\boldsymbol{\theta}}_2, \hat{\boldsymbol{\Sigma}}_2)$

$$\boldsymbol{\theta}_2 | \mathbf{y}_2 \sim N(\hat{\boldsymbol{\theta}}_2, \hat{\boldsymbol{\Sigma}}_2)$$

where $\hat{\boldsymbol{\theta}}_2 = [7.35, 0.90]$ and $\hat{\boldsymbol{\Sigma}}_2 = -\hat{\mathbf{I}}_2^{-1} = [0.1142, 0.0529; 0.0529, 0.0489]$.

Figure 6.4 shows both the original and approximated posterior distribution $\pi(\boldsymbol{\theta}_2)$.

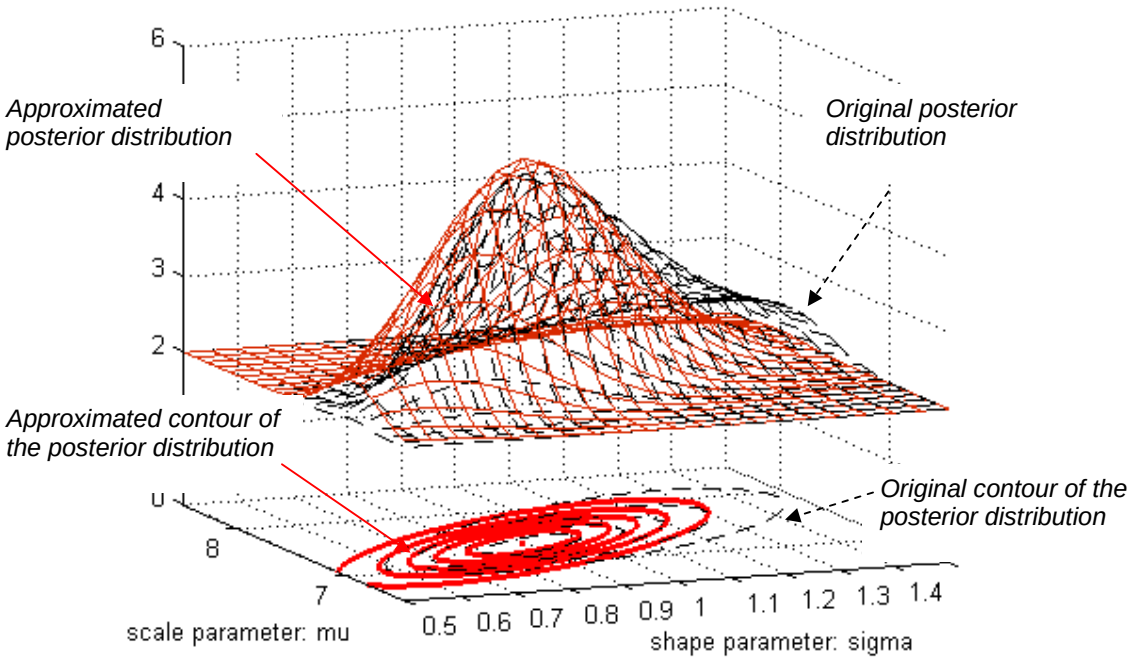

Figure 6.4 Posterior distribution and its normal approximation at the high stress level

6.4.2. Test Design and Data Analysis at Lower Stress Levels

6.4.2.1 Information Transfer and Decay

Given the approximated posterior distribution of $\boldsymbol{\theta}_2$ and the prior knowledge about the activation energy Ea, the prior distribution $\vartheta(\boldsymbol{\theta}_i)$ at any lower temperature level can be constructed using (6.10). In this project, empirical engineering experience suggests that Ea most likely ranges from 0.8 to 1.2.

As briefly discussed in Section 6.3.2.1, the knowledge on Ea always involves a certain amount of uncertainty, and the information on $\boldsymbol{\theta}_i$ contained in the prior distribution $\vartheta(\boldsymbol{\theta}_i)$ therefore decays as the testing temperature decreases from the highest level 85^0C. The rate of information decay is determined by the amount of uncertainty associated to Ea. The higher the uncertainty, the faster the information

decays. In the most extreme cases when no information about Ea is available, the decay rate becomes infinity, i.e. the prior distribution of $\boldsymbol{\theta}_i$ cannot be constructed at lower temperature levels.

To illustrate the information transfer and decay from the highest to lower temperature level, we construct two prior distributions for $\boldsymbol{\theta}_i$ respectively at 45^0C and 65^0C using equation (6.10). The results are given in Figure 6.5.

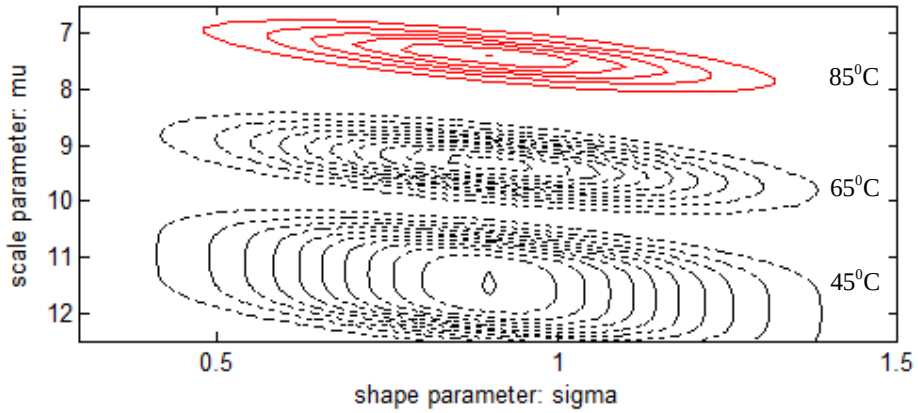

Figure 6.5 Illustration of the constructed prior distributions

As clearly shown by this figure, the constructed prior distribution $\vartheta(\boldsymbol{\theta}_i)$ becomes diffuse as the testing temperature decreases. In other words, the information contained in the prior distribution decays as the temperature level moving away from the 85^0C. This is the observation that is intuitively correct: As only the test at the highest temperature 85^0C has been conducted, we naturally have higher uncertainty on SS life distribution at those testing levels with lower temperature.

6.4.2.2 Motivations of Using an Auxiliary Acceleration Factor

Based on the constructed $\vartheta(\boldsymbol{\theta}_i)$, engineers calculated the expected number of failures

at each lower temperature level before they planned the test at lower temperature level. Figure 6.6 below shows their results. As seen from this figure, in order to see more than 4 or 5 failures, the lowest temperature should be at least 63^0C which is almost standing on the middle point between 45^0C and 85^0C . Hence, the degree of extrapolation was considered to be too high.

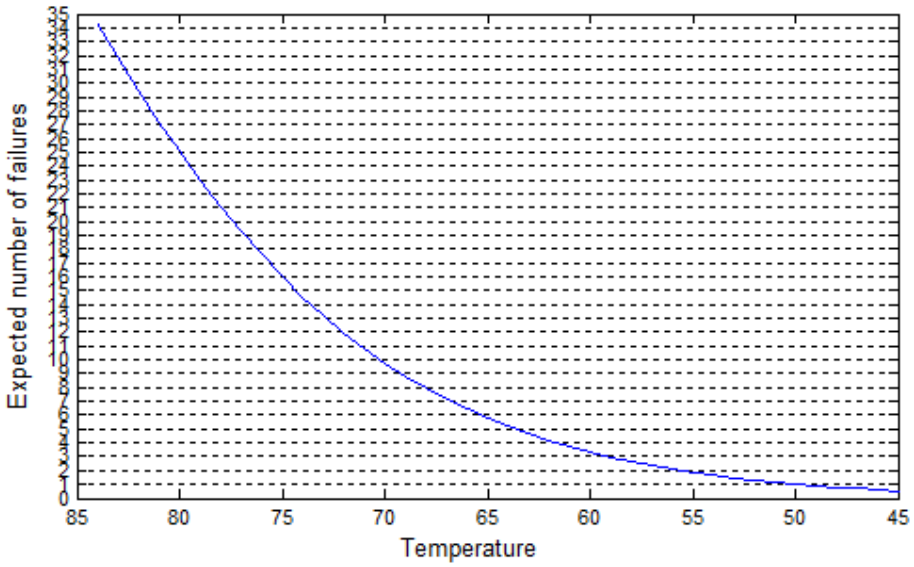

Figure 6.6 Expected number of failures at each lower temperature level

In fact, this problem can be well understood from another interesting perspective of view by comparing the information expected to be obtained from units tested at a particular temperature level to that conveyed by the constructed prior distribution at the same stress level. To conduct this comparison, we need the ratio defined as follows

$$\eta = \frac{\det \mathbf{I}_{\boldsymbol{\theta}_i}}{\det \mathbf{I}^{\vartheta_i}} \tag{6.22}$$

where $\mathbf{I}^{\vartheta_i}$ and $\mathbf{I}_{\boldsymbol{\theta}_i}$ is respectively defined in equation (6.17) and (6.18).

Figure 6.7 plots the ratio η against temperature level. As clearly seen, since very few failures are expected when the temperature is low, the information obtained from

testing the rest controller prototypes at a low temperature level ($<74^0$C) is even less than the information contained in the constructed prior distributions. Then, one natural question raised is that why the tests at lower stress levels are still needed rather than testing all units at the highest stress level.

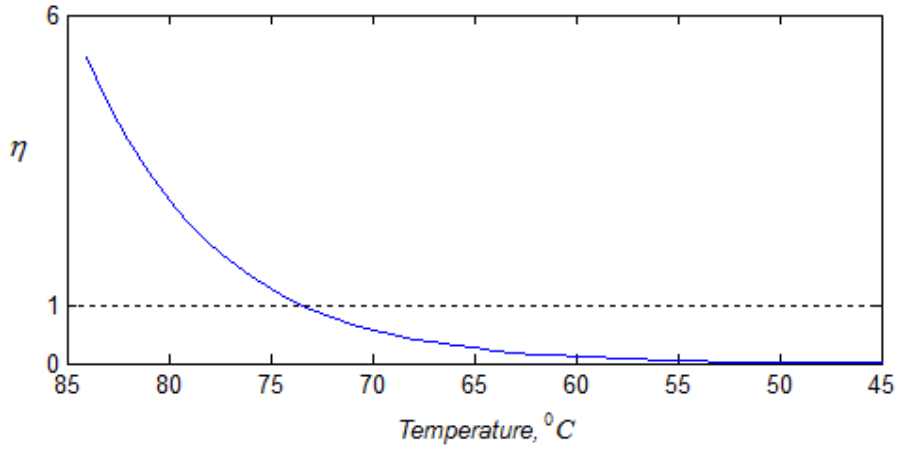

Figure 6.7 Plots of the ratio η against testing temperature

Hence, in this project, there existed a strong motivation to use an auxiliary acceleration factor. Among the three candidates AAF including relative humidity (RH), on/off cycle frequency, and voltage, RH was eventually chosen as the AAF as its effect on the life of the soft starter has been well defined from previous experiments. Correspondingly, the Arrhenius life-stress model given in (6.21) was extended to the Hallberg-Peck relationship as follows so as to incorporate the AAF

$$\mu(T,H) = \beta_0 + \frac{Ea}{k} \times \frac{1}{T} + p \times \log\left(\frac{H}{H_0}\right) \tag{6.22}$$

where H is the relative humidity level in test; $H_0 = 60\%$ is nominal humidity level at use condition; p is the humidity acceleration constant; and T, Ea and k is defined in (6.21). Furthermore, the assumption that the scale parameter σ is a constant independent of stress still holds.

6.4.2.3 Test Design at Low Temperature Level

The planning information needed for the test at low temperature are now summarized as follows,

- The posterior distribution $\pi(\boldsymbol{\theta}_2)$ obtained from the test under the highest temperature;
- The specified range of the activation energy, $0.8 \le Ea \le 1.2$;
- The number of controller units, 76; and the test duration left, 1080 hours;
- The pre-specified humidity acceleration constant, $p = 3$. According the design specifications, the nominal relative humidity 60%, and the maximum humidity should not exceed 90%; Furthermore, the AAF has a two-step step-stress loading pattern based on the LCEM cumulative exposure model as discussed in Section 6.3;
- The target time compression, $\psi_1 = 3$;

Given the planning information above, we obtain the optimum plan as summarized by Table 6.2 using equation (6.20).

As seen in Table 6.2, the test is firstly conducted at highest temperature 85^0C with humidity fixed to the nominal value 60% (Point A in Figure 6.8). At this stress point, the probability of failure is around 0.32, which is considered high enough for engineers to quickly obtain enough failures. However, when the temperature level descends to 53^0C with the humidity level fixed (Point B in Figure 6.8), the probability of failure quickly drops to an extremely low value which is less than 0.01. Hence, an AAF is loaded following the profile given in Table 6.2. According to this profile, the test is firstly conducted on 53^0C and 60% humidity level for 170.5 hours (Point C. Here, point B and C are overlapped). Then, the humidity level is increased to 90% (Point D) and

the test is stopped till maximum test duration 1080 hours is reached. Note that, no auxiliary acceleration stress is applied in the first 170.5 hrs at the low temperature level as the target time compression is achieved. Since the model presented in this chapter requires stronger assumptions than that of ordinary CSALT, the auxiliary acceleration stress should be used only when it is truly necessary.

Table 6.2 Accelerated life test plan for the cost reduction electronic controller

Condition i	Temperature, ^0C	Humidity Level, %	Test Time, hr	Sample Size
Use	45	60		
Low	53	See Loading profile	1080	76
High	85	60	720	44

Humidity Loading Profile at 54 ^0C Temperature Level

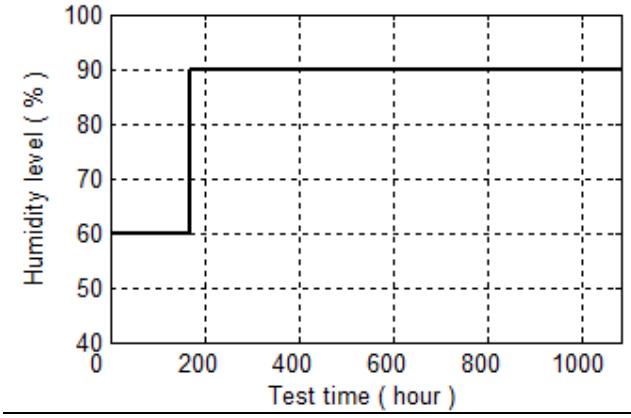

Low Humidity Level: 60%
High Humidity Level: 90%
Holding Time: 170.5 hrs

Expected Failures:
Interval [0, 170.5] : No failure
Interval [170.5,1080]: 5 failures
Interval [1080, ∞): 71 censored

For this plan, the asymptotic standard error of the estimate $y_p(1)$ equals 0.3408

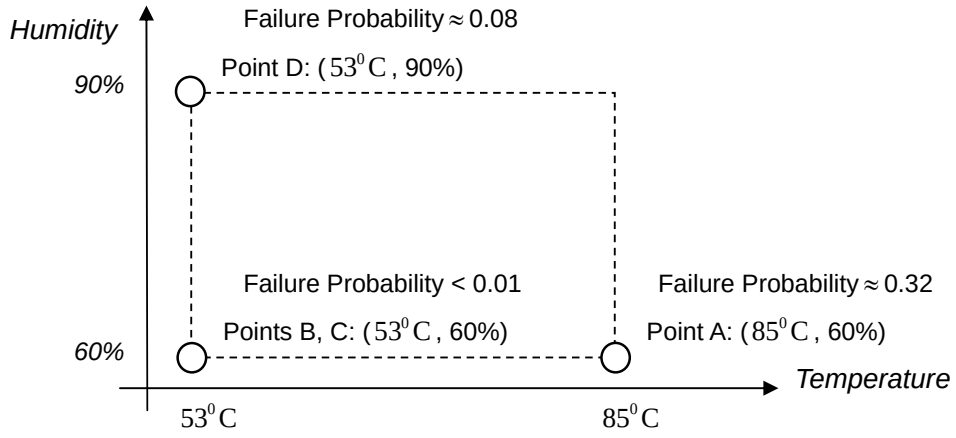

Figure 6.8 Illustration of the sequential ALT plan with auxiliary acceleration factor

6.4.2.4 Sensitivity of the Optimum Plan to Mis-specification of *p*

In our model, the effect of the auxiliary acceleration factor is assumed to be known, but what if the value of *p* is mis-specified? How does the optimum stress combination, sample allocation, and the loading pattern of the auxiliary acceleration factor change if we perturb the value of *p*? These are the questions that we try to answer in this section.

However, it turns out to be extremely difficult to establish the closed-form relationship between the optimum plans and *p*. Generally speaking, the specified effect *p* affects the planning results only through the expected information $\mathbf{I}_{\boldsymbol{\theta}_i}$ at lower stress levels. Here, we let the specified *p* range from 2.8 to 3.5 with step size 0.1, and re-design the test at low temperature level. The results are given in Table 6.3.

Table 6.3 Sensitivity of the optimum plan to p

Specified p	Optimum Low Temperature		Optimum Low Humidity		Optimum Holding Time		Standard Deviation of $y_{0.1}(1)$	
	Planned Value	Relative Change, RT	Planned Value	Relative Change, RH	Planned Value	Relative Change, RHT	Planned Value	Relative Change, RSD
3	53^0C	0	60 %	0	170.5 hr	0	0.3408	0
2.8	53^0C	0	60 %	0	57.5 hr	-66.4 %	0.3375	-0.9 %
2.9	53^0C	0	60 %	0	116.0 hr	-31.9 %	0.3400	-0.2 %
3.1	53^0C	0	60 %	0	221.0 hr	29.6 %	0.3429	0.6 %
3.2	53^0C	0	60 %	0	268.0 hr	57.2 %	0.34438	1.1 %
3.3	53^0C	0	60 %	0	312.0 hr	82.8 %	0.3476	2.0 %
3.4	53^0C	0	60 %	0	352.5 hr	106.7 %	0.3501	2.8 %
3.5	53^0C	0	60 %	0	391.0 hr	129.1 %	0.35341	3.7 %

Figure 6.9 plots the relative change of the optimum temperature level, optimum low humidity, optimum holding time of low humidity, and the expected standard deviation of $y_{0.1}(1)$ against the specified p. It is immediately seen that the optimum holding time is the only quantity that is sensitive to the specified p, whereas the optimum temperature, optimum low humidity, and the expected standard deviation of $y_{0.1}(1)$ appears to be robust to the specified p.

To understand why this is the case, recall the Hallberg-Peck stress-life model given in (6.22). When p is getting larger, the effect of humidity on product becomes stronger. As a result, it is no longer necessary to test the products at a high humidity level for a long time, hence, the holding time of the low humidity increases so as to maintain a fixed time compression. Since the time compression target is always achieved, the expected standard deviation of $y_{0.1}(1)$ does not vary too much, and we do not have to change the optimum low temperature and low humidity used in the test.

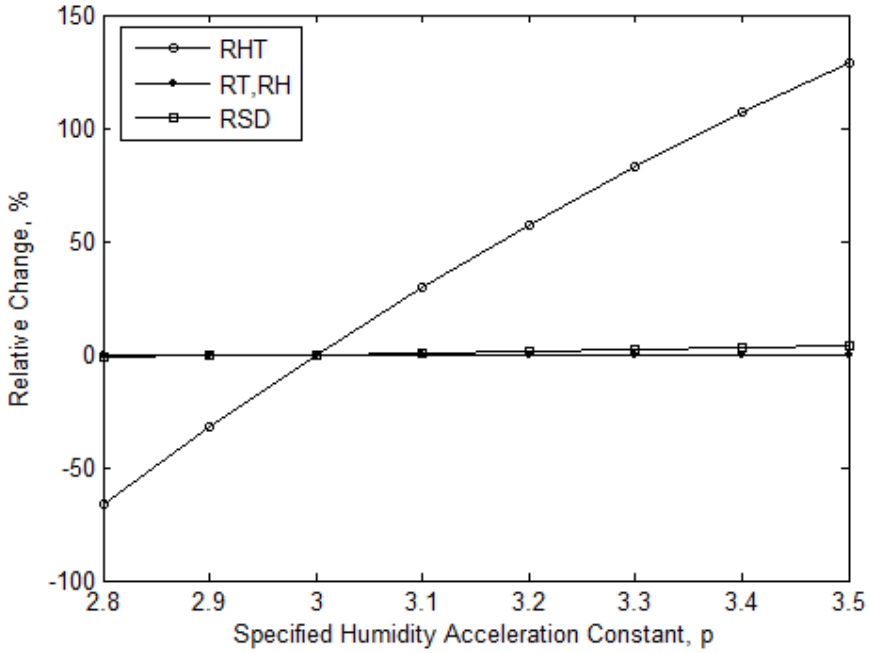

Figure 6.9 Sensitivity of optimum plan to p

6.4.2.5 Evaluation of the Developed Plan

Next, the developed ALT plan is evaluated using the Monte Carlo simulation, see e. g. Meeker and Escobar (1998), Zhang and Meeker (2006), to see if the plan achieves its intended precision level for the estimate of interest.

For each simulation run, given the testing results obtained at the highest temperature from Table 6.2, we simulate failure times for the 76 controller units at low temperature level according to the plan given in Table 6.3, assuming that both the Hallberg-Peck relationship and those specified planning inputs are true. Based on the simulated dataset, the estimate $\hat{y}_{0.1}(1)$ of the 0.1 life percentile at the use temperature is obtained. A total of *N* simulation runs are to be conducted based on the above procedure so as to compute the sample standard deviation $\mathrm{SD}(\hat{y}_{0.1}(1))$.

To gauge the total number of simulation runs needed to obtain a stable estimate, we progressively run the simulation for 10 independent repeated trails and track the sample standard deviation $\mathrm{SD}(\hat{y}_{0.1}(1))$. Figure 6.10 plots the calculated sample standard deviation $\mathrm{SD}(\hat{y}_{0.1}(1))$ against simulation runs for each trial. It is clearly seen that, the variation of $\mathrm{SD}(\hat{y}_{0.1}(1))$ is getting smaller as the number of simulation runs increases and a total of 5000 simulation runs should suffice.

Figure 6.11 presents the histogram of the results, 5000 estimates of $\hat{y}_{0.1}(1)$ at use temperature, obtained from the first simulation trial. This figure describes the amount of variability would be expected if we repeated the ALT over and over. It is seen from Figure 6.11, the sample standard deviation $\mathrm{SD}(\hat{y}_{0.1}(1)) = 0.3721$, which is slightly higher than the large-sample approximate standard error $\mathrm{Ase}(\hat{y}_{0.1}(1)) = 0.3408$ given from Table 6.3.

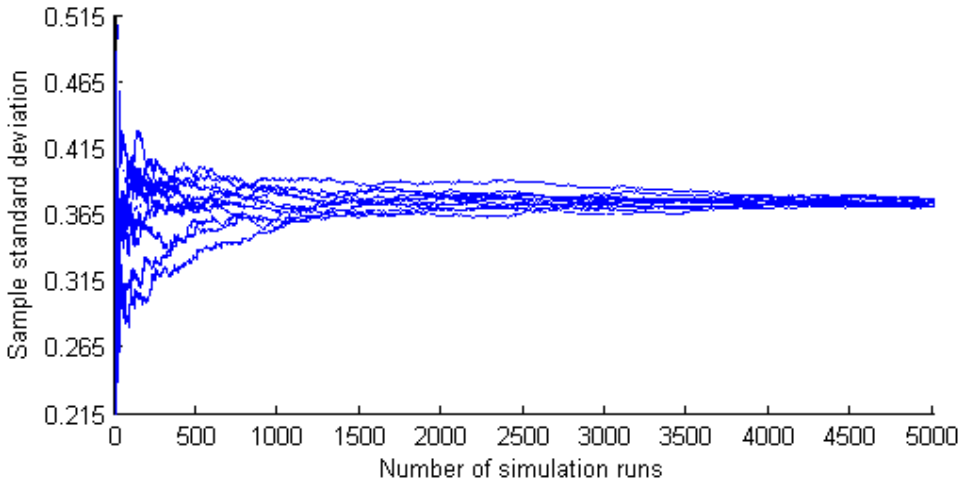

Figure 6.10 Plot of the sample standard deviation $\mathrm{SD}(\hat{y}_{0.1}(1))$ against simulation runs

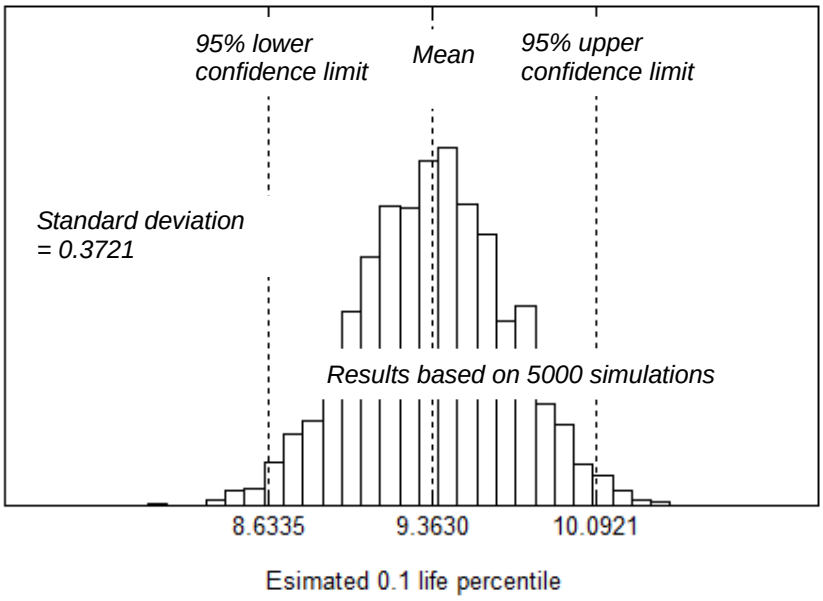

Figure 6.11 Simulation evaluation of the developed ALT plan

6.5. Conclusions

In this chapter, we presented a Bayesian planning method for sequentially design a constant-stress accelerated life test. Particularly, an auxiliary acceleration factor was used to amplify the failure probability of testing items at low stress levels. It was proposed that the auxiliary acceleration factor follows a step-stress loading pattern based on a cumulative exposure model LCEM with a target time compression fixed. To apply this method, the effect of the auxiliary acceleration factor must be known and must not interact with other acceleration factors. In the case study, the proposed approach was illustrated by the Hallberg-Peck model with the humidity acceleration factor known.

Chapter 7. Planning for Sequential ALT Based on the Maximum Likelihood (ML) Theory

7.1. Introduction

In Chapter 5, a Bayesian method was adopted to plan sequential constant-stress ALTs. In this chapter, we shall see how the classical planning method, which is based on the maximum likelihood (ML) theory, can be extended to accommodate the situation when ALT is sequentially conducted.

In what follows, Section 7.2 describes the framework of the planning method for a constant-stress ALT with multiple stress levels. Section 7.3 illustrates the application of the proposed method using the adhesive bond reliability testing example.

7.1.1. The Model

The model presented in Section 5.1.1 is used throughout this chapter.

7.2. The Framework of the ML Planning Approach

We present in this section, based on the ML theory, the framework of the sequential planning approach. Although it can be easily generalized to ALT with multiple stress levels, the following discussion only focuses on an ALT with 3 constant stress levels.

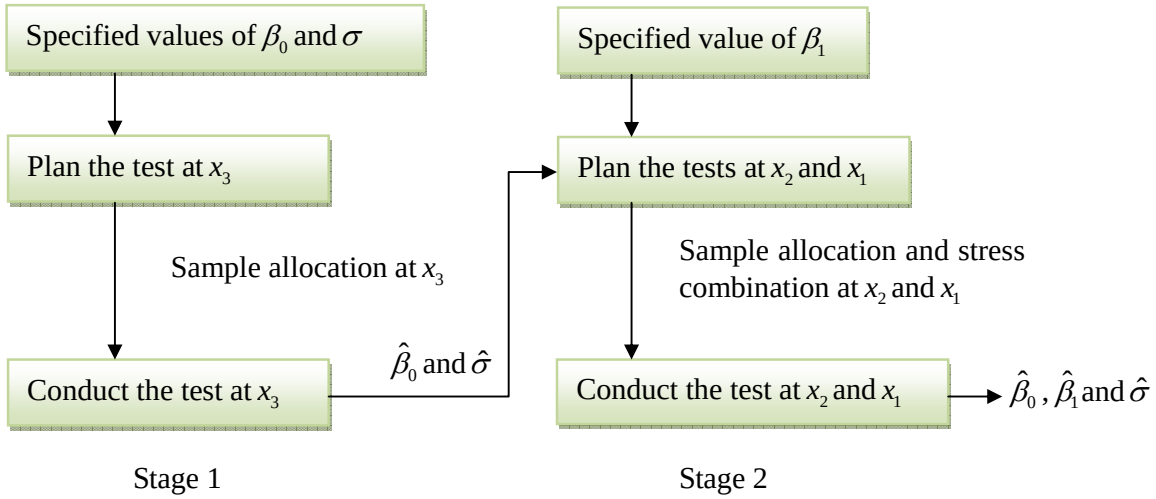

Figure 7.1Framework of the ML planning approach

As shown in Figure 7.1, two stages are involved in the framework. At stage 1, test at the highest stress level x_3 is firstly planned given the specified values of β_0 and σ. In practice, the true values of β_0 and σ are never known exactly, hence, engineers have to guess these values based on their engineering knowledge. When the test the highest stress level x_3 is done, the ML estimates of $\hat{\beta}_0$ and $\hat{\sigma}$ can be easily derived. At stage 2, based on the estimates ($\hat{\beta}_0$, $\hat{\sigma}$) and the pre-specified value of β_1, test runs at the lowest stress and middle stress are planned by optimizing both sample allocation and stress level combination. Compared to the planning information on β_0 and σ, information on the slope β_1 is relatively easier to obtain from handbooks or certain physical/chemical knowledge of products' failure mechanism. When the popular Arrhenius model is used, for example, specifying β_1 is equivalent to specifying the activation energy E_a which has been well defined especially for consumer electronics. Note that, although sample size and test duration are usually assumed to be fixed in many previous studies, in reality, however, engineers might also be interested in the trade-off between sample size/test

duration and statistical precision. It is this trade-off that generates the full picture and makes our decisions more flexible. In what follows, each stage is described in detail.

7.2.1. STAGE 1: Test Planning at the Highest Stress Level

The approach presented in Section 6.3.1 is used to plan the test at the highest stress level. That is, given the planning inputs: 1) the censoring time c_3, and the number of failures R_3 expected to see; 2) the values for both parameters β_0 and σ; and 3) a confidence level α, the number of units needed in the test at x_3 is obtained by solving the equation

$$\sum_{i=0}^{R_H-1} C_{n_H}^{i} p^{i} \left(1-p\right)^{n_H-i} = 1-\alpha \tag{7.1}$$

This is exactly the binomial bogey testing which are commonly used for product reliability demonstration, and the value $1-\alpha$ is then referred as the consumer's risk (Yang 2007, pp.384).

7.2.2. STAGE 2: Test Planning at the Lowest and Middle Stress Level

7.2.2.1. Planning Inputs

After the test at the highest stress x_3 has been done, we move to the second stage of sequential ALT planning. To plan the tests at lower stresses, i.e. the lowest and middle stresses, one needs to:

- Estimate β_0 and σ from the testing data obtained at the highest stress level.

  Based on the ML theory, the estimate $(\hat{\beta}_0, \hat{\sigma})$ is found by maximizing the log-likelihood function

$$l(\beta_0, \sigma) = \sum_{j=1}^{n_3} \left(\kappa_{3j} (-\log \sigma + z_{3j} - \exp z_{3j}) - (1 - \kappa_{3j}) \exp \zeta_3 \right) \quad (7.2)$$

where the subscript $\cdot_{ij}$ corresponds to the *jth* failure at stress i

- Specify the slope parameter β_1.
- Specify the sample size $n_1 + n_2$ available for tests at x_1 and x_2.
- Specify the position and sample allocation of x_2.

  Since the middle stress is typically added to check the non-linearity of the stress-life model, we constrain the middle stress level to be halfway between x_1 and x_3. In addition, to avoid the developed 3-stress plan from degenerating to a 2-stress optimum plan, we let the proportion of sample allocated to stresses x_1 and x_2 follows $n_2 / (n_1 + n_2) = \pi$.

7.2.2.2. The Fisher Information

Collect all 3 ALT model parameters in a vector $\boldsymbol{\theta} = (\beta_0, \beta_1, \sigma)$. Let $\hat{\mathbf{I}}_3$ denote the observed Fisher information on $\boldsymbol{\theta}$ from the test at the highest stress level x_3; $\mathbf{I}_1$ and $\mathbf{I}_2$ respectively denote the expected information on $\boldsymbol{\theta}$ to be obtained from tests at low and middle stresses, then, the asymptotic covariance matrix $\boldsymbol{\Sigma}$ of the MLE $\hat{\boldsymbol{\theta}}$ is given by

$$\boldsymbol{\Sigma} = (\hat{\mathbf{I}}_3 + \mathbf{I}_1 + \mathbf{I}_2)^{-1} \quad (7.3)$$

Using the results of Nelson and Meeker (1978), the observed information matrix $\hat{\mathbf{I}}_3$ is derived as in equation (7.4). Note that, as the test at x_3 does not contain any information on the slope β_1 of the stress-life model, the second row and column of $\hat{\mathbf{I}}_3$ must be zeros

$$\hat{\mathbf{I}}_3 = \begin{bmatrix} \sum_{j=1}^{n_3} A(z_{3j},\zeta_3) & 0 & \sum_{j=1}^{n_3} B(z_{3j},\zeta_3) \\ 0 & 0 & 0 \\ \sum_{j=1}^{n_3} B(z_{3j},\zeta_3) & 0 & \sum_{j=1}^{n_3} C(z_{3j},\zeta_3) \end{bmatrix}$$

where

$$A(z,\zeta) = \frac{x_0^2}{\sigma^2}(\kappa e^z + (1-\kappa)e^\zeta) \tag{7.4}$$

$$B(z,\zeta) = \frac{x_0}{\sigma^2}(-x_0(\kappa(e^z-1)+(1-\kappa)e^\zeta)+\kappa z e^z+(1-\kappa)\zeta e^\zeta)$$

$$C(z,\zeta) = \frac{1}{\sigma^2}\left\{-2(\kappa(ze^z-z-1)+(1-\kappa)\zeta e^\zeta)+\kappa(1+z^2e^z)+(1-\kappa)\zeta^2 e^\zeta\right\}$$

$\mathbf{I}_1$ and $\mathbf{I}_2$ is the expected information on $\boldsymbol{\theta}$ respectively obtained from tests at low and middle stress. Based on the definition of Fisher information, expressions of $\mathbf{I}_1$ and $\mathbf{I}_2$ can be derived as

$$\mathbf{I}_1 = \frac{(n_1+n_2)\cdot(1-\pi)}{\sigma^2}\begin{bmatrix} D(\zeta_1) & x_1\cdot D(\zeta_1) & E(\zeta_1) \\ x_1\cdot D(\zeta_1) & x_1^2\cdot D(\zeta_1) & x_1\cdot E(\zeta_1) \\ E(\zeta_1) & x_1\cdot E(\zeta_1) & F(\zeta_1) \end{bmatrix}$$

$$\mathbf{I}_2 = \frac{(n_1+n_2)\cdot\pi}{\sigma^2}\begin{bmatrix} D(\zeta_2) & x_2\cdot D(\zeta_2) & E(\zeta_2) \\ x_2\cdot D(\zeta_2) & x_2^2\cdot D(\zeta_2) & x_2\cdot E(\zeta_2) \\ E(\zeta_2) & x_2\cdot E(\zeta_2) & F(\zeta_2) \end{bmatrix} \tag{7.5}$$

where

$$D(\zeta) = 1-(\exp(-\exp\zeta))$$

$$E(\zeta) = \int_0^{e^\zeta} \omega e^{-\omega}\log\omega d\omega + (1-D(\zeta))\zeta e^\zeta$$

$$F(\zeta) = D(\zeta) + \int_0^{e^\zeta} \omega e^{-\omega}\log^2\omega d\omega + (1-D(\zeta))\zeta^2 e^\zeta$$

7.2.2.3. The Test Planning Problem

The optimization criterion here is to minimize the large-sample (asymptotic) variance $\text{var}(\hat{y}_p)$ of the estimate $\hat{y}_p$ at use stress $x_0 = 1$. Hence, the optimization problem is formulated as

$$\begin{aligned} \text{Min} \quad & \text{var}(\hat{y}_p) = [1,1,u_p]\boldsymbol{\Sigma}[1,1,u_p]^T \\ \text{s.t} \quad & x_2 = (x_1 + x_3)/2 = x_1/2 \\ & n_2/n_1 = \pi/(1-\pi) \end{aligned} \tag{7.6}$$

In the literature, this type of criterion is known as the *c*-optimality, and interested readers may refer to an excellent reference by Atkinson and Donev (2007) for more details. In the next section, we illustrate the application of the proposed framework using a numerical example.

7.3. NUMERICAL EXAMPLE

7.3.1. Reliability Estimation of an Adhesive Bond

Suppose an ALT is conducted to estimate the 0.1 life quantile of certain adhesive bond at the use operating temperature. Necessary planning information is summarized as below,

- 300 adhesive bond units and 230days are available for the test.
- Temperature is used as the acceleration factor. In particular, the use temperature is 50^0C according to the design specifications, whereas the highest temperature allowed in the test is 120^0C. That is, the testing region ranges from 50^0C to 120^0C.
- Weibull distribution is used to model the adhesive bond data as suggested by previous testing results on similar products. Equivalently, the logarithm failure times follow SEV distribution with location μ and scale σ.
- Arrhenius relationship is taken as the underlying stress-life model on the testing region ranging from 50^0C to 120^0C, i.e.

$$\mu = \log A + \frac{\text{Activation energy}, E_a}{\text{Boltzmann constant}, k_B = 8.6171\times10^{-5}} \cdot \frac{1}{T}$$

Let $s = 1/T$ and $x = (s - s_k)/(s_0 - s_k)$, the re-parameterization of the Arrhenius model yields the linear stress-life model as

$$\mu = \beta_0 + \beta_1 \cdot x$$

where $\beta_0 = \log A + E_a \cdot k_B^{-1} \cdot S_0 \quad \beta_1 = E_a \cdot k_B^{-1} \cdot (S_0 - S_k)$

In this example, engineering experiences suggest that $\log A = -16.733$ and $E_a = 0.7265$. Hence, we have the pre-specified values $\beta_0 = 4.72$ and $\beta_1 = 4.65$ as the planning inputs.

- The scale parameter σ is constant independent of testing temperature, and is specified as $\sigma = 0.6$.

7.3.2. STAGE 1: Planning for the Test Run at the Highest Stress Level

Given the planning inputs $\beta_0 = 4.72$, $\sigma = 0.6$ and $\alpha = 0.9$, equation (7.1) generates the contour plot, as shown in Figure 7.2, of the required sample size n_3 against the specified number of failures R_3 and the confidence level α. Apparently, the required sample size n_3 increases as either R_3 or c_3 increases.

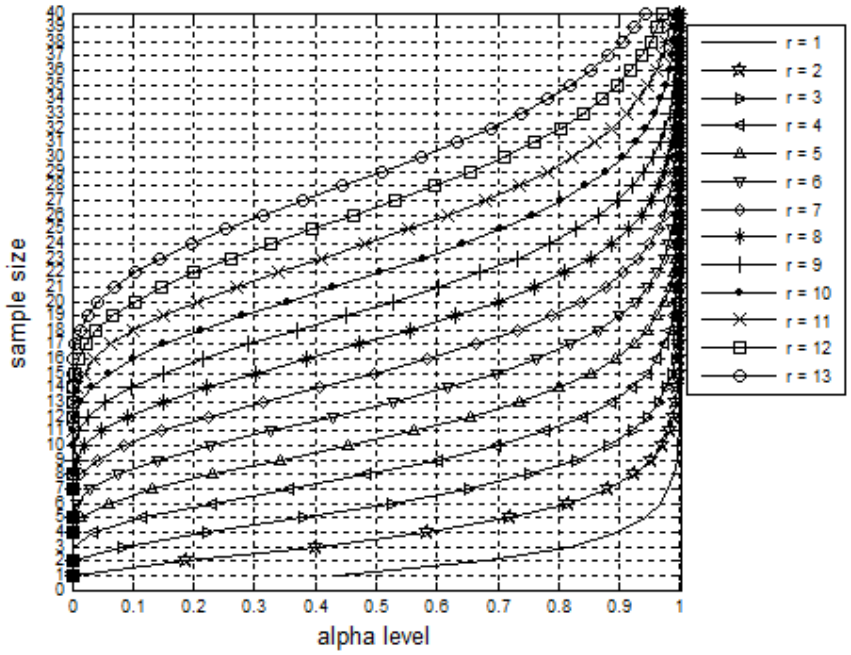

Figure 7.2 Plot of n_3 for different number of failures R_3 and the confidence level α

Suppose $R_3 = 12$ failures are expected within $c_3 = 80$ days, 35 adhesive bond units are tested at the highest temperature level 120^0 C as indicated by Figure 7.2.

The testing data at the highest stress level are presented in Table 7.1. It is seen that, 27 adhesive bonds fail within 80days during the test at 120^0 C temperature level. Maximize the likelihood function given by equation (7.2), we have the MLE of both β_0 and σ as

$$(\hat{\beta}_0, \hat{\sigma}) = \arg\max l(\beta_0, \sigma) = \arg\max \left\{ \sum_{j=1}^{n_3} \left(\kappa_{3j} (-\log\sigma + z_{3j} - \exp z_{3j}) - (1-\kappa_{3j}) \exp\zeta_3 \right) \right\}$$
$$= (4.0125, 0.8747)$$

Table 7.1 Simulated failure times at the highest temperature level

Failure times (day)
5 74 31 42 10 19 45 <u>80</u> 15 46 31 17 7 21 <u>80</u> 50 6 8 50 10 <u>80</u> 56 15 <u>80</u> <u>80</u> 79 <u>80</u> 32 67 <u>80</u> <u>80</u> 20 46 7 44

7.3.3. STAGE 2 Planning for Test Runs at the Lowest and Middle Stress Level

Based on the ML estimates ($\hat{\beta}_0, \hat{\sigma}$) and equation (7.4), we can compute each entry of the observed Fisher information matrix $\hat{\mathbf{I}}_3$. However, to derive the Fisher information $\mathbf{I}_1$ and $\mathbf{I}_2$, additional planning information is needed as discussed in Section 7.2.2.2.

- The pre-specified slope parameter, $\beta_1 = 4.65$;
- The censoring times of tests at stress levels x_1 and x_2, $c_1 = c_2 = 150$days;
- The sample size $n_1 + n_2 = 300 - n_3 = 265$;
- $\pi = 0.1$, i.e. 10% units are allocated at the middle stress level x_2;
- $p = 0.1$, i.e. the 10% smallest extreme value percentile at use stress is of interest.

Then, using equations (7.5) and (7.6), we are able to conduct the numerical search of optimum ALT plan as shown in Figure 7.3. It is seen that, the minimum value of $\text{var}^*(\hat{y}_{0.1}) \approx 0.12$ is achieved when $x_1^* = 0.52\,(80^0\text{C})$ and $x_2^* = x_1^*/2 = 0.26$ (99^0C). Table 7.2 summarizes the complete sequential plan.

Table 7.2 Developed sequential ALT plan for the adhesive bond ALT

Stage	Condition	Stress Level		Test Duration	Failure Probability	Allocation	Expected Failures
		Temp	Std.				
1	High	120C	0	80 days	0.43	35	15
2	Mid	99C	0.26	150 days	0.19	27	5
	Low	80C	0.52		0.03	238	7

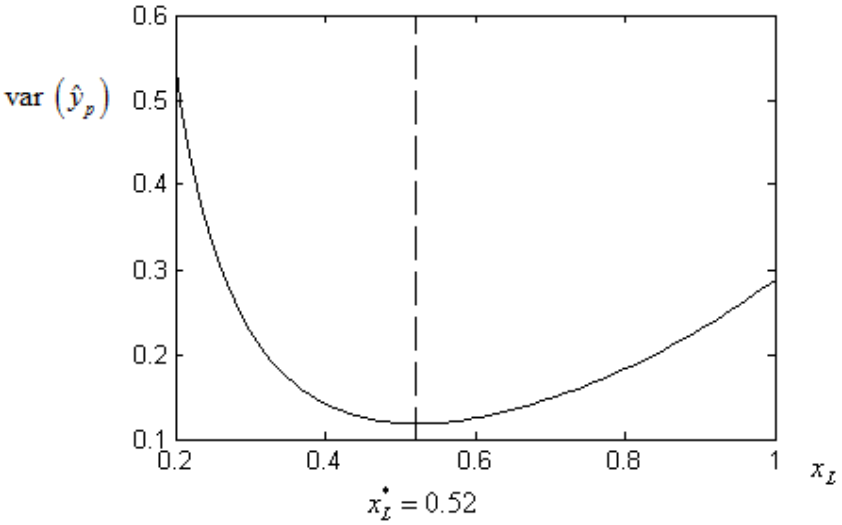

Figure 7.3 Plot of $\text{var}^*(\hat{y}_{0.1})$ against x_1

One salient advantage of sequential experiment is that subsequent decisions can be flexibly made based on the results of previous testing outputs. For example, engineers might be interested in whether it is profitable to apply more test units or longer test duration. To answer this question, we let $\bar{n}_L$ be the baseline or default sample size available for tests at stresses x_1 and x_2; ω (>0) be a proportional adjuster of $\bar{n}_L$ such that $n_L = \bar{n}_L \cdot \omega$.

For the adhesive bond ALT example, the default samples size $\bar{n}_L$ is 265, and the testing duration c at both stresses x_1 and x_2 are 150 days. Using equations (7.5) and (7.6), we obtain the contour plot of the optimum $\text{var}^*(\hat{y}_{0.1})$ against different values of ω and censoring time c. As seen from Figure 7.4, in order to reduce a fixed amount of variance $\text{var}^*(\hat{y}_{0.1})$, the amount of additional test duration or sample size required depends on the current $\text{var}^*(\hat{y}_{0.1})$. The smaller the $\text{var}^*(\hat{y}_{0.1})$, the larger the additional sample size/test duration. For example, suppose the target variance level is 0.1 instead of 0.12, one may increase the test duration to 175 hrs (from point "A" to "B"); or

increase the sample size to 265×1.25=339 (from point "A" to "C"); or simultaneously increase both sample size and test duration (e.g. from point "A" to "D") depending on certain considerations, say, the cost of the test (Tang and Xu 2005).

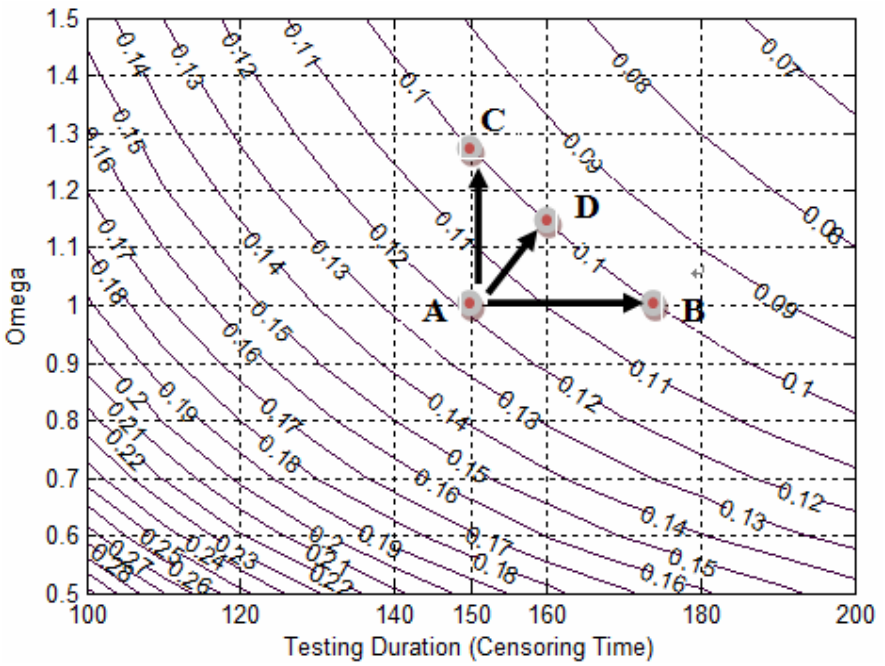

Figure 7.4 Contour plot of $\mathrm{var}^{*}(\hat{y}_{0.1})$ against sample size and test duration

7.4. DISCUSSIONS AND CONCLUSIONS

The sequential ALT planning can be used as a strategy to enhance the robustness of ALT plan against mis-specification of model parameters, especially when there is a high margin of parameter specification error.

To visualize the key idea behind the sequential planning approach as well as its advantages, we re-visit the numerical example presented in Section 7.3, and let

$\mathbf{i}_i$: expected Fisher information from a single observation at stress x_i, $\quad \forall i = 1,2,3$

$\det^{jk} \mathbf{i}_i$: the *jkth* element of the determinant of matrix $\mathbf{i}_i$, $\quad \forall i, j, k = 1,2,3$

In particular, we assume that σ is known so as to make the discussion clearer. Then, at any stress x_i, we have,

$$\det \mathbf{i}_i = \begin{bmatrix} \det^{11} \mathbf{i}_i & \det^{12} \mathbf{i}_i \\ \det^{12} \mathbf{i}_i & \det^{22} \mathbf{i}_i \end{bmatrix} \qquad \forall i = 1, 2, 3$$

, where $\det^{11} \mathbf{i}_i$ and $\det^{22} \mathbf{i}_i$ will be respectively interpreted as the expected information to be obtained on parameter β_0 and β_1.

Figure 7.5 plots both $\det^{11} \mathbf{i}_i$ and $\det^{22} \mathbf{i}_i$ at each stress levels given different specified values of β_0 and β_1. As seen from this figure, the expected information is much more sensitive to the specified value of β_0. In many applications, unfortunately, the value of β_0 is extremely difficult to be specified, and the margin of error can be very large. Hence, by conducting the test in a sequential manner, we are able to secure the accuracy of the specified value of β_0. In fact, based on the failure data obtained at the highest stress level, a confidence interval of β_0 can be constructed. Then, as shown in Figure 7.6, the value of β_0 can be confined to a range which covers the true value at a given confidence level. As we have discussed in the introduction part, the value of β_1 is relatively easier to obtain as it is often associated to products' failure mechanism, hence, the proposed sequential planning framework has its advantages in developing more robust ALT plans. Of course, one possible side effect of conducting an ALT sequentially is that the test duration might be longer.

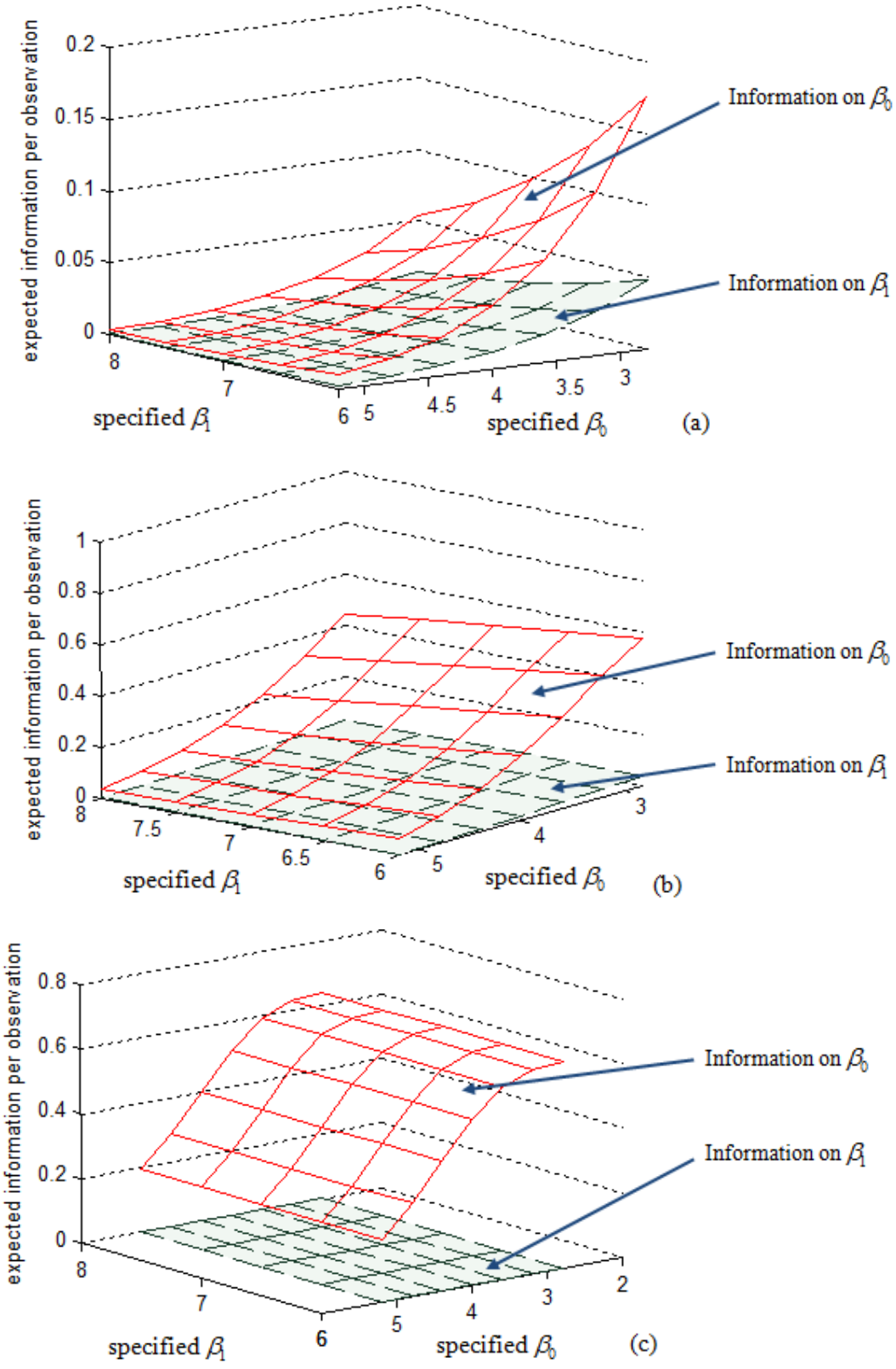

Figure 7.5 Expected information per observation (a) at x_1; (b) at x_2; (c) at x_3

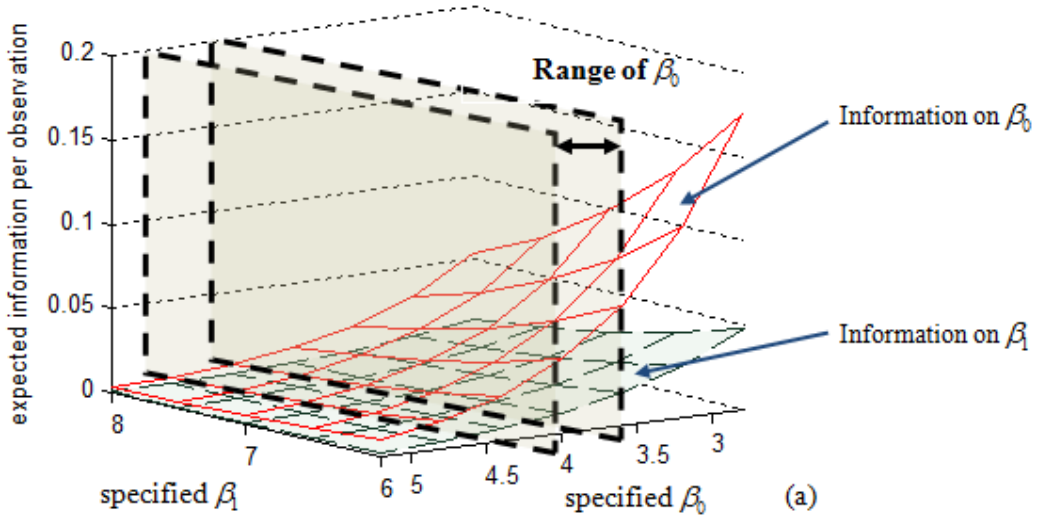
expected information per observation
0.2
0.15
0.1
0.05
0
Range of β_0
Information on β_0
Information on β_1
8
7
6
5
4.5
4
3.5
3
specified β_1
specified β_0
(a)

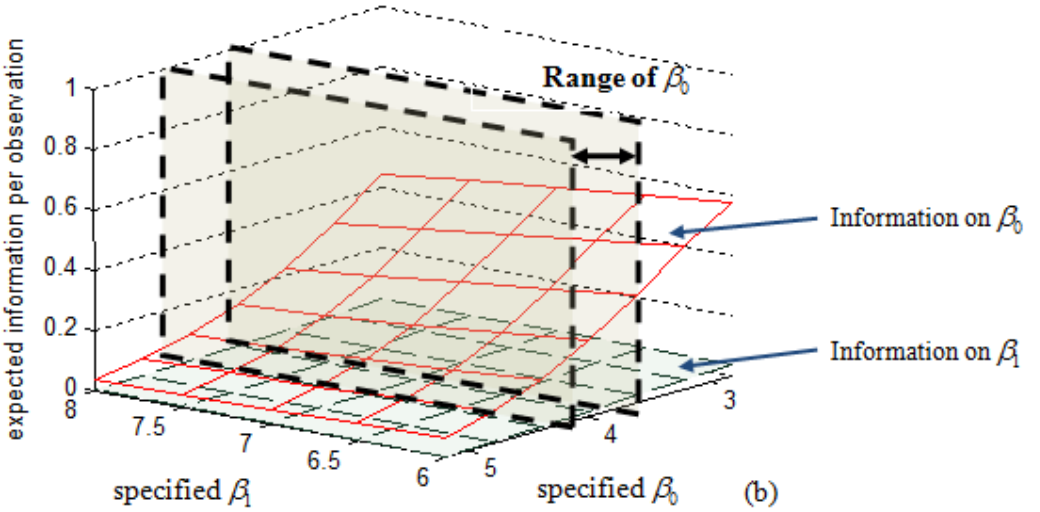
expected information per observation
1
0.8
0.6
0.4
0.2
0
Range of β_0
Information on β_0
Information on β_1
8
7.5
7
6.5
6
5
4
3
specified β_1
specified β_0
(b)

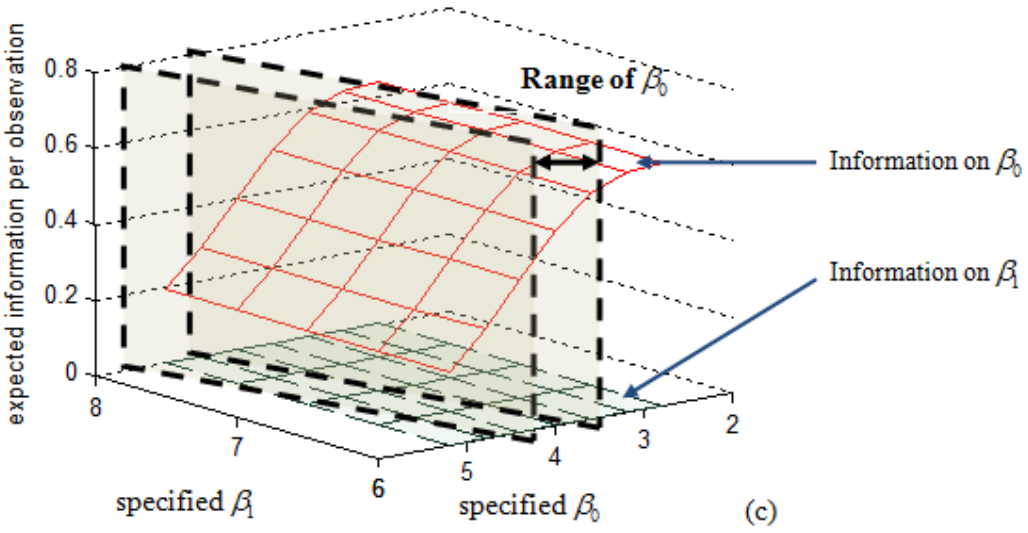

Figure 7.6 Pre-estimation of β_0 under the sequential planning framework

(a) at x_1; (b) at x_2; (c) at x_3

Chapter 8. Case Study: Planning and Inference of an Electronic Controller Sequential ALT

8.1. Introduction

8.1.1. Background and Experiment Purpose

This case study deals with an ALT project in which engineers assessed the reliability of a newly developed cost reduction electronic controller installed on one of their domestic products. The sequential planning and inference scheme was successfully implemented in this testing project which involves temperature, humidity and power cycles.

Facing the escalating pressure from competitors in the field, the design team of the company lately developed a new electronic controller with lower manufacturing cost. As this new product is a simplified version of the original design, a decline in reliability is expected. To quickly assess whether the new design still meets the reliability target within 45 days, product engineers launched this accelerated life testing project using 60 controller prototypes. Both temperature and humidity were taken as accelerating factors in this experiment. According to the products' specifications, the nominal temperature and relative humidity are respectively 45C and 50%, and the 10% percentile of products' lifetime should not be less than 2 years. Furthermore, the power cycle was also taken into account in order to fully simulate the working conditions of the controller.

8.1.2. The Acceleration Model

Since Weibull distribution had been successfully used to model data of the original version of the controller, engineers adopted the assumption of Weibull failure times with scale parameter α and shape parameter β. Besides, it is assumed that β is a constant independent of stress, whereas α depends on both temperature and relative humidity through Hallberg-Peck relationship

$$AF = \frac{\alpha(318K, 60\%)}{\alpha(T, RH)} = \left(\frac{RH}{60\%}\right)^{p} \times \exp\left\{\left(\frac{Ea}{k}\right) \times \left(\frac{1}{318k} - \frac{1}{T}\right)\right\} \quad (8.1)$$

where

AF : Acceleration Factor

RH : Relative Humidity in Test

T : Temperature in Test

Ea : Activation Energy

k : Boltzman's Constant

p : Humidity Acceleration Factor

8.2. The Experiment

To protect proprietary information in what follows, I simulated data from the fitted model for the original application and re-scaled the data. Furthermore, I also masked the name of the actual dominate failure mode and called it “failure mode 820314”.

8.2.1. Planning and Inference under the Highest Stress

8.2.1.1 Test Design

Under the sequential framework of ALT planning, test at the highest stress level is conducted first. For the acceleration model to hold, the highest temperature and relative humidity are respectively fixed to 85C and 90%. To plan the test at the highest

stress level x_H, engineers firstly specified both values for the scale parameter α_H and the shape parameter σ at the test condition in which $T = 85C$ and $RH = 90\%$. The specification was done using previous test results of the original version of the controller. Based on this information, the shape parameter $\sigma \approx 1$, the humidity acceleration factor $p \approx 3$, and the activation energy $Ea \approx 1ev$. Hence, as the 10% percentile of the lifetime is 2 years (17520 hours) according to controller design specifications, α_H was computed as

$$\alpha_H = \alpha_0 \Big/ \left(\frac{RH = 90\%}{60\%}\right)^p \times \exp\left\{\left(\frac{Ea}{k}\right) \times \left(\frac{1}{318k} - \frac{1}{T = 358}\right)\right\} = 835\text{hrs}$$

where (8.2)

$$1 - \exp\{-17520/\alpha_0\} = 0.1$$

Figure 8.1 shows the contour plot of the sample size needed for the test at the highest stress level against test duration and expected number of failures.

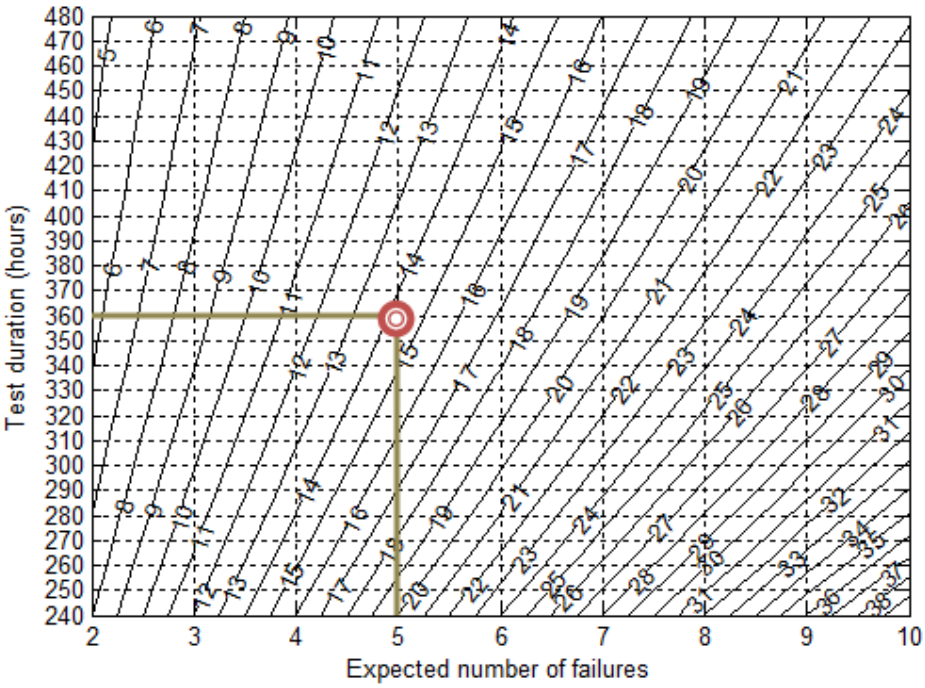

Figure 8.1 Contour plot of sample size needed in the test

In this project, 15 days were assigned to the test at the highest stress level, and 5

failures were expected. From the reading of Figure 8.1, 14 controllers were tested.

8.2.1.2 Test Procedure

During the test, the controllers were fixed by the mechanical fixture in a temperature/humidity chamber. All systems that have microprocessor controls were programmed with test software; all wiring inside the chamber was rated for 125C operation; the function test was done optically so that test engineers can determine whether the “failure mode 820314” has occurred.

The temperature/humidity/voltage loading profile is given in Figure 8.2. The power cycles are 5 hours on and 1 hour off for a 6 hours cycle.

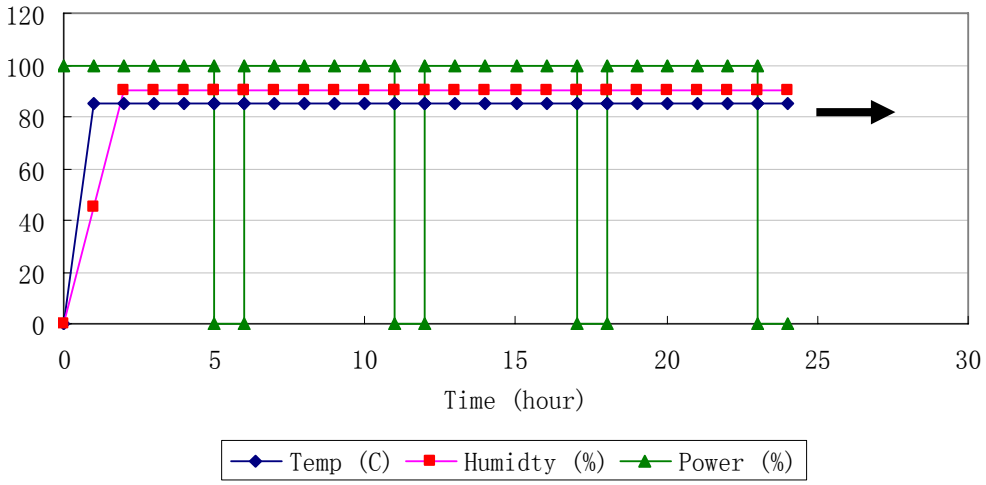

Figure 8.2 Temp/Humidity/Voltage Loading Profile

8.2.1.3 Test Data Analysis

The test results, as reported in Table 8.1, were obtained after 15 days. Before conducting the data analysis, engineers firstly checked the assumption of Weibull failure times. From the Weibull probability plot in Figure 8.3, there was no significant evidence indicating a violation of this assumption.

Table 8.1 Testing data collection form

CONTROLLER ACCELERATED LIFE TEST DATA COLLECTION FORM

Ref No: 0829x1 **Page:** 1 **of:** 1 **Data:** Jun, 2007

Testing Item Name: Cost Reduction Controller	Project Engineer: Victor Liu

Data:

No.	Temperature (C)	Humidity (%)	Failure/Censoring Time (hrs)	Failure Mode	Notes
1	85	95	355.28	820314	
2	85	95	12.76	820314	
3	85	95	360	820314	
4	85	95	47.25	820314	
5	85	95	155.90	820314	
6	85	95	73.92	820314	
7	85	95	360	820314	
8	85	95	171.07	820314	
9	85	95	82.21	820314	
10	85	95	360	820314	
11	85	95	360	820314	
12	85	95	219.81	820314	
13	85	95	262.04	820314	
14	85	95	339.58	820314	

Total Number of Failures: 10

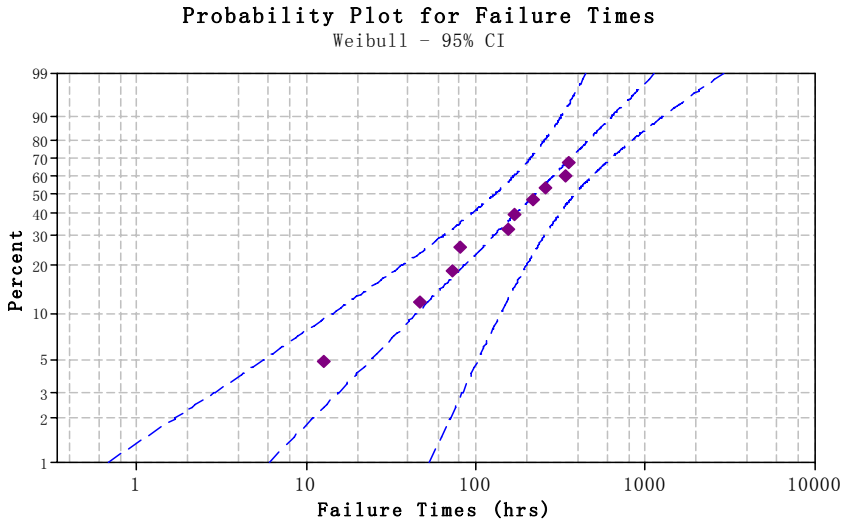

Figure 8.3 Weibull probability plot for failure times

Then, based on the data reported from the table above, information on

both $\mu_H = \log(\alpha_H)$ and $\sigma = 1/\beta$ in log-scale was quantified using the posterior distribution $\pi(\mu_H, \sigma)$. Figure 8.4 shows the deducted posterior distribution. In this project, the mode of the posterior distribution was taken as the Bayesian estimate $\hat{\boldsymbol{\theta}}_H = [\hat{\mu}_H, \hat{\sigma}]$, then, $\hat{\mu}_H = 5.74$ and $\hat{\sigma} = 0.855$ as indicted in Figure 8.4.

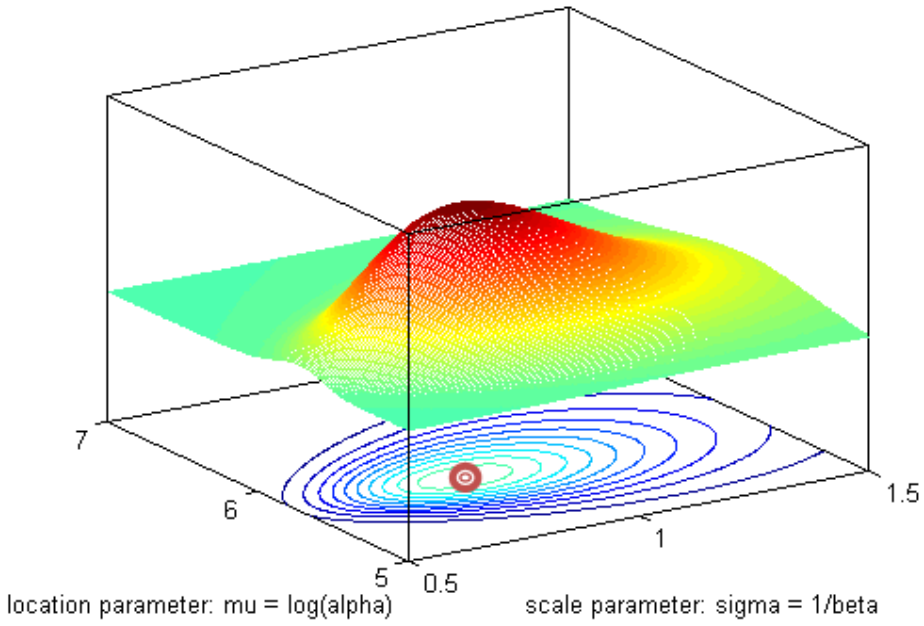

Figure 8.4 Posterior distribution $\pi(\mu_H, \sigma)$ at the highest stress level

As the actual number of failures obtained from the test is much larger than the expected number of failures, engineers realized that they might have overrated the controller reliability at the highest stress level. At this moment, however, they did not have sufficient information to judge whether this deviation is caused by a decline in controller reliability or a mis-specification of the humidity acceleration factor *p* as well as the activation energy *Ea* . Hence, they proceeded to conduct further testing at lower stress levels. Here, in order to relax the burden of the heavy computation in what follows, the posterior distribution $\pi(\mu_H, \sigma)$ was approximated by a bivariate normal

distribution as shown in Figure 8.5.

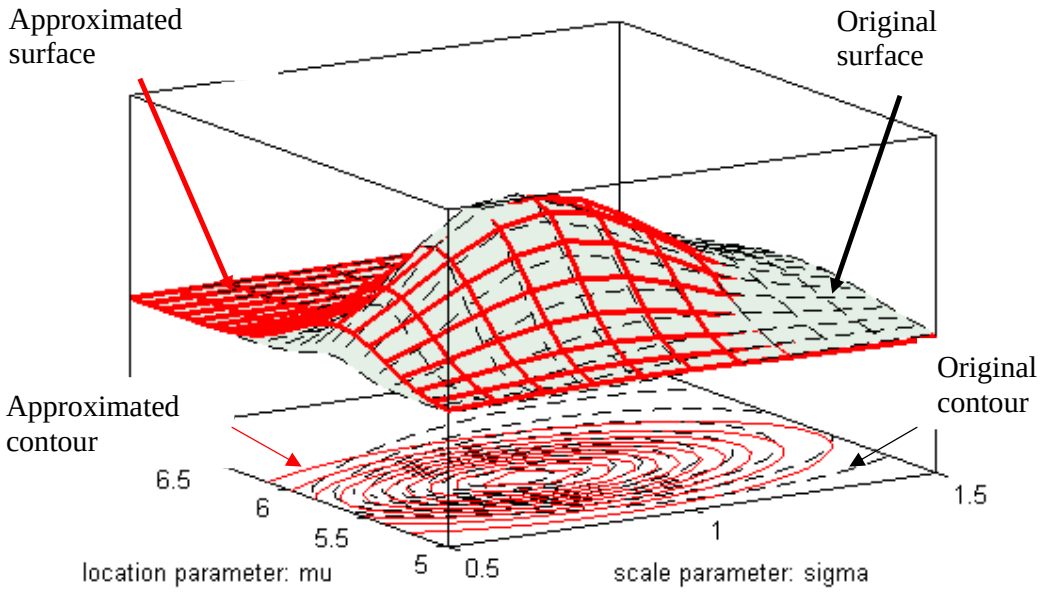

Figure 8.5 Normal approximation of the posterior distribution $\pi(\mu_H, \sigma)$

8.2.2. Planning and Inference under Lower Stresses

8.2.2.1 Tests Design

After the test under the highest stress was done, engineers proceeded to plan the subsequent tests involving three temperature-humidity combinations. As seen in Figure 8.6, these combinations include: 1) test at low temperature and low humidity (the lowest stress level); 2) test at high temperature and low humidity (the middle stress level 1); and 3) test at low temperature and high humidity. The sample allocation to these three stress levels follows 8:1:1 ratio.

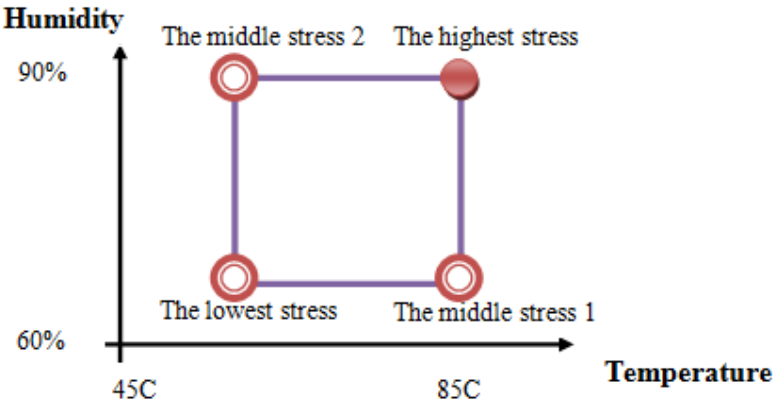

Figure 8.6 Experiment design

Given the specified ranges for both humidity acceleration factor $p \in [2.5, 3.5]$ and activation energy $Ea \in [0.7, 1.2]$, Figure 8.7 shows the expected variance of the estimator for the 0.1 percentile at use condition against the low temperature level and the low humidity level. Based on the reading from the figure, product engineers obtained the optimal test plan as summarized in Table 8.2.

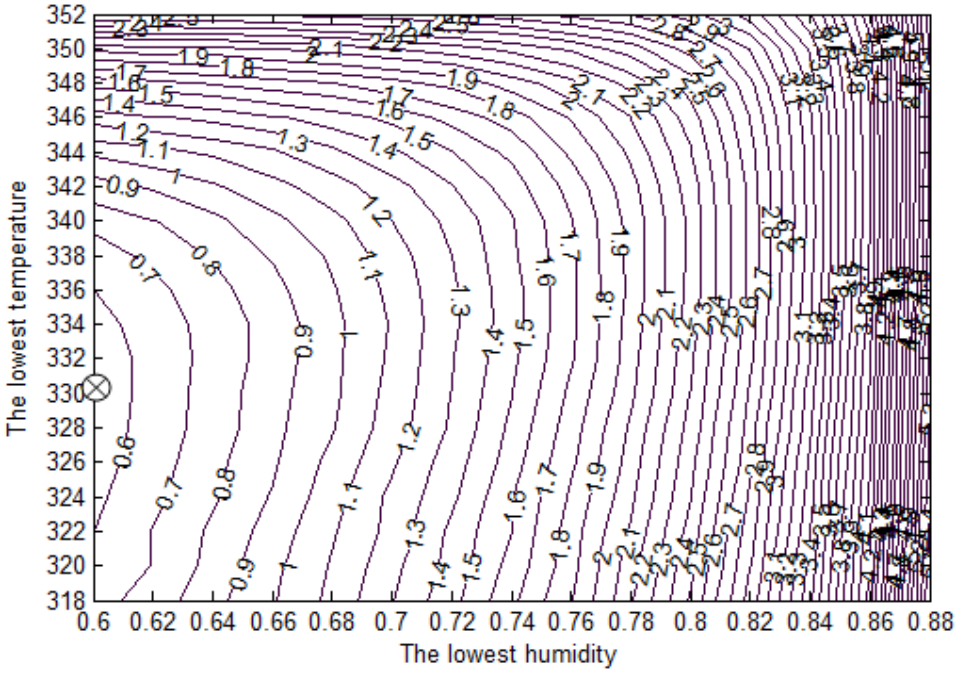

Figure 8.7 Expected variance of the estimator at different low temperature level and the low humidity level

Table 8.2 Developed test plan

CONTROLLER ACCELERATED LIFE TEST PLAN

Ref No: 0233x8 **Page:** 1 **of:** 1 **Data:** Jun, 2007
Testing Item Name: Cost Reduction Controller **Project Engineer:** Victor Liu
Testing Purpose: Estimate the 0.1 life percentile at 45C and 60% humidity
Expected Variance of the Estimator: 1.701

Plan:

Test Stage	Temperature (C)	Humidity (%)	Test Duration (hrs)	Sample Size	Expected Failures
1	85	95	360	14	5
2	85	60	720	5	3
	58	95	720	5	1
	58	60	720	36	1

8.2.2.2 Simulation Assessment of the Developed Plan

Before conducting the tests, engineers quickly run a simulation in order to assess the developed plan. In each simulation run, p and Ea are randomly generated from their specified ranges, then, based on the generated values and test results obtained from the highest stress level, failure times at each lower stress levels were simulated. From every batch of failure times, engineers computed the asymptotic variance of the estimator for the 0.1 life percentile at use condition. Figure 8.8 presented the simulation results involving 1000 simulation runs. As seen from this figure, the expected variance (1.701) only slightly higher than the mean of the simulated variance (1.6), hence, engineers proceeded to the run the tests.

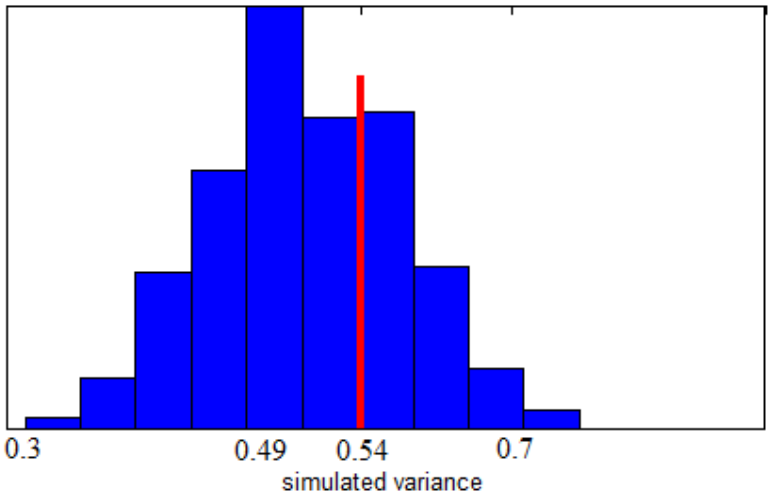

Figure 8.8 Simulation assessment of test plan

8.2.2.3 Test Procedure

During the test, the controllers were fixed by the mechanical fixture in a temperature/humidity chamber. All systems that have microprocessor controls were programmed with test software; all wiring inside the chamber was rated for 125C operation; the function test was done optically so that test engineers can determine whether the “failure mode 820314” has occurred. The temperature/humidity/voltage loading profiles are given in Figure 8.9.

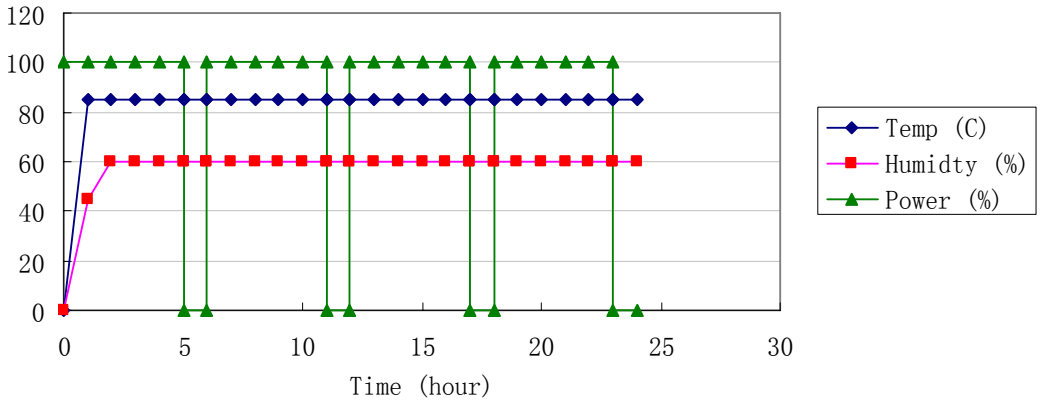

(a) The middle stress 1: high temperature – low humidity

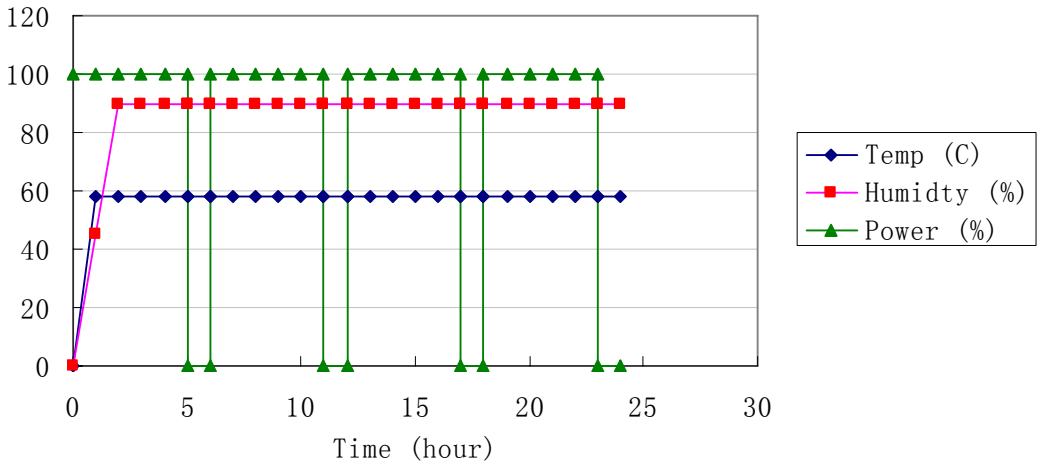

(b) The middle stress 2: low temperature – high humidity

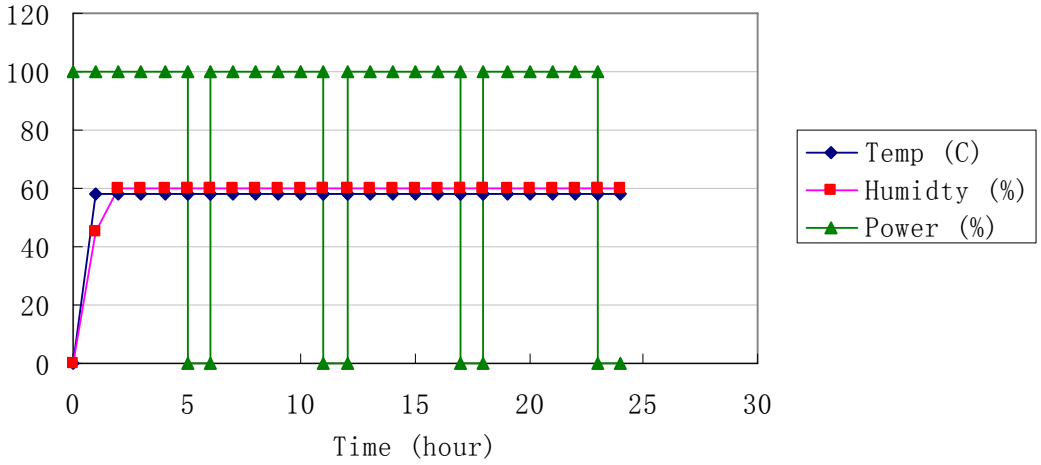

(c) The lowest stress level: high temperature – high humidity

Figure 8.9 Temp/Humidity/Voltage Loading Profiles

8.2.2.4 Test Data Analysis

The test results, as reported in Table 8.3, were obtained after 30 days.

Table 8.3 Testing data collection form

CONTROLLER ACCELERATED LIFE TEST DATA COLLECTION FORM

Ref No: 0829x1 **Page:** 1 **of:** 1 **Data:** Jun, 2007

Testing Item Name: Cost Reduction Controller	Project Engineer: Victor Liu

Data:

No.	Temperature (C)	Humidity (%)	Failure/Censoring Time (hrs)	Failure Mode	Notes
1	58	60	29.80	820314	
2	58	60	720.00	820314	
3	58	60	720.00	820314	
…	…	…			
36	58	60	720.00	820314	

Total Number of Failures: 1

Data:

No.	Temperature (C)	Humidity (%)	Failure/Censoring Time (hrs)	Failure Mode	Notes
1	85	60	334.09	820314	
2	85	60	632.88	820314	
3	85	60	720.00	820314	
4	85	60	720.00	820314	
5	85	60	720.00	820314	

Total Number of Failures: 2

Data:

No.	Temperature (C)	Humidity (%)	Failure/Censoring Time (hrs)	Failure Mode	Notes
1	58	90	131.45	820314	
2	58	90	720.00	820314	
3	58	90	720.00	820314	
4	58	90	720.00	820314	
5	58	90	720.00	820314	

Total Number of Failures: 1

Engineers analyzed these failure data, Figure 8.10 shows both deduced prior distribution and derived posterior distribution at each lower stress levels. Table 8.4 summarizes the analysis results.

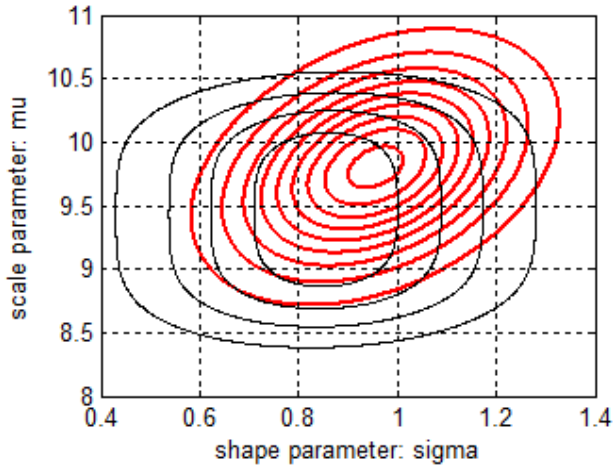

(a) The lowest stress level: low temperature, low humidity

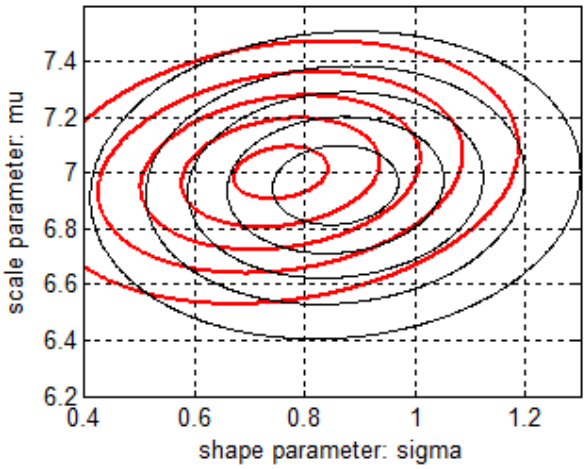

(b) The middle stress level 1: high temperature, low humidity

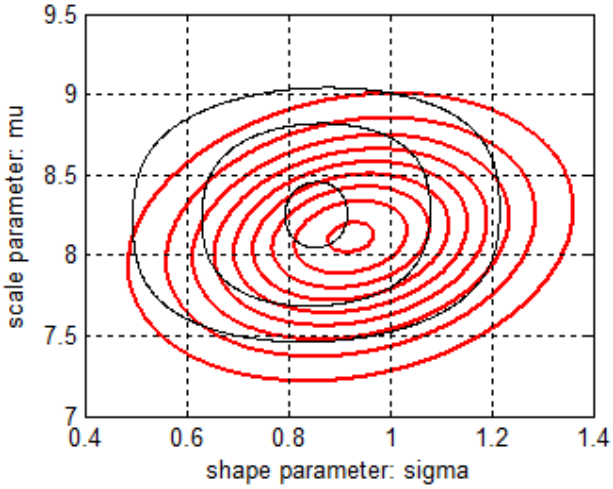

(c) The middle stress level 2: low temperature, high humidity

Figure 8.10 Prior and posterior distribution at each lower stress levels

Table 8.4 Data analysis results

CONTROLLER ACCELERATED LIFE TEST DATA ANALYSIS REPORT

Ref No: 0829x1 **Page:** 1 **of:** 1 **Data:** Aug, 2007

Testing Item Name: Cost Reduction Controller	Project Engineer: Victor Liu

Analysis Results:

Stress Level	Temperature (C)	Humidity (%)	Analysis Results						
			Scale: mu	Shape: sigma	0.1 life percentile		variance (log-scale)	Lower bound at 95% level	
					In log-scale	In hours		In log-scale	In hours
High	85	90	5.740	0.855	3.816	45.4	0.3204	2.886	17.9
Mid 1	85	60	7.000	0.756	5.299	200.1	0.2959	4.404	81.8
Mid 2	58	90	8.110	0.924	6.031	416.1	0.3215	5.101	164.2
Low	58	60	9.800	0.956	7.649	2097.7	0.2746	6.787	886.2
Use	45	60			8.853	6995.3	0.4606	7.7367	2290.9

8.2.3. Conclusions

Since 2290.9 hours are far less than 2 years, the reliability of the cost reduction controller does not meet the requirement. In fact, when the test at the highest stress level was done, engineers had already found that the actual number of failures was far more than the expected number. At that moment, however, they could not decide whether this deviation was due to an overestimation of product reliability or a mis-specification of the stress-life model parameters. Until the whole tests were done, they finally realized that re-design and improvements in controller reliability are needed. From this simple case study, we have seen one real application of the sequential ALT planning and inference scheme in manufacturing industry, in which some key stress-life model parameters are well understood from engineering empirical knowledge.

Chapter 9. Planning and Analysis of Accelerated Life Test for Repairable Systems with Independent Competing Risks

9.1. Introduction

This chapter describes a Bayesian method of planning an accelerated life test for repairable systems with multiple *s*-independent failure modes. At any testing stress, failure times of each failure mode are assumed to constitute a Power Law Process (PLP). The scale parameter of the failure process is a log-linear function of stress, whereas the shape parameter is a constant independent of stress. We use both Bayesian *D*-optimality and *Ds*-optimality to develop the two-stress optimum as well as the three-stress compromise ALT plan. Particularly, the prior elicitation is discussed, the Fisher information matrix is derived, and the global optimality of the two-stress ALT plan is verified using the general equivalence theorem. We provide a numerical example to illustrate the proposed planning method, and employed a Bayesian curve fitting method based on the Dirichlet process mixture of normals to evaluate the posterior distribution when the sample size is relatively small.

9.1.1. Accelerated Life Test for Repairable Systems

As we have seen in previous chapters, a significant amount of research has been done on both test planning and data analysis for non-repairable system ALT. However, the problem of planning an ALT for repairable systems has not yet been fully investigated.

Even if for non-repairable systems, since the number of prototypes are usually small in the R&D phase, failed products, if possible, can be repaired and continuously tested (see e.g. Guida and Giorgio 1995, Yun et al. 2006, Guerin et al. 2004).

In the literature, most of the studies of repairable systems ALT are mainly focused on data analysis. Guida and Giorgio (1995) presented an important method for analyzing ALT data from repairable systems. In their study, repairable systems are modeled by the Power Law Process (PLP) with covariates. Both proportional intensity (PI) and accelerated time (AT) regression models are conceived in formulating the dependence of the failure process on the covariates (stress), and the maximum likelihood (ML) solutions are derived for parameter estimation. It is noted that, the use of the PLP in modeling the failure process implicitly implies that the repair restores the system to the intensity just before failure. According to the classification of Pham and Wang (1994), this type of repair is termed as the 'minimal repair'. In Guerin et al. (2004), based on the same 'minimal repair' assumption, the authors derived two useful ALT models for repairable systems, namely, the Arrhenius-exponential model, and the Peck-Weibull model. In many cases, the repair action does make a system younger, if not as good as new. This situation was considered in Yun et al. (2006) and the PI regression model was used for analyzing the ALT data.

Little work has been done on the planning of an ALT for repairable systems. Considering the economic factors, the early work of Flehinger (1965) developed optimum test plans for repairable systems test assuming (homogeneous) Poisson process. Recently, Guo and Pan (2008) provided a theoretical method that helps to

determine the minimal sample size and test duration for demonstration tests of repairable systems.

9.1.2. Accelerated Life Test with Competing Risks

A complex system, either non-repairable or repairable, may fail due to one of a series of failure modes, or competing risks (see Chapter 7, Nelson 1990). A good real-life example of repairable systems subject to competing risks was presented in Langseth and Lindqvist (2006). In that study, the authors provided a data analysis for a particular compressor system based on the dataset from the Offshore Reliability Data (OREDA) Database.

Most of the literature on ALT ignores the possibility of multiple failure modes. For those that did consider competing risks, the focus is mainly on data analysis. For example, assuming independent failure modes and type I/type II/progressive censoring, Klein and Basu (1981) obtained ML estimators when the underlying life distributions are Weibull with equal or unequal shape parameters. Zhao and Elsayed (2004) presented a method for analyzing ALT data considering both system hard failure and degradation. The lifetime of hard failure was modeled by Weibull distribution and the system degradation was assumed to follow a Brownian motion process.

Very few studies have been done on ALT planning with competing risks, and the planning of an ALT for repairable systems with competing risks have not been explored yet. Recently, Pascual (2008) presented an important work for planning of an ALT for non-repairable system. In that study, it was assumed that the failure modes

have respective latent failure times, and the minimum of these times corresponds to the product life. Further, these latent failure times were assumed to be independently Weibull with unknown shape parameter. Optimum plans were obtained based on different planning criteria motivated by practical considerations.

9.1.3. ALT Planning for Repairable Systems with Competing Risks

In this chapter, we propose a Bayesian approach to planning a constant-stress ALT for repairable systems with competing risks. Usually, preliminary estimates of unknown model parameters are needed so as to assess the statistical efficiency of a test plan. For the ALT planning approaches based on the likelihood theory, the asymptotic variance of the MLE is used as a yardstick in determining the optimum plan, and the developed plan is locally optimum depending on the "best guess" of the unknown model parameter values (see Chernoff (1972)). Hence, if the margin of parameters specification error is high and the requisite level of statistical precision cannot be achieved as planned. Motivated by this fact, various Bayesian methods for planning an ALT for non-repairable systems have been explored by many researchers. Some important results were presented in Chaloner and Larntz (1992), Zhang and Meeker (2006), Singpurwalla (2006), and etc. Compared to other ALT planning approaches based on the likelihood theory, Bayesian planning approaches generally enhance the robustness of the developed plans against mis-specifications of ALT models.

For the planning problem addressed in this chapter, the number of unknown model parameters could be large as it is proportional to the number of failure modes. Hence,

assuming these parameters are known at the planning stage can easily lead to a “false sense of statistical precision (Zhang and Meeker 2006)”. Based on this reasoning, we shall employ a Bayesian framework for planning an ALT for repairable systems with competing risks.

In Section 9.2, we briefly review the Power Law Process with covariates, and the statistical model of the repairable systems ALT with more than one failure modes is presented. Section 9.3 derives the expected Fisher information matrix for any given testing plan, and Section 9.4 discusses the specification of the prior which quantifies the uncertainly of unknown model parameters based on empirical engineering knowledge. In Section 9.5, details of the Bayesian planning problem are presented. This involves optimally choosing both sample allocation and stress combinations for a testing plan. In particular, the Bayesian *D*-optimality and *Ds*-optimality are used as the planning criteria. In Section 9.6, a numerical example is presented to illustrate the proposed Bayesian planning approach, and the equivalent theorem provided in Whittle (1973) is used to check the optimal approximate plan is indeed globally optimal. Section 9.7 employs a Bayesian curving fitting method based on Dirichlet process mixture of normals to evaluate the posterior distribution when the sample size is small.

9.2. The Modeling of ALT for Repairable Systems

This section develops the ALT model for repairable system with competing risks. Section 9.2.1 introduces both the Power Law Process (PLP) that models the failure process; as well as the acceleration model that formulates the dependence of the failure

process on testing conditions. Section 9.2.2 describes the modeling for competing risks; Based on the results in Section 9.2.1 and 9.2.2, Section 9.2.3 generalizes the ALT model for repairable system with competing risks.

9.2.1. The Power Law Process and the Acceleration Model

Consider a constant-stress ALT where N repairable systems are tested at m possibly transformed stress levels s_i for $i = 1, ..., m$ and $m \geq 2$. Particularly, $N_i = N \cdot \pi_i$ systems are allocated to stress level s_i and tested for T_i units of time. Let s_m denotes the highest stress level which is pre-fixed, and s_0 denotes the normal use stress level. We standardize s_i

$$x_i = \frac{s_i - s_m}{s_0 - s_m}$$

such that $0 = x_m \leq x_i \leq x_0 = 1$ for $i = 1, 2, ..., m$.

At any stress level x_i, each system is subject to k risks or causes of failure. Upon the occurrence of each failure, the system is immediately repaired, and the repair time is assumed to be negligible.

9.2.1.1. The Power Law Process

Assuming that repair times are negligible, the occurrence of consecutive failures of a repairable system constitutes a stochastic point process, say $N(t)$. One commonly used stochastic model is the Non-Homogeneous Poisson Process (NHPP) as described by Rigdon and Basu (1989). Such a model implicitly implies that the system reliability restores to the level it was in just before the occurrence of the failure, i.e. the system is as bad as old after repair. According to the classification of Pham and Wang (1994),

this type of repair is termed as the ‘minimal repair’.

A NHPP is often specified in terms of the intensity $v(t)$, and the most popular form of $v(t)$ is given as

$$v(t) = \left(\frac{\beta}{\alpha}\right) \cdot \left(\frac{t}{\alpha}\right)^{\beta-1} \qquad \alpha > 0, \quad \beta > 0 \tag{9.1}$$

and the cumulative mean number of failures in the time interval $(0,t]$ is then computed as,

$$\Lambda(t) = \int_0^t v(t)dt = \int_0^t \frac{\beta}{\alpha} \cdot \left(\frac{t}{\alpha}\right)^{\beta-1} dt = \left(\frac{t}{\alpha}\right)^{\beta} \tag{9.2}$$

A NHPP with the intensity specified as (9.1) is referred as the Power Law Process (PLP). PLP has many nice properties for modeling repairable system. For example, the shape parameter β determines how system reliability improves or deteriorates over time. When $\beta < 1$, the intensity is decreasing, hence, the PLP is a useful model for the system burn-in phase. When $\beta > 1$, the intensity is increasing, hence, the PLP is a good model for the system wear-out phase. And particularly when $\beta = 1$, the intensity is a constant and the underlying process reduces to the well-known (Homogeneous) Poisson Process with Exponential inter-arrival time. In addition, by comparing intensity (9.1) to that of Weibull distribution, it is not difficult to recognize that the time to the first failure under the PLP exactly follows Weibull distribution with scale parameter α and shape parameter β.

9.2.1.2. The Acceleration Model

In this chapter, the PLP is used to model the failure process due to particular risk at

given testing condition i for $i = 1, 2, ..., m$. Clearly, it is desirable to model the dependence of the failure process on testing conditions. In the literature, both the Proportional Intensity (PI) and Accelerated Time (AT) approaches are proposed.

PI approach (Cox 1972) assumes the mean number of failures under testing condition i in a time interval $(0, t]$ is u_i times of that under baseline condition in the same time interval, i.e. $\Lambda_i(t) = \Lambda_0(t) \cdot u_i$; while AT approach (Nelson 1990) assumes that the mean number of failures under testing condition i in a time interval $(0, t]$ equals that under baseline condition in the time interval $(0, u_i \cdot t]$.

As shown by Guida and Giorgio (1995), both approaches give the same result under the PLP model. According to their results, the effect of the testing stress x_i is to alter the scale parameter α while leaving the shape parameter β unchanged. Hence, we have

$$\alpha_i = \alpha_0 / u_i \quad , \quad \beta_i = \beta_0 \qquad \forall\ i = 1, 2, ..., m \tag{9.3}$$

The result shown in (9.3) is extremely important as it provides the theoretical basis for the following modeling of repairable system ALT with competing risks.

9.2.2. Modeling for Competing Risks

At any stress level x_i , each system is subject to k known risks. Hence, for each system on test, a sequence of failure times for each risk r ($r = 1, 2, ..., k$) is obtained. We assume that these failure times are either observed (exact) or right censored.

In particular, for system j at stress x_i , let $n_{i,j}^{(r)}$ denotes the total number of failures due to risk r for $r = 1, 2, ..., k$; $t_{i,j}^{(r)}(1), t_{i,j}^{(r)}(2), ..., t_{i,j}^{(r)}(n_{i,j})$ denote the exact failure times

due to risk r; and T_i denotes the censoring time at stress x_i. Then, Table 9.1 lists the observations for system j at condition i.

Table 9.1 Observations for system j at condition i

Risks	Number of Failures	Observed (Exact) Failure Times	Censoring Time
1	$n_{i,j}^{(1)}$	$t_{i,j}^{(1)}(1), t_{i,j}^{(1)}(2), \ldots, t_{i,j}^{(1)}(n_{i,j}^{(1)})$	T_i
2	$n_{i,j}^{(2)}$	$t_{i,j}^{(2)}(1), t_{i,j}^{(2)}(2), \ldots, t_{i,j}^{(2)}(n_{i,j}^{(2)})$	T_i
$\vdots$	$\vdots$	$\vdots$	$\vdots$
k	$n_{i,j}^{(k)}$	$t_{i,j}^{(k)}(1), t_{i,j}^{(k)}(2), \ldots, t_{i,j}^{(k)}(n_{i,j}^{(k)})$	T_i

At any stress level x_i, the failure times $t_{i,j}^{(r)}(1), t_{i,j}^{(r)}(2), \ldots, t_{i,j}^{(r)}(n_{i,j})$ for risk r are modeled by a PLP process. Hence, apply equations (9.1) and (9.2), the failure intensity at any stress x_i w.r.t. risk r is

$$v_i^{(r)}(t) = \left(\frac{\beta_i^{(r)}}{\alpha_i^{(r)}}\right)^{\beta_i^{(r)}} \left(\frac{t}{\alpha_i^{(r)}}\right)^{\beta_i^{(r)}-1} \tag{9.4}$$

and the cumulative mean number of failures w.r.t. risk r until any time t is

$$\Lambda_i^{(r)}(t) = \left(\frac{t}{\alpha_i^{(r)}}\right)^{\beta_i^{(r)}} \tag{9.5}$$

Let $\alpha_0^{(r)}$ and $\beta_0^{(r)}$ respectively denote the (baseline) value of $\alpha^{(r)}$ and $\beta^{(r)}$ at normal operating condition, then, under either PI or AT approach, equation (9.3) implies that

$$\alpha_i^{(r)} = \alpha_0^{(r)} / u_i^{(r)} \quad , \quad \beta_i^{(r)} = \beta_0^{(r)} \qquad \forall\ i = 1, 2, \ldots, m\ ,\ r = 1, 2, \ldots, k \tag{9.6}$$

That is, the effect of the testing stress x_i is to alter the scale parameter $\alpha^{(r)}$ while leaving the shape parameter $\beta^{(r)}$ unchanged.

9.2.3. Modeling of ALT for Repairable Systems with Competing Risks

In summary, an ALT for repairable systems with competing risks is modeled as follows,

- For each system j ($j = 1, 2, ..., N_i$) at stress level x_i ($i = 1, 2, ..., m$), the sequence of failure times $t_{i,j}^{(r)}(1), t_{i,j}^{(r)}(2), ..., t_{i,j}^{(r)}(n_{i,j})$ due to any risk r ($r = 1, 2, ..., k$) constitutes the power law process (PLP) with scale parameter $\alpha_i^{(r)}$ and shape parameter $\beta_i^{(r)}$.
- Let $u_i^{(r)} = \exp[\gamma^{(r)} \cdot (1 - x_i)]$, equation (9.6) implies that

  $$\alpha_i^{(r)} = \alpha_m^{(r)} \cdot \exp(\gamma^{(r)} x_i) \quad , \quad \gamma^{(r)} > 0 \tag{9.7}$$

  i.e. we have a log-linear relationship

  $$\mu_i^{(r)} = \mu_m^{(r)} + \gamma_1^{(r)} x_i = \gamma_0^{(r)} + \gamma_1^{(r)} x_i \quad \text{where } \mu = \log(\alpha), \mu_m^{(r)} = \gamma_0^{(r)} \tag{9.8}$$

  After the test has been performed, it is always important to verify this stress-life relationship based on the data. At the planning stage, assuming $u_i^{(r)} = \exp[\gamma^{(r)} \cdot (1 - x_i)]$ is motivated by:

  - It yields the (log) linear model of (9.8), which maintain the flexibility and simplicity of the model;
  - Mathematically, it guarantees the intensity, $u_i^{(r)}$, to be nonnegative for all $\gamma^{(r)}$ and x_i.
  - Many important stress-life model can be linearized, including the Arrhenius-type and inverse power models;
- Failure processes due to different risks might not necessarily have the same shape parameter $\beta_i^{(r)} = 1/\sigma_i^{(r)}$. However, for any given risk r, equation (9.3) implies that

the shape parameter $\beta_i^{(r)}$ is an unknown constant independent of stress under either PI or AT model, i.e. $\sigma^{(r)} = \sigma_i^{(r)}$ given risk r for $i = 0,1,...,m$

Hence, this ALT model consists of a $3 \times k$ vector $\boldsymbol{\theta} = (\boldsymbol{\theta}^{(1)}, \boldsymbol{\theta}^{(2)}, ..., \boldsymbol{\theta}^{(k)})$ as its parameters, where the component $\boldsymbol{\theta}^{(r)} = (\gamma_0^{(r)}, \gamma_1^{(r)}, \sigma^{(r)})$ for $r = 1, 2, ..., k$.

9.3. The Fisher Information Matrix

Based on the model developed, the Fisher information matrix for an ALT plan $\boldsymbol{\xi}$ is defined as

$$\mathbf{I}(\boldsymbol{\theta}; \boldsymbol{\xi}) = -E\left[\frac{\partial^2 l(\boldsymbol{\theta})}{\partial \boldsymbol{\theta} \partial \boldsymbol{\theta}}\right] \tag{9.9}$$

where $l(\boldsymbol{\theta})$ is the log-likelihood of the model parameter $\boldsymbol{\theta}$, which can be written as a summation of the log-likelihood $l_{i,j}^{(r)}(\boldsymbol{\theta}^{(r)})$ contributed from system j at stress x_i with respect to risk r

$$l(\boldsymbol{\theta}) = \sum_{i=1}^{m} \sum_{j=1}^{N_i} \sum_{r=1}^{k} l_{i,j}^{(r)}(\boldsymbol{\theta}^{(r)}) \tag{9.10}$$

Here, since each failure mode is assumed to be *s*-independent, let $\mathbf{I}(\boldsymbol{\theta}^{(r)}; \boldsymbol{\xi})$ be the expected information with respect to risk r obtained from all m stress levels, it is immediately seen that the Fisher information matrix $\mathbf{I}(\boldsymbol{\theta}; \boldsymbol{\xi})$ for the plan $\boldsymbol{\xi}$ is a $3k \times 3k$ block diagonal matrix with $\mathbf{I}(\boldsymbol{\theta}^{(r)}; \boldsymbol{\xi})$ as the *rth* block

$$\mathbf{I}(\boldsymbol{\theta}; \boldsymbol{\xi}) = -E\left[\frac{\partial^2 l(\boldsymbol{\theta})}{\partial \boldsymbol{\theta} \partial \boldsymbol{\theta}'}\right] = \underbrace{\begin{bmatrix} \mathbf{I}(\boldsymbol{\theta}^{(1)}; \boldsymbol{\xi}) & & & \\ & \mathbf{I}(\boldsymbol{\theta}^{(2)}; \boldsymbol{\xi}) & & \\ & & \ddots & \\ & & & \mathbf{I}(\boldsymbol{\theta}^{(k)}; \boldsymbol{\xi}) \end{bmatrix}}_{3 \times k} \tag{9.11}$$

To obtain the expression of $\mathbf{I}(\boldsymbol{\theta}^{(r)}; \boldsymbol{\xi})$, we let

$$\mathbf{I}(\boldsymbol{\theta}^{(r)};\boldsymbol{\xi}) = \sum_{i=1}^{m}\sum_{j=1}^{N_i} I_{i,j}^{(r)}$$

where $I_{i,j}^{(r)}$ is the expected information obtained from any system j at stress x_i with respect to risk r. Similar to equation (9.9), $I_{i,j}^{(r)}$ is defined as

$$I_{i,j}^{(r)} = -E\left[\frac{\partial^2\left(l_{i,j}^{(r)}(\boldsymbol{\theta}^{(r)})\right)}{\partial\boldsymbol{\theta}^{(r)}\partial\boldsymbol{\theta}^{(r)\prime}}\right] \tag{9.12}$$

We now derive the closed-form expression of $I_{i,j}^{(r)}$. For system j at stress x_i, let $0 < t_{i,j}^{(r)}(1) < t_{i,j}^{(r)}(2) < \ldots < t_{i,j}^{(r)}(n_{i,j}) < T_i$ be the failure times with respect to risk r before time T_i. The joint density of $n_{i,j}^{(r)}$ and $t_{i,j}^{(r)}(1), t_{i,j}^{(r)}(2), \ldots, t_{i,j}^{(r)}(n_{i,j})$ is given by (Rigdon and Basu 2000, pp.136)

$$f\left(n_{i,j}^{(r)}, t_{i,j}^{(r)}(1), t_{i,j}^{(r)}(2), \ldots, t_{i,j}^{(r)}(n_{i,j})\right)$$
$$= \begin{cases} \dfrac{\left(\beta^{(r)}\right)^{n_{i,j}^{(r)}}}{\left(\alpha_i^{(r)}\right)^{n_{i,j}^{(r)}\cdot\beta^{(r)}}}\left(\prod_{l=1}^{n_{i,j}^{(r)}} t_{i,j}^{(r)}(l)\right)^{\beta^{(r)}-1}\exp\left(-\left(\dfrac{T_i}{\alpha_i^{(r)}}\right)^{\beta^{(r)}}\right) & , \quad n_{i,j}^{(r)} \geq 1 \\ \exp\left(-\left(\dfrac{T_i}{\alpha_i^{(r)}}\right)^{\beta^{(r)}}\right) & , \quad n_{i,j}^{(r)} = 0 \end{cases}$$

Making the change of variables $\alpha = \exp(\mu)$, $\beta = 1/\sigma$, and $t = \exp(y)$, we have the joint density of $n_{i,j}^{(r)}$ and $-\infty < y_{i,j}^{(r)}(1) < y_{i,j}^{(r)}(2) < \cdots y_{i,j}^{(r)}(n_{i,j}^{(r)}) < c_i$

$$f\left(n_{i,j}^{(r)}, y_{i,j}^{(r)}(1), y_{i,j}^{(r)}(2), \cdots, y_{i,j}^{(r)}(n_{i,j}^{(r)})\right)$$
$$= \begin{cases} \left(\dfrac{1}{\sigma^{(r)}}\right)^{n_{i,j}^{(r)}}\exp\left(-\dfrac{n_{i,j}^{(r)}\mu_i^{(r)}}{\sigma^{(r)}}\right)\left(\prod_{l=1}^{n_{i,j}^{(r)}}\exp\left(\dfrac{y_{i,j}^{(r)}(l)}{\sigma^{(r)}}\right)\right)\exp\left(-\exp\left(\dfrac{c_i-\mu_i^{(r)}}{\sigma^{(r)}}\right)\right) & , n_{i,j}^{(r)} \geq 1 \\ \exp\left(-\exp\left(\dfrac{c_i-\mu_i^{(r)}}{\sigma^{(r)}}\right)\right) & , n_{i,j}^{(r)} = 0 \end{cases}$$

The log-likelihood $l_{i,j}^{(r)}(\boldsymbol{\theta}_i^{(r)})$ is thus

$$l_{i,j}^{(r)}(\boldsymbol{\theta}; n_{i,j}^{(r)}, y_{i,j}^{(r)}(1), y_{i,j}^{(r)}(2), \cdots, y_{i,j}^{(r)}(n_{i,j}^{(r)}))$$
$$= \sum_{l=1}^{n_{i,j}^{(r)}}\left(\log\frac{1}{\sigma^{(r)}} + \frac{y_{i,j}^{(r)}(l) - (\gamma_0^{(r)} + \gamma_1^{(r)}x_i)}{\sigma^{(r)}}\right) - \exp(\zeta_i)$$

where $\zeta_i = \dfrac{c_i - (\gamma_0^{(r)} + \gamma_1^{(r)} x_i)}{\sigma^{(r)}}$.

Let $A_{i,j}^{(r)}(l) = -\log\sigma^{(r)} + (\sigma^{(r)})^{-1}(y_{i,j}^{(r)}(l) - (\gamma_0^{(r)} + \gamma_1^{(r)} x_i))$ and $B_i^{(r)} = \exp(\zeta_i)$, we then have

$$\frac{\partial^2 A_{i,j}^{(r)}(l)}{\partial\boldsymbol{\theta}_i \partial\boldsymbol{\theta}_i'} = \frac{1}{(\sigma^{(r)})^2}\begin{bmatrix} 0 & 0 & 1 \\ & 0 & x_i \\ & & 1 + 2(\sigma^{(r)})^{-1}(y_{i,j}^{(r)}(l) - (\gamma_0^{(r)} + \gamma_1^{(r)} x_i)) \end{bmatrix}$$

$$= \frac{1}{(\sigma^{(r)})^2}\begin{bmatrix} 0 & 0 & 1 \\ & 0 & x_i \\ \text{symmetric} & & 1 + 2z_{i,j}^{(r)}(l) \end{bmatrix}$$

$$\frac{\partial^2 B_i^{(r)}}{\partial\boldsymbol{\theta}_i \partial\boldsymbol{\theta}_i'} = \frac{1}{(\sigma^{(r)})^2}\begin{bmatrix} \exp(\zeta_i) & x_i\exp(\zeta_i) & \zeta_i\exp(\zeta_i) + \exp(\zeta_i) \\ & x_i^2\exp(\zeta_i) & x_i\zeta_i\exp(\zeta_i) + x_i\exp(\zeta_i) \\ \text{symmetric} & & \zeta_i^2\exp(\zeta_i) + 2\zeta_i\exp(\zeta_i) \end{bmatrix}$$

where $z_{i,j}^{(r)}(l) = (\sigma^{(r)})^{-1}(y_{i,j}^{(r)}(l) - (\gamma_0^{(r)} + \gamma_1^{(r)} x_i))$, and it is the *only* quantity that is a function of the logarithm failure time *y*. Hence, the information $I_{i,j}^{(r)}(\boldsymbol{\theta}^{(r)} \,|\, n_{i,j}^{(r)})$ conditioning on the number of failures $n_{i,j}^{(r)}$ is

$$I_{i,j}^{(r)}(\boldsymbol{\theta}^{(r)} \,|\, n_{i,j}^{(r)}) = E\left[-\frac{\partial^2\left(l_{i,j}^{(r)}(\boldsymbol{\theta} \,|\, n_{i,j}^{(r)})\right)}{\partial\boldsymbol{\theta}_i \partial\boldsymbol{\theta}_i'}\right]$$

$$= \frac{-1}{(\sigma^{(r)})^2}\left[\begin{bmatrix} 0 & 0 & n_{i,j}^{(r)} \\ & 0 & n_{i,j}^{(r)} x_i \\ \text{symmetric} & & n_{i,j}^{(r)} + 2\sum_{l=1}^{n_{i,j}^{(r)}} E(z_{i,j}^{(r)}(l)) \end{bmatrix} - \frac{\partial^2 B_i^{(r)}}{\partial\boldsymbol{\theta}_i \partial\boldsymbol{\theta}_i'}\right]$$

To derive the closed-form expression of the expectation $E(z_{i,j}^{(r)}(l))$ of $z_{i,j}^{(r)}(l)$, we need the Theorem 26 presented in Rigdon and Basu (2000) on page 59. The theorem states that, if a *PLP* is observed until time t, then, conditioning on the number of failures n, the random failure times $t_1 < t_2 < \cdots < t_n$ are distributed as *n order statistics* from the distribution with Cdf, $F(x) = \Lambda(x)/\Lambda(t) = (x/t)^{\beta}$ for $0 < x \le t$.

Hence, conditioning on the number of failures $n_{i,j}^{(r)}$, the pdf of the l^{th} failure time of system j at stress i with respect to risk r can be derived as,

$$f(t_{i,j}^{(r)}(l)) = \frac{\Gamma(n_{i,j}^{(r)}+1)}{\Gamma(l)\Gamma(n_{i,j}^{(r)}-l+1)}\left[\left(\frac{t_{i,j}^{(r)}(l)}{T_i}\right)^{\frac{1}{\sigma^{(r)}}}\right]^{l-1}\left[1-\left(\frac{t_{i,j}^{(r)}(l)}{T_i}\right)^{\frac{1}{\sigma^{(r)}}}\right]^{n_{i,j}^{(r)}-l}\frac{1}{\sigma^{(r)}T_i}\left(\frac{t_{i,j}^{(r)}(l)}{T_i}\right)^{\frac{1}{\sigma^{(r)}}-1}$$

where Γ is the Gamma function. Making the change of variable $t=\exp(y)$, we have

$$f(y_{i,j}^{(r)}(l)) = \frac{\Gamma(n_{i,j}^{(r)}+1)}{\Gamma(l)\Gamma(n_{i,j}^{(r)}-l+1)}\cdot\frac{1}{\sigma^{(r)}}\cdot\left[\exp\left(\frac{y_{i,j}^{(r)}(l)-c_i}{\sigma^{(r)}}\right)\right]^{l}\left[1-\exp\left(\frac{y_{i,j}^{(r)}(l)-c_i}{\sigma^{(r)}}\right)\right]^{n_{i,j}^{(r)}-l}$$

and the $E(z_{i,j}^{(r)}(l))$ is evaluated by

$$E(z_{i,j}^{(r)}(l)) = \int_{-\infty}^{c_i}\frac{y_{i,j}^{(r)}(l)-(\gamma_0^{(r)}+\gamma_1^{(r)}x_i)}{\sigma^{(r)}}\cdot f(y_{i,j}^{(r)}(l))dy_{i,j}^{(r)}(l)$$

Let $\kappa_{i,j}^{(r)}(l)=\exp((y_{i,j}^{(r)}(l)-c_i)/\sigma^{(r)})$, $a=l$, and $b=n-a+1$, we obtain,

$$\begin{aligned}E(z_{i,j}^{(r)}(l)) &= \int_0^1 \log(\kappa_{i,j}^{(r)}(l))\cdot B^{-1}(a,b)\cdot(\kappa_{i,j}^{(r)}(l))^{a-1}\cdot(1-\kappa_{i,j}^{(r)}(l))^{b-1}d\kappa_{i,j}^{(r)}(l)\\ &\quad+\zeta_i\cdot\int_0^1 B^{-1}(a,b)\cdot(\kappa_{i,j}^{(r)}(l))^{a-1}\cdot(1-\kappa_{i,j}^{(r)}(l))^{b-1}d\kappa_{i,j}^{(r)}(l)\\ &= (\psi(a)-\psi(a+b))+\zeta_i\end{aligned}$$

where ψ is the Digamma function defined as $\psi(x)=\partial\log\Gamma(x)/\partial x$; and $B(a,b)$ is the Beta function defined as $\Gamma(a)\Gamma(b)/\Gamma(a+b)$. Note that

$$B^{-1}(a,b)\cdot(\kappa_{i,j}^{(r)}(l))^{a-1}\cdot(1-\kappa_{i,j}^{(r)}(l))^{b-1}$$

is exactly the pdf of the Beta distribution for random variable $0<\kappa_{i,j}^{(r)}(l)<1$.

Averaging over $n_{i,j}^{(r)}$, the expected Fisher information $I_{i,j}^{(r)}$ is obtained as

$$I_{i,j}^{(r)} = \sum_{n_{i,j}^{(r)}=0}^{\infty} I_{i,j}^{(r)}(\boldsymbol{\theta}^{(r)}\,|\,n_{i,j}^{(r)})\cdot p(n_{i,j}^{(r)})$$

where $p(\cdot)$ is the probability of observing $n_{i,j}^{(r)}$ failures from system j at stress i with respect to risk r. Here, the random variable $n_{i,j}^{(r)}$ has a Poisson distribution with mean $(T_i/\alpha_i^{(r)})^{\beta^{(r)}}$ (see Rigdon and Basu 2000, pp.136),

$$p(n_{i,j}^{(r)}) = \frac{[(T_i/\alpha_i^{(r)})^{\beta^{(r)}}]^{n_{i,j}^{(r)}} \exp[-(T_i/\alpha_i^{(r)})^{\beta^{(r)}}]}{n_{i,j}^{(r)}!}, \quad n_{i,j}^{(r)} = 0,1,2,...$$

9.4. The Prior Distribution

Prior elicitation is an important issue in planning an ALT using Bayesian approaches. Very often, prior distributions are constructed either from historical data of previous test (e.g. Clyde et al. 1996) or from subjective opinion based on empirical engineering knowledge (e.g. Kadane 1996). In this chapter, available prior information on the unknown ALT model parameters $\boldsymbol{\theta} = (\boldsymbol{\theta}^{(1)}, \boldsymbol{\theta}^{(2)}, ..., \boldsymbol{\theta}^{(k)})$ is quantified in terms of joint prior distributions of $\boldsymbol{\theta}^{(r)} = (\gamma_0^{(r)}, \gamma_1^{(r)}, \sigma^{(r)})$ for $r = 1, 2, ..., k$.

The slope $\gamma_1^{(r)}$ parameter is associated to particular acceleration mechanism. Useful information on $\gamma_1^{(r)}$ is usually obtainable from preliminary testing, engineering experience, physical knowledge about the system, or engineering handbooks such as MIL-HDBK-217E. In this chapter, a lognormal prior distribution $m^{(r)} = m(\gamma_1^{(r)})$ for $\gamma_1^{(r)}$ is used as in reference Zhang and Meeker (2006).

The interpretation of $\sigma^{(r)}$ is clear as it measures the reliability improvement or deterioration of the system. In this chapter, a lognormal prior distribution $g^{(r)} = g(\sigma^{(r)})$ for $\sigma^{(r)}$ is used as in reference Zhang and Meeker (2006).

As the interpretation of $\gamma_0^{(r)}$ is less clear, the prior of $\gamma_0^{(r)}$ is obtained in an indirect way by specifying a prior distribution of the cumulative mean number of failures $\Lambda_0^{(r)}$ in a given time interval $(0, t]$ at use stress level x_0 . Suppose $\mu_{\Lambda_0^{(r)}}$ and $\sigma^2_{\Lambda_0^{(r)}}$ respectively denote the mean and variance of $\Lambda_0^{(r)}$ based on our

prior knowledge, Guida et al. (1989) suggests a Gamma prior distribution for the quantity $\Lambda_0^{(r)}$ as follows

$$h^{(r)} = h(\Lambda_0^{(r)}) = \frac{b^a}{\Gamma(a)}\left(\Lambda_0^{(r)}\right)^{a-1}\exp(-b\Lambda_0^{(r)}), \quad \Lambda_0^{(r)} > 0$$

where (9.13)

$$a = \mu^2_{\Lambda_0^{(r)}} \Big/ \sigma^2_{\Lambda_0^{(r)}} \quad , \quad b = \mu_{\Lambda_0^{(r)}} \Big/ \sigma_{\Lambda_0^{(r)}}$$

Then, assume that the prior information on $\Lambda_0^{(r)}$, $\gamma_1^{(r)}$ and $\sigma^{(r)}$ are independent, we obtain the joint density of $(\gamma_0^{(r)}, \gamma_1^{(r)}, \sigma^{(r)})$ by making the change of variable $\Lambda_0^{(r)} = \exp[(\sigma^{(r)})^{-1}(c - \gamma_0^{(r)} - \gamma_1^{(r)})]$

$$\begin{aligned} w^{(r)} &= w(\gamma_0^{(r)}, \gamma_1^{(r)}, \sigma^{(r)}) \\ &= -m^{(r)} \cdot g^{(r)} \cdot \frac{\partial \exp[(\sigma^{(r)})^{-1}(c - \gamma_0^{(r)} - \gamma_1^{(r)})]}{\partial \gamma_0^{(r)}} h(\exp[(\sigma^{(r)})^{-1}(c - \gamma_0^{(r)} - \gamma_1^{(r)})]) \\ &= m^{(r)} \cdot g^{(r)} \cdot \frac{b^a}{\sigma^{(r)} \cdot \Gamma(a)} \cdot \exp\left(a \cdot \frac{c - \gamma_0^{(r)} - \gamma_1^{(r)}}{\sigma^{(r)}} - b \cdot \exp\left(\frac{c - \gamma_0^{(r)} - \gamma_1^{(r)}}{\sigma^{(r)}} \right) \right) \end{aligned}$$

(9.14)

Finally, since different risks are assumed to be *s*-independent in this chapter, the joint prior distribution of $\boldsymbol{\theta} = (\boldsymbol{\theta}^{(1)}, \boldsymbol{\theta}^{(2)}, ..., \boldsymbol{\theta}^{(k)})$ is $\vartheta(\boldsymbol{\theta}) = \prod_{r=1}^{k} w^{(r)}$.

9.5. The Bayesian Planning Problem

The planning of an ALT involves choosing both the optimum stress combinations and sample allocations. Specifically, the testing (experiment) region here is between the use stress $x_0 = 1$ and the highest stress $x_m = 0$, and the plan $\boldsymbol{\xi}$ must choose a $(m-1)$-tuple $\mathbf{X} = (x_1, x_2, ..., x_{m-1})$ that determines on which stresses the test is to be conducted, as well as another $(m-1)$-tuple $\boldsymbol{\Pi} = (\pi_1, \pi_2, ..., \pi_{m-1})$ that specifies the proportion of samples (i.e. $\sum_{i=1}^{m} \pi_i = 1$) to be allocated to each stress x_i for $i = 1, 2, ..., m$.

In the context of Bayesian design, the optimum ALT plan ξ^* is the one that maximizes the pre-defined utility function $U(\xi)$. In the literature, different goals of ALT can motivate different choices of utility functions $U(\xi)$. This is in line with Lindley's arguments that "a good way to design experiments is to specify a utility function reflecting the purpose of the experiment, to regard the design choice as a decision problem and to select a design that maximizes the expected utility (Chaloner and Verdinelli, 1995)". In general, there will be no plan ξ which is uniformly best, i.e., which maximizes the utility function $U(\xi)$ regardless of the formulation of $U(\xi)$ (Pilz, 1991).

9.5.1. The Planning Criterion

9.5.1.1. The Choice of Utility Function

In the context of Bayesian design, the optimum ALT plan ξ^* maximizes a pre-defined utility function $U(\xi)$. If we adopt the idea of Zellner (1988) and view the inference as information processing involving input information and output information, the optimum ALT plan is the one that maximizes the pre-posterior expectation of the Kullback-Leibler distance between the posterior $\pi(\boldsymbol{\theta}|\mathbf{t},\xi)$ and prior distribution $\vartheta(\boldsymbol{\theta})$ over the marginal distribution of (unobserved) testing data $\mathbf{t}$

$$U(\xi)=\int\left\{\int \log\frac{\pi(\boldsymbol{\theta}|\mathbf{t},\xi)}{\vartheta(\boldsymbol{\theta})}\cdot\pi(\boldsymbol{\theta}|\mathbf{t},\xi)d\boldsymbol{\theta}\right\}p(\mathbf{t}|\xi)d\mathbf{t}$$

Or equivalently, the expected gain in Shannon information

$$U(\xi)=\int\int \log\pi(\boldsymbol{\theta}|\mathbf{t},\xi)\cdot p(\mathbf{t},\boldsymbol{\theta}|\xi)d\boldsymbol{\theta}d\mathbf{t} \qquad (9.15)$$

In general, there will be no plan ξ which is uniformly best, i.e., which maximizes the utility function $U(\xi)$ regardless of the formulation of $U(\xi)$. In practice, different goals of ALT can motivate different choices of utility functions $U(\xi)$, which is in line with Lindley's arguments that "a good way to design experiments is to specify a utility function reflecting the purpose of the experiment, to regard the design choice as a decision problem and to select a design that maximizes the expected utility (Chaloner and Verdinelli 1995)". The recent work of Pascual (2008) also embodies this idea of choosing planning criteria.

9.5.1.2. The Evaluation of Expected Utility

The estimation of the exact expected utility in (9.15) can be done using the Markov chain Monte Carlo (MCMC) method introduced in Muller and Parmigiani (1996). In practice, however, such estimation can be computationally intractable. Hence, the approximation of the expected utility that provides an easy-to-interpret simplification to the planning problem is particularly important for industrial applications.

Several normal approximations are available for the utility $U(\xi)$ presented in (9.15), see Berger (1985), pp. 224, and also see Kass and Slate (1994) for some diagnostics of the posterior normality. In this chapter, we let $\tilde{\boldsymbol{\theta}}$ denote the posterior mode, i.e. the generalized MLE (Berger 1985, pp.133), of the parameter $\boldsymbol{\theta}$, and approximate the posterior distribution $\pi(\boldsymbol{\theta})$ by a normal distribution $N\left(\tilde{\boldsymbol{\theta}}, (\mathbf{I}(\tilde{\boldsymbol{\theta}};\xi))^{-1}\right)$. Then, the utility $U(\xi)$ presented in (9.15) is approximated by

$$U(\xi) \approx -\frac{3k}{2}\log(2\pi) - \frac{3k}{2} + \frac{1}{2}\int \log\det(\mathbf{I}(\boldsymbol{\theta};\xi)) \cdot \vartheta(\boldsymbol{\theta})\, d\boldsymbol{\theta} \qquad (9.16)$$

Dropping those constant terms, we obtain the Bayesian *D*-optimality criterion that maximizes

$$\phi_1(\xi) \approx \int \log\det(\mathbf{I}(\boldsymbol{\theta};\xi)) \cdot \vartheta(\boldsymbol{\theta})\, d\boldsymbol{\theta} \tag{9.17}$$

The Bayesian *D*-optimality criterion minimizes the expected generalized variance of $\hat{\boldsymbol{\theta}}$ over the marginal distribution of (unobserved) testing data $\mathbf{t}$ which makes it is an appropriate criterion for estimating the unknown model parameter $\boldsymbol{\theta}$. It is also noted that the *D*-optimum plan is invariant under nonsingular transformation of parameters. Interested readers might refer to Atkinson and Donev (1992) for the eight important properties of *D*-optimum designs.

In some cases, we note that experimenters are only interested in a subset of $\boldsymbol{\theta}$ and treat others as nuisance parameters. This arises when the nuisance parameters are important for modeling purposes, but they are not of primary interest. Then, D_s -optimality criterion can be used in place of the *D*-optimality criterion. Re-parameterize and partition $\boldsymbol{\theta}$ so that we are interested in the first part $\boldsymbol{\theta}_1$ of $\boldsymbol{\theta} = [\boldsymbol{\theta}_1, \boldsymbol{\theta}_2]$. Then, the information matrix given in equation (9.11) can be partitioned as

$$\mathbf{I}(\boldsymbol{\theta};\xi) = \begin{bmatrix} \mathbf{I}(\boldsymbol{\theta}_1;\xi) & 0 \\ 0 & \mathbf{I}(\boldsymbol{\theta}_2;\xi) \end{bmatrix} \tag{9.18}$$

In order to estimate $\boldsymbol{\theta}_1$ as precisely as possible, i.e., to minimize the generalized variance of $\hat{\boldsymbol{\theta}}_1$, D_s -optimality leads to maximizing the following planning criterion

$$\phi_2(\xi) \approx \int \frac{\det(\mathbf{I}(\boldsymbol{\theta};\xi))}{\det(\mathbf{I}(\boldsymbol{\theta}_2;\xi))} \cdot \vartheta(\boldsymbol{\theta})\, d\boldsymbol{\theta} \tag{9.19}$$

Numerical methods are needed to obtain optimum ALT plans by maximizing (9.17) and (9.19).

9.5.2. The General Equivalence Theorem

In order to verify the global optimality of the developed ALT plans, the general equivalence theorem (GET) introduced by Whittle (1973), which has been widely used (e.g. Pascual 2008, Chaloner and Larntz 1992, and Zhang and Meeker 2006), can be applied.

Whittle (1973) proved the GET in the context of linear design, and Chaloner and Larntz (1989) applied it to Bayesian design. Let ξ be a probability measure on the testing region $X = [0,1]$, and our planning problem is to find such a measure ξ that maximizes $\phi_1(\xi)$ or $\phi_2(\xi)$. Here, both $\phi_1(\xi)$ and $\phi_2(\xi)$ are concave directly following the results given in Firth and Hinde (1997).

Further define the Frechet derivative of the criterion $\phi(\xi)$ at ξ in the direction of ξ_x as follows

$$d(\xi, x) = \lim_{\varepsilon \downarrow 0} \left(\varepsilon^{-1} \left[\phi\{(1-\varepsilon)\xi + \varepsilon \xi_x\} - \phi(\xi) \right] \right)$$

Then, the following equivalence theorem gives the conditions for the plan ξ^* to be globally optimal.

Theorem (Whittle 1973): If $\phi(\xi)$ is concave, an optimal design ξ^* can be equivalently characterized by any of the three conditions:

(a) ξ^* maximizes $\phi(\xi)$; (b) ξ^* minimizes $\sup_{x \in X} d(\xi, x)$; (c) $\sup_{x \in X} d(\xi^*, x) = 0$.

Hence, we have

Theorem 9.1: If $\phi_1(\xi)$ is concave, then, $\phi_1(\xi^*)$ is the global maximum iff

$$\sup_{0 \le x \le 1} \left\{ -\dim(\boldsymbol{\theta}) + \int \operatorname{tr}\left(\mathbf{I}(\boldsymbol{\theta}; \xi_x)(\mathbf{I}(\boldsymbol{\theta}; \xi^*))^{-1} \right) \cdot \vartheta(\boldsymbol{\theta}) \, d\boldsymbol{\theta} \right\} = 0 \qquad (9.20)$$

Theorem 9.2: If $\phi_2(\xi)$ is concave, then, $\phi_2(\xi^*)$ is the global maximum iff

$$\sup_{0\le x\le 1}\left\{-\dim(\boldsymbol{\theta}_1)+\int\left\{\mathrm{tr}\left(\mathbf{I}(\boldsymbol{\theta};\xi_x)(\mathbf{I}(\boldsymbol{\theta};\xi^*))^{-1}\right)-\mathrm{tr}\left(\mathbf{I}(\boldsymbol{\theta}_2;\xi_x)(\mathbf{I}(\boldsymbol{\theta}_2;\xi^*))^{-1}\right)\right\}\cdot\vartheta(\boldsymbol{\theta})\,d\boldsymbol{\theta}\right\}=0 \tag{9.21}$$

9.6. A Numerical Case Study

In this section, we present a numerical example to illustrate the application of the proposed Bayesian ALT planning methods. Both the statistically optimum two-stress plan and the compromise three-stress plan are developed.

9.6.1. Accelerated Life Test for Diesel Engine

We present a numerical case study to illustrate the application of the proposed Bayesian ALT planning methods. Consider a newly designed 6-cyliner $6.8\,\mathrm{dm}^3$ swept volume diesel automotive engine. To investigate the effects of the operation condition on engine reliability, an accelerated life test program was launched with 8 engine prototypes. During the test, engineers mounted each engine to a truck, and run these trucks for 150,000km at different stress levels x which consist of elaborately designed combinations of speed, load, and road conditions. For example, $x=0$ if the truck runs on a mountain track at full load; $x=0.75$ if the truck runs on a circuit track at maximum speed; and of course, $x=1$ if the truck runs at pre-defined use speed, load, and road conditions. In what follows, we shall assume x to be continuous between 0 and 1 without explicitly mentioning the relationships between x and the combination of speed, load, and road conditions.

For a clear illustration, we assume that only two types of s-independent failure modes, denoted as the type-I and type-II failure, were monitored in the test. Upon failure, the kilometer-to-failure was recorded, and the engine was repaired immediately. For each failure mode, the failure process at any stress is modeled by PLP with the scale parameter which is a log-linear function of the stress x as in equation (9.8); and the shape parameter is a constant independent of stress.

9.6.2. Prior Specification

To plan an ALT for the diesel engine, prior distributions for the unknown model parameters $\boldsymbol{\theta}^{(r)} = (\gamma_0^{(r)}, \gamma_1^{(r)}, \sigma^{(r)})$ for $r = 1, 2$ must be elicited as discussed in 9.4. Here, previous experience with the failure mechanisms suggests that the slope parameter $\gamma_1^{(1)}$ and $\gamma_1^{(2)}$ for the type-I and type-II failure mode is near 1 and 1.5, respectively. Hence, a lognormal distribution $m^{(1)} = m(\gamma_1^{(1)})$ is used as the prior distribution for $\gamma_1^{(1)}$, with mean -0.013 and standard deviation chosen such that a central 95% probability interval for $\gamma_1^{(1)}$ is approximately between 0.7 and 1.3

$$m^{(1)} = m(\gamma_1^{(1)}) = \frac{1}{0.15\gamma_1^{(1)}} \phi_{\text{nor}} \left[\frac{\log(\gamma_1^{(1)}) - (-0.013)}{0.15} \right]$$

Similarly, a lognormal distribution $m^{(2)} = m(\gamma_1^{(2)})$ is used as the prior distribution for $\gamma_1^{(2)}$, with mean 0.400 and standard deviation chosen such that a central 95% probability interval for $\gamma_1^{(2)}$ is approximately between 1 and 2

$$m^{(2)} = m(\gamma_1^{(2)}) = \frac{1}{0.15\gamma_1^{(2)}} \phi_{\text{nor}} \left[\frac{\log(\gamma_1^{(2)}) - 0.4}{0.15} \right]$$

The pdf of both $m^{(1)}$ and $m^{(2)}$ are graphed in Figure 9.1.

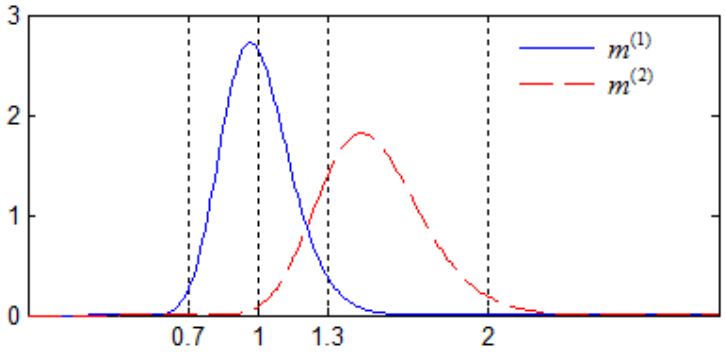

Figure 9.1 Prior distributions of $m^{(1)}$ and $m^{(2)}$

In practice, the lack of precise information about the shape parameter $\beta^{(r)}$ usually motives the use of a moderately informative prior distribution $g^{(r)}$, see example Rigdon and Basu (2000) and Zhang and Meeker (2006). In this case study, the failure intensity of the diesel engine is thought to be increasing with time, i.e. the shape parameter $\beta^{(r)}$ is most likely to be greater than 1 for both failure modes.

Hence, a lognormal distribution $g^{(1)} = g(\sigma^{(1)})$ of $\sigma^{(1)} = 1/\beta^{(1)}$ for the type-I failure mode is used, with mean $E(\sigma^{(1)}) = -0.85$ and the standard deviation chosen such that a central 95% probability interval for $\sigma^{(1)}$ is approximately between 0.35 and 0.50.

$$g^{(1)} = g(\sigma^{(1)}) = \frac{1}{0.1\sigma^{(1)}}\phi_{\text{nor}}\left[\frac{\log(\sigma^{(1)}) - (-0.85)}{0.1}\right]$$

Similarly, a lognormal distribution $g^{(2)} = g(\sigma^{(2)})$ of $\sigma^{(2)}$ for the type-II failure mode is used with mean $E(\sigma^{(2)}) = -0.70$, and the standard deviation chosen such that a central 95% probability interval for $\sigma^{(2)}$ is approximately between 0.40 and 0.60.

$$g^{(2)} = g(\sigma^{(2)}) = \frac{1}{0.1\sigma^{(2)}}\phi_{\text{nor}}\left[\frac{\log(\sigma^{(2)}) - (-0.70)}{0.1}\right]$$

The pdf of both $g^{(1)}$ and $g^{(2)}$ are graphed in Figure 9.2.

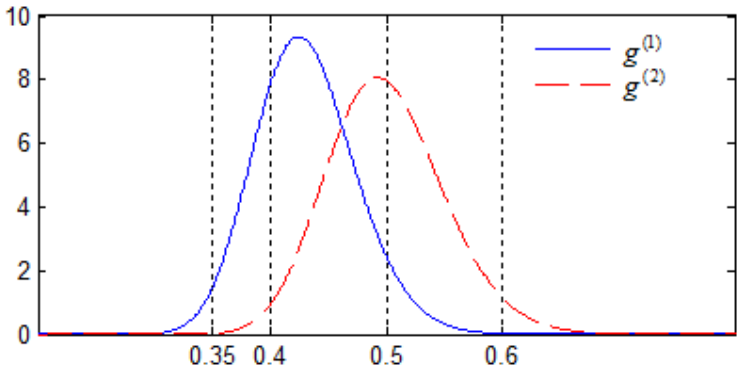

Figure 9.2 Prior distributions of $g^{(1)}$ and $g^{(2)}$

As discussed in Section 9.4, the prior of $\gamma_0^{(r)}$ is usually obtained in an indirect way by specifying a prior of the cumulative mean number of failures $\Lambda^{(r)}$ within 10^6 km at use stress $x=1$. Suppose $\mu_{\Lambda^{(1)}}=80$ and $\sigma^2_{\Lambda^{(1)}}=10$ are respectively chosen as the mean and variance of $\Lambda^{(1)}$, and $\mu_{\Lambda^{(2)}}=100$ and $\sigma^2_{\Lambda^{(2)}}=10$ are respectively chosen as the mean and variance of $\Lambda^{(2)}$, the joint density of $\boldsymbol{\theta}^{(r)}=(\gamma_0^{(r)},\gamma_1^{(r)},\sigma^{(r)})$ for $r=1,2$ is obtained from equation (9.14),

$$
\begin{aligned}
w^{(1)} &= w(\gamma_0^{(1)},\gamma_1^{(1)},\sigma^{(1)}) \\
&= m^{(1)}\cdot g^{(1)}\cdot\frac{8^{640}}{\sigma^{(1)}\cdot\Gamma(640)}\cdot\exp\left(640\cdot\frac{c-\gamma_0^{(1)}-\gamma_1^{(1)}}{\sigma^{(1)}}-8\cdot\exp\left(\frac{c-\gamma_0^{(1)}-\gamma_1^{(1)}}{\sigma^{(1)}}\right)\right) \\
w^{(2)} &= w(\gamma_0^{(2)},\gamma_1^{(2)},\sigma^{(2)}) \\
&= m^{(2)}\cdot g^{(2)}\cdot\frac{10^{1000}}{\sigma^{(2)}\cdot\Gamma(10^3)}\cdot\exp\left(10^3\cdot\frac{c-\gamma_0^{(2)}-\gamma_1^{(2)}}{\sigma^{(2)}}-10\cdot\exp\left(\frac{c-\gamma_0^{(2)}-\gamma_1^{(2)}}{\sigma^{(2)}}\right)\right)
\end{aligned}
$$

where $c=\log(15\times10^4)$ is the censoring kilometer in log-scale.

9.6.3. Numerical Search for a Two-Stress Optimum Plan

If all model parameters contained in $\boldsymbol{\theta}$ are of interest, maximizing (9.17) yields the optimum two-stress ALT plan $\boldsymbol{\xi}^*$ for the diesel engine test. The planning space

is x_i and π_i for $i = 1, 2$, with constraints $0 \le x_i, \pi_i \le 1$, and $\sum_{i=1}^{2} \pi_i = 1$. Specifically, since the highest stress level $x_2 = 0$ has been fixed, we are searching on a 2-dimension space for the optimum level of the low stress x_1 and the proportion of sample π_1 allocated to x_1. Figure 9.3 shows the contour plot of $\phi_1(\xi)$ with respect to x_1 and π_1. The cross of the dashed lines indicates the position of the optimum point $x_1^* = 0.81$ and $\pi_1^* = 0.33$ that yields the maximum $\phi_1(\xi^*) = 34.4652$.

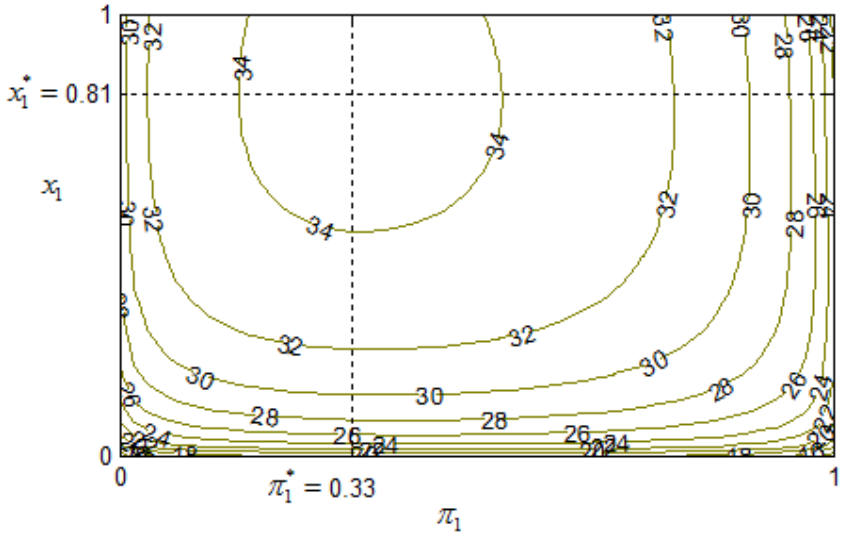

Figure 9.3 Contour plot of the numerical search for two-stress optimum ALT plan

In fact, the two-stress optimum ALT plan yields the maximum $\phi_1(\xi)$ over all possible test designs. That is, any *m*-stress plans for $m > 2$ eventually degenerates to a two-stress plan to yield the maximum $\phi_1(\xi)$. This global optimality of the developed two-stress plan ξ^* can be verified by the general equivalence theorem (GET) introduced in Section 9.5. Figure 9.4 plots the directional derivative $d(\xi^*, x)$ as a function

of $x \in [0,1]$. It is immediately seen that $\sup d(\xi^*, x) = 0$ for $x \in [0,1]$, indicating the plan ξ^* that allocates $\pi_1^* = 0.33$ proportion of sample to the low stress $x_1^* = 0.81$ is globally optimum.

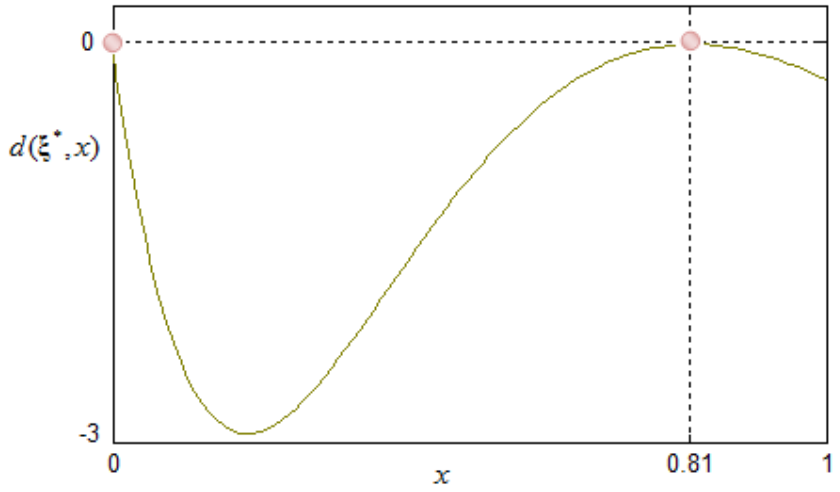

Figure 9.4 The plot of the directional derivative $d(\xi^*, x)$ as a function of $x \in [0,1]$

Similarly, if only $\boldsymbol{\theta}^{(1)} = (\gamma_0^{(1)}, \gamma_1^{(1)}, \sigma^{(1)})$ or $\boldsymbol{\theta}^{(2)} = (\gamma_0^{(2)}, \gamma_1^{(2)}, \sigma^{(2)})$ is of interest, maximizing the criterion (9.19) with respect to x_1 and π_1 develop the optimum ALT plan. Figure 9.5 shows the contour plots of $\phi_2(\xi)$ with respect to x_1 and π_1 when $\boldsymbol{\theta}^{(1)}$ and $\boldsymbol{\theta}^{(2)}$ is of interest, respectively.

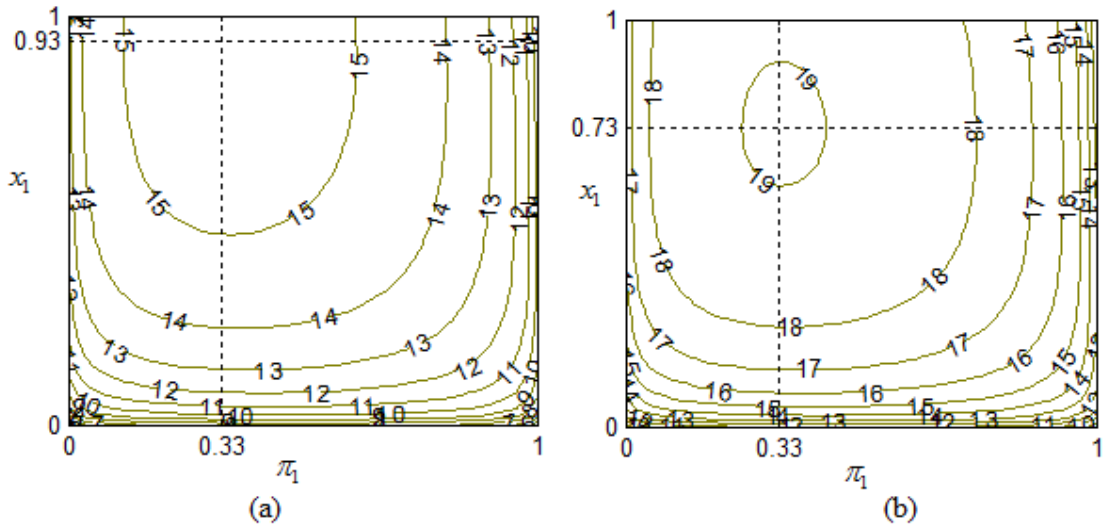

Figure 9.5 Contour plot of the numerical search for two-stress optimum ALT plan

(a) When $\boldsymbol{\theta}^{(1)}$ is of interest; (b) When $\boldsymbol{\theta}^{(2)}$ is of interest

As summarized in Table 9.2, if the test is conducted to estimate $\boldsymbol{\theta}^{(1)}$, the optimum plan $\boldsymbol{\xi}^*$ allocates $\pi_1^* = 0.33$ proportion of sample to the low stress $x_1^* = 0.93$; if the test is conducted to estimate $\boldsymbol{\theta}^{(2)}$, the optimum plan $\boldsymbol{\xi}^*$ allocates $\pi_1^* = 0.33$ proportion of sample to the low stress $x_1^* = 0.73$.

Table 9.2 Optimum two-Stress ALT plans for the diesel engine test

(Sample size $N = 8$, Censoring distance $T = 15 \times 10^4$ km)

Criterion		(x_1, π_1)	Expected No. of Type-I Failures Per System		Expected No. of Type-II Failures Per System		$U(\boldsymbol{\xi}^*)$	$\phi(\boldsymbol{\xi}^*)$
			x_1	x_2	x_1	x_2		
$\phi_1(\boldsymbol{\xi})$		(0.81, 0.33)	1.5	10.0	4.0	45.2	8.7190	34.4652
$\phi_2(\boldsymbol{\xi})$	Type-I Failure	(0.93, 0.33)	1.2	10.0	2.8	45.2	3.4662	15.4460
	Type-II Failure	(0.73, 0.33)	1.8	10.0	5.1	45.2	5.2690	19.0517

Figure 9.6 plots the directional derivative $d(\xi^*, x)$ as a function of $x \in [0,1]$ for both plans. It is seen that $\sup d(\xi^*, x) = 0$ for $x \in [0,1]$, indicating the global optimality of both plans.

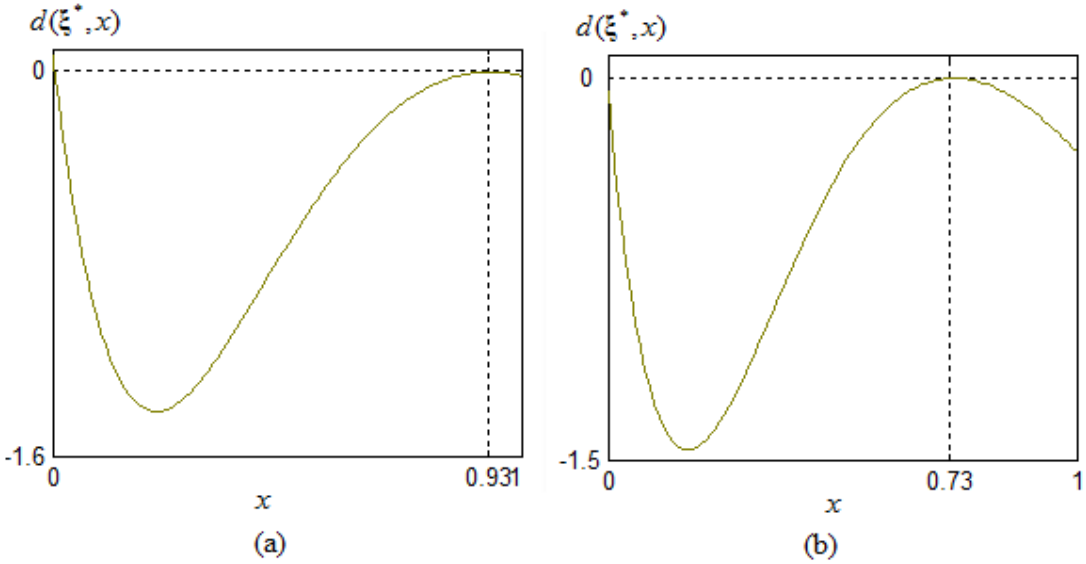

Figure 9.6 Plot of the directional derivative $d(\xi^*, x)$ as a function of $x \in [0,1]$

(a) When $\boldsymbol{\theta}^{(1)}$ is of interest; (b) When $\boldsymbol{\theta}^{(2)}$ is of interest

9.6.4. Numerical Search for Three-Stress Compromise Plan

In practice, the two-stress optimum ALT plan is not robust to misspecification of model parameters and assumptions. It is more often used as a bench mark of the testing plan, unless the model, pre-specified parameters, and testing data are all valid (see Nelson 1990, pp. 341 for detailed discussions).

It is well-known that the assumption of linear stress-life relationship cannot be validated with a two-stress plan. To avoid this drawback, a third (middle) testing stress is added. Since the two-stress ALT is globally optimal as we had discussed above,

adding the third testing stress reduces the statistical efficiency of the plan, and the developed three-stress ALT plan is therefore called the compromise plan.

To keep the three-stress compromise plan from degenerating to a two-stress optimum plan, we let $\pi_2 = 0.25$, i.e. 2 units are allocated to the middle level. In addition, since the middle stress level is added mainly to check the linearity of the stress-life model, we also let the middle stress be halfway between the low and high stress, i.e. we have $x_2 = x_1/2$. Then, maximizing (9.17) and (9.19) respectively, the compromise plans are obtained as summarized in Table 9.3.

Table 9.3 Compromise three-stress ALT plans for the diesel engine test

Criterion		(x_1, x_2, π_1)	Expected No. of Type-I Failures Per System			Expected No. of Type-II Failures Per System			$U(\xi^*)$	$\phi(\xi^*)$
			x_1	x_2	x_3	x_1	x_2	x_3		
$\phi_1(\xi)$		(1, 0.5, 0.15)	0.9	3.1	10.0	2.3	10.1	45.2	8.6448	34.3168
$\phi_2(\xi)$	Type-I	(1, 0.5, 0.17)	0.9	3.1	10.0	2.3	10.1	45.2	3.3997	15.3130
	Type-II	(1, 0.5, 0.09)	0.9	3.1	10.0	2.3	10.1	45.2	5.2509	19.0155

(Sample size $N = 8$, Proportion of sample allocated to the middle stress $\pi_2 = 0.25$, Censoring distance $T = 150{,}000$ km)

In the next section, a discussion will be presented based on the key observations of numerical example.

9.6.5. Efficiency Loss of Compromise Plans

A good compromise plan has more practical advantages with acceptable loss of statistical efficiency. To investigate the efficiency loss of the developed three-stress diesel engine compromise plans, we define the relative *D*-efficiency of the compromise plan as below

$$\eta(\xi^*_{com}) = \exp\left(\left\{\phi(\xi^*_{com}) - \phi(\xi^*_{opt})\right\}\right) \tag{9.22}$$

where ξ^*_{com} denotes the developed three-stress compromise plan, and ξ^*_{opt} denotes the statistically optimum two-stress plan.

In addition, we also define the adjusted relative *D*-efficiency as shown in (9.23)

$$\eta_a(\xi^*_{com}) = \exp\left(\frac{1}{\rho}\cdot\left\{\phi(\xi^*_{com}) - \phi(\xi^*_{opt})\right\}\right) \tag{9.23}$$

where ρ equals the total number of parameters of interest so that the relative efficiency measure $\eta_a(\xi^*_{com})$ does not depend on the dimension of the problem. This definition can be directly derived from the *D*-efficiency of an arbitrary design defined in Atkinson and Donev (1992), pp. 116.

Table 9.4 shows the relative *D*-efficiency of the three diesel engine compromise ALT plan with respect to the corresponding statistical two-stress optimum plan. It is seen that, by sacrificing an acceptable amount of loss in statistical efficiency, we obtain the three-stress compromise plans which are more robust in practice.

Table 9.4 Efficiency loss of the three-stress compromise plan

Compromise Plans	$\phi(\xi^*_{com})$	$\phi(\xi^*_{opt})$	ρ	$\eta(\xi^*_{com})$	$\eta_a(\xi^*_{com})$
When $\boldsymbol{\theta}$ is of interest	34.3168	34.4652	6	0.8621	0.9756
When $\boldsymbol{\theta}^{(1)}$ is of interest	15.3130	15.4460	3	0.8755	0.9566
When $\boldsymbol{\theta}^{(2)}$ is of interest	19.0155	19.0517	3	0.9644	0.9880

9.6.6. Evaluation of ALT Plans

After an ALT plan is developed, Monte-Carlo simulation is an insightful tool to visualize the sampling uncertainty, e.g. Zhang and Meeker 2006, Meeker et al 2005. For the diesel engine ALT, we use simulation in this section to evaluate the compromise three-stress ALT plan when both failure modes are of interest, i.e. $\boldsymbol{\theta} = [\boldsymbol{\theta}^{(1)}, \boldsymbol{\theta}^{(2)}]$ is to be estimated. Other developed plans can be evaluated utilizing the same approach.

When $\phi_1(\boldsymbol{\xi})$ is the criterion, the expected information matrix $\mathbf{I}(\boldsymbol{\theta};\boldsymbol{\xi}^*)$ of the compromise three-stress ALT plan $\boldsymbol{\xi}^*$ developed in Table 9.3 is computed as

$$\mathbf{I}(\boldsymbol{\theta};\boldsymbol{\xi}^*) = \begin{bmatrix} \mathbf{I}(\boldsymbol{\theta}^{(1)};\boldsymbol{\xi}^*) & \\ & \mathbf{I}(\boldsymbol{\theta}^{(2)};\boldsymbol{\xi}^*) \end{bmatrix}$$

where

$$\mathbf{I}(\boldsymbol{\theta}^{(1)};\boldsymbol{\xi}) = \begin{bmatrix} 307.54 & 22.12 & 414.01 \\ & 13.70 & 19.10 \\ & & 1772.8 \end{bmatrix}, \quad \mathbf{I}(\boldsymbol{\theta}^{(2)};\boldsymbol{\xi}) = \begin{bmatrix} 993.43 & 49.34 & 2779.1 \\ & 29.17 & 100.52 \\ & & 14556 \end{bmatrix}$$

Hence, the large-sample approximate variance-covariance matrix for $\hat{\boldsymbol{\theta}}^{(1)}$ and $\hat{\boldsymbol{\theta}}^{(2)}$ is respectively the inverse of $\mathbf{I}(\boldsymbol{\theta}^{(1)};\boldsymbol{\xi})$ and $\mathbf{I}(\boldsymbol{\theta}^{(2)};\boldsymbol{\xi})$

$$\boldsymbol{\Sigma}_{\boldsymbol{\theta}^{(1)}} = \begin{bmatrix} 5.33 & -6.97 & -1.17 \\ & 83.23 & 0.73 \\ & & 0.83 \end{bmatrix} \times 10^{-3} \quad , \quad \boldsymbol{\Sigma}_{\boldsymbol{\theta}^{(2)}} = \begin{bmatrix} 2.32 & -2.46 & -0.43 \\ & 37.72 & 0.21 \\ & & 0.15 \end{bmatrix} \times 10^{-3}$$

(9.24)

Then, based on the developed compromise three-stress ALT plan, we simulate the failure times using the model parameters randomly sampled from the prior distribution $\vartheta(\boldsymbol{\theta})$, and obtain the generalized MLE (Berger 1985, pp. 133) $\hat{\boldsymbol{\theta}} = [\hat{\boldsymbol{\theta}}^{(1)}, \hat{\boldsymbol{\theta}}^{(2)}]$ using a non-informative prior distribution for $\boldsymbol{\theta}$. After 200 repetitions of the above process, Figure 9.7 plots the histograms for the estimates $\hat{\gamma}_0^{(1)}$, $\hat{\gamma}_1^{(1)}$, $\hat{\sigma}^{(1)}$, $\hat{\gamma}_0^{(2)}$, $\hat{\gamma}_1^{(2)}$ and $\hat{\sigma}^{(2)}$. It is seen that, the sample standard deviation of $\mathrm{SD}(\hat{\gamma}_0^{(1)})$, $\mathrm{SD}(\hat{\gamma}_1^{(1)})$, $\mathrm{SD}(\hat{\sigma}^{(1)})$, $\mathrm{SD}(\hat{\gamma}_0^{(2)})$, $\mathrm{SD}(\hat{\gamma}_1^{(2)})$, and $\mathrm{SD}(\hat{\sigma}^{(2)})$ respectively well agrees with the corresponding asymptotic standard error $\mathrm{Ase}(\hat{\gamma}_0^{(1)})$, $\mathrm{Ase}(\hat{\gamma}_1^{(1)})$, $\mathrm{Ase}(\hat{\sigma}^{(1)})$, $\mathrm{Ase}(\hat{\gamma}_0^{(2)})$, $\mathrm{Ase}(\hat{\gamma}_1^{(2)})$,and $\mathrm{Ase}(\hat{\sigma}^{(2)})$. Here, the asymptotic standard error is directly derived from the large-sample approximate variance-covariance matrix given in (9.24).

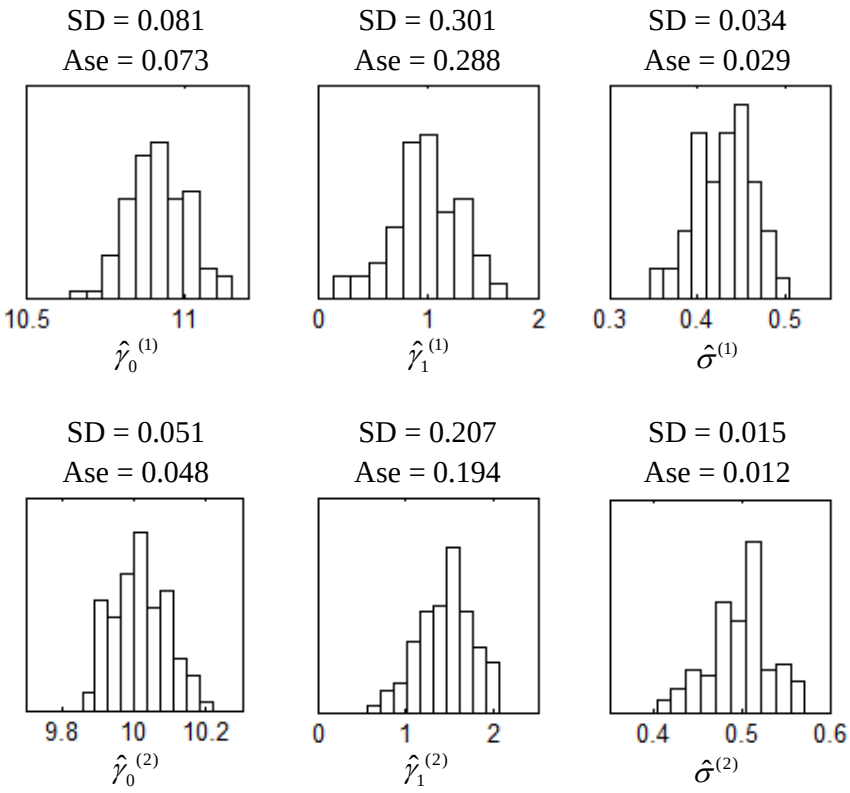

Figure 9.7 Simulation assessment of the plan

9.7. Analysis of Testing Data

Given testing data, posterior distribution of parameters of interest can be found using the Bayes' Rule (e.g. Singpurwalla 2006). When the sample size is moderately large, various normal approximations greatly simplifies the evaluation of posterior distribution and usually perform reasonably well in practice (Berger 1985, pp. 224).

However, only 8 engine prototypes are available in the diesel engine ALT example. In fact, this is not a trivial case in practice as the number of prototypes is usually small during product R&D phase. Recall what we have mentioned in the introduction, one

important reason to repair failed prototypes in a life test is due to lack of samples (see e.g. Guida and Giorgio 1995, Yun et al. 2006, and Guerin et al. 2004). Hence, in this section, we employ the Bayesian curve fitting method proposed in Muller and Parmigiani (1996) and Muller et al (1996) to evaluate of the posterior distribution, and particularly compare this method to the large-sample based normal approximation of posterior distribution. Several important reliability measures for repairable systems are estimated using both methods.

To clearly demonstrate the data analysis as well as the comparison study, suppose engineers are only interested in the parameter $\boldsymbol{\theta}^{(1)} = (\gamma_0^{(1)}, \gamma_1^{(1)}, \sigma^{(1)})$ of the type-I failure mode, and treat $\boldsymbol{\theta}^{(2)} = (\gamma_0^{(2)}, \gamma_1^{(2)}, \sigma^{(2)})$ as nuisance. Hence, based on the plan developed in Table 9.2, a two-stress ALT is conducted with 3 engines allocated to the low stress. The testing results are presented in Table 9.5.

Given the testing data, the posterior distribution $\pi(\boldsymbol{\theta}^{(1)})$ of $\boldsymbol{\theta}^{(1)}$ is

$$\pi(\boldsymbol{\theta}^{(1)} \left| \text{data}) \propto f(\boldsymbol{\theta}^{(1)}) \cdot l(\boldsymbol{\theta}^{(1)}; \text{data}) \right.$$

where $f(\boldsymbol{\theta}^{(1)})$ is the prior distribution $\boldsymbol{\theta}^{(1)}$ used for data analysis, and $l(\boldsymbol{\theta}^{(1)})$ is the likelihood of $\boldsymbol{\theta}^{(1)}$ given the testing data. Recall the planning criteria defined in (9.17) and (9.19), we therefore use a non-informative prior distribution $f(\boldsymbol{\theta}^{(1)})$ for $\boldsymbol{\theta}^{(1)}$ in analyzing the data.

In practice, the exact evaluation of $\pi(\boldsymbol{\theta}^{(1)})$ can be computational intractable. Hence, $\pi(\boldsymbol{\theta}^{(1)})$ is usually approximated using normal distribution as follows (Berger 1985, pp. 224)

$$\boldsymbol{\theta}^{(1)} \Big| \text{data} \sim N\left(\tilde{\boldsymbol{\theta}}^{(1)}, (\mathbf{I}(\tilde{\boldsymbol{\theta}}^{(1)}))^{-1}\right)$$

where $\tilde{\boldsymbol{\theta}}^{(1)}$ denote the MLE of $\boldsymbol{\theta}^{(1)}$, and $\mathbf{I}(\tilde{\boldsymbol{\theta}})$ is the information observed at $\tilde{\boldsymbol{\theta}}^{(1)}$.

Table 9.5 Kilometers to failure of the diesel engine on test

Stress Level	Kilometers to Failure ($\times 10^5$)						
Low	Engine 8:						
	1.4972						
	Engine 2:						
	0.9806						
	Engine 6:						
	0.1249	1.3304					
High	Engine 1:						
	0.2840	0.3182	0.4664	0.5252	0.6763	0.7840	0.8744
	1.0337	1.1279	1.1669	1.2278	1.3119	1.4561	
	Engine 5:						
	0.3833	0.8264	1.2253	1.2281	1.3001	1.4080	1.4108
	1.4320	1.4945					
	Engine 7:						
	0.4817	0.6066	0.8096	0.8673	0.9870	0.9883	1.0641
	1.1511	1.1822	1.1903	1.2045			
	Engine 2:						
	0.5891	0.8338	0.8704	1.0615	1.1384	1.2009	1.2153
	1.2391	1.2638	1.3124				
	Engine 4:						
	0.4103	0.4158	0.4752	0.6999	0.7388	0.9662	1.0496

When the sample size is small, the normality of $\pi(\boldsymbol{\theta}^{(1)})$ might not be guaranteed.

One may refer to Kass and Slate (1994) for diagnostics of posterior normality. In Muller and Parmigiani (1996) and Muller et al (1996), the authors proposed a Bayesian curve fitting method using Dirichlet process mixture (DPM) of normal distributions. The salient idea is to reconstruct the posterior distribution by multivariate normal mixtures using the Monte Chain Monte-Carlo integration and density estimation. Specifically, given a sample $\{\theta_1, \theta_2, ..., \theta_n\}$ generated from the posterior distribution, this method fitting the following model to the points $\{\theta_1, \theta_2, ..., \theta_n\}$

$$\theta_i \sim N(\mu_i, \Sigma_i)$$
$$\mu_i, \Sigma_i \sim G$$
$$G \sim DP(G_0, \alpha)$$
$$G_0(\Sigma, \mu) = W(\Sigma^{-1}; s, (sS)^{-1}) \cdot N(\mu; m, B) \qquad \text{for } i = 1, 2, ..., n$$

Here, W is the Wishart distribution, and DP refers to a Dirichlet process. The hyper-parameters S, m, B, α respectively has hyper-priors $W(S; q, q^{-1}R)$, $N(m; a, A)$, $W(B^{-1}; c, (cC)^{-1})$ and $\Gamma(\alpha; a_0, b_0)$.

Based on this model, a Gibbs sampling scheme was presented to produce a Markov chain that eventually yields an approximation of the posterior distribution of $\{\theta_1, \theta_2, ..., \theta_n\}$.

Figure 9.8 below shows the sampled values of $\boldsymbol{\theta}^{(1)}$ from the posterior distribution $\pi(\boldsymbol{\theta}^{(1)})$ using the Markov Chain Monte-Carlo simulation, the normally approximated posterior distribution, as well as the re-constructed posterior distribution $\pi(\boldsymbol{\theta}^{(1)})$ using Dirichlet process mixture of normals. It is seen that the re-constructed posterior distribution $\pi(\boldsymbol{\theta}^{(1)})$ using Dirichlet process mixture of normals tends to concentrate on the high density region of the sampled $\boldsymbol{\theta}^{(1)}$.

In our experiment, when the reconstruction of $\pi(\boldsymbol{\theta}^{(1)})$ converges, the Dirichlet process mixture of normals happens to consist of only one normal distribution as its component. This allows us to use the normal probability plot to conduct a fair comparison between the normally approximated and DPM re-constructed posterior distribution. Figure 9.9 below plots the sampled $\boldsymbol{\theta}^{(1)}$ on a normal probability plot paper, and also shows the fitted marginal distributions of $\gamma_0^{(1)}$, $\gamma_1^{(1)}$ and $\sigma^{(1)}$ respected from the normally approximated and DPM re-constructed posterior distribution. Here, the plotting position on the vertical axis is the inverse of the standard normal distribution Φ_{NOR} evaluated at the estimated $\hat{F} = (i - 0.3)/(n + 0.4)$, and the plotting position on the horizontal axis is the ordered sampled values. It is immediately seen that, the DPM re-constructed posterior distributions gives closer fit to the posterior distribution, particularly for the marginal posterior distributions of $\gamma_0^{(1)}$ and $\sigma^{(1)}$.

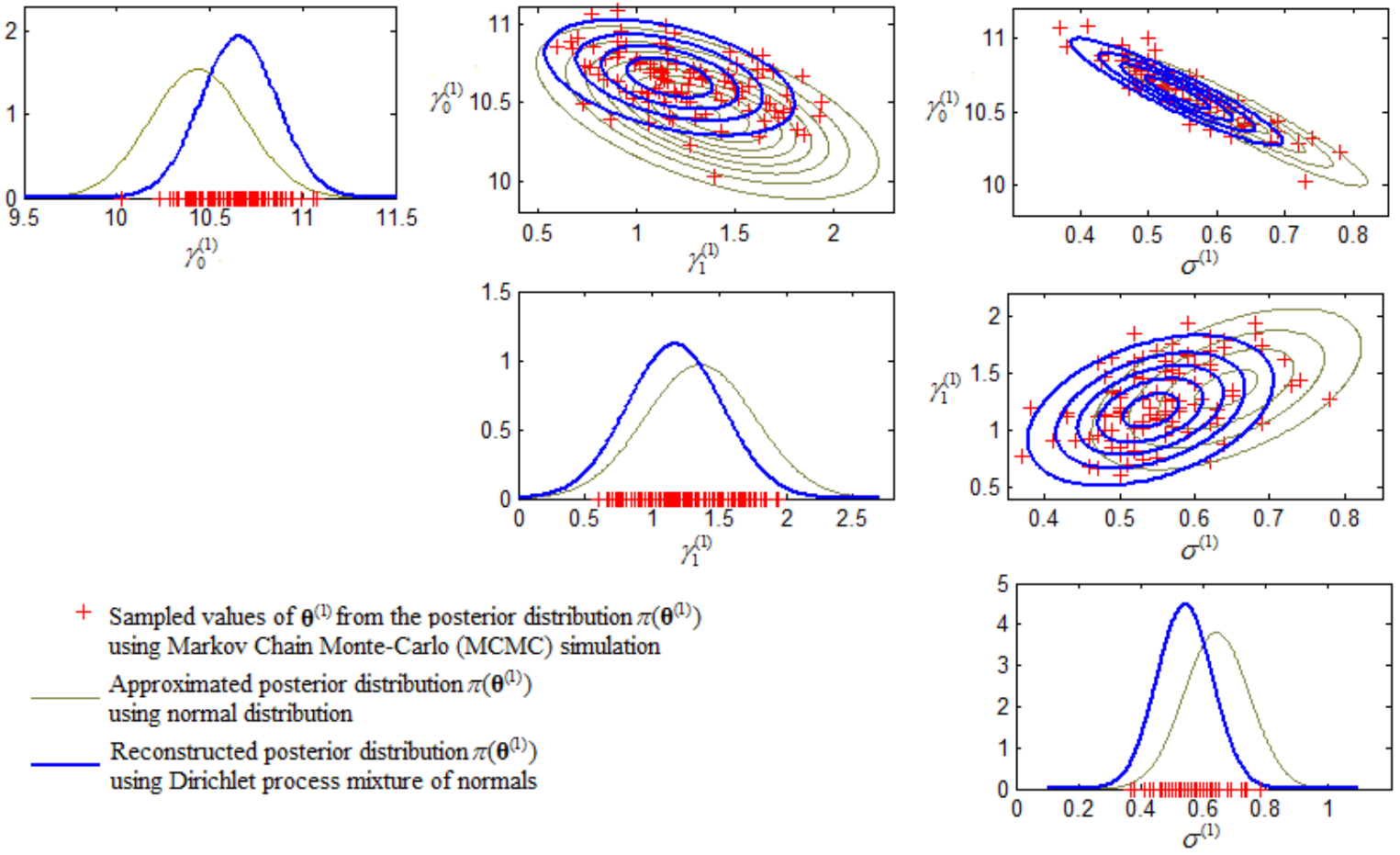

Figure 9.8 The Approximation of the posterior distribution

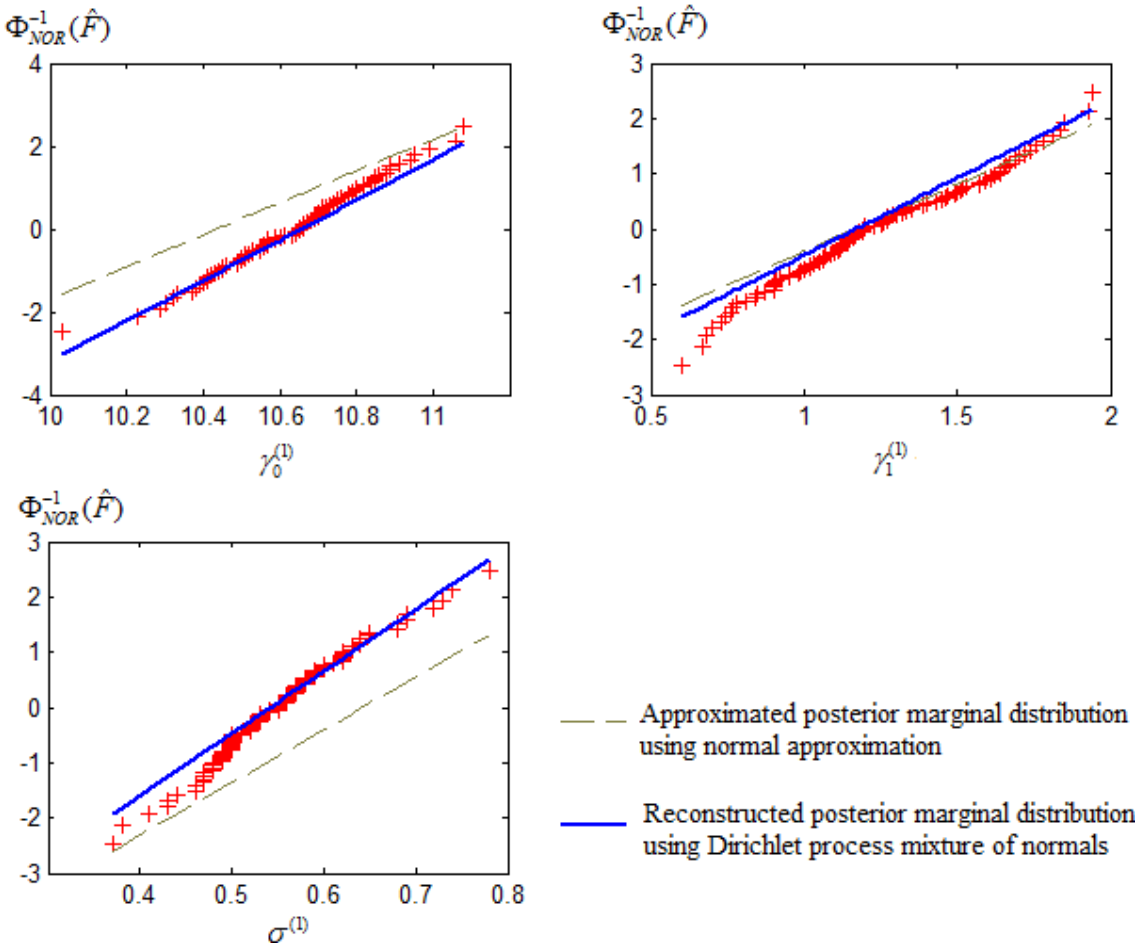

Figure 9.9 Comparison of the approximated and DMP re-constructed posterior marginal distribution

Using the both normally approximated and DPM re-constructed, Table 9.6 below provides the point estimation as well as the lower bound with 95% confidence level for some commonly used key reliability measures of the diesel engine at use condition, only considering the type-I failure mode.

Table 9.6 Estimated key reliability measures of the diesel engine at use condition (Type-I failure mode)

Reliability Measures	Using the Normally Approximated Posterior Distribution		Using the DPM Re-constructed Posterior Distribution	
	Point Estimation	Lower Bound with 95% Confidence	Point Estimation	Lower Bound with 95% Confidence
10% Life Quantile	3.41×10^4 km	1.56×10^4 km	4.37×10^4 km	2.07×10^4 km
Median Life	11.09×10^4 km	5.96×10^4 km	11.80×10^4 km	6.41×10^4 km
Number of Repairs within the first 10^5 Km	0.73	0.24	0.67	0.17
Failure Intensity at 10^6 Km	0.66 repairs per 10^4 km	0.12 repairs per 10^4 km	1.72 repairs per 10^4 km	0.21 repairs per 10^4 km

9.8. Conclusion

This chapter described a Bayesian method for planning a single-variable constant-stress ALT of repairable systems with multiple failure modes. For each failure mode, the failure process was modeled by a Power Law Process. A log linear relationship was assumed to describe the relationship between the unknown scale parameter and testing stress, while the shape parameter is a constant independent of stress. Here, different failure modes were assumed to be *s*-independent, and the corresponding failure processes might not have the same shape parameters. To develop the optimal plan, the Bayesian D-optimality and Ds-optimality were adopted, and the Generalized Equivalence Theorem was used to verify the global optimality of the developed plans. Furthermore, we provided a diesel engine testing example to illustrate the proposed planning approach. Particularly, a Bayesian curve fitting method called Dirichlet process mixture of normal distributions was employed to analyze the

testing data since the sample size is relatively small.

Chapter 10. Conclusions

This dissertation proposed a framework of sequential constant-stress accelerated life test (ALT). Both inference and planning methods were thoroughly discussed. Sufficient numerical (case) studies were presented, and necessary comparison studies based on both theoretical derivations and simulation techniques were provided. Important issues involves the set-up of the framework, the data analysis under right censoring scheme, the selection of prior distributions, the elicitation and quantification of empirical engineering knowledge, the robustness of the estimator as well as the test plan, the approximation of probability density, the experiment design under multiple conflicting objectives, and etc.

The original idea of the sequential data analysis came to my mind when I prepared the term paper of IE6123-reliability. In regression analysis, one of the most commonly used assumptions is the independent assumption of observations associated to different explanatory variables. However, in many industrial applications such as ALT, test results obtained at one particular stress level may provide certain clue on the life distribution at other stress levels, provided that certain amount of information on the stress-life relationships is available. Fortunately, this is the case in many ALT applications. Using empirical engineering knowledge, or test results from older generations of the product, product engineers are usually able to elicit some useful information on stress-life relationships. For example, they might roughly know the range of the activation energy, or they might be able to specify the most probable value. Hence, from my point of view, the key problem is not whether we should incorporate this empirical information, which might risk the objectivity of the analysis, but to come out with an effective method that employs such information.

As indicated by the literature review provided in Chapter 2, current Bayesian methods, which could be very useful in some situations, suffer from the difficulty of choosing appropriate prior distributions. This difficulty is of two-fold. One, it is difficult to choose the right form of the prior distribution; Two, it is difficult to quantify the value of information into the prior distribution. Hence, people may argue that the objectivity of Bayesian analysis is questionable. From another perspective of view, however, ALT is only one essential part of the product life-cycle reliability engineering. This is a cycle that consists of multiple decisions under different scenarios, and most of these decisions are never made pure objectively. In engineering applications, although Bayesian methods might violate the data objectivity when they are not properly used, this does not necessarily mean that a better decision can be made if we disregard the prior knowledge. Again, the question here is how to come out with an effective Bayesian method and this is the key motivation of this study.

Based on this reasoning, Chapter 3 presented the sequential ALT framework and its Bayesian inference. Under this framework, test at the highest stress level is firstly conducted. When this test is completed, we have some information on the intercept of the stress-life model as well as the scale of the failure time distribution (in log scale). Then, by specifying the range of the slope parameter, prior distributions at any stress level can be deduced. However, since engineers are never able to specify the exact value of the slope parameter, uncertainty always exists over this parameter. As discussed in Chapter 6, this causes an information-decay during the information-transmission among stress levels. The higher the uncertainty; the larger the decay rate. So, in order to maximize the information obtained at the lower stress levels, an auxiliary acceleration factor was introduced Chapter 6 that amplifies the failure probability when the stress level is low. In Chapter 4, the effects of the specified

slope parameter was thoroughly investigated and numerical examples were presented to visualize such effects. Here, I need to point out that the choice of a uniform prior distribution for the slope parameter may not be optimal. The adoption of this form of distribution is due to it can be conveniently used in reality. Further studies are definitely needed here so as to make the method of sequential ALT analysis a more complete one. Chapter 5 presented the planning method for the sequential ALT, and Chapter 7 approaches the same problem but from a non-Bayesian perspective of view. Comparison studies between the methods presented in these two sections are important, particularly results in closed-forms.

After a case study presented in Chapter 8, we investigated the planning of an ALT for repairable systems with multiple competing risks in Chapter 9. In reality, many systems/products are repairable and experience multiple failure modes in their lifetime. More important, as prototypes are usually costly at the R&D phase, failed testing units are fixed in order to cut down the total number of samples needed for the test. Hence, the method proposed in Chapter 9 provides reliability engineers with an effective method to plan such a test when testing units are fixed upon failure, and the mechanism of failures are not unique.

Bibliography

[1]. Ahmad, N. and Islam, A., Optimal Accelerated Life Designs for Burr Type XII Distributions under Periodic Inspection and Type-I Censoring, Naval Research Logistics, 43, pp. 1049-77. 1996.

[2]. Ahmad, N., Islam, A., Kumar, R., and Tuteja, R.K., Optimal Design of Accelerated Life Test Plans under Periodic Inspection and Type-I Censoring: the Case of Rayleigh Failure Law, South African Statistical Journal, 28, pp. 27-35. 1994.

[3]. Ahmad, N., and Islam, A., and Salam, A., Analysis of Optimal Accelerated Life Test Plans for Periodic Inspection: the Case of Exponentiated Weibull Failure Model," International Journal of Quality and Reliability Management, 23, pp. 1019-46, 2006.

[4]. Al-Bayyati, H.A., and Arnold, J.C., On Double-Stage Estimation in Simple Linear Regression Using Prior Knowledge Technometrics, 14, pp. 405-414. 1972

[5]. Atkinson, A.C., and Donev, A.N., Optimum Experimental Designs, New York: Oxford University Press Inc. 1992.

[6]. Atkinson, A.C., and Donev, A.N., Optimum Experimental Designs, with SAS. New York: Oxford University Press Inc. 2007.

[7]. Achcar, J.A., and Louzada-Neto, F. A Bayesian approach for accelerated life tests considering the Weibull distribution, Computational Statistics, 7, pp. 355-369. 1992.

[8]. Aitkin, M. A Note on the Regression Analysis of Censored Data, Technometrics, 23, pp. 161-164. 1981.

[9]. Alhadeed, A.A. and Yang, S.S. Optimal Simple Step-Stress Plan for Khamis-Higgins Model, IEEE Transactions on Reliability, 51, pp. 212-215. 2002.

[10]. Atkinson, A.C. and Donev, A.N., Optimum Experimental Designs. London: Clarendon Press, 1992.

[11]. Bai, D.S., and Yun, H.J., Accelerated Life Tests for Products of Unequal Size, IEEE Transactions on Reliability, 45, pp. 611-618, 1996.

[12]. Bain, L.J. and Engelhardt, M., Statistical Analysis of Reliability and Life-Testing Models: Theory and Methods. Marcel Dekker, New York. 1991.

[13]. Balakrishnan, N., Han, D., Optimal Step-Stress Testing for Progressively Type-I censored Data from Exponential Distribution. Journal Statistical Planning and Inference, In Press, available online. 2009.

[14]. Balakrishnan, N. and Xie, Q. Exact Inference for a Simple Step-Stress Model with Type-II Hybrid Censored Data from the Exponential Distribution, Journal of Statistical Planning and Inference, 137, pp. 2543-2563. 2007a.

[15]. Balakrishnan, N. and Xie, Q. Exact Inference for a Simple Step-Stress Model with Type-I Hybrid Censored Data from the Exponential Distribution, Journal of Statistical Planning and Inference, 137, pp. 3268-3290. 2007b.

[16]. Barlow, R.E. Toland, R.H. and Freeman, T. A Bayesian Analysis for the Stress-Rupture Life of Kevlar/Epoxy Spherical Pressure Vessels. In Accelerated Life Testing and Experts' Opinions in Reliability, ed by C.A. Clarotti and D.V. Lindley, pp. 203-235. Amsterdam: North-Holland. 1988.

[17]. Berger, J.O. Statistical Decision Theory and Bayesian Analysis, 2nd edition. New York: Springer-Verlag. 1985.

[18]. Bessler S, Chernoff H, and Marshall A. An Optimal Sequential Accelerated Life Test. Technometrics 4, pp.367-379. 1962.

[19]. Birkes, D. and Dodge, Y. Alternative Methods of Regression. New York: Wiley. 1993.

[20]. Buckley, J. and James, I. Linear Regression with Censored Data, Biometrika, 66, pp. 429-436. 1979.

[21]. Bugaighis, M.M. Efficiencies of MLE and BLUE for Parameters of an Accelerated Life-Test Model, IEEE Transactions on Reliability, 37, pp. 230-233. 1988.

[22]. Chaloner, K. and Larntz, K. Bayesian Design of Accelerated Life Testing. Journal of Statistical Planning and Inference, 33, pp. 245-259. 1992.

[23]. Chaloner, K. and Verdinelli, I. Bayesian Experimental Design: A Review. Statistical Science, 10, pp. 273-304. 1995.

[24]. Chernoff, H. Optimal Accelerated Life Designs for Estimation, Technometrics, 4, pp. 381-408. 1962.

[25]. Chernoff, H. Sequential Analysis and Optimum Design. Philadelphia: Society for Industrial and Applied Mathematics (SIAM). 1972.

[26]. Chernoff H, Sequential Design of Experiments. Annals of Mathematical Statistics 30, pp. 755-770. 1959.

[27]. Chatterjee, S. and Price, B. Regression Analysis by Example, 2nd Edition. New York: Wiley. 1991.

[28]. Clyde, M.A. Bayesian Optimal Designs for Approximate Normality. *Ph. D Dissertation*. University of Minnesota. 1993.

[29]. Clyde, M.A. Muller, P. and Parmigiani, G. Inference and design strategies for a hierarchical logistic regression model, in D. Berry and D. Stangl, Ed. Bayesian Biostatistics: Marcel Dekker, 1996.

[30]. Cox, D.R. Regression models and life-tables (with discussion), Journal of the Royal Statistician Society, Series B, vol 34, 1972, pp 187-220.

[31]. Cox, D.R. and Hinkley, D. Theoretical Statistics. USA: Chapman & Hall/CRC. 2000.

[32]. David, F.N., and Neyman, J., Extension of the Markoff Theorem on Least Squares, Statistical Research Memoirs, 2, pp. 105-116, 1938.

[33]. DeGroot, M.H. and Goel, P.K. Bayesian Estimation and Optimal Design in Partially Accelerated Life Testing, Naval Research Logistics, 26, pp. 223-235. 1979.

[34]. DeGroot, M.H. and Goel, P.K. Bayesian Design and Analysis of Accelerated Life Testing with Step Stress. In Accelerated Life Testing and Experts' Opinions in Reliability, ed by C.A. Clarotti and D.V. Lindley, pp. 193-199. Amsterdam: North-Holland. 1988.

[35]. Edgeman R, Lin DKJ, Sequential Analysis of an Accelerated Life Model. International Journal of Quality and Reliability Management, 14, pp.598-605, 1997.

[36]. Efron, B. Why isn't everyone a Bayesian, The American Statistician, 40, pp. 1-5. 1986.

[37]. Escobar L.A., Meeker, W.Q, Planning accelerated life test plans with two or more experimental factors. Technometrics, 37, pp. 411-427. 1995.

[38]. Eubank, R.L., A Density-Quantile Function Approach to Optimal Spacing Selection, Annals of Statistics, 9, pp. 494-500, 1981.

[39]. Eubank, R.L., A Note on Optimal and Robust Spacing Selection, Technical Report, SMU/DS/TR-176, Department of Statistics, Southern Methodist University, 1983.

[40]. Fard, N, Li, C., Optimal simple step stress accelerated life test design for reliability prediction. J. Statist. Plann. Inference. In press, available online. 2009.

[41]. Fiacco, A.V., and McCormick, G.P. Nonlinear Programming: Sequential Unconstrained Minimization Techniques. NY: Wiley. 1968.

[42]. Firth, D and Hinde, J.P. On Bayesian D-optimum design criteria and the equivalence theorem in non-linear models. Journal of the Royal Statistical Society, B, 59, 793-797. 1997.

[43]. Fisher, R.C., Nonparametric Empirical Bayes Estimation of the Poisson Failure Rate, Ph. D Dissertation, University of New Mexico, Albuquerque, NM. 1990.

[44]. Flehinger, B.J. Product test planning for repairable systems, Technometrics, vol 7, pp. 485-494, 1965.

[45]. Friedman, M. and Kandel, A. Fundamentals of Computer Numerical Analysis. Boca Raton: CRC Press. 1994.

[46]. Frohner, F.H. Analytic Bayesian Solution of the Two-Stage Poisson-Type Problem in Probabilistic Risk Analysis, Risk Analysis, 5, 217-225, 1985.

[47]. Frohner, F.H. The Two-Stage Poisson-Type Problem in Probabilistic Risk

Analysis, 5, 231-234, 1985.

[48]. Ginebra, J., and Sen, A., Minimax Approach to Accelerated Life Tests. IEEE Transactions on Reliability, 47, pp. 261-267. 1998

[49]. Gouno, E. An inference method for temperature step-stress accelerated life testing. Quality and Reliability Engineering International, 17, pp. 11-18. 2001.

[50]. Guerin, F., Dumon., B and Lantieri, P. Accelerated life testing on repairable systems, in The Annual Reliability and Maintainability Symposium, Jan. 2004.

[51]. Guida, M. and Giorgio, M. Reliability analysis of accelerated life-test data from a repairable system, IEEE Trans. on Reliability, 44, pp 337-346, Jun, 1995.

[52]. Guida, M. Calabria, R. and Pulcini, G. Bayes inference for a non-homogeneous Poisson process with power intensity law, IEEE Trans. on Reliability, 28, pp. 206-211, 1989.

[53]. Guo, H. and Pan, R. On determining sample size and testing duration of repairable system test, in *The Annual Reliability and Maintainability Symposium*, Jan. 2008.

[54]. Harter, H.L. and Moore, A.H. Maximum-Likelihood Estimation, from Doubly Censored Samples, of the Parameters of the First Asymptotic Distribution of Extreme Values. Journal of the American Statistical Association, 63, pp. 889-901. 1968.

[55]. Hassanein, K.M., Simultaneous Estimation of the Parameters of the Extreme Value distribution by Sample Quantiles, Technometrics, 14, pp.63-70, 1972.

[56]. Haykin, S. Neural Networks – A Comprehensive Foundation, 2nd Edition. New Jersey: Prentice-Hall. 1999.

[57]. Hooper, J.H. and Amster, S.J. Analysis and presentation of reliability data. In Handbook of Statistical Methods for Engineers and Scientists, ed by Harrison M. Wadsworth. New York: McGraw Hill. 1990

[58]. Islam, A., and Ahmad, N., Optimal Design of Accelerated Life Tests for the Weibull Distribution under Periodic Inspection and Type-I Censoring, Microelectronics and Reliability, 34, 1459-68, 1994.

[59]. Jeng, S.L., Joseph, R.V., Wu, C.F., Modeling and analysis strategies for failure amplification method, J. Qual. Techno., 40, pp. 128-139. 2008.

[60]. Jin, Z. Lin, D. and Ying, Z. On Least-Squares Regression with Censored Data, Biometrika, 92, pp. 147-161. 2006.

[61]. Joseph, V.R. and Wu, C.F., Failure Amplification method: An Information Maximization Approach to Categorical Response Optimization, Technometrics, 46, pp. 1-11. 2004.

[62]. Kadane, J. Bayesian Methods and Ethics in a Clinical Trial Design: John Wiley & Sons, 1996.

[63]. Kahn, H.D. Least Squares estimation for the Inverse Power Law for Accelerated Life Tests, Applied Statistics, 28, pp. 40-46. 1979.

[64]. Kass, R.E. and Slate, E, H. Some Diagnostics of Maximum Likelihood and Posterior Non-normality, Annals of Statistics, 22, pp. 668-695. 1994.

[65]. Kenney, J. F. Keeping, E. S. Mathematics of statistics, 2nd edition. Van Nostrand, New Jersy. 1951.

[66]. Klein, J.P. and Basu, A.P. Weibull accelerated life tests when there are competing causes of failure, Communications in Statistics--Theory and

Methods, vol. A10, pp. 2073-2100, 1981.

[67]. Klein, J.P. and Moeschberger, M.L. Survival Analysis: Techniques for Censored and Truncated Data. New York: Springer. 2004

[68]. Liao, C. M., Tseng, S. T. Optimal design for step-stress accelerated degradation tests. IEEE Transactions on Reliability, 55, pp. 59-66. 2006.

[69]. Langseth, H. and Lindqvist, B. H. Competing risks for repairable systems: A data study, Journal of Statistical Planning and Inference, vol. 136, pp. 1687-1700, 2006.

[70]. Lawless, J.F. Statistical Models and Methods for Lifetime Data. New York: Wiley. 1982.

[71]. Leemis, L.M. Reliability: Probabilistic Models and Statistical Methods. Englewood Cliffs: Prentice-Hall. 1995.

[72]. Lindley, D.V. On the measure of information provided by an experiment. Annals of Statistics, 27, pp. 986-1005, 1956.

[73]. Lindley D.V. The Future of Statistics – A Bayesian 21st Century, Advances in Applied Probability, 7, pp. 106 -115. 1975.

[74]. Liu, X. and Tang, L.C. A Sequential Constant-Stress Accelerated Life Testing Scheme and Its Bayesian Inference. Quality and Reliability Engineering International, 91-105, 2009.

[75]. Liu, X., Tang, L.C., Auxiliary Acceleration Factor for Sequential Accelerated Life Tests: A Case Study. In IEEE International Conference on Industrial Engineering and Engineering Management. 2008.

[76]. Liu, X. and Tang, L.C. Planning and Inference for Sequential Accelerated Life

Tests. Journal of Quality Technology, 2009, to appear.

[77]. Liu, X. and Tang, L.C., Statistical Planning of Sequential Constant-Stress Accelerated Life Test with Stepwise Loaded Auxiliary Acceleration Factor. Journal of Statistical Planning and Inference, 2009, to appear.

[78]. Liu, X. and Tang, L.C., Accelerated Life Test Plans for Repairable Systems with Independent Competing Risks. IEEE Transactions on Reliability, 2009, to appear.

[79]. Liu, X. and Tang, L.C., Planning a Sequential Accelerated Life Tests Based on the Maximum Likelihood Theory. Working paper.

[80]. Liu, X., and Tang, L.C., A Computerized Double-Stage Estimation for Sequential Accelerated Life Test Data. Working paper.

[81]. Liu, X., and Tang, L.C., Planning of Accelerated Life Test Plans under Non-Destructive Intermittent Inspections Using the Principle of Optimum Spacing. 1st International Conference on the Interface between Statistics and Engineering, Invited talk, July 13-15, 2009, Beijing, China

[82]. Livingston, H. “SSB-1: Guidelines for Using Plastic Encapsulated Microcircuits and Semiconductors in Military, Aerospace, and Other Rugged Applications”, Proceedings of DMSMS conference 2000.

[83]. Martz, R.A. Waller, R.A., and Fickas, E.T. Bayesian Reliability Analysis of Series Systems of Binomial Subsystems and Components. Technometrics, 30, pp 143-153. 1988.

[84]. Mazzuchi, T.A. and Singpurwalla, N.D. Inferences from Accelerated Life Tests: Some Recent Results. In Accelerated Life Testing and Experts’ Opinions in Reliability, ed by C.A. Clarotti and D.V. Lindley, pp. 181-191. Amsterdam: North-Holland. 1988.

[85]. Meeker, W.Q. A Comparison of Accelerated Life Test Plans for Weibull and Lognormal Distributions and Type I Censoring. Technometrics, 26, pp. 157-172. 1984.

[86]. Meeker, W.Q., Planning Life Tests in which Units are Inspected for Failures, IEEE Transactions on Reliability, R-35, 571-578, 1986.

[87]. Meeker, W.Q. and Escobar, L.A. A Review of Recent Research and Current Issues in Accelerated Testing. International Statistical Review, 61, pp. 147-168. 1993.

[88]. Meeker, W.Q. and Escobar L.A. Planning Accelerated Life Test Plans with Two or More Experimental Factors, Technometrics, 37, pp. 411-427. 1995.

[89]. Meeker, W.Q. and Escobar, L.A. Statistical Methods for Reliability Data. New York: Wiley. 1998.

[90]. Meeker, W.Q. and Hahn, G.J. How to Plan an Accelerated Life Test – Some Practical Guidelines, ASQC Basic References in Quality Control: Statistical Techniques. 1985.

[91]. Meeker, W.Q. Hahn, G.J. and Doganaksoy, N. Planning Reliability Assessment, Quality Progress, 38, pp. 90-93. 2005.

[92]. Meeter, C. and Meeker, W.Q. Optimum Acceleration Life Tests with a Non-Constant Scale Parameter. Technometrics, 36, pp. 71-83. 1994.

[93]. Meinhold, R.J. and Singpurwalla, N.D. Understanding the Kalman Filter. The American Statistician, 37, pp. 123-127. 1983.

[94]. Meinhold, R.J. and Singpurwalla, N.D. A Kalman-Filter Approach for Extrapolations in Certain Dose-Response, Damage Assessment, and

Accelerated-Life-Testing Studies. The American Statistician, 41, pp. 101-106. 1987.

[95]. Michlin, Y.H., Meshkov, L., and Grunin, I, Improvement on 'Sequential Testing' in MIL-HDBK-781A and IEC 61124. IEEE Transactions on Reliability, 57, pp.379-387. 2008.

[96]. MIL-STD-883, Test Methods and Procedures for Microelectronics, available from Naval Publications and Forms Center, 5801 Tabor Aver., Philadelphia, PA 19120. 1985.

[97]. Monroe, E and Pan, Rong, Experimental Design Considerations for Accelerated Life Tests with Nonlinear Constraints and Censoring. 40, pp. 355-347, 2008.

[98]. Montgomery, D and Runger, G, Applied Statistics and Probability for Engineers, 3rd Edition, NY: John Wiley & Sons. 2003.

[99]. Morris M, A Sequential Experimental Design for estimating a Scale Parameter from Quantal Life Testing. Technometrics, 29, pp. 173-181, 1987.

[100]. Mosteller, F., On Some Useful Inefficient Statistics, Annals of Mathematical Statistics, 17, pp. 175-213, 1946.

[101]. Muller, P. and Parmigiani, G. Numerical evaluation of information theoretic measures. In Bayesian Analysis in Statistics and Econometrics: Essays in Honor of Arnold Zellner. D.A Berry, K.M. Chaloner and J.F. Geweke, eds., pp. 397-406. Wiley, 1996.

[102]. Muller, P. Erkanli, A. and West, M. Bayesian curve fitting using multivariate normal mixtures. Biometrika, 83, pp. 67-79. 1996.

[103]. Nelson, W. Graphical Analysis of Accelerated Life Test Data with a Mix of

Failure Modes, IEEE Transactions on Reliability, R-24, pp. 230-237. 1975a.

[104]. Nelson, W. Analysis of Accelerated Life Test Data – Least Squares Methods for the Inverse Power Law Model, IEEE Transactions on Reliability, R-24, pp. 103-107. 1975b.

[105]. Nelson, W. Applied Life Data Analysis. New York: Wiley. 1982.

[106]. Nelson, W. Accelerated Testing: Statistical Models, Test Plans, and Data Analysis. New York: Wiley. 1990.

[107]. Nelson, W. A Bibliography of Accelerated Test Plans, IEEE Transactions on Reliability, 54, pp. 194-197. 2005.

[108]. Nelson, W. A Bibliography of Accelerated Test Plans Part II - References, IEEE Transactions on Reliability, 54, pp. 370-373. 2005.

[109]. Nelson, W. and Hahn, G.J. Linear Estimation of a Regression Relationship from Censored Data – Part I. Simple Methods and Their Application, Technometrics, 14, pp. 247-269. 1972.

[110]. Nelson, W. and Hahn, G.J. Linear Estimation of a Regression Relationship from Censored Data – Part II. Best Linear Unbiased Estimation and Theory, Technometrics, 15, pp. 133-150. 1973.

[111]. Nelson, W. and Kielpinski, T. Theory for Optimum Censored Accelerated Life Tests for Normal and Lognormal Life Distributions. Technometrics, 18, pp. 15-114. 1976.

[112]. Nelson, W. and Meeker, W. Theory for Optimum Censored Accelerated Life Tests for Weibull and Extreme Value Distributions. Technometrics, 20, pp. 171-177. 1978.

[113]. Ogawa, J., Contributions to the Theory of Systematic Statistics, I, Osaka Mathematical Journal, 3, 175-209, 1951.

[114]. Pascual, F.G. and Montepiedra, G. Model-Robust Test Plans with Applications in Accelerated Life Testing, Technometrics, 45, pp. 47-57. 2003a.

[115]. Pascual, F.G. and Montepiedra, G. On Minimax Designs When There Are Two Candidate Models, Journal of Statistical Computation and Simulation, 72, pp. 841-862, 2003b.

[116]. Pascual, F. Accelerated Life Test Plans Robust to Misspecification of the Stress-Life Relationship, Technometrics, 48, pp. 11-25. 2006.

[117]. Pascual, F. Meeker, W. and Escobar, L. Accelerated Life Test Models and Data Analysis. In Handbooks of Engineering Statistics, ed by H. Pham, pp.397-425. New York: Springer-Verlag. 2006.

[118]. Pascual, F. Accelerated Life Test Planning with Independent Weibull Competing Risks with Known Shape Parameter. IEEE Transactions on Reliability, 56, pp. 85-93. 2007.

[119]. Pascual, F., Accelerated Life Test Planning with Independent Weibull Competing Risks, IEEE Transactions on Reliability, 57, pp.435-444, 2008.

[120]. Pathak, P. Singh, A. and Zimmer, W. Bayes Estimation of Hazard and Acceleration in Accelerated Testing. IEEE Transactions on Reliability, 40, pp. 615-621. 1991.

[121]. Pham, H. and Wang, H. Imperfect maintenance, European Journal of Operational Research, 94, pp. 425-438. 1996.

[122]. Pilz, J. Bayesian Estimation and Experimental Design in Linear Regression Models. Germany: John Wiley & Sons. 1991.

[123]. Porter, A. Accelerate Testing and Validation: Testing, Engineering, and Management Tolls for Lean Development. Oxford: Elsevier. 2004.

[124]. Rigdon, S.E. and Basu, A.P. The power law process: A model for the reliability of repairable systems. Journal of Quality Technology, vol 21, pp 251-260, Oct, 1989.

[125]. Rigdon, S.E. and Basu, A.P. Statistical Methods for the Reliability of Repairable Systems. : John Wiley & Sons, Inc. 2000.

[126]. Robert, C.P. and Casella, G. Monte Carlo Statistical Methods. New York: Springer. 1999.

[127]. Schmee, J. and Hahn, G.J. A Simple Method for Regression Analysis with Censored Data, Technometrics, 21, pp. 417-432. 1979.

[128]. Schmee, J. and Hahn, G.J. A Computer Program for Simple Regression with Censored Data, Journal of Quality Technology, 13, pp. 264-269. 1981.

[129]. Seo, S.K., and Yun, B.J., Accelerated Life Test Plans under Intermittent Inspection and Type-I Censoring: The Case of Weibull Failure Distribution, Naval Research Logistics, 38, pp. 1-22, 1991.

[130]. Sikand, S.S., Hariram, S.S. and Patel, J. Reliability of the Engine Electronic Controls and a Novel Approach to Improve Service Life. SAE transactions, 114, 1276-1284, 2005.

[131]. Singpurwalla, N.D. Reliability and Risk – A Bayesian Perspective. New York: Wiley. 2006.

[132]. Sohn, S.Y., Accelerated Life-Tests for Intermittent destructive Inspection, with Logistic Failure-Distribution," IEEE Transactions on Reliability, 46, pp.

122-129, 1997.

[133]. Tang, L.C. Planning accelerated life tests for censored two-parameter exponential distributions, Naval Research Logistics, 46, pp.169-186. 1999.

[134]. Tang, L.C. Multiple-Steps Step-Stress Accelerated Test. In Handbooks of Reliability Engineering, ed by H. Pham, pp.441-455. New York: Springer-Verlag. 2003.

[135]. Tang, L.C. Statistical Approaches to Planning of Accelerated Reliability Testing. In Handbooks of Engineering Statistics, ed by H. Pham, pp.427-440. New York: Springer-Verlag. 2006.

[136]. Tang, L.C., and Liu, X., A Two-Phase Analysis for a Large Fleet of Repairable Systems. The 36th International Conference on Computers and Industrial Engineering. 2006.

[137]. Tang, L.C., Goh, T.N., Sun, Y.S., Ong, H.L., Planning accelerated life tests for censored two-parameter exponential distributions, Naval Research Logistics, 46, pp. 169-186, 1999.

[138]. Tang, L.C. Tan, A.P. and Ong, S.H. Planning Accelerated Life Tests with Three Constant Stress Levels. Computer and Industrial Engineering, 42, pp. 439-446. 2002.

[139]. Tang, L.C. and Xu, K. A Multiple Objective Framework for Planning Accelerated Life Tests, IEEE Transactions on Reliability, 54, pp. 58-63. 2005.

[140]. Tang, L.C, Ng, Q.Y. Cheong, W.T. and Goh, J.S. Reliability assessment for particle-induced failures in multi-generation hard disk drives. Microsystem Technologies, 13, pp.891-894. 2007.

[141]. Teng, S.L. and K.P. Yeo. A Least-Squares Approach to Analyzing Life-Stress

Relationship in Step-Stress Accelerate Life Tests, IEEE Transactions on Reliability, 51, pp. 177-182. 2002.

[142]. Tojeiro, C.A.V. Louzada-Neto, F. and Bolfarine, H. A Bayesian Analysis for Accelerated Lifetime Tests Under an Exponential Power Law Model with Threshold Stress, Applied Statistics, 31, pp. 685-691. 2004.

[143]. Tseng, S.T. Planning Accelerated Life Tests for Selecting the Most Reliable Product. Journal of Statistical Planning and Inference, 41, pp. 215-230. 1994

[144]. Van Dorp, J.R. Mazzuchi, T.A. Fornell, G.E. and Pollock, L.R. A Bayes Approach to Step-Stress Accelerated Life Testing, IEEE Transactions on Reliability, 45, pp. 491-498. 1996.

[145]. Van Dorp, J.R. and Mazzuchi, T.A. A General Bayes Exponential Inference Model for Accelerated Life Testing, Journal of Statistical Planning and Inference, 119, pp. 55-74. 2004.

[146]. Van Dorp, J.R. and Mazzuchi, T.A. A General Bayes Weibull Inference Model for Accelerated Life Testing, Reliability Engineering and System Safety, 90, pp. 140-147. 2005.

[147]. Verdinelli, I. Polson, N. and Singpurwalla, N.D. Shannon Information and Bayesian Design for Prediction in Accelerated Life Testing. In Reliability and Decision Making, ed R.E. Barlow et al, pp. 247-256. New York: Chapman & Hall/CRC. 1993.

[148]. Viertl, R. Statistical Methods in Accelerated Life Testing, Gottingen: Vandenhoeck & Ruprecht. 1988.

[149]. Wetherill, G.B. and Glazebrook, K.D. Sequential Methods in Statistics, 3rd Edition. London: Chapman and Hall.1986.

[150]. Whittle, P., Some general points in the theory of optimal experimental design, Journal of the Royal Statistician Society, Series B, 35, pp. 123-130, 1973.

[151]. Yang, G.B. Optimum Constant-Stress Accelerated Life-Test Plans, IEEE Transactions on Reliability, 43, pp. 575-581. 1994.

[152]. Yang, G.B. and Jin, L. Best Compromise Test Plans for Weibull Distributions with Different Censoring Times, Quality and Reliability Engineering International, 10, pp. 411-415. 1994.

[153]. Yang, G.B. Life Cycle Reliability Engineering, New Jersey: Wiley & Sons, 2007.

[154]. Yang, G. Accelerated Life Tests at Higher Usage Rate, IEEE Transactions on Reliability, 54, pp.5 3-57. 2005.

[155]. Yang, G. and Zaghati, Z. Accelerated Life Tests at Higher Usage Rates: A Case Study. In Proc. Reliability and Maintainability Symposium, 2006, pp. 313-317.

[156]. Yang, G. Optimum Plans for Step-Stress Accelerated Life Tests at Higher Usage Rates. In Proc. Reliability and Maintainability Symposium, 2008, 11A1.

[157]. Yeo, K.Y., Tang, L.C. Planning step-stress life-test with a target acceleration-factor. IEEE Trans. Reliab. 48, pp. 61-67. 1999

[158]. Yum, B.J., and Choi, S.C., Optimal Design of Accelerated Life Tests under Periodic Inspection, Navel Research Logistics, 36, 779-795, 1989.

[159]. Yun, W.Y. Kim, E.S., and Cha, J.H. Accelerated life test data analysis for repairable systems, Communications in Statistics – Theory and Methods, vol 35, pp. 1803-1814, 2006.

[160]. Zellner, A. Optimal information processing and Bayes' theorem. The American Statistician, vol 42, pp. 278-284. 1988.

[161]. Zhang, Y. and Meeker, W.Q. Bayesian Methods for Planning Accelerated Life Tests, Technometrics, 48, pp. 49-60. 2006.

[162]. Zhao, W.B. and Elsayed, E.A. An accelerated life testing under competing failure modes. in The Annual Reliability and Maintainability Symposium, Jan. 2004.

[163]. Zhao, W.B. and Elsayed, E.A. Optimum accelerated life testing plans based on proportional mean residual life. Quality and Reliability Engineering International, 21, pp. 701-713. 2005.

Appendix

Table A.1 ALT data for Device-A (Data from Meeker and Escobar 1998)

Hours	Status	Number of Devices	Temperature, C
5000	Censored	30	10
1298	Failed	1	40
1390	Failed	1	40
3187	Failed	1	40
3241	Failed	1	40
3261	Failed	1	40
3313	Failed	1	40
4501	Failed	1	40
4568	Failed	1	40
4841	Failed	1	40
4982	Failed	1	40
5000	Censored	90	40
581	Failed	1	60
925	Failed	1	60
1432	Failed	1	60
1586	Failed	1	60
2452	Failed	1	60
2734	Failed	1	60
2772	Failed	1	60
4106	Failed	1	60
4674	Failed	1	60
5000	Censored	11	60
283	Failed	1	80
361	Failed	1	80
515	Failed	1	80
638	Failed	1	80
854	Failed	1	80
1024	Failed	1	80
1030	Failed	1	80
1045	Failed	1	80
1767	Failed	1	80
1777	Failed	1	80
1856	Failed	1	80
1951	Failed	1	80
1964	Failed	1	80
2884	Failed	1	80
5000	Censored	1	80